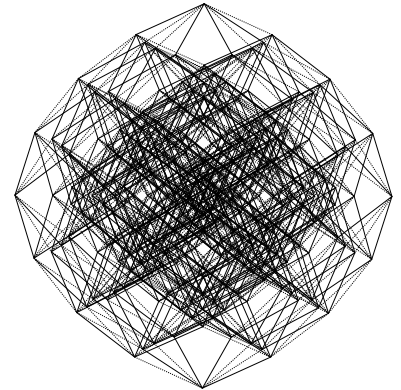
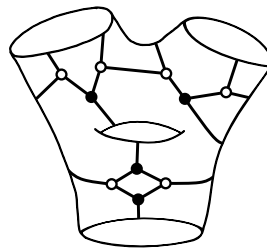
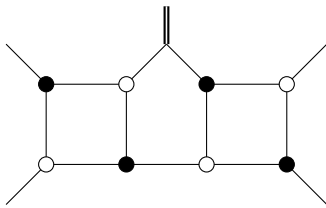


Integrability in weakly coupled super Yang–Mills theory: form factors, on-shell methods and Q-operators



Dissertation
zur Erlangung des akademischen Grades
doctor rerum naturalium
(Dr. rer. nat.)
im Fach Physik
eingereicht an der Mathematisch-Naturwissenschaftlichen Fakultät
der Humboldt-Universität zu Berlin
von
David Meidinger, M.Sc.

Präsidentin der Humboldt-Universität zu Berlin
Prof. Dr.-Ing. Dr. Sabine Kunst

Dekan der Mathematisch-Naturwissenschaftlichen Fakultät
Prof. Dr. Elmar Kulke

Gutachter
Prof. Dr. Matthias Staudacher
Prof. Dr. Jan Plefka
Prof. Dr. Dmytro Volin

Tag der mündlichen Prüfung: 26.01.2018

Hiermit erkläre ich, die Dissertation selbstständig und nur unter Verwendung der angegebenen Hilfen und Hilfsmittel angefertigt zu haben. Ich habe mich anderwärts nicht um einen Doktorgrad beworben und besitze einen entsprechenden Doktorgrad nicht. Ich erkläre die Kenntnisnahme der dem Verfahren zugrunde liegenden Promotionsordnung der Mathematisch-Naturwissenschaftlichen Fakultät I der Humboldt-Universität zu Berlin vom 27. Juni 2012.

ZUSAMMENFASSUNG

Diese Arbeit untersucht die superkonforme $\mathcal{N} = 4$ Yang-Mills-Theorie ($\mathcal{N} = 4$ SYM) bei schwacher Kopplung, mit dem Ziel eines tieferen Verständnisses von Größen der Theorie als Zustände des integrablen Modells, von dem vermutet wird, dass es der planaren Theorie zu Grunde zu liegt. Die Grundlage hierfür bilden moderne On-Shell-Methoden, insbesondere für Formfaktoren und nicht-planare On-Shell-Diagramme. Die Untersuchung von Streuamplituden hat Verknüpfungen zwischen On-Shell-Methoden und der Yangschen Invarianz der Theorie aufgezeigt; die am besten vom Blickwinkel der Integrabilität aus verstandenen Observablen sind hingegen die Zweipunktfunktionen zusammengesetzter Operatoren. Formfaktoren interpolieren zwischen diesen Größen und sind deshalb ein vielversprechender Untersuchungsgegenstand für eine einheitliche Beschreibung der integrablen Struktur der Theorie.

Zu diesem Zweck leiten wir On-Shell-Diagramme für Formfaktoren des chiralen Energie-Impuls-Tensor-Multipletts aus der Britto-Cachazo-Feng-Witten-Rekursion her, und untersuchen deren Eigenschaften. Sie erlauben die Herleitung eines Graßmannschen Integrals für diese Formfaktoren, d.h. einer Darstellung als Konturintegral in Graßmann-Mannigfaltigkeiten. Für Komponenten mit nächst-zu-maximaler Helizität (NMHV) bestimmen wir die entsprechende Integrationskontur. Dies erlaubt es das Integral mit einer Twistor-String-inspirierten Formulierung in Beziehung zu setzen. Mit Hilfe dieser On-Shell-Methoden zeigen wir dass sowohl Formfaktoren des chiralen Energie-Impuls-Tensor-Multipletts, als auch On-Shell-Funktionen mit Einfügungen beliebiger Operatoren Eigenzustände integrierbarer Transfermatrizen sind. Die entsprechenden Eigenwertgleichungen verallgemeinern die Yangsche Invarianz der On-Shell-Funktionen von Amplituden. Wir zeigen weiterhin dass ein Teil der Yangschen Symmetrien trotz der Operatoreinfügung erhalten bleibt. Da die On-Shell-Diagramme von Formfaktoren in einem gewissen Sinne nichtplanar sind, erweitern wir unsere Untersuchung auf allgemeine nichtplanare On-Shell-Funktionen. Wir zeigen dass diese Funktionen, obwohl sie erst in höheren Ordnungen der $1/N$ -Entwicklung auftreten, einen Teil der Yangschen Symmetrien erhalten. Weitere, von Transfermatrizen generierte Symmetrien können ebenfalls hergeleitet werden, und zeigen insbesondere dass Diagramme auf Zylindern als Intertwiner fungieren. Alle untersuchten Größen lassen sich als Graßmannsche Integrale darstellen, deren Integranden, wie wir zeigen, selbst als Zustände integrierbarer Spinketten zu verstehen sind.

On-Shell-Diagramme basieren auf Größen der führenden Ordnung der Störungsrechnung. Als einen Schritt hin zur Berechnung der Eigenzustände des integrablen Modells zu höheren Schleifenordnungen untersuchen wir zusammengesetzte Operatoren. Hier erlaubt die Quanten-Spektral-Kurve (Quantum Spectral Curve, QSC) die nichtperturbative Berechnung ihres Spektrums, liefert jedoch keine Information zur Form der Zustände selbst. Die QSC kann als algebraisches Q-System verstanden werden, welches in Operatorform durch Baxter Q-Operatoren formulierbar sein sollte. Diese Formulierung enthielte die vollständige Information über die Eigenzustände. Um auf eine solche Operatorform der QSC hinzuwirken untersuchen wir die Q-Operatoren nichtkompakter Superspinketten, insbesondere jene welche $\mathcal{N} = 4$ SYM zur führenden Schleifenordnung beschreibt. Wir entwickeln ein effiziente Methode zur Berechnung der Matrixelemente der Q-Operatoren. Dies erlaubt es das gesamte Q-System durch endliche Matrizen für jeden Anregungssektor zu realisieren, und liefert die Grundlage für perturbative Rechnungen mit der QSC in Operatorform.

SUMMARY

This thesis investigates weakly coupled $\mathcal{N} = 4$ superconformal Yang-Mills theory ($\mathcal{N} = 4$ SYM), aiming at a better understanding of on-shell and off-shell quantities as states of the integrable model that is conjectured to underlie the planar limit of the theory. The basis for this investigation are modern on-shell methods, in particular for form factors and non-planar on-shell functions. The study of scattering amplitudes has revealed links between on-shell methods and the Yangian symmetry of the model; the most well-understood objects from the viewpoint of integrability however are the two-point correlators of composite operators. Form factors are quantities interpolating between off-shell correlation functions and on-shell scattering amplitudes, and are therefore a promising subject of study for a unified description of the integrable structure of the theory.

We use the Britto-Cachazo-Feng-Witten recursion relations to develop on-shell diagrams for form factors of the chiral stress-tensor multiplet, and investigate their properties. The diagrams then allow to derive a Grassmannian integral for these form factors, i.e. a representation as a contour integral inside a Grassmannian. We show how to obtain the contour of this integral for next-to-maximally-helicity-violating (NMHV) form factors, and use this knowledge to relate the integral to a twistor string inspired formulation. Based on these on-shell methods, we show that both form factors of the chiral stress-tensor multiplet as well as on-shell functions with insertions of arbitrary operators are eigenstates of integrable transfer matrices. The corresponding eigenvalue equations can be seen as symmetries generalizing the Yangian invariance of amplitude on-shell functions. In addition, a part of these Yangian symmetries remain unbroken by the operator insertion. Motivated by the fact that on-shell diagrams of form factors can be understood as being nonplanar, we consider general nonplanar on-shell functions. Despite appearing in subleading contributions of the $1/N$ -expansion, we prove that these quantities exhibit a partial Yangian invariance, inherited from the integrability of the planar theory. We also derive symmetries generated by transfer matrices, and show that on-shell diagrams on cylinders can be understood as intertwiners. All these quantities can be written as Grassmannian integrals and interestingly, their integrands can be regarded as states of integrable spin chains themselves.

On-shell diagrams involve quantities at lowest order in perturbation theory. To make progress towards the calculation of the higher loop eigenstates of the integrable model, we consider single trace operators, for which the Quantum Spectral Curve (QSC) exists as a beautiful and concise way of determining the spectrum of these states non-perturbatively. This formulation however carries no information about the form of the states. The QSC is an algebraic Q-system, for which an operatorial form in terms of Baxter Q-operators should exist, containing the complete information on the eigenstates in addition to the eigenvalues. To initiate the developments of an operatorial formulation of the QSC, we investigate the Q-operators of non-compact super spin chains, in particular those of the integrable spin chain describing $\mathcal{N} = 4$ SYM at the one-loop level, and devise efficient methods to evaluate their matrix elements. This allows to obtain the entire Q-system in terms of finite dimensional matrices for each magnon sector. These can be used as input data for perturbative calculations using the QSC in operatorial form.

CONTENTS

1 Introduction 3

Superconformal Yang–Mills theory and the AdS/CFT correspondence 3 *Integrability in $\mathcal{N}=4$ SYM* 5
Scattering amplitudes: on-shell methods and integrability 8 *Overview* 10

I On-shell methods for form factors

2 On-shell methods for scattering amplitudes 17

Kinematics & on-shell superfields 17 *Scattering amplitudes* 21 *On-shell techniques* 24 *On-shell diagrams* 28
The Graßmannian integral 31

3 On-shell diagrams for form factors 35

Form factors 36 *The chiral stress–tensor multiplet* 37 *From BCFW to on-shell diagrams* 38 *Inverse soft limits* 39
Cyclicity and equivalence moves 40 *A relation to amplitude diagrams* 40 *Multiple top–cell diagrams* 42
Permutations 44 *Leading singularities and on-shell functions* 45

4 Form factors as Graßmannian integrals 47

Graßmannian geometry and the off-shell momentum 48 *Gluing the operator into on-shell diagrams* 49
Gluing the top–form 51 *Twistor and momentum twistor space* 55 *More examples* 60

5 The BCFW contour for NMHV 65

The NMHV top–forms 66 *Extracting the geometry from diagrams* 67 *The contour in closed form* 71

6 The Graßmannian and the connected prescription 75

Brief review of the connected prescription for form factors 76 *Graßmannian integrals from the connected prescription* 77
Relating the formulations 79

II On-shell methods and integrability

7 Yangian invariants and R-operators 87

The RTT realization of the Yangian 88 *Transfer matrices and Hamiltonians* 92 *Yangian invariance* 93
Deformations 95 *Construction of on-shell functions via R-operators* 96 *Yangian invariance of R-operator states* 99

8 Integrability construction for form factors 101

The minimal form factor as a vacuum state 101 *Permutations, bridges and R-operators* 102 *Deformed MHV form factors* 103
Form factor on-shell functions as spin chain eigenstates 106

9 Yangian symmetries of nonplanar on-shell diagrams 113

Nonplanar on-shell diagrams 114 *Motivation* 114 *Setup & notation* 115 *Monodromy matrix identities* 116
Transfer matrix identities 119 *Example: Five–point MHV on a cylinder* 121

10 Partial Yangian invariance of form factors 125

Dual Jordan–Schwinger realization 126 *Construction with R-operators* 126 *Yangian symmetries* 127
Symmetries from the original representation 129

11 The Graßmannian integral as a map between spin chains 131

A formula for transfer matrices in terms of rotations in the space of particles 131 *Action on Graßmannian integrals* 132
The \mathfrak{gl}_k spin chain 134

III Towards states at higher loops

12 The Quantum Spectral Curve & Baxter Q-operators 139

Composite operators in $\mathcal{N}=4$ SYM 140 The Quantum Spectral Curve 142 Q-operators 146

13 Q-operators for non-compact super spin chains 149

Lax operators for the Q-system from Yang-Baxter equations 150 Monodromy construction of Q-operators 152
Non-compact representations 154 Case study: spin $-s$ Heisenberg models 155 Overview of non-compact Q-systems 158

14 Evaluating Q-operators 161

Ladder decomposition of \mathcal{R} -operators 162 Lowest level \mathcal{R} -operators for oscillator representations of $\mathfrak{u}_{p,q|r+s}$ 163
Generating the operatorial Q-system 170 Expressions for higher-level Lax operators 174

15 Q-operators for $\mathcal{N}=4$ SYM 177

Representation and conventions 177 Q-functions for the BMN vacuum in fully twisted $\mathcal{N}=4$ SYM 179
A matrix example: local charges, untwisting, and single trace operators 182

16 Conclusion 189

Acknowledgments 197

Bibliography 199

PUBLICATIONS

This thesis is based on the following publications by the author:

Rouven Frassek, David Meidinger, Dhritiman Nandan, Matthias Wilhelm
On-shell diagrams, Grassmannians and integrability for form factors
JHEP **01** (2016) 182
[arXiv:1506.08192](#)

Rouven Frassek and David Meidinger
Yangian-type symmetries of non-planar leading singularities
JHEP **05** (2016) 110
[arXiv:1603.00088](#)

Rouven Frassek, Christian Marboe, David Meidinger
Evaluation of the operatorial Q-system for non-compact super spin chains
JHEP **09** (2017) 18
[arXiv:1706.02320](#)

David Meidinger, Dhritiman Nandan, Brenda Penante, Congkao Wen
A note on NMHV form factors from the Grassmannian and the twistor string
JHEP **09** (2017) 24
[arXiv:1707.00443](#)

Introduction

Quantum field theories in general, and gauge theories in particular, have proven to be the fundamental building blocks of our understanding of nature at microscopic scales. The Glashow-Weinberg-Salam model of the electroweak interactions together with Quantum Chromodynamics describing the strong nuclear force combine into the Standard Model of particle physics. This model successfully describes the dynamics of subatomic matter and after the discovery of the Higgs particle¹ has firmly been verified experimentally in its entirety, up to the TeV scale. Nevertheless, fundamental physics remains far from being fully understood. Some of its open problems will likely require new physics beyond the Standard Model, such as the nature of dark matter, the hierarchy problem, and the missing UV-complete description of quantum gravity. Other problems concern the theoretical and formal depth of our knowledge: the dynamics of nonperturbative and in particular strongly coupled gauge theories still remain poorly understood analytically; even perturbative calculations are extremely challenging and have only been performed to very few orders for many processes.

Although some of its properties deviate from realistic gauge theories, the maximally supersymmetric Yang-Mills theory in four space-time dimensions ($\mathcal{N}=4$ SYM) provides a unique opportunity to study a gauge theory in a far more comprehensive way. The large amount of symmetries of this theory facilitates many practical calculations, often in unexpected ways. Via the AdS/CFT correspondence, it does not only provide a nonperturbative definition of a string theory and therefore for a quantum theory of gravity; it also opens a window into the strong coupling dynamics of gauge theories. Most importantly, its conjectured integrability in the planar limit allows to access many observables nonperturbatively, and promises to solve the theory exactly. It is therefore a powerful theoretical tool to advance our understanding of gauge theories in general.

1.1 Superconformal Yang-Mills theory and the AdS/CFT correspondence

The action of $\mathcal{N}=4$ SYM can be obtained from the 10-dimensional Yang-Mills theory with $\mathcal{N}=1$ supersymmetry by dimensional reduction.² The massless Kaluza-

¹ ATLAS Collaboration, Aad *et al.*, “Observation of a new particle in the search for the Standard Model Higgs boson with the ATLAS detector at the LHC”, [1207.7214](#); and CMS Collaboration, Chatrchyan *et al.*, “Observation of a new boson at a mass of 125 GeV with the CMS experiment at the LHC”, [1207.7235](#)

² Brink, Schwarz, Scherk, “Supersymmetric Yang-Mills Theories”, *Nucl. Phys. B*121 (1977) 77–92

4 | Introduction

Klein modes of the fields in 10D give rise to an $\mathcal{N}=4$ multiplet in 4D, consisting of the gluons, four Weyl fermions $\psi_{\alpha A}$ and their conjugates, as well as six scalars $\phi_{AB} = -\phi_{BA}$; here $A = 1, 2, 3, 4$ is an index of the $SU(4)$ R-symmetry. All these fields transform in the adjoint representation of the gauge group $SU(N)$. The theory is conformally invariant,³ to all orders of perturbation theory;⁴ it is the four-dimensional quantum field theory with the maximal amount of space-time (super) symmetry.⁵ We note that the theory is furthermore invariant under S-duality, i.e. $SL(2, \mathbb{Z})$ transformations of the complexified coupling constant.

Most remarkably, $\mathcal{N}=4$ SYM appears to be quantum integrable, at least in the planar limit, i.e. for the leading contribution of the expansion in $\frac{1}{N}$, where $N - 1$ is the rank of the gauge group. This property, which will be the focus of this work, will be explained in more detail shortly. It provides one of the main reasons to study $\mathcal{N}=4$ SYM. But also from a purely field theoretic perspective, the theory has many special properties. Hidden in the perturbative expansion in terms of Feynman diagrams, the theory is indeed much simpler than it appears at first sight, and this simplicity is made explicit by modern on-shell techniques.⁶

Finally, the arguably most spectacular aspect of the theory is its role in the AdS/CFT correspondence. In his seminal work⁷ building up on previous observations on the scattering from black branes,⁸ Maldacena conjectured that string theories on anti-de-Sitter (AdS) backgrounds are dual to conformal field theories (CFTs) on the boundary of the AdS space. The details of this conjecture were quickly elaborated,⁹ in particular the mapping between observables. The basic relation which underlies the duality is the identification of the partition functions of the string and the CFT model:

$$Z_{\text{string/SUGRA}}[\phi|_{z=0} = \phi_0] = Z_{\text{CFT}}[J = \phi_0]. \quad (1.1)$$

For the string partition function, one imposes boundary values ϕ_0 at the boundary of AdS_5 (spatial infinity at $z = 0$) for the fields ϕ , which are interpreted as sources J for composite operators with the same charges in the conformal field theory. This identification rests on the basic fact that the isometries of AdS spaces can be identified with the group of conformal transformations in the CFT, leading to an identical classification of states. For an extensive review of AdS/CFT dualities, the reader is referred to Aharony et al. (2000).¹⁰

While many instances of this duality have been explored, such as the AdS_4 case with a supersymmetric Chern-Simons theory on the boundary,¹¹ the most prominent and most well-studied example is the duality between $\mathcal{N}=4$ SYM and type IIB string theory on $\text{AdS}_5 \times S^5$. This string theory can be formulated as a symmetric coset sigma model,¹² with target space $\frac{PSU(2,2|4)}{SO(4,1) \times SO(5)}$, such that its symmetries match with the superconformal group $PSU(2,2|4)$ which governs $\mathcal{N}=4$ SYM on the CFT side of the correspondence.

Defining the 't Hooft coupling for $\mathcal{N}=4$ SYM as $\lambda = g_{\text{YM}}^2 N$ where N is the number of colors, and the effective string tension as $T = R^2/(2\pi\alpha')$, with α' the inverse string tension and R the identical radii of AdS_5 and S^5 , the coupling constants of the theories can be related by

$$\lambda = 4\pi^2 T^2, \quad \frac{1}{N} = \frac{g_{\text{str}}}{4\pi^2 T^2}. \quad (1.2)$$

³ Sohnius, West, “Conformal Invariance in $\mathcal{N}=4$ Supersymmetric Yang–Mills Theory”, *Phys. Lett.* **B100** (1981) 245

⁴ Green, Schwarz, Brink, “ $\mathcal{N}=4$ Yang–Mills and N=8 Supergravity as Limits of String Theories”, *Nucl. Phys.* **B198** (1982) 474–492; Grisaru, Rocek, Siegel, “Zero Three Loop beta Function in $\mathcal{N}=4$ Superyang–Mills Theory”, *Phys. Rev. Lett.* **45** (1980) 1063–1066; Mandelstam, “Light Cone Superspace and the Ultraviolet Finiteness of the $\mathcal{N}=4$ Model”, *Nucl. Phys.* **B213** (1983) 149–168; and Brink, Lindgren, Nilsson, “The Ultraviolet Finiteness of the $\mathcal{N}=4$ Yang–Mills Theory”, *Phys. Lett.* **B123** (1983) 323–328

⁵ Haag, Lopuszanski, Sohnius, “All Possible Generators of Supersymmetries of the S Matrix”, *Nucl. Phys.* **B88** (1975) 257

⁶ Arkani–Hamed, Cachazo, Kaplan, “What is the Simplest Quantum Field Theory?”, [0808.1446](#)

⁷ Maldacena, “The Large N limit of superconformal field theories and supergravity”, [hep-th/9711200](#), [*Adv. Theor. Math. Phys.* **2**,231(1998)]

⁸ Gubser, Klebanov, Peet, “Entropy and temperature of black 3–branes”, [hep-th/9602135](#); Gubser, Klebanov, Tseytlin, “String theory and classical absorption by three–branes”, [hep-th/9703040](#); Klebanov, “World volume approach to absorption by nondilatonic branes”, [hep-th/9702076](#); and Gubser, Klebanov, “Absorption by branes and Schwinger terms in the world volume theory”, [hep-th/9708005](#)

⁹ Witten, “Anti–de Sitter space and holography”, [hep-th/9802150](#); and Gubser, Klebanov, Polyakov, “Gauge theory correlators from noncritical string theory”, [hep-th/9802109](#)

¹⁰ Aharony, Gubser, Maldacena, Ooguri, Oz, “Large N field theories, string theory and gravity”, [hep-th/9905111](#)

¹¹ Aharony, Bergman, Jafferis, Maldacena, “ $\mathcal{N}=6$ superconformal Chern–Simons–matter theories, M2–branes and their gravity duals”, [0806.1218](#)

¹² Metsaev, Tseytlin, “Type IIB super–string action in $\text{AdS}_5 \times S^5$ background”, [hep-th/9805028](#)

Therefore the AdS/CFT correspondence provides a weak-strong duality between the models: for small λ , we have the picture of a perturbative field theory, while the worldsheet theory is strongly coupled; for large λ the field theory is strongly coupled, while worldsheet theory reduces to the supergravity limit. Amazingly this identification of coupling constants shows that the AdS/CFT correspondence provides a realization of the idea that quantum gravity can be defined holographically,¹³ via the older intuition that the topological large- N expansion relates Yang-Mills theories to string theories.¹⁴

The fact that the duality relates opposite extremes of the coupling constants has different implications: On one hand, it allows to non-perturbatively define a string theory for the first time, and provides insights into the strongly coupled dynamics of a non-abelian gauge theory; on the other hand, it renders checks or even a proof of the correspondence very difficult. Apart from quantities which are protected by supersymmetry or have large charges, gauge and string theory calculations do not provide answers in overlapping regions of the parameter space. Here the integrability of the AdS₅/CFT₄ system¹⁵ comes into play, allowing to calculate and match other quantities at intermediate values of the coupling. Although we will only be concerned with integrability of the field theory side of the AdS/CFT correspondence, we note that the superstring on AdS₅ × S⁵ is also (classically) integrable.¹⁶ This is a general property of symmetric coset sigma models, for a compact review see Magro (2012).¹⁷

1.2 Integrability in $\mathcal{N}=4$ SYM

The study of quantum integrable system has a long history, dating back to Bethe's seminal work¹⁸ proposing an elegant solution for the quantum mechanical problem of a periodic one-dimensional magnet, i.e. a closed chain of spins with nearest-neighbor exchange interactions. His method is now known as the Coordinate Bethe Ansatz, and understood to belong to a whole family of related techniques and concepts which allow to define and solve the special models exhibiting quantum integrability. Works in this area range from the Quantum Inverse Scattering method of the Leningrad school¹⁹ to the mathematical theory of quantum groups,²⁰ to experimental realizations of these models.²¹

Despite being a rare property especially for realistic models, the stringent mathematical structure of quantum integrability allowed to construct a large class of integrable models. These models are always two-dimensional. This includes 1+1-dimensional discrete quantum systems such as spin chains, which are closely related to statistical lattice models,²² but also two-dimensional field theories, see Dorey (1996)²³ for an introduction. Quantum integrability allows to solve these models exactly, i.e. to compute the scattering matrices of excitations, the eigenstates of the Hamiltonian and their energies, as well as the tower of higher conserved charges which is the hallmark of integrability.

Despite the fact that the 't Hooft limit and the description by a string sigma model via the AdS/CFT correspondence provide $\mathcal{N}=4$ SYM with a two-dimen-

13 Susskind, "The World as a hologram", [hep-th/9409089](#)

14 't Hooft, "A Planar Diagram Theory for Strong Interactions", *Nucl. Phys.* B72 (1974)a 461; and 't Hooft, "A Two-Dimensional Model for Mesons", *Nucl. Phys.* B75 (1974)b 461–470

15 For an extensive but not quite up-to-date review see Beisert *et al.*, "Review of AdS/CFT Integrability: An Overview", [1012.3982](#).

16 Bena, Polchinski, Roiban, "Hidden symmetries of the AdS₅ × S⁵ superstring", [hep-th/0305116](#)

17 Magro, "Review of AdS/CFT Integrability, Chapter II.3: Sigma Model, Gauge Fixing", [1012.3988](#)

18 Bethe, "Zur Theorie der Metalle", *Zeitschrift für Physik* 71 (1931), no. 3, 205–226

19 Faddeev, "Instructive history of the quantum inverse scattering method", *Acta Applicandae Mathematicae* 39 (1995) 69–84, [10.1007/BF00994626](#)

20 Drinfeld, "Quantum groups", *J. Sov. Math.* 41 (1988) 898–915

21 Batchelor, Foerster, "Yang-Baxter integrable models in experiments: from condensed matter to ultracold atoms", [1510.05810](#)

22 Baxter, "Exactly solved models in statistical mechanics", 1982,

23 Dorey, "Exact S matrices", [hep-th/9810026](#)

- 24 Lipatov, “Evolution equations in QCD”, in “Perspectives in hadronic physics. Proceedings, Conference, Trieste, Italy, May 12–16, 1997”, pp. 413–427, 1997
- 25 Minahan, Zarembo, “The Bethe ansatz for $\mathcal{N} = 4$ Super Yang–Mills”, [hep-th/0212208](#); we also refer the reader to earlier work on the integrability of the renormalization of certain operators in QCD, see Braun, Derkachov, Manashov, “Integrability of three particle evolution equations in QCD”, [hep-ph/9805225](#).
- 26 Beisert, “The complete one loop dilatation operator of $\mathcal{N} = 4$ Super Yang–Mills theory”, [hep-th/0307015](#); Beisert, Staudacher, “The $\mathcal{N} = 4$ SYM integrable super spin chain”, [hep-th/0307042](#); and Beisert, Kristiansen, Staudacher, “The Dilatation operator of conformal $\mathcal{N} = 4$ Super Yang–Mills theory”, [hep-th/0303060](#)
- 27 Beisert, Staudacher, “The $\mathcal{N} = 4$ SYM integrable super spin chain”, [hep-th/0307042](#); we note that the problem of solving the Bethe equations efficiently has recently been addressed in Marboe, Volin, “The full spectrum of AdS₅/CFT₄ I: Representation theory and one-loop Q-system”, [1701.03704](#).
- 28 Fendley, Schoutens, Nienhuis, “Lattice fermion models with supersymmetry”, [cond-mat/0307338](#); Hagendorf, “Spin chains with dynamical lattice supersymmetry”, [1207.0357](#); Meidinger, Mitev, “Dynamic Lattice Supersymmetry in $\mathfrak{gl}(n|m)$ Spin Chains”, [1312.7021](#); Hagendorf, Liénardy, “Open spin chains with dynamic lattice supersymmetry”, [1612.02951](#); and Matsui, “Spinon excitations in the spin-1 XXZ chain and hidden supersymmetry”, [1607.04317](#)
- 29 Beisert, Dippel, Staudacher, “A Novel long range spin chain and planar $\mathcal{N} = 4$ super Yang–Mills”, [hep-th/0405001](#); Bargheer, Beisert, Loebbert, “Boosting Nearest-Neighbour to Long-Range Integrable Spin Chains”, [0807.5081](#); Beisert, Erkal, “Yangian symmetry of long-range $\mathfrak{gl}(N)$ integrable spin chains”, [0711.4813](#); and Beisert, “The $\mathfrak{su}(2|3)$ dynamic spin chain”, [hep-th/0310252](#)

sional structure, the appearance of integrability in the planar limit is truly remarkable. Since the theory is conformal, the state-operator map allows to describe the Hilbert space via the gauge invariant composite operators of the theory. In the planar limit, only single trace operators play a role, as interactions between different traces are $\frac{1}{N}$ -suppressed. These operators are color traces over products of the fundamental fields of the theory, evaluated at the same point in space-time. The two-point correlation functions of these operators are fixed by conformal symmetry, up to a scalar value, the anomalous dimension. The operators acquire these anomalous dimensions via quantum corrections: they need to be renormalized, and the leading poles in the corresponding Z-factors give rise to the anomalous scaling behavior. Importantly, operators with the same charges under the symmetry generators will typically mix in this process, giving the Z-factors a matrix structure. This defines the dilatation operator, the diagonalization of which is called the spectral problem. Since the anomalous dimensions together with the structure constants in the Operator Product Expansion (OPE) in principle determine the theory completely, their calculation is – or maybe was – an important problem, and the first one to be tackled by integrability.

Lipatov first conjectured planar $\mathcal{N} = 4$ SYM to be a quantum integrable model in 1997.²⁴ Concrete evidence was found a few years later when Minahan and Zarembo discovered that the one-loop dilatation operator, acting on states in the \mathfrak{so}_6 subsector composed of single trace operators involving only the six scalars of the theory, is in fact identical to the Hamiltonian of an integrable spin chain with \mathfrak{so}_6 symmetry.²⁵ Here the “spins” on the chain are \mathfrak{so}_6 vectors, and their space is spanned by the different scalar fields, or rather their flavor structure. Only nearest-neighbor interactions can occur, since other Feynman diagrams are $\frac{1}{N}$ -suppressed. Due to the cyclicity of the color trace, the spin chain obeys periodic boundary conditions, and only the cyclic states with zero total lattice momentum correspond to operators in the field theory. This result was shown to generalize to the full theory, where the dilatation operator can be understood as the Hamiltonian of a non-compact $\mathfrak{psu}_{2,2|4}$ spin chain.²⁶ This system can be diagonalized by the Bethe Ansatz, such that the one-loop anomalous dimensions can conveniently be obtained by solving the Bethe equations.²⁷

Compared to the models studied in the literature on integrability, the $\mathcal{N} = 4$ SYM spin chain is characterized by some unusual features, which first appear at the two-loop level. In particular, the Hamiltonian, i.e. the dilatation operator, is not invariant under the symmetry algebra, but rather a generator of it. It furthermore receives perturbative quantum corrections which therefore also affect the other generators. From the field theoretical structure of the perturbative expansion it follows that these corrections contain long-range interactions, and even interactions changing the number of sites on the spin chain, such that the length ceases to be a good quantum number. While length-changing structures do appear in a variety of integrable spin chain models,²⁸ the situation is much more involved for $\mathcal{N} = 4$ SYM. A considerable amount of work on the integrability of $\mathcal{N} = 4$ SYM concerned possible Bethe Ansatz descriptions for these long-range and length-changing interactions.²⁹

To circumvent these difficulties, Staudacher proposed to apply an “Asymptotic Bethe Ansatz”, i.e. to study the S-matrix of magnons scattering on spin chains of infinite length.³⁰ Based on the available data for subsectors, this allowed to conjecture all loop asymptotic Bethe equations.³¹ Bootstrapping the exact S-matrix from symmetries, and determining the dressing phase, then allowed to derive these equations.³² Despite neglecting finite size effects, the Asymptotic Bethe Ansatz not only formed the basis for later non-approximate methods, but also allowed to derive exact results. The most noteworthy example is the BES equation.³³ It determines the cusp anomalous dimension, i.e. the divergence of a cusped Wilson line or equivalently the soft-collinear IR behavior of scattering amplitudes to all loop orders.

Finite size effects can perturbatively be incorporated via Lüscher corrections.³⁴ The Thermodynamic Bethe Ansatz³⁵ (TBA) provides a way of systematically resumming these corrections and has been used extensively in the study of $\mathcal{N}=4$ SYM. The TBA equations are notoriously difficult to solve, or even to define for all states. Building on a large corpus of work dedicated to the search for more compact representations of the TBA, the Quantum Spectral Curve³⁶ (QSC) was derived recently. The QSC poses the spectral problem as a Riemann-Hilbert problem for a small number of functions. It combines the system of Q-functions on an algebraic level with a specification of the analytic structure of these functions via their asymptotics – encoding the charges of the states – and their singularities. The core equations algebraically relate the branches of different functions. The QSC has proved to be an efficient method for obtaining operator dimensions at very high loop orders, or non-perturbatively via numerical solutions, and is generally considered to be the final solution of the spectral problem.

Although the progress of using the integrability of planar $\mathcal{N}=4$ SYM was most spectacular for the calculation of anomalous dimensions or equivalently the two-point functions of single trace operators, many other quantities have been investigated successfully from the integrability perspective. One important class of such quantities are three-point functions of these operators, which are completely determined by the anomalous dimensions and the structure constants of the theory. Together with the two-point functions, they thus contain all the data needed to employ the OPE for the calculation of any correlator. Based on early work calculating the lowest order contributions to these structure constants as overlaps of spin chain states,³⁷ recently a framework was proposed for formulating these overlaps non-perturbatively in the coupling.³⁸ It decomposed the structure constants into hexagon form factors (worldsheet form factors of twist operators), which can be bootstrapped using integrability. These ideas are currently being considered as tools to obtain also higher-point correlation functions directly, circumventing the OPE.³⁹ Another very interesting class of observables, especially from the viewpoint of the AdS/CFT correspondence, are smooth Maldacena-Wilson loops, which are likely the quantities making the hidden symmetries of the theory as manifest as possible.⁴⁰ These symmetries, generated by the Yangian of the superconformal algebra, play a distinct role for a particularly important quantity, the S-matrix of the theory.

- 30 Staudacher, “The Factorized S-matrix of CFT/AdS”, [hep-th/0412188](#)
- 31 Beisert, Staudacher, “Long-range psu(2,2|4) Bethe Ansatz for gauge theory and strings”, [hep-th/0504190](#)
- 32 Beisert, “The SU(2|2) dynamic S-matrix”, [hep-th/0511082](#); Beisert, Eden, Staudacher, “Transcendentality and Crossing”, [hep-th/0610251](#); Janik, “The $AdS_5 \times S^5$ superstring worldsheet S-matrix and crossing symmetry”, [hep-th/0603038](#); and Volin, “Minimal solution of the AdS/CFT crossing equation”, [0904.4929](#)
- 33 Beisert, Eden, Staudacher, “Transcendentality and Crossing”, [hep-th/0610251](#); and Eden, Staudacher, “Integrability and transcendentality”, [hep-th/0603157](#)
- 34 Lüscher, “Volume Dependence of the Energy Spectrum in Massive Quantum Field Theories. 1. Stable Particle States”, *Commun. Math. Phys.* **104** (1986) 177; and Janik, “Review of AdS/CFT Integrability, Chapter III.5: Lüscher Corrections”, [1012.3994](#)
- 35 Zamolodchikov, “Thermodynamic Bethe Ansatz in Relativistic Models. Scaling Three State Potts and Lee-Yang Models”, *Nucl. Phys.* **B342** (1990) 695–720; and Bajnok, “Review of AdS/CFT Integrability, Chapter III.6: Thermodynamic Bethe Ansatz”, [1012.3995](#)
- 36 Gromov, Kazakov, Leurent, Volin, “Quantum Spectral Curve for Planar $\mathcal{N} = \text{Super-Yang-Mills}$ Theory”, [1305.1939](#); and Gromov, Kazakov, Leurent, Volin, “Quantum spectral curve for arbitrary state/operator in AdS_5/CFT_4 ”, [1405.4857](#)
- 37 Escobedo, Gromov, Sever, Vieira, “Tailoring Three-Point Functions and Integrability”, [1012.2475](#)
- 38 Basso, Komatsu, Vieira, “Structure Constants and Integrable Bootstrap in Planar $\mathcal{N} = 4$ SYM Theory”, [1505.06745](#)
- 39 Fleury, Komatsu, “Hexagonalization of Correlation Functions”, [1611.05577](#); Basso, Coronado, Komatsu, Lam, Vieira, Zhong, “Asymptotic Four Point Functions”, [1701.04462](#); and Eden, Sfondrini, “Tessellating cushions: four-point functions in $\mathcal{N} = 4$ SYM”, [1611.05436](#)
- 40 Müller, Münkler, Plefka, Pollok, Zarembo, “Yangian Symmetry of smooth Wilson Loops in $\mathcal{N} = 4$ super Yang-Mills Theory”, [1309.1676](#); and Beisert, Müller, Plefka, Vergu, “Integrability of smooth Wilson loops in $\mathcal{N} = 4$ superspace”, [1509.05403](#)

- 41 Bern, Dixon, Dunbar, Kosower, “One loop n point gauge theory amplitudes, unitarity and collinear limits”, [hep-ph/9403226](#); and Bern, Dixon, Dunbar, Kosower, “Fusing gauge theory tree amplitudes into loop amplitudes”, [hep-ph/9409265](#)
- 42 Britto, Cachazo, Feng, “New recursion relations for tree amplitudes of gluons”, [hep-th/0412308](#); and Britto, Cachazo, Feng, Witten, “Direct proof of tree-level recursion relation in Yang-Mills theory”, [hep-th/0501052](#)
- 43 Witten, “Perturbative gauge theory as a string theory in twistor space”, [hep-th/0312171](#)
- 44 Roiban, Spradlin, Volovich, “On the tree level S matrix of Yang-Mills theory”, [hep-th/0403190](#)
- 45 Cachazo, He, Yuan, “Scattering equations and Kawai-Lewellen-Tye orthogonality”, [1306.6575](#)
- 46 Hodges, “Eliminating spurious poles from gauge-theoretic amplitudes”, [0905.1473](#)
- 47 Adamo, “Twistor actions for gauge theory and gravity”, PhD thesis, Cambridge U., DAMTP, 2013, [1308.2820](#),
- 48 Arkani-Hamed, Cachazo, Cheung, Kaplan, “A Duality For The S Matrix”, [0907.5418](#); and Arkani-Hamed, Bourjaily, Cachazo, Goncharov, Postnikov, Trnka, “Scattering Amplitudes and the Positive Grassmannian”, Cambridge University Press, 2016, [1212.5605](#)
- 49 Arkani-Hamed, Trnka, “The Amplituhedron”, [1312.2007](#); and Arkani-Hamed, Trnka, “Into the Amplituhedron”, [1312.7878](#)
- 50 Brandhuber, Heslop, Travaglini, “MHV amplitudes in $\mathcal{N} = 4$ super Yang-Mills and Wilson loops”, [0707.1153](#); Drummond, Henn, Korchemsky, Sokatchev, “On planar gluon amplitudes/Wilson loops duality”, [0709.2368](#); and Alday, Roiban, “Scattering Amplitudes, Wilson Loops and the String/Gauge Theory Correspondence”, [0807.1889](#)
- 51 Drummond, Henn, Korchemsky, Sokatchev, “Dual superconformal symmetry of scattering amplitudes in $\mathcal{N} = 4$ super-Yang-Mills theory”, [0807.1095](#); and Brandhuber, Heslop, Travaglini, “A Note on dual superconformal symmetry of the $\mathcal{N} = 4$ super Yang-Mills S-matrix”, [0807.4097](#)
- 52 Drummond, Henn, Plefka, “Yangian symmetry of scattering amplitudes in $\mathcal{N} = 4$ super Yang-Mills theory”, [0902.2987](#)

1.3 Scattering amplitudes: on-shell methods and integrability

Scattering amplitudes are perhaps the most basic quantities in quantum field theories, and the last decades have seen a rapid advance of the methods to calculate them. Many novel techniques have been developed that far surpass standard perturbative calculations based on Feynman diagrams in terms of efficiency. They follow a general pattern, avoiding Feynman diagrams and more generally all quantities which are not gauge invariant; they exploit the analytic structure of the S-matrix, and make use of the tools of complex analysis. Noteworthy examples of these developments are the generalized unitarity method⁴¹ and the Britto-Cachazo-Feng-Witten (BCFW) recursion relations.⁴² These and other methods have also led to novel and far more compact representations of the amplitudes, often making use of better variables to express them, such as in the spinor-helicity and twistor space formalisms. In this respect, it was Witten’s proposal of formulating gauge theory amplitudes as correlators of a topological string model on twistor space⁴³ which resulted in an ongoing stream of works deriving novel representations of amplitudes: from the connected prescription⁴⁴ and its generalization to all space-time dimensions and many theories in the CHY formulation based on the scattering equations⁴⁵ to a general resurrection of twistor space ideas. These included a geometric understanding of certain amplitudes in twistor space as volumes of polytopes,⁴⁶ as well as formulations of gauge theories directly in twistor space.⁴⁷ It also paved way for the discovery of on-shell diagrams and Grassmannian integral representations of amplitudes,⁴⁸ which will play a key role in the following, and subsequently to the amplituhedron proposal, defining amplitudes in purely geometric terms.⁴⁹ It is important to note that while many of these techniques are available for various theories, $\mathcal{N} = 4$ SYM often played a crucial role in their development. Moreover, it are these techniques which make the hidden simplicity of the theory manifest.

The integrability of planar $\mathcal{N} = 4$ SYM also governs the scattering amplitudes of the theory. In contrast to the spectral problem, where the starting point for the investigation of integrability was the observation that the spectral problem admits an integrable spin chain description, for amplitudes the most important manifestation of integrability comes in the form of hidden symmetries. As a consequence of the Ward identities following from the superconformal invariance of the action, tree-level scattering amplitudes in $\mathcal{N} = 4$ SYM are also superconformally invariant. The duality between scattering amplitudes and lightlike polygonal Wilson loops⁵⁰ was a strong motivation to consider scattering amplitudes formulated in terms of dual momenta, i.e. the momenta naturally associated to the dual graphs, and to the Wilson loop picture. It was found that tree-level amplitudes are indeed covariant under the action of the superconformal algebra in this dual space.⁵¹ The Yangian of $\mathfrak{psu}_{2,2|4}$ emerges as the closure of this dual superconformal symmetry and the ordinary one.⁵² This infinite-dimensional symmetry algebra extends the ordinary Lie symmetry by a tower of higher levels of non-local generators and is the hallmark symmetry of integrable models. While

it is typically not a symmetry of finite size spin chains, it nevertheless underlies the entire construction via the Quantum Inverse Scattering method. The Yangian will play an important role also in this work, and will be discussed in more detail later. For a general overview of Yangian symmetry in $\mathcal{N}=4$ SYM, we refer the reader to Beisert (2011);⁵³ for a recent investigation of this symmetry on the level of the action of $\mathcal{N}=4$ SYM see Beisert et al. (2017).⁵⁴

Importantly, the formulation of scattering processes which makes Yangian symmetry most easily accessible are on-shell diagrams and the Grassmannian integral.⁵⁵ Each on-shell diagram contributing to the amplitude via the BCFW recursion relations is itself a Yangian invariant. There is also on-going work considering the role of the Yangian in the amplituhedron picture, see Ferro et al. (2016).⁵⁶ In the spectral problem, the symmetry generators of $\mathcal{N}=4$ SYM receive quantum corrections, since the dilatation operator has continuous eigenvalues which depend on the coupling constant, and the closure of the algebra propagates these corrections to the other generators. Something analogous happens for scattering amplitudes, where the source of these anomalies are the IR divergences which are inherently part of loop corrections to the amplitudes.⁵⁷ This structure is believed to determine scattering amplitudes to all loop order.⁵⁸

The Yangian can be formulated in terms of monodromy matrices which play a key role in the Quantum Inverse Scattering method. These matrices combine all Yangian generators into a single operator depending on a spectral parameter. In the context of scattering amplitudes in $\mathcal{N}=4$ SYM, this RTT formulation allowed to give tree-level amplitudes an interpretation as special spin chains states, invariant under the action of the monodromy matrix.⁵⁹ This opened up the possibility to investigate the invariants using Bethe Ansatz techniques, but also allowed to construct them via special R-matrices. Remarkably, these R-matrices turned out to be deformations of BCFW-bridges, which can be used to build up the on-shell diagrams appearing from the BCFW recursion relations. This means that each such on-shell diagram is Yangian invariant on its own, and connects on-shell methods with the integrability and spin chain perspective. This construction naturally introduces deformations, related to inhomogeneities of the spin chain sites. These deformations can be interpreted as spectral parameters, such that the deformed amplitudes can themselves be given an interpretation as R-matrices, or generalizations of such operators.

Independently of these developments investigating scattering amplitudes from the spin chain point of view, a framework for computing amplitudes – or rather polygonal Wilson loops – was proposed in Basso et al. (2013, 2015a,b).⁶⁰ This approach computes the Wilson loop by considering the propagation of excitations on the flux tube between the sides of the Wilson loop, regarded as probe quarks. The pieces of this propagation are glued together using the Wilson loop OPE developed in Alday et al. (2011),⁶¹ while the flux tube excitations and their scattering are bootstrapped assuming integrability, as excitations on top of the GKP string. The excitations are described by a generalization of the BES result for the cusp anomaly.⁶² This formulation is inherently non-perturbative in the coupling constant, but perturbative in the number of excitations.

- 53 Beisert, “On Yangian Symmetry in Planar $\mathcal{N}=4$ SYM”, [1004.5423](#)
- 54 Beisert, Garus, Rosso, “Yangian Symmetry and Integrability of Planar $\mathcal{N}=4$ Supersymmetric Yang–Mills Theory”, [1701.09162](#)
- 55 Drummond, Ferro, “Yangians, Grassmannians and T–duality”, [1001.3348](#); and Drummond, Ferro, “The Yangian origin of the Grassmannian integral”, [1002.4622](#)
- 56 Ferro, Łukowski, Orta, Parisi, “Yangian Symmetry for the Tree Amplituhedron”, [1612.04378](#)
- 57 Bargheer, Beisert, Loebbert, “Exact Superconformal and Yangian Symmetry of Scattering Amplitudes”, [1104.0700](#)
- 58 Caron-Huot, He, “Jumpstarting the All-Loop S–Matrix of Planar $\mathcal{N}=4$ Super Yang–Mills”, [1112.1060](#)
- 59 Chicherin, Derkachov, Kirschner, “Yang–Baxter operators and scattering amplitudes in $\mathcal{N}=4$ super–Yang–Mills theory”, [1309.5748](#); Frassek, Kanning, Ko, Staudacher, “Bethe Ansatz for Yangian Invariants: Towards Super Yang–Mills Scattering Amplitudes”, [1312.1693](#); Ferro, Łukowski, Meneghelli, Plefka, Staudacher, “Spectral Parameters for Scattering Amplitudes in $\mathcal{N}=4$ Super Yang–Mills Theory”, [1308.3494](#); Broedel, de Leeuw, Rosso, “A dictionary between R–operators, on–shell graphs and Yangian algebras”, [1403.3670](#); and Kanning, Łukowski, Staudacher, “A shortcut to general tree–level scattering amplitudes in $\mathcal{N}=4$ SYM via integrability”, [1403.3382](#)
- 60 Basso, Sever, Vieira, “Spacetime and Flux Tube S–Matrices at Finite Coupling for $\mathcal{N}=4$ Supersymmetric Yang–Mills Theory”, [1303.1396](#); Basso, Caetano, Cordova, Sever, Vieira, “OPE for all Helicity Amplitudes”, [1412.1132](#); and Basso, Caetano, Cordova, Sever, Vieira, “OPE for all Helicity Amplitudes II. Form Factors and Data Analysis”, [1508.02987](#)
- 61 Alday, Gaiotto, Maldacena, Sever, Vieira, “An Operator Product Expansion for Polygonal null Wilson Loops”, [1006.2788](#)
- 62 Basso, “Exciting the GKP string at any coupling”, [1010.5237](#)

1.4 Overview

These developments show that modern on-shell methods are not only useful tools for the calculation of scattering amplitudes – in the case of $\mathcal{N}=4$ SYM they provide representations directly linking these quantities to integrability. Indeed, work in this area does not only indicate that integrability determines the theory outside of the spectral problem, but also shows that other quantities can be accommodated as states in the integrable model at weak coupling. Even more importantly, on-shell methods seem to provide the best language to make integrability – which is obscured in the perturbative expansion via Feynman diagrams – manifest, as for example in the case of the Yangian invariance of on-shell diagrams. For correlators of composite operators and other off-shell objects, such methods have not yet been developed to the same extent as for amplitudes. On the other hand, this is the area where the structure of integrability has been uncovered in most detail, with the Quantum Spectral Curve providing a completely non-perturbative description of the eigenfunctions of the Q-operators and transfer matrices which determine the spectrum of these states.

The aim of this thesis is to extend these developments in two directions, and to bring both into closer proximity. We first develop on-shell methods, including on-shell diagrams and Grassmannian integrals, for form factors. These quantities describe the overlap of on-shell states with the states created by composite operators. They therefore provide a bridge between fully on-shell amplitudes and off-shell correlation functions. We use these on-shell representations to derive identities for form factor on-shell functions which can be considered as novel, integrability-related symmetries, but also allow to give these quantities an interpretation as spin chain states, bridging the gap between amplitudes and composite operators from this viewpoint. The form factor diagrams can be understood as inherently nonplanar; this motivates the study of general nonplanar on-shell diagrams, appearing as leading singularities in loop calculations. We remarkably find that they are still partially Yangian invariant. This provides a hint that integrability leaves its traces beyond the planar limit. The identities we find also allow to think of some of the functions as intertwiners of the integrable spin chain. We finally consider the Baxter Q-operators of non-compact super spin chains, and develop methods to calculate them explicitly. In particular this allows to consider the one-loop spectral problem in $\mathcal{N}=4$ SYM, and is an important first step to lift the Quantum Spectral Curve to the operatorial level, and to determine the eigenstates of the model at higher loop order, where the spin chain picture starts to break down.

This thesis consists of three parts, each beginning with a chapter reviewing the necessary background, followed by chapters containing the original contributions of the author.^{63,64} The detailed structure of this work is as follows:⁶⁵

In **Part I**, we develop several on-shell formulations for tree-level form factors of the chiral stress-tensor multiplet in $\mathcal{N}=4$ SYM; in analogy to the case of ampli-

63 These chapters aim at answering one specific question each, and are written to be as self-contained as possible. We therefore included also slightly longer calculations in the main text, instead of putting them into appendices.

64 As the reader certainly has already noticed, we put (abbreviated) references into sidenotes (in lighter font compared to actual “footnotes”) whenever they are cited. This is meant for the ease of reading and to prevent annoying page-skipping. Note that this implies that some references appear at multiple places. A complete, alphabetically sorted list of references with the full bibliographical information can be found on page 199.

65 In the following, we indicate the original paper by the author each chapter is based on via its arXiv number, cf. the list of publications preceding this chapter. Some text of these publications has been used in the respective chapters.

tudes, these representations will be a good starting point for the investigation of form factors from the viewpoint of integrability.

Chapter 2 presents background on scattering amplitudes and some of the on-shell techniques for calculating them, with a focus on on-shell diagrams and their Grassmannian integral representations.

Chapter 3 [1506.08192] We show that form factors of the chiral stress-tensor multiplet can be represented by simple generalizations of on-shell diagrams with the minimal form factor as an additional vertex. We discuss some of the properties of these diagrams, present a way to directly relate them to amplitude diagrams, and show that in contrast to amplitudes, multiple “top-cell” diagrams are needed to encode a full tree-level form factor.

Chapter 4 [1506.08192] Based on the on-shell diagrams we then derive a Grassmannian integral representation for form factors. We first discuss how to accommodate the off-shell kinematics of the operator insertion in the Grassmannian picture, and then show how to obtain the Grassmannian integral by gluing together the on-shell part of the diagram with the minimal form factor. This allows to find top-dimensional forms on the Grassmannian, leading to integrals in spinor-helicity as well as twistor and momentum twistor variables. Some example form factors are then calculated based on this representation.

Chapter 5 [1707.00443] As its amplitude counterpart, the Grassmannian integral for form factors does not include a description of the “contour”, i.e. the combination of residues which combine into the tree-level form factor. In this chapter we derive this contour for NMHV form factors, based on the BCFW recursion relations and the resulting geometry in the Grassmannian.

Chapter 6 [1707.00443] For amplitudes, there exists an alternative representation in terms of Grassmannian integrals which can directly be derived from Witten’s twistor string. This formulation includes a precise description of the contour. Recently a similar formulation was proposed for form factors. In this chapter we first write this formula for the NMHV case in Grassmannian form, and show that it has a recursive structure identical to its amplitude counterpart. This provides an interpretation of the recursion as adding particles via inverse soft factors. We then discuss the relation of this Grassmannian formulation to the integral based on on-shell diagrams.

Part II is dedicated to the investigation of the integrability properties of on-shell functions, beyond planar amplitude functions. We discover new symmetries for these functions, and discuss their interpretation as spin chain states.

Chapter 7 reviews quantum integrability in general and RTT realization of the Yangian in particular. We define monodromy and transfer matrices in the representation needed for on-shell functions, using spinor-helicity variables. We also review inhomogeneous versions of these constructions, leading to deformations of physical scattering amplitudes which recently received a lot of interest. The

spin chain monodromies allow to define Yangian invariants elegantly as their eigenvectors. We then show how the R-operator construction for on-shell functions can be used to prove their Yangian invariance.

Chapter 8 [1506.08192] We then show that a similar construction in terms of R-operators can be used for form factor on-shell functions. In contrast to amplitudes, these are not Yangian invariants. The integrability-based formulation however allows to show that they are nevertheless eigenstates of integrable transfer matrices; this can be viewed as a manifestation of hidden symmetries, but also allows to interpret these functions as well-defined spin chain states. We discuss that these statements are not particular to form factor on-shell functions of the chiral stress-tensor multiplet, but apply to arbitrary operator insertions.

Chapter 9 [1603.00088] Another exciting generalization of the on-shell formalism are nonplanar on-shell diagrams, appearing as leading singularities in higher-loop calculations of $\frac{1}{N}$ -suppressed contributions to scattering amplitudes. We show that one can sensibly define the action of the Yangian on the corresponding on-shell functions. Remarkably, Yangian invariance turns out to be only partially broken. We derive the remaining hidden symmetries, and in particular present an exact intertwining relation for diagrams on cylinders, which shows that these diagrams can be regarded as members of the family of commuting operators of the integrable model related to the Yangian.

Chapter 10 [unpublished] Using the strategies developed for nonplanar on-shell diagrams, we return to form factor on-shell functions and prove that – apart from being transfer matrix eigenstates – they also retain invariance under the higher levels of the Yangian.

Chapter 11 [unpublished] presents the observation that Grassmannian integrals with arbitrary integrand, such as those appearing for form factors and nonplanar on-shell diagrams, provide a map between certain states of non-compact \mathfrak{gl}_k spin chains (with k the MHV degree), and the spin chain of $\mathcal{N}=4$ SYM. Concretely we show that it maps the transfer matrices of these models into each other. We describe the resulting spin chain models and show that in the MHV case, the model is a spin chain which previously appeared in the context of high energy scattering in QCD.

In the final **Part III** of this thesis, we consider states of the $\mathcal{N}=4$ SYM spin chain corresponding to single trace operators. On the eigenvalue level, these states are described non-perturbatively by the Quantum Spectral Curve, which is based on a Q-system. With the aim of lifting the QSC to the operatorial level, and to find the eigenstates of the integrable model behind $\mathcal{N}=4$ SYM at higher loop order, we define the operatorial Q-system of non-compact super spin chains, such as $\mathcal{N}=4$ SYM at one-loop. We focus on the calculation of explicit matrix representatives of the Q-operators in individual magnon blocks. For non-compact spin chains, these calculations are rather involved. Still they are a necessary prerequisite to employ perturbative solution methods of the QSC.

Chapter 12 We first review composite single trace operators in $\mathcal{N} = 4$ SYM and their oscillator representation. The determination of the anomalous scaling dimensions of these operators constitutes the spectral problem, to which the Quantum Spectral Curve provides a concise solution. This formulation, which we briefly describe in this chapter, is based on a system of Q-functions. These in turn are known to be the eigenvalues of Baxter Q-operators. We give a short introduction to the monodromy, or oscillator construction of these operators, which will form the basis of the following work.

Chapter 13 [1706.02320] We then give a derivation of the Lax operators used in this construction, for rational super spin chains with arbitrary representations of Jordan-Schwinger type at the sites of the spin chain. These are then used to construct the Q-operators. For the case of representations of the non-compact algebras $u_{p,q|r+s}$, the Lax operators, in the form in which they can be derived from a Yang-Baxter equation, contain infinite sums. These make it difficult to use them in explicit calculations, and result in Q-operators which are given in terms of special functions with poles in the spectral parameter. To showcase these properties, we discuss spin $-s$ Heisenberg models in detail. We then give an overview over general non-compact Q-systems, highlighting which Q-operators are non-rational functions of the spectral parameter.

Chapter 14 [1706.02320] To make an application to $\mathcal{N} = 4$ SYM possible, it is necessary to find an efficient method to explicitly evaluate the Q-system, in particular the non-rational Q-operators. To this end, we derive a compact integral representation for the Lax-operators of the lowest level, from which the matrix elements of the operators can easily be determined. It also provides a way of writing the non-rational operators in terms of finite sums. We then show how to evaluate the supertraces over the auxiliary Fock spaces to obtain the matrix elements of the lowest level Q-operators. For each magnon block, this yields these operators in the form of explicit finite-dimensional matrices. Finally we show how the entire Q-system can be determined from this data, solving the functional relations in an efficient way.

Chapter 15 [1706.02320 & unpublished] In this chapter we show how to specialize these more generally applicable methods to the $\mathcal{N} = 4$ SYM spin chain and consider some single trace operators to discuss a variety of phenomena which are important for the QSC. As an example of how the method can be applied to obtain the one-loop Q-functions of an entire class of states, we calculate them for the BMN vacuum of arbitrary length in the fully twisted theory. Due to the twists, these Q-functions are already rather involved. We furthermore discuss a magnon block with excitations. This allows to showcase the mixing of states, the emergence of local charges and the untwisting limit. We also discuss the parametrization of the twists which has an impact on the interpretation of the states as single trace operators in the non-commutative field theory. This is an important ingredient for the twisted QSC.

We summarize our findings in **chapter 16**, and discuss open questions.

I

**ON-SHELL METHODS
FOR FORM FACTORS**

2

On-shell methods for scattering amplitudes

Scattering amplitudes are perhaps the most important quantities of any QFT in particle physics, and directly relevant for experimental measurements. Nevertheless, they are notoriously hard to calculate using the standard techniques of perturbative QFT. Since the 1980s, a new set of techniques has gradually emerged, that involve no Feynman diagrams. These methods use only on-shell quantities, and in particular avoid non-gauge-invariant quantities even in intermediate steps of the calculation. A key role is played by the analytic structure of the S-matrix.

In this chapter we want to discuss some of these developments. We first introduce useful variables for the description of the scattering of massless particles, and discuss the on-shell superfield of $\mathcal{N}=4$ SYM. After some general remarks on the structure of scattering amplitudes, we describe some techniques that allow to calculate them efficiently, in particular the Britto-Cachazo-Feng-Witten (BCFW) recursion relations and the generalized unitarity method. We then come to the topics that are most important for the following chapters: The representation of scattering amplitudes via on-shell diagrams, and the Graßmannian integral.

Of course this chapter can only give a brief outline of this field of research. We aim at providing an overview which introduces the necessary notation, techniques and formulas to compare the results for form factors in the next chapters with similar results for amplitudes. Fortunately, in-depth reviews are available on this subject; apart from the references in this chapter, we refer the reader to the excellent books Elvang and Huang (2013, 2015)¹ and Henn and Plefka (2014).²

2.1 Kinematics & on-shell superfields

Scattering amplitudes in Yang-Mills theories are parametrized in terms of the kinematics of the particles participating in the scattering process. For n particles there are n massless four-momenta $p^\mu = (p^0, p^i) = (E, p^i)$ obeying momentum conservation,

$$p_1 + p_2 + \cdots + p_{n-1} + p_n = 0, \quad p^2 = \eta_{\mu\nu} p^\mu p^\nu = 0, \quad (2.1)$$

¹ Elvang, Huang, “Scattering Amplitudes”, **1308.1697**; and Elvang, Huang, “Scattering Amplitudes in Gauge Theory and Gravity”, Cambridge University Press, 2015,

² Henn, Plefka, “Scattering Amplitudes in Gauge Theories”, *Lect. Notes Phys.* **883** (2014) pp.1–195

with the Minkowski metric $\eta_{\mu\nu} = \text{diag}(+1, -1, -1, -1)$. Furthermore, each of the particles carries a specific helicity which needs to be specified. For any Yang-Mills theory there are at least two gluon states with helicity ± 1 ; if the theory is supersymmetric, there are further fermion and possibly scalar states with helicity $\pm \frac{1}{2}$ and zero, respectively.

A substantial part of the recent progress in the study of scattering amplitudes is based on some reparametrizations of this kinematical data, which automatically satisfy either momentum conservation or the masslessness condition, and on which the symmetries of scattering amplitudes act in simpler way compared to momentum space. Therefore these choices of variables can simplify practical calculations and sometimes open up avenues for entirely new formal developments. This section introduces spinor-helicity and supertwistor variables. They are fundamental to the on-shell techniques for form factors we develop in the following chapters as well as for the investigation of their integrability properties.

spinor-helicity variables

Any four-momentum can equivalently be written as a two-by-two hermitian matrix, by defining

$$p^{\alpha\dot{\alpha}} = p^\mu \sigma_\mu^{\alpha\dot{\alpha}} = \begin{pmatrix} p^0 + p^3 & p^1 - ip^2 \\ p^1 + ip^2 & p^0 - p^3 \end{pmatrix} \quad (2.2)$$

where σ_μ are the Pauli matrices

$$\sigma_0 = \begin{pmatrix} 1 & 0 \\ 0 & 1 \end{pmatrix}, \quad \sigma_1 = \begin{pmatrix} 0 & 1 \\ 1 & 0 \end{pmatrix}, \quad \sigma_2 = \begin{pmatrix} 0 & -i \\ i & 0 \end{pmatrix}, \quad \sigma_3 = \begin{pmatrix} 1 & 0 \\ 0 & -1 \end{pmatrix}. \quad (2.3)$$

The Lorentz group acts by conjugation as $SL(2, \mathbb{C})$ on the momenta in the form (2.2). The invariant $p^2 = m^2$ is given by the determinant in this representation,

$$\det(p^{\alpha\dot{\alpha}}) = (p^0)^2 - (p^1)^2 - (p^2)^2 - (p^3)^2 = m^2. \quad (2.4)$$

For the massless particles of Yang-Mills theory, this implies that the determinant of the matrix $p^{\alpha\dot{\alpha}}$ vanishes; the matrix is thus of rank one and can be written as an outer product

$$p^{\alpha\dot{\alpha}} = \lambda^\alpha \tilde{\lambda}^{\dot{\alpha}}. \quad (2.5)$$

The variables λ^α and $\tilde{\lambda}^{\dot{\alpha}}$ are called spinor-helicity variables and are two component spinors; note that they are commuting, i.e. they have bosonic statistics.³ They automatically implement the masslessness condition of on-shell momenta, and allow to write scattering amplitudes in vastly simpler forms.

The decomposition of the momentum implies that scalings of the spinors of the form

$$(\lambda, \tilde{\lambda}) \mapsto (t\lambda, t^{-1}\tilde{\lambda}) \implies p \mapsto p \quad (2.6)$$

leaves the momentum they represent unchanged. This invariance is called little group scaling. For real momenta in Minkowski signature, the spinor-helicity

³ To our knowledge, the first paper to describe the use of these variables for the calculation of scattering amplitudes is Kleiss, Stirling, "Spinor techniques for calculating $p\bar{p} \rightarrow W_\pm/Z_0 + \text{jets}$ ", *Nuclear Physics B* **262** (1985), no. 2, 235 – 262.

variables satisfy

$$\lambda = \pm(\tilde{\lambda})^* \quad (2.7)$$

where the plus sign is for positive and the minus sign for negative energy states. This constrains the little group scalings (2.6) to be pure phases.

For each type of spinor, we can use the $SU(2)$ -invariant ε tensor,

$$\varepsilon_{\alpha\beta} = \varepsilon_{\dot{\alpha}\dot{\beta}} = \begin{pmatrix} 0 & 1 \\ -1 & 0 \end{pmatrix}, \quad (2.8)$$

to construct Lorentz invariants. These are typically denoted by angle and square brackets

$$\langle ij \rangle = \varepsilon_{\alpha\beta} \lambda_i^\alpha \lambda_j^\beta = \lambda_i^1 \lambda_j^2 - \lambda_i^2 \lambda_j^1, \quad [ij] = \varepsilon_{\alpha\beta} \tilde{\lambda}_i^\alpha \tilde{\lambda}_j^\beta = \tilde{\lambda}_i^1 \tilde{\lambda}_j^2 - \tilde{\lambda}_i^2 \tilde{\lambda}_j^1, \quad (2.9)$$

and are antisymmetric

$$\langle ji \rangle = -\langle ij \rangle, \quad [ji] = -[ij], \quad \langle ii \rangle = [ii] = 0. \quad (2.10)$$

We can express the usual Mandelstam invariants using the spinor-helicity variables as

$$s_{ij} = (p_i + p_j)^2 = \langle ij \rangle [ji]. \quad (2.11)$$

A useful formula for many practical calculations is the Schouten identity

$$\langle ij \rangle \langle kl \rangle = \langle ik \rangle \langle jl \rangle + \langle il \rangle \langle kj \rangle \quad (2.12)$$

which expresses the fact that any three two-vectors are linearly dependent.

The polarization vectors needed in Feynman diagram calculations can also be represented via the spinors (2.5). We refer the reader to the introductory literature on modern methods for scattering amplitudes such as Dixon (2014, 1996)⁴ for further information on this topic, since the direct methods we present in the following calculate the amplitude directly, without reference to Feynman diagrams.

4 Dixon, "A brief introduction to modern amplitude methods", [1310.5353](#); and Dixon, "Calculating scattering amplitudes efficiently", [hep-ph/9601359](#)

On-shell superfields

All on-shell states of the component fields of $\mathcal{N}=4$ SYM can be combined into a chiral superfield.⁵ Introducing Grassmann variables $\tilde{\eta}^A$, with $A = 1, \dots, 4$, we define the superfield by

$$\Psi = g^+ + \tilde{\eta}^A \bar{\psi}_A + \frac{1}{2!} \tilde{\eta}^A \tilde{\eta}^B \phi_{AB} + \frac{1}{3!} \varepsilon_{ABCD} \tilde{\eta}^A \tilde{\eta}^B \tilde{\eta}^C \psi^D + \tilde{\eta}^1 \tilde{\eta}^2 \tilde{\eta}^3 \tilde{\eta}^4 g^- \quad (2.13)$$

Here g^\pm are the gluon states with helicity ± 1 , $\bar{\psi}_A$ and ψ^D are the four plus four gluinos with helicity $\pm 1/2$, and $\phi_{AB} = -\phi_{BA}$ are the six scalars. The variables $\tilde{\eta}$ can be thought of as carrying helicity $1/2$; therefore we can define superamplitudes of the superfield with homogeneous helicity. The complete set of kinematical data for these amplitudes are then the super spinor-helicity variables $\{\lambda_i^\alpha, \tilde{\lambda}_i^{\dot{\alpha}}, \tilde{\eta}_i^A\}$, and the $\tilde{\eta}$ variables can be used to pick out component amplitudes.

5 Nair, "A Current Algebra for Some Gauge Theory Amplitudes", *Phys. Lett. B* **214** (1988) 215–218

Twistors

It is important to note that the superconformal algebra $\mathfrak{psu}_{2,2|4}$ is not realized linearly in the spinor-helicity variables (or momentum space, for that matter). For example, the generators of translations are realized by $\lambda^\alpha \tilde{\lambda}^{\dot{\alpha}}$, i.e. by multiplication with the momentum, while the special conformal transformations are second order differential operators $\partial^2 / \partial \lambda^\alpha \partial \tilde{\lambda}^{\dot{\alpha}}$.

In $(+ + - -)$ signature,⁶ the spinor-helicity variables λ and $\tilde{\lambda}$ would be real and independent, with real little group scaling. Therefore, in this signature it is possible to perform a Fourier transformation on the λ variables alone,

$$\bullet \rightarrow \int d^2 \lambda_j \exp(-i \tilde{\mu}_j^\alpha \lambda_{j\alpha}) \bullet . \quad (2.14)$$

This results in the superconformal algebra acting linearly as $\mathfrak{sl}_{4|4}$ on the *supertwistor* variables

$$\mathcal{W}_i = (\tilde{\mu}_i, \tilde{\lambda}_i, \tilde{\eta}_i) . \quad (2.15)$$

The observation that scattering amplitudes can be obtained from a string theory in twistor space⁷ led to renewed interest in the use of twistor variables, and to entirely new representations of scattering amplitudes. Twistors were originally introduced in Penrose (1967),⁸ for reviews see Penrose (1999); Huggett and Tod (1994).⁹ The supersymmetric extensions was first considered in Ferber (1978).¹⁰

Region momenta

Another important set of variables are the so-called region, or dual momenta y_i . They can be defined, together with dual supermomenta ϑ_i , by

$$\begin{aligned} p_i &= \lambda_i \tilde{\lambda}_i = y_i - y_{i+1} , \\ q_i &= \lambda_i \tilde{\eta}_i = \vartheta_i - \vartheta_{i+1} . \end{aligned} \quad (2.16)$$

Note that this implies that

$$y_i - y_j = p_i + \dots + p_{j-1} . \quad (2.17)$$

As we will see, the color structure of (super) Yang-Mills scattering amplitudes provides an ordering of the momenta p_i at tree-level and for planar loop integrands, which fixes the dual momenta (2.16) up to translation invariance. Note that the term “dual momenta” stems from the fact that they are the natural variables associated to the dual Feynman graphs.

Provided that we impose the periodicity condition $y_{n+1} = y_1$, the definition (2.16) of the dual momenta automatically implies momentum conservation for the original momenta p_i . Due to this cyclicity, one can think of the momenta as describing the (light-like) edges of a polygon in y -space, the vertices of which are given by the y_i , see figure 2.1. Although the dual momenta still have mass-dimension one, they can be interpreted as points in a configuration space. This is

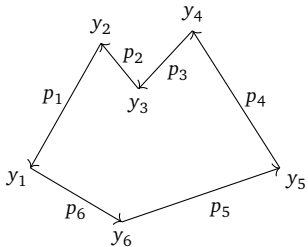


Figure 2.1: The dual momenta y_i can be understood as the vertices of a lightlike polygon, with edges given by the null momenta p_i .

6 Note that at tree-level, the reality conditions on the spinors do not influence the analytic expressions for the amplitudes, and therefore the choice of signature does not matter. If explicit numerical values are desired, one of course needs to analytically continue to Minkowski signature.

7 Witten, “Perturbative gauge theory as a string theory in twistor space”, [hep-th/0312171](https://arxiv.org/abs/hep-th/0312171)

8 Penrose, “Twistor algebra”, *J. Math. Phys.* **8** (1967) 345

9 Penrose, “The Central programme of twistor theory”, *Chaos Solitons Fractals* **10** (1999) 581–611; and Huggett, Tod, “An Introduction to Twistor Theory”, 1994

10 Ferber, “Supertwistors and Conformal Supersymmetry”, *Nucl. Phys. B* **132** (1978) 55–64

the kinematic basis of the duality between scattering amplitudes and light-like polygonal Wilson loops.¹¹

The observation that tree-level scattering amplitudes are covariant under superconformal transformations in the dual y -space (the dual superconformal symmetry¹²), was the starting point for the investigation of scattering amplitudes from the viewpoint of integrability, which we will discuss in chapter 7.

Momentum twistors

Starting from the dual (super) momenta, we can define another set of twistor variables, the momentum twistors,¹³ which we define to be

$$\mathcal{X}_i = (\lambda_i, \mu_i, \eta_i) \quad (2.18)$$

where λ_i is the holomorphic spinor for momentum p_i , and μ_i, η_i are given via the incidence relations

$$\mu_i = \lambda_i y_i = \lambda_i y_{i+1}, \quad \eta_i = \lambda_i \vartheta_i = \lambda_i \vartheta_{i+1}. \quad (2.19)$$

This definition maps the point (y_i, ϑ_i) in super Minkowski space to a line in momentum twistor space $\mathbb{CP}^{3|4}$, given by (2.18) and (2.19) and parametrized by $\lambda_i \in \mathbb{CP}^1$. The incidence relations can be inverted in order to express $\tilde{\lambda}$ and $\tilde{\eta}$ in terms of the components of the supertwistors,

$$\begin{aligned} \tilde{\lambda}_i &= \frac{\langle i+1 i \rangle \mu_{i-1} + \langle i i-1 \rangle \mu_{i+1} + \langle i-1 i+1 \rangle \mu_i}{\langle i-1 i \rangle \langle i i+1 \rangle}, \\ \tilde{\eta}_i &= \frac{\langle i+1 i \rangle \eta_{i-1} + \langle i i-1 \rangle \eta_{i+1} + \langle i-1 i+1 \rangle \eta_i}{\langle i-1 i \rangle \langle i i+1 \rangle}. \end{aligned} \quad (2.20)$$

Just as for the twistors defined above, there is a $\mathfrak{sl}_{4|4}$ acting linear on these variables. For momentum twistors, this $\mathfrak{sl}_{4|4}$ however does not correspond to the superconformal, but to the dual superconformal algebra. Defining the bosonic part of the supertwistors (2.18) as $Z_i = (\lambda_i, \mu_i)$, we see that the bosonic invariants of this action are given by

$$\langle i j k l \rangle = \det(Z_i Z_j Z_k Z_l) = \epsilon_{ABCD} Z_i^A Z_j^B Z_k^C Z_l^D. \quad (2.21)$$

These four-bracket can be related to the kinematic invariants via

$$(y_i - y_j)^2 = (p_i + \dots + p_{j-1})^2 = \frac{\langle i-1, i, j-1, j \rangle}{\langle i-1 i \rangle \langle j-1 j \rangle}. \quad (2.22)$$

This equation furthermore shows that since $(y_i - y_{i+1})^2 = p_i^2 = 0$, the lines $(i-1, i)$ and $(i, i+1)$ intersect.

2.2 Scattering amplitudes

Scattering amplitudes are the transition amplitudes of free asymptotic states in the infinite past to those in the infinite future. One can use crossing symmetry to

11 Brandhuber, Heslop, Travaglini, “MHV amplitudes in $\mathcal{N} = 4$ super Yang–Mills and Wilson loops”, [0707.1153](#); Drummond, Henn, Korchemsky, Sokatchev, “On planar gluon amplitudes/Wilson loops duality”, [0709.2368](#); Drummond, Korchemsky, Sokatchev, “Conformal properties of four-gluon planar amplitudes and Wilson loops”, [0707.0243](#); Alday, Roiban, “Scattering Amplitudes, Wilson Loops and the String/Gauge Theory Correspondence”, [0807.1889](#); and Berkovits, Maldacena, “Fermionic T-Duality, Dual Superconformal Symmetry, and the Amplitude/Wilson Loop Connection”, [0807.3196](#)

12 Drummond, Henn, Korchemsky, Sokatchev, “Dual superconformal symmetry of scattering amplitudes in $\mathcal{N} = 4$ super-Yang–Mills theory”, [0807.1095](#); and Brandhuber, Heslop, Travaglini, “A Note on dual superconformal symmetry of the $\mathcal{N} = 4$ super Yang–Mills S-matrix”, [0807.4097](#)

13 Hodges, “Eliminating spurious poles from gauge-theoretic amplitudes”, [0905.1473](#)

put all n particles into the final state, defining the amplitude as

$$\mathcal{A}_n = {}_{\text{out}}\langle 1, \dots, n | 0 \rangle_{\text{in}} = \langle 1, \dots, n | \mathbf{S} | 0 \rangle, \quad (2.23)$$

where in the second equality we introduced the scattering operator, or S-matrix, which is the time evolution operator from $t = -\infty$ to $t = +\infty$. The states are composed out of n on-shell fields defined in (2.13).

Using standard field theory techniques, scattering amplitudes can be calculated using the momentum-space Feynman diagrams of the corresponding correlation function, with external legs amputated by the LSZ reduction.¹⁴ These calculations typically involve an extremely large number of diagrams which are not individually gauge invariant. In the following, we will mostly consider the tree-level contributions to scattering amplitudes.

Note that the amplitudes as we defined them are really super amplitudes that contain all amplitudes of the component fields when expanded in the Graßmann variables. In components, the generators measuring the helicity of individual particles are given by $h_i = -\frac{1}{2}(\lambda_i^\alpha \frac{\partial}{\partial \lambda_i^\alpha} - \tilde{\lambda}_i^{\dot{\alpha}} \frac{\partial}{\partial \tilde{\lambda}_i^{\dot{\alpha}}})$; in the supersymmetric setting, we can define the superhelicity by

$$\mathbf{h}_i = -\frac{1}{2} \left(\lambda_i^\alpha \frac{\partial}{\partial \lambda_i^\alpha} - \tilde{\lambda}_i^{\dot{\alpha}} \frac{\partial}{\partial \tilde{\lambda}_i^{\dot{\alpha}}} - \tilde{\eta}_i^A \frac{\partial}{\partial \tilde{\eta}_i^A} \right). \quad (2.24)$$

Comparing with (2.13), we see that the on-shell superfield carries superhelicity $+1$, such that the full amplitude is homogeneous:

$$\mathbf{h} \mathcal{A}_n = \sum_{i=1}^n \mathbf{h}_i \mathcal{A}_n = \sum_{i=1}^n \mathcal{A}_n = n \mathcal{A}_n. \quad (2.25)$$

In $\mathcal{N}=4$ SYM all fields are in the adjoint representation of the gauge group which we take to be $SU(N)$. If we call the generators of this representation T^a , with commutation relations $[T^a, T^b] = i\sqrt{2}f^{abc}T^c$, then each three-point vertex contributes a factor of the structure constant f^{abc} and each four-point vertex a factor $f^{abe}f^{cde}$ when calculating a Feynman diagram. The structure constants can be eliminated in favor of traces of the generators using $i\sqrt{2}f^{abc} = \text{Tr}(T^a T^b T^c) - \text{Tr}(T^a T^c T^b)$. One can show that after performing further color algebra, tree-level amplitudes have a color structure without products of traces,

$$\mathcal{A}_n = g^{n-2} \sum_{\sigma \in S_n/Z_n} \text{Tr}(T^{a_{\sigma(1)}} \dots T^{a_{\sigma(n)}}) \mathbf{A}_n(\sigma(1), \dots, \sigma(n)), \quad (2.26)$$

where $g = \frac{\sqrt{\lambda}}{4\pi}$. The traces differ only by permutations of the labels, and therefore the same is true for the coefficients \mathbf{A}_n , which are called partial, or color-ordered amplitudes. The external legs of these quantities carry a fixed cyclic ordering inherited from the color trace. It is generally simpler to calculate $\mathbf{A}_n(1, \dots, n)$ which is a singlet in color space, and recover the full amplitude via (2.26).

The partial superamplitudes can furthermore be expanded into terms with a homogeneous degree in the Graßmann variables,

$$\mathbf{A}_n = \mathbf{A}_{n,2} + \mathbf{A}_{n,3} + \dots + \mathbf{A}_{n,n-3} + \mathbf{A}_{n,n-2}, \quad (2.27)$$

¹⁴ Lehmann, Symanzik, Zimmermann, "Zur Formulierung quantisierter Feldtheorien", *Il Nuovo Cimento* (1955-1965) 1 (1955), no. 1, 205–225

where $A_{n,k} \propto \tilde{\eta}^{4k}$ are R-symmetry singlets. The term $A_{n,2}$ is called the MHV amplitude, because it contains the amplitude with two negative and $n - 2$ positive helicity gluons as a component. Using crossing symmetry, the two negative helicity gluons can be interpreted as two incoming gluons with positive helicity, and then the total helicity changes by the maximal amount from the incoming to the outgoing state. Following this terminology, $A_{n,3}$ is called next-to-MHV or NMHV and in general $A_{n,k}$ is an N^{k-2} MHV amplitude. The term with the highest power of Grassmann variables, $A_{n,n-2}$, is referred to as $\overline{\text{MHV}}$.

The Parke-Taylor amplitude

The MHV amplitudes are considerably simpler than those with a higher MHV degree.¹⁵ It is sometimes useful to factor this part of the amplitude out of the expansion (2.27) and to write the amplitude as

$$A_n = A_{n,2}(1 + \mathcal{P}_{n,3} + \cdots + \mathcal{P}_{n,n-2}). \quad (2.28)$$

A particularly simple expression exists for these MHV amplitudes with an arbitrary number of legs. This so-called Parke-Taylor formula states that

$$A_{n,2}(1, \dots, n) = \frac{\delta^4(P) \delta^8(Q)}{\langle 12 \rangle \langle 23 \rangle \cdots \langle n-1 n \rangle \langle n1 \rangle}. \quad (2.29)$$

Here P and Q are the total momentum and super momentum,¹⁶

$$P^{\alpha\dot{\alpha}} = \sum_{i=1}^n \lambda_i^\alpha \tilde{\lambda}_i^{\dot{\alpha}}, \quad Q^{\alpha A} = \sum_{i=1}^n \lambda_i^\alpha \tilde{\eta}_i^A. \quad (2.30)$$

Parke and Taylor¹⁷ originally found the absolute value squared of this amplitude (in the non-supersymmetric version) in terms of four momenta. Using (2.11) and (2.7) one can see that this square has the same structure as (2.29), with the denominator given in terms of the products $p_i \cdot p_{i+1}$. spinor-helicity variables thus allowed “to take the square root” of this amplitude squared, resulting in the compact formula (2.29), which, for large enough n , would take pages to write down using products of momenta.

Three-point amplitudes

It is a basic fact that scattering amplitudes of three massless particles vanish identically for kinematical reasons. One can easily see this going to the center-of-momentum frame of two incoming particles; momentum conservation then implies that the outgoing particle has $p = 0$.

If, however, the momenta of the particles are complexified, three-particle momentum conservation allows for two discrete kinematical solutions.¹⁸ To determine these solutions, we note that momentum conservation simultaneously implies the following conditions:

$$\begin{aligned} p_1 = -p_2 - p_3 &\implies (p_2 + p_3)^2 = \langle 23 \rangle [32] = 0, \\ p_2 = -p_3 - p_1 &\implies (p_3 + p_1)^2 = \langle 31 \rangle [13] = 0, \\ p_3 = -p_1 - p_2 &\implies (p_1 + p_2)^2 = \langle 12 \rangle [21] = 0. \end{aligned} \quad (2.31)$$

¹⁵ Of course, by parity, the same can be said starting from the $\overline{\text{MHV}}$ amplitudes.

¹⁶ Note that a fermionic delta function, such as $\delta^8(Q)$, is identical to its argument: $\delta^8(Q) = \prod_{\alpha,A} Q^{\alpha A}$.

¹⁷ Parke, Taylor, “An Amplitude for n Gluon Scattering”, *Phys. Rev. Lett.* 56 (1986) 2459

¹⁸ Indeed these constraints determine the three-point amplitudes of any massless theory uniquely. In particular this implies that they are protected from loop corrections, up to the renormalization of the coupling constant.

These equations have two solutions for complexified momenta,

$$\text{all } \langle ij \rangle = 0 \quad \text{or} \quad \text{all } [ij] = 0, \quad (2.32)$$

i.e. either all the spinors λ_i are collinear or all $\tilde{\lambda}_i$. Lorentz invariance, the scaling property (2.25) and the requirement that the expressions are non-singular for these special kinematics then fix the three-point amplitudes to be

$$A_{3,2} = \frac{\delta^4(\lambda_1 \tilde{\lambda}_1 + \lambda_2 \tilde{\lambda}_2 + \lambda_3 \tilde{\lambda}_3) \delta^8(\lambda_1 \tilde{\eta}_1 + \lambda_2 \tilde{\eta}_2 + \lambda_3 \tilde{\eta}_3)}{\langle 12 \rangle \langle 23 \rangle \langle 31 \rangle}, \quad (2.33)$$

$$A_{3,1} = \frac{\delta^4(\lambda_1 \tilde{\lambda}_1 + \lambda_2 \tilde{\lambda}_2 + \lambda_3 \tilde{\lambda}_3) \delta^4([12] \tilde{\eta}_3 + [23] \tilde{\eta}_1 + [31] \tilde{\eta}_2)}{[12][23][31]}.$$

The MHV amplitude $A_{3,2}$ constrains $\tilde{\lambda}_1 \propto \tilde{\lambda}_2 \propto \tilde{\lambda}_3$, while the $\overline{\text{MHV}}$ amplitude $A_{3,1}$ enforces $\lambda_1 \propto \lambda_2 \propto \lambda_3$. Even though they are not physical, these amplitudes play an important role for the techniques presented in the following. In particular we will use a graphical notation, denoting them by black and white vertices,

$$\begin{array}{c} 1 \\ | \\ \bullet \\ / \quad \backslash \\ 3 \quad 2 \end{array} = A_{3,2}(1, 2, 3), \quad \begin{array}{c} 1 \\ | \\ \circ \\ / \quad \backslash \\ 3 \quad 2 \end{array} = A_{3,1}(1, 2, 3). \quad (2.34)$$

2.3 On-shell techniques

We next discuss some on-shell techniques for the calculation of scattering amplitudes: BCFW recursion relations, their generalization to all loop-orders in planar $\mathcal{N}=4$ SYM, and the generalized unitarity method.

BCFW recursion relations

The discovery of the BCFW recursion relations,¹⁹ which we present here in their supersymmetric version,²⁰ marked a milestone in the renewed interest in methods to determine the S-matrix directly, exploiting its analytic properties. The idea behind this method is to make use of the universal factorization behavior of scattering amplitudes, which is made manifest in their representation in terms of Feynman diagrams, via the tools of complex analysis.

Consider some color-ordered amplitude at tree-level. Although the recursion relations aim at calculating without using Feynman diagrams, the existence of a representation in terms of these diagrams implies that the amplitude factorizes into two sub-amplitudes whenever a propagator in one of these diagrams diverges because the momentum flowing through it hits the mass shell. Since we are considering partial amplitudes which impose a cyclic order on the external momenta, this only happens when the sum of a number of consecutive momenta has vanishing norm. The aim of the BCFW recursion relations is to exploit this universal behavior in order to reconstruct the full amplitude from the set of these

¹⁹ Britto, Cachazo, Feng, “New recursion relations for tree amplitudes of gluons”, [hep-th/0412308](#); and Britto, Cachazo, Feng, Witten, “Direct proof of tree-level recursion relation in Yang-Mills theory”, [hep-th/0501052](#)

²⁰ Brandhuber, Heslop, Travaglini, “A Note on dual superconformal symmetry of the $\mathcal{N} = 4$ super Yang-Mills S-matrix”, [0807.4097](#); Arkani-Hamed, Cachazo, Kaplan, “What is the Simplest Quantum Field Theory?”, [0808.1446](#); and Elvang, Freedman, Kiermaier, “Recursion Relations, Generating Functions, and Unitarity Sums in $\mathcal{N} = 4$ SYM Theory”, [0808.1720](#)

factorization channels, which only involve amplitudes with fewer legs. To access the factorization poles in a controlled way, the momenta have to be complexified; this allows to perform a shift on two of the momenta,

$$\begin{aligned} \hat{\lambda}_i &= \lambda_i - \alpha \lambda_j, & \hat{\tilde{\lambda}}_i &= \tilde{\lambda}_i, & \hat{\eta}_i &= \tilde{\eta}_i, \\ \hat{\lambda}_j &= \lambda_j, & \hat{\tilde{\lambda}}_j &= \tilde{\lambda}_j + \alpha \tilde{\lambda}_i, & \hat{\eta}_j &= \tilde{\eta}_j + \alpha \tilde{\eta}_i, \end{aligned} \quad (2.35)$$

which simultaneously respects momentum conservation and preserves the on-shell condition, $\hat{p}_i^2 = \hat{p}_j^2 = 0$. In the following we indicate that this shift has been performed on some quantity by hats, i.e. for $f = f(\lambda, \tilde{\lambda}, \tilde{\eta})$, we denote $\hat{f} = f(\hat{\lambda}, \hat{\tilde{\lambda}}, \hat{\tilde{\eta}})$. We furthermore assume that the particles i and j are adjacent in the color ordering, $j = i + 1$.

If this shift is applied to a scattering amplitude, the undeformed amplitude can be recovered by a contour integral around zero

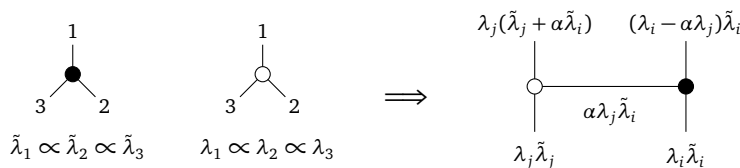
$$A_{n,k} = \oint_{\alpha=0} \frac{\hat{A}_{n,k}(\alpha)}{\alpha}. \quad (2.36)$$

The basic idea of the BCFW recursion is to use the residue theorem to write the integral as a sum over the residues of all other poles of $\hat{A}_{n,k}$ in the complex α plane. But every such pole corresponds precisely to a factorization channel. Because the momenta are massless and the shift (2.35) preserves this property, it follows that all possible propagators which contain either \hat{p}_i or \hat{p}_j are linear functions of α ; if both momenta appear, the propagator is independent of α since $\hat{p}_i + \hat{p}_j = p_i + p_j$. If we denote a propagator depending on the shift by $\frac{1}{\hat{p}_I^2}$, where I refers to the set of momenta, $P_I = \sum_{i \in I} p_i$, then one can furthermore easily see that $\text{Res}_{\hat{p}_I^2=0} \frac{1}{\hat{p}_I^2} = \frac{1}{P_I^2}$. Therefore, we can write the amplitude as a sum over all factorization channels which separate particles i and j :

$$A_{n,k} = \sum_{\text{factorization channels}} \hat{A}_L \frac{1}{P_I^2} \hat{A}_R. \quad (2.37)$$

In each term, α is fixed to the value which renders $\hat{p}_I^2 = 0$. Of course for each distribution of external momenta, this sum also includes a sum over intermediate particle states. Furthermore we assume that the shifted amplitude has no pole at $\alpha \rightarrow \infty$. For $\mathcal{N}=4$ SYM, this is the case for adjacent shifts $j = i \pm 1$; for other cases see for example Henn and Plefka (2014).²¹

Before we write down the super BCFW recursion relations in their explicit form, we note that the shift (2.35) can be realized via the so-called BCFW bridge, which is composed of the three-point amplitudes. Recalling that kinematically, $A_{3,2}$ enforces the collinearity of the $\tilde{\lambda}$ variables and $A_{3,1}$ the collinearity of the λ 's, we see that the bridge, shown in figure 2.2, precisely implements the shift (2.35).



21 Henn, Plefka, "Scattering Amplitudes in Gauge Theories", *Lect. Notes Phys.* 883 (2014) pp.1–195

Figure 2.2: The BCFW bridge.

This bridge is to be attached via super phase space integrations to the factorized amplitude. It then provides the integration $\int \frac{d\alpha}{\alpha}$, remaining as a part of the phase space integrations not fixed by kinematic constraints:

$$\begin{array}{c} \dots \\ \text{---} \end{array}
 \left(\text{Diagram of amplitude } f \text{ with a bridge between two legs} \right)
 = \int \frac{d\alpha}{\alpha}
 \left(\text{Diagram of amplitude } \hat{f} \text{ with a bridge between two legs} \right)
 \dots
 \quad (2.38)$$

In the recursion relation (2.37), this integral is fixed term by term via the on-shell condition of the propagator on which the amplitude factorizes. We can thus write the recursion relations for $\mathcal{N}=4$ SYM in the form

$$A_{n,k} = \sum_{\substack{n',n'',k',k'' \\ n'+n''=n+2 \\ k'+k''=k+1}} \left(\text{Diagram of } A_{n',k'} \text{ and } A_{n'',k''} \text{ connected by a bridge} \right)
 \quad (2.39)$$

One of the successes of the BCFW recursion relations was their solution in closed form.²² This yielded compact expressions for all $\mathcal{N} = 4$ SYM tree amplitudes which in particular include all gluon amplitudes as components.

All loop recursion

In the discussion above we have seen that tree-level amplitudes are determined by their singularities, i.e. by their sets of possible factorizations. The BCFW bridge, applied to the entire set of these singularities can be understood as a way of lifting them, i.e. to produce a function with precisely these singularities, that is the amplitude.

At least for planar $\mathcal{N} = 4$ SYM, a similar statement can be made at loop level. Of course, the full amplitude has a complicated analytic structure, but its integrand, which can be uniquely defined for planar amplitudes using the dual momenta as discussed in section 2.1, is a rational function determined by the Feynman rules, just like tree-level amplitudes. Indeed, ℓ -loop $\mathcal{N} = 4$ SYM amplitude integrands are completely determined by so called forward limits, in addition to the possible factorization channels.²³ These forward limits correspond to a loop-momentum going on-shell, and thus to single cuts of amplitudes. On these cuts, the amplitude is determined by the $\ell - 1$ loop amplitude with two more legs carrying opposite on-shell momenta $\pm p_l$ with $p_l^2 = 0$.

Similar to the factorizations at tree-level, these singularities can be lifted by the BCFW bridge. This leads to the all-loop recursion relations²⁴

²² Drummond, Henn, "All tree-level amplitudes in $\mathcal{N} = 4$ SYM", 0808.2475

²³ Caron-Huot, "Loops and trees", 1007.3224

²⁴ Arkani-Hamed, Bourjaily, Cachazo, Caron-Huot, Trnka, "The All-Loop Integrand For Scattering Amplitudes in Planar $\mathcal{N} = 4$ SYM", 1008.2958; and Arkani-Hamed, Bourjaily, Cachazo, Goncharov, Postnikov, Trnka, "Scattering Amplitudes and the Positive Grassmannian", Cambridge University Press, 2016, 1212.5605

$$\begin{aligned}
 A_{n,k}^{(\ell)} = & \text{Diagram 1} + \sum_{\substack{n',n'',k',k'',\ell',\ell'' \\ n'+n''=n+2 \\ k'+k''=k+1 \\ \ell'+\ell''=\ell-1}} \text{Diagram 2}, \\
 \end{aligned}
 \tag{2.40}$$

where the first term is the forward limit of the $\ell - 1$ loop amplitude, and the other terms are channels where the amplitude factorizes into products of lower loop amplitudes, with loop numbers $\ell' + \ell'' = \ell$. We see that this equation generalizes the BCFW recursion (2.39), where the first term is absent.²⁵

Generalized Unitarity

Generalized unitarity²⁶ is one of the most successful modern techniques for loop calculations. It is based on a completely different idea compared to the classical unitary method, but still employs cuts to reconstruct the full amplitude. These cuts are taken by replacing propagators in the loop integrals by delta functions which force the momentum flowing through the propagator to become on-shell, with positive energy,²⁷

$$i \frac{1}{p^2} \longrightarrow 2\pi \delta(p^2) \theta(p^0). \tag{2.41}$$

This can also be understood as considering the real and four-dimensional loop integration as a contour integral in \mathbb{C}^4 , and choosing a torus contour around the pole of the propagator.

For theories in four dimensions, only four types of scalar integrals can appear in Feynman diagram calculation at one loop: the box, the triangle, the bubble and the tadpole. This is a consequence of the fact that all momenta in the propagators can be expanded in terms of four linearly independent momentum vectors.²⁸ All of these integrals have been calculated in closed form.²⁹ We can therefore write any one-loop amplitude in this basis of master integrals I_t ,

$$A_n^{(1)} = \sum_{\substack{t \in \text{topologies} \\ i \in \text{assignments} \\ \text{of momenta}}} c_{t,i} I_{t,i} + \text{rational terms}. \tag{2.42}$$

The rational, i.e. branch-cut-free terms appear due to the need to regularize the integrals, and are absent for supersymmetric theories. For $\mathcal{N}=4$ SYM amplitudes, only box integrals contribute, and there are no rational terms. The idea is now to fix the coefficients $c_{t,i}$, which are rational functions of the external kinematics, by applying cuts (2.41) to both sides of this equation.

First consider the box integral. The four propagators have the loop momentum shifted by cyclic sets of the external momenta. For each possible such set, we can apply the four corresponding cuts (2.41), which localizes the integral

25 We remark that the way the loop integrations appear in this recursion is subtle, see footnote 36 below; therefore the recursion should rather be thought of as a recursion of the loop integrand.

26 Bern, Dixon, Dunbar, Kosower, “One loop n point gauge theory amplitudes, unitarity and collinear limits”, [hep-ph/9403226](#); Bern, Dixon, Dunbar, Kosower, “Fusing gauge theory tree amplitudes into loop amplitudes”, [hep-ph/9409265](#); and Britto, Cachazo, Feng, “Generalized unitarity and one-loop amplitudes in $\mathcal{N} = 4$ super-Yang-Mills”, [hep-th/0412103](#)

27 Often the notation $\delta^+(p^2) = \delta(p^2)\theta(p^0)$ is used for this combination.

28 In dimensional regularization, also pentagon integrals contribute, see Bern, Dixon, Kosower, “Dimensionally regulated pentagon integrals”, [hep-ph/9306240](#).

29 't Hooft, Veltman, “Scalar One Loop Integrals”, *Nucl. Phys. B*153 (1979) 365–401

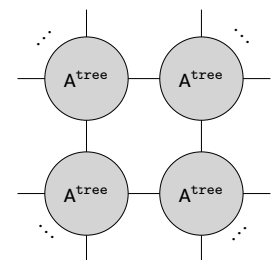


Figure 2.3: The leading singularity of a one-loop amplitude.

30 One might have to sum over multiple solutions to the equations imposed by the cuts.

31 Bern, Carrasco, Dixon, Johansson, Roiban, “The Ultraviolet Behavior of N=8 Supergravity at Four Loops”, 0905.2326

32 Bern, Carrasco, Johansson, Kosower, “Maximally supersymmetric planar Yang–Mills amplitudes at five loops”, 0705.1864

33 Bourjaily, Herrmann, Trnka, “Prescriptive Unitarity”, 1704.05460

34 These edges are undirected since the $\mathcal{N}=4$ on-shell multiplet is CPT self-conjugate.

completely.³⁰ The left hand side of (2.42) is then given by a product of tree amplitudes; schematically we can draw them as in figure 2.3. These cuts in which all loop integrations are localized, are called leading singularities. On the right hand side only one term contributes, given in terms of the cut of the master integral, and this fixes the corresponding coefficient. For $\mathcal{N}=4$ SYM amplitudes, fixing all box coefficients is sufficient. For other theories, or other quantities in $\mathcal{N}=4$ SYM, one can continue to determine the coefficients of the triangle and bubble integrals. Since the contributions from the integrals with more propagators, which can have the same triple or lower cuts, are already known, triple cuts are sufficient for the triangle coefficients, and double cuts for the bubbles.

The method is extremely efficient, even beyond one-loop. A noteworthy application is the program of checking the finiteness of $\mathcal{N}=8$ supergravity.³¹ For a higher-loop application in $\mathcal{N}=4$ SYM, see for example Bern et al. (2007).³² We finally note that the method continues to be developed and improved, see e.g. Bourjaily et al. (2017).³³

2.4 On-shell diagrams

On-shell diagrams provide a graphical language for the quantities and techniques discussed so far. They are graphs with two types of vertices, representing the two three-point amplitudes, which are drawn as black and white vertices as in equation (2.34). The internal edges³⁴ represent on-shell phase space integrations over intermediate states of the form (2.13),

$$\int \frac{d^2\lambda d^2\tilde{\lambda}}{\text{Vol}[GL(1)]} d^4\tilde{\eta}. \tag{2.43}$$

Here the “Vol[GL(1)]” shorthand notation indicates that the integration is only over spinor-helicity variables which are inequivalent under the little group scaling (2.6).

Scattering amplitudes, as well as many related quantities, can be expressed via these diagrams. Consider the BCFW recursion relations for tree amplitudes, given in equation (2.39); by fully recursing this equation, we end up with a sum of terms only involving three-point amplitudes, i.e. on-shell diagrams. The simplest example is the four-point amplitude, which can be written as

$$A_{4,2} = \begin{array}{c} \text{---} \circ \text{---} \\ | \quad | \\ \text{---} \bullet \text{---} \end{array} \begin{array}{c} \text{---} \bullet \text{---} \\ | \quad | \\ \text{---} \circ \text{---} \end{array} = \begin{array}{c} \text{---} \bullet \text{---} \\ | \quad | \\ \text{---} \circ \text{---} \end{array} \begin{array}{c} \text{---} \circ \text{---} \\ | \quad | \\ \text{---} \bullet \text{---} \end{array} \tag{2.44}$$

Note that in the recursion relations, $A_{3,1}$ cannot appear on the left side, and $A_{3,2}$ not on the right side of the factorization, since these terms would have constrained kinematics, see the discussion after equation (2.33). Therefore, the four-point amplitude is given by a single diagram, sometimes called a “box”.

An example where the recursion generates multiple terms is given by the six-point NMHV amplitude,

$$\begin{aligned}
 A_{6,3} &= \begin{array}{c} \text{Diagram 1} \\ \parallel \\ \text{Diagram 2} \\ \parallel \\ \text{Diagram 3} \end{array} + \begin{array}{c} \text{Diagram 4} \\ \parallel \\ \text{Diagram 5} \\ \parallel \\ \text{Diagram 6} \end{array} + \begin{array}{c} \text{Diagram 7} \\ \parallel \\ \text{Diagram 8} \\ \parallel \\ \text{Diagram 9} \end{array} \\
 &= \begin{array}{c} \text{Diagram 10} \\ + \\ \text{Diagram 11} \\ + \\ \text{Diagram 12} \end{array}
 \end{aligned}
 \tag{2.45}$$

The all-loop recursion (2.40) leads to on-shell diagrams representing loop amplitudes. As an example we consider the four-point one-loop amplitude. According to the recursion, it is given by

$$A_{4,2}^{(1)} = \begin{array}{c} \text{Diagram 1} \\ = \\ \text{Diagram 2} \\ = \\ \text{Diagram 3} \end{array}
 \tag{2.46}$$

Note that there are no factorization channels contributing in this case, since the three-point amplitudes do not receive quantum corrections. Therefore the only term comes from the forward limit. Of the three terms in (2.45) only one is non-vanishing in this limit.³⁵ The second equality follows from equivalence moves which will be discussed below, and the resulting diagram makes it obvious that the maximal cut is given by the box diagram (2.44), the four-point tree amplitude. To this end, note that the “bubbles” correspond to loop integrations, as will be explained shortly.³⁶

Finally, it is evident that any leading singularities appearing in the generalized unitarity method can be expressed by on-shell diagrams; this follows from simply representing the occurring tree amplitudes as on-shell diagrams. Due to the all-loop recursion, even non-maximal cuts can be drawn as a diagram.

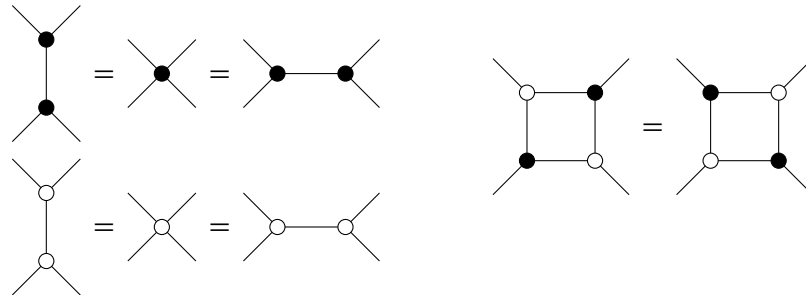
35 Arkani-Hamed, Bourjaily, Cachazo, Goncharov, Postnikov, Trnka, “Scattering Amplitudes and the Positive Grassmannian”, Cambridge University Press, 2016, [1212.5605](#)

36 We remark already here that the precise way in which these bubbles are related to the loop integrations is very subtle. The bubbles define the integrand in terms of integration variables which very different from the components of the loop momenta and, to our knowledge, there is no known way of determining the contour of integration for them.

Equivalence moves

The analytic functions encoded by on-shell diagrams are invariant under certain diagrammatic equivalence moves, which are shown in figure 2.4.

Figure 2.4: Equivalence moves for on-shell diagrams.



The first two moves are called “merge-unmerge”; they are based on the observation that each black vertex, representing the three-point MHV amplitude (2.34), enforces the collinearity of the anti-holomorphic spinors $\tilde{\lambda}_i$ of its external legs (and similar for the $\tilde{\eta}_i$), while any white vertex, i.e. any three-point $\overline{\text{MHV}}$ amplitude forces the holomorphic spinors λ_i to be collinear. Thus, if two (or more) vertices of the same color are directly connected, they can be merged into a single vertex which represents the combined constraint that all four external legs obey the corresponding collinearity condition. Unmerging the vertex into two three-valent vertices with a different assignment of external legs then gives the first two moves presented in figure 2.4.

The third move (often called “box move”) is simply the diagrammatic statement that the four-point amplitude is cyclicly invariant.

There is a further move, which does not strictly represent an equivalence. If a “bubble” as shown in figure 2.5 is present, the full diagram encodes the same expression as the diagram where the bubble is deleted, times a dlog integration which factors out. Diagrams free of such bubbles (in any representation obtainable from the equivalence moves described above) are called reduced.

Figure 2.5: A bubble corresponds to an integration which factors out of the expression.

$$\text{---} \circ \text{---} = \left(\int \frac{d\alpha}{\alpha} \right) \times \text{---}$$

Permutations

On-shell diagrams are in one-to-one correspondence with permutations

$$\sigma = \begin{pmatrix} 1 & 2 & 3 & \dots & n \\ \downarrow & \downarrow & \downarrow & \dots & \downarrow \\ \sigma(1) & \sigma(2) & \sigma(3) & \dots & \sigma(n) \end{pmatrix} \equiv (\sigma(1), \sigma(2), \sigma(3), \dots, \sigma(n)). \quad (2.47)$$

The relation implies that for each diagram the associated permutation encodes the same information as the diagram itself. The exact correspondence can be obtained using so-called left-right paths: For every external particle, draw a path entering the diagram at the leg corresponding to that particle and turning right at every black vertex and left at every white vertex:³⁷

37 Arkani-Hamed, Bourjaily, Cachazo, Goncharov, Postnikov, Trnka, “Scattering Amplitudes and the Positive Grassmannian”, Cambridge University Press, 2016, 1212.5605

$$\begin{array}{c} 1 \\ \nearrow \searrow \\ \bullet \\ \nwarrow \nearrow \\ 3 \quad 2 \end{array} \rightarrow \sigma = (3, 1, 2), \quad \begin{array}{c} 1 \\ \nearrow \searrow \\ \circ \\ \nwarrow \nearrow \\ 3 \quad 2 \end{array} \rightarrow \sigma = (2, 3, 1). \quad (2.48)$$

If the path ends on particle j , set $\sigma(i) = j$. The permutation associated to a given on-shell diagram is invariant under the equivalence moves in figure 2.4 and therefore encodes the same information as the diagram.³⁸

In the reverse direction, a representative on-shell diagram can be constructed from the permutation as follows. First, the permutation is decomposed into a product of transpositions, where the multiplication corresponds to the right action, i.e.

$$\sigma_1 \triangleleft \sigma_2 = (\sigma_2(\sigma_1(1)), \dots, \sigma_2(\sigma_1(n))). \quad (2.49)$$

This sequence should be of minimal length, but is not unique, due to the equivalence moves. It is possible to consider only adjacent transpositions.³⁹ Second, each such transposition (i, j) is interpreted as a BCFW bridge,

$$\begin{array}{c} | \\ \circ \\ | \\ j \end{array} \text{ --- } \begin{array}{c} | \\ \bullet \\ | \\ i \end{array}, \quad (2.50)$$

connecting the legs i and j . One can then build up the diagram by stacking these bridges on top of each other, and removing the legs at the top. This construction will be discussed in greater detail in chapter 7, where it will be related to integrability.

2.5 The Graßmannian integral

We have seen that a remarkable range of quantities related to scattering amplitudes can be represented as on-shell diagrams. A unifying description for the analytic expressions these diagrams encode can be given in terms of an integral over an auxiliary Graßmannian $G(k, n)$, the set of k -planes in n -dimensional space.

The geometry of momentum conservation and the Graßmannian

The fundamental idea behind the Graßmannian integral representations of on-shell diagrams is to understand momentum conservation in a geometric way.⁴⁰ The n massless momenta which define the external data of a scattering process are represented by the spinors λ_i^α and $\tilde{\lambda}_i^{\dot{\alpha}}$. Instead of viewing this data as a set of n pairs of two-vectors, they can be thought of as two two-dimensional planes in \mathbb{C}^n : the first plane is spanned by the n -vectors $\lambda^1 = (\lambda_1^1, \dots, \lambda_n^1)$ and $\lambda^2 = (\lambda_1^2, \dots, \lambda_n^2)$, and similar for the variables $\tilde{\lambda}_i^{\dot{\alpha}}$. From this point of view, momentum

³⁸ Although it does not play a key role in the following, we remark here that one should really associate a so-called *decorated permutation* with $i \leq \sigma(i) \leq i + n$ to each diagram. The additional information encoded by the label i with $\sigma(i) > n$ has some impact on the decomposition into BCFW bridges mentioned below.

³⁹ These statements follow from the properties of the corresponding permutation group; note in particular that even decompositions into only adjacent transpositions are not unique.

⁴⁰ Arkani-Hamed, Cachazo, Cheung, Kaplan, "A Duality For The S Matrix", 0907.5418

conservation is expressed as the orthogonality of these planes:

$$0 = \sum_{i=1}^n \lambda_i \tilde{\lambda}_i = \lambda \cdot \tilde{\lambda}. \quad (2.51)$$

This interpretation opens the possibility to linearize this constraint, i.e. to impose separate constraints on the two types of spinors. To this end, one introduces an auxiliary k -plane C . The space of such k -planes in \mathbb{C}^n is the Grassmannian $G(k, n)$. Each point in this space can be represented by a $k \times n$ matrix C of full rank; the rows of this matrix are n -vectors that span the plane. Of course this set of vectors is not unique: left multiplication of C by any $GL(k)$ matrix just rotates the vectors into each other and rescales them, leaving the plane invariant. The fact that the two-planes λ and $\tilde{\lambda}$ are orthogonal can then be phrased as the requirement that $\tilde{\lambda}$ is orthogonal to the k -plane C , while λ is contained in it. The latter requirement is equivalent to saying that λ is orthogonal to the orthogonal complement of C , which can be represented by a $(n-k) \times n$ matrix C^\perp fulfilling $C(C^\perp)^T = 0$.⁴¹ We can thus write momentum conservation as

$$(C \cdot \tilde{\lambda})_I^{\dot{\alpha}} = \sum_{i=1}^n C_{Ii} \tilde{\lambda}_i^{\dot{\alpha}} = 0 \quad \text{and} \quad (C^\perp \cdot \lambda)_J^\alpha = \sum_{i=1}^n C_{Ji}^\perp \lambda_i^\alpha = 0, \quad (2.52)$$

where $I = 1, \dots, k$ and $J = 1, \dots, n-k$. Note that these equations constrain both the kinematics as well as the plane C . Although we focused on the momentum, a similar argument can be made for the supermomentum; for it to be conserved, we need to further impose $C \cdot \tilde{\eta} = 0$.

The Grassmannian integral is based on the idea that scattering amplitudes can be written in a way which uses these constraints. The k -plane C is only an auxiliary object, and it turns out that one has to average over all possible planes subject to the constraints. We can thus introduce the Grassmannian integral as

$$\int \frac{d^{k \times n} C}{\text{Vol}[GL(k)]} \Omega_{n,k} \delta^{2 \times k}(C \cdot \tilde{\lambda}) \delta^{4 \times k}(C \cdot \tilde{\eta}) \delta^{2 \times (n-k)}(C^\perp \cdot \lambda) \quad (2.53)$$

where we integrate over all matrices C which are not related by a $GL(k)$ transformation.⁴² The integrand $\Omega_{n,k}$ indeed does only depend on the plane C and not on the kinematical data – in a sense, the integral therefore separates the dynamics from the kinematics. Counting the powers of the Grassmann variables, we see that the integral over $G(k, n)$ will give the amplitude $A_{n,k}$, as discussed below. The contour of integration is left unspecified in this equation.

We will discuss in a moment the form $\Omega_{n,k}$ appearing in the integral (2.53). Two simple examples are already given by the three-point amplitudes,

$$A_{3,2}(1, 2, 3) = \int \frac{d^{2 \times 3} C}{\text{Vol}[GL(2)]} \frac{1}{(12)(23)(31)} \delta^4(C \cdot \tilde{\lambda}) \delta^8(C \cdot \tilde{\eta}) \delta^2(C^\perp \cdot \lambda), \quad (2.54)$$

$$A_{3,1}(1, 2, 3) = \int \frac{d^{1 \times 3} C}{\text{Vol}[GL(1)]} \frac{1}{(1)(2)(3)} \delta^2(C \cdot \tilde{\lambda}) \delta^4(C \cdot \tilde{\eta}) \delta^4(C^\perp \cdot \lambda). \quad (2.55)$$

which can easily be seen to give the expressions in equation (2.33). Here and in the following we denote the $k \times k$ minors of the matrix C by parentheses, with labels indicating the columns, i.e. $(i_1, \dots, i_k) = \det(C_{i_1}, \dots, C_{i_k})$.

41 Of course the matrix C^\perp is not unique given C ; this does not matter in the following.

42 In practice this integration over inequivalent matrices can be achieved by “fixing the gauge”, i.e. by setting k columns of C to orthogonal unit k -vectors.

Graßmannian integral for general diagrams

For general on-shell diagrams, a Graßmannian integral formula as given in (2.53) could be obtained by “gluing” the Graßmannian formulas (2.54) and (2.55) for each three-point amplitude vertex, i.e. by performing the phase space integrations (2.43) for all internal edges.⁴³ Although these formulas simplify this task by linearizing the constraints on the external kinematics, there are more direct ways of constructing the Graßmannian integral.

The method we briefly describe makes use of edge variables α_i to parametrize the matrix C . As their name suggests, they are naturally associated to edges of the on-shell diagram. In fact, they are the variables parametrizing the BCFW shifts (2.35) induced by the bridges (see figure 2.2) into which the diagram can be decomposed as outlined in section 2.4 and described in more detail in section 7.5, where we discuss the relation of this construction to integrability. In principle one can therefore obtain a Graßmannian integral representation from such a decomposition.

A method which does not directly refer to a particular decomposition of the diagram makes use of so-called boundary measurements. First give the on-shell diagram a perfect orientation: assign an orientation to each edge such that each white vertex is connected to one incoming and two outgoing edges and each black vertex to two incoming and one outgoing edges. Then attach a variable α_e to each edge e . For every vertex, one of the variables of the connected edges can be removed. Under the perfect orientation graph will have k “sources” and $n - k$ “sinks”, where n is the number of particles and k the MHV degree. The columns of the C matrix corresponding to the k sinks are given by $C_{is} = \delta_{is}$ for each sink s . The remaining entries are fixed as follows: for each source i and sink j set the entry of the C matrix

$$C_{ij} = - \sum_{\text{paths } \Gamma \text{ from } i \text{ to } j} \prod_{\text{edges } e \in \Gamma} \alpha_e, \quad (2.56)$$

where any closed directed loops are summed as geometric series, $\sum_{\text{loop}} \prod_e \alpha_e = (1 - \prod_e \alpha_e)^{-1}$. The Graßmannian integral (2.53) is then given by

$$\int \prod_{i=1}^m \frac{d\alpha_i}{\alpha_i} \delta^{2 \times k}(C(\alpha) \cdot \tilde{\lambda}) \delta^{4 \times k}(C(\alpha) \cdot \tilde{\eta}) \delta^{2 \times (n-k)}(C^\perp(\alpha) \cdot \lambda), \quad (2.57)$$

where m is the number of edge variables.

The top-form

The C matrices associated to on-shell diagrams constructed by this method, or rather their equivalence classes, correspond to the cells of the positroid stratification⁴⁴ of the positive Graßmannian. This sub-manifold of the Graßmannian $G_+(k, n) \subset G(k, n)$ is the restriction to the points for which all minors of the C matrix of the form $(i_1 \cdots i_k)$ for $i_1 < \cdots < i_k$ are positive. The residue of the integral (2.57) at $\alpha_e = 0$ gives the integral representation of the diagram obtained from

⁴³ Arkani-Hamed, Bourjaily, Cachazo, Goncharov, Postnikov, Trnka, “Scattering Amplitudes and the Positive Grassmannian”, Cambridge University Press, 2016, [1212.5605](#)

⁴⁴ Postnikov, “Total positivity, Grassmannians, and networks”, [math/0609764](#); and Knutson, Lam, Speyer, “Positroid Varieties: Juggling and Geometry”, [1111.3660](#)

the original diagram by removing edge e . The corresponding C matrix describes a co-dimension one boundary of the original cell in the Grassmannian.

There is a unique top-form, of dimension $k \times (n - k)$, corresponding to the entire positive Grassmannian, of which the integrals of all other diagrams with given k and n can be obtained by taking residues. Since it is top-dimensional, it can directly be expressed in terms of the entries of the C matrix, without a special parametrization. Due to the $GL(k)$ invariance, it only involves the $k \times k$ minors of this matrix, and is given by

$$\mathcal{G}_{n,k} = \int \frac{d^{k \times n} C}{\text{Vol}[GL(k)]} \frac{\delta^{2 \times k}(C \cdot \tilde{\lambda}) \delta^{4 \times k}(C \cdot \tilde{\eta}) \delta^{2 \times (n-k)}(C^\perp \cdot \lambda)}{(1 \cdots k)(2 \cdots k+1) \cdots (n-1 \cdots k-2)(n \cdots k-1)}. \quad (2.58)$$

Without derivation, we also give the Grassmannian integral in the other variables introduced in section 2.1. Under the half-Fourier transformation (2.14) the integral transforms into

$$\mathcal{G}_{n,k}^{\mathcal{W}} = \int \frac{d^{k \times n} C}{\text{Vol}[GL(k)]} \frac{\delta^{(4|4) \times k}(C \cdot \mathcal{W})}{(1 \cdots k)(2 \cdots k+1) \cdots (n-1 \cdots k-2)(n \cdots k-1)}. \quad (2.59)$$

Here superconformal symmetry is made manifest by the $\mathfrak{sl}_{4|4}$ invariance of the delta functions. The change of variables to momentum twistor variables allows to factor the MHV amplitude (2.29) out of (2.58), such that one is left with an integral of the same form as (2.59), but over the Grassmannian $G(k-2, n)$,⁴⁵

$$\mathcal{G}_{n,k} = A_{n,2} \int \frac{d^{(k-2) \times n} C}{\text{Vol}[GL(k-2)]} \frac{\delta^{(4|4) \times (k-2)}(C \cdot \mathcal{Z})}{(1 \cdots k-2)(2 \cdots k-1) \cdots (n-1 \cdots k-4)(n \cdots k-3)}. \quad (2.60)$$

In each case, the Grassmannian integral can be used to calculate the corresponding scattering amplitude; however it needs to be supplemented by a contour for the unfixed integration variables, which picks out a correct combination of residues.

While the review in this chapter has focused entirely on scattering amplitudes in $\mathcal{N} = 4$ SYM, many of the tools presented here are more widely applicable. The BCFW recursion relations were originally formulated for gluon-amplitudes in pure Yang-Mills theories, but are available for many theories. General unitarity can in principle be applied to any perturbative calculation in any quantum field theory. On-shell diagrams and Grassmannian integrals were discussed for theories with less supersymmetry in Benincasa and Gordo (2016); Benincasa (2015),⁴⁶ and for gravity in Heslop and Lipstein (2016); Herrmann and Trnka (2016).⁴⁷ There has also been some work on nonplanar on-shell diagrams, which will be discussed from the viewpoint of their (Yangian) symmetries in chapter 9, see the references there.

In the next chapters we will extend these developments to another class of quantities in $\mathcal{N} = 4$ SYM, form factors of composite operators.

⁴⁵ Arkani-Hamed, Cachazo, Cheung, “The Grassmannian Origin Of Dual Superconformal Invariance”, 0909.0483; and Elvang, Huang, Keeler, Lam, Olsson, Roland, Speyer, “Grassmannians for scattering amplitudes in 4d $\mathcal{N} = 4$ SYM and 3d ABJM”, 1410.0621

⁴⁶ Benincasa, Gordo, “On-shell diagrams and the geometry of planar $N < 4$ SYM theories”, 1609.01923; and Benincasa, “On-shell diagrammatics and the perturbative structure of planar gauge theories”, 1510.03642

⁴⁷ Heslop, Lipstein, “On-shell diagrams for $\mathcal{N} = 8$ supergravity amplitudes”, 1604.03046; and Herrmann, Trnka, “Gravity On-shell Diagrams”, 1604.03479

3

On-shell diagrams for form factors

In the last chapter we saw that on-shell diagrams provide a compact and useful representation for scattering amplitudes, and a graphical language for modern methods to calculate them. Form factors describe the overlap of asymptotic on-shell multi-particle states with states created by composite operators. They are thus a class of quantities which interpolate amplitudes, which are purely on-shell and can be understood as the form factor of the identity operator, and off-shell objects involving multiple composite operators, in particular their correlation functions.

In this chapter we show that form factors can – just as amplitudes – systematically be represented by on-shell diagrams. This will allow to derive a Graßmannian integral representation for them in the next chapter, showing that this framework can be extended to other quantities. In later chapters these diagrams will also be the our starting point for the development of integrability approaches to form factors.

We first briefly discusses form factors in general (section 3.1), and those of the chiral stress-tensor multiplet in particular (section 3.2). We will almost exclusively focus on super form factors of this multiplet, which are the most widely studied form factors in $\mathcal{N}=4$ SYM. In section 3.3 we will show how on-shell diagram representations for form factors can be developed from the BCFW recursion relations. After discussing inverse soft limits in section 3.4, which are a feature these diagrams share with their amplitude counterparts, we will derive a useful relation to amplitude diagrams in section 3.6. This relation allows to find “top-cell” diagrams, which will be used to derive the Graßmannian integral. In contrast to amplitudes, one has to consider many such diagrams, as will be shown in section 3.7. Finally, we discuss several ways in which the relation between on-shell diagrams and (decorated) permutations can be extended to this setting (section 3.8).

*This chapter is based on
the author's publication
Frassek, Meidinger, Nandan, Wilhelm,
“On-shell diagrams, Graßmannians
and integrability for form factors”,
1506.08192.*

3.1 Form factors

Form factors are a generalization of scattering amplitudes. They are defined as the overlap of an n -particle asymptotic on-shell state with the state created by a gauge invariant composite operator \mathcal{O} at space-time point x out of the vacuum,

$$\hat{\mathcal{F}}_{\mathcal{O},n}(x) = {}_{\text{out}}\langle 1, \dots, n | \mathcal{O}(x) | 0 \rangle_{\text{in}}. \quad (3.1)$$

Intuitively, form factors can be interpreted as the amplitude of the decay of the state created by the operator \mathcal{O} into these n particles. This definition generalizes scattering amplitudes, cf. (2.23), which are the form factors of the identity operator. Note that $\hat{\mathcal{F}}_{\mathcal{O},n}(x) = \exp(i \sum_{j=1}^n p_j \cdot x) \hat{\mathcal{F}}_{\mathcal{O},n}(0)$ due to translation invariance. We will exclusively work with the Fourier transform

$$\mathcal{F}_{\mathcal{O}}(q) = \int d^4x e^{-iqx} \hat{\mathcal{F}}_{\mathcal{O}}(x) = (2\pi)^4 \delta^4\left(\sum_{i=1}^n p_i - q\right) \hat{\mathcal{F}}_{\mathcal{O}}(0), \quad (3.2)$$

where the operators carries momentum q . Since the operator is a color singlet, the color structure of tree-level form factors is given by the following expression

$$\mathcal{F}_{\mathcal{O},n} = g^{n-L} \sum_{\sigma \in S_n/Z_n} \text{Tr}(T^{a_{\sigma(1)}} \dots T^{a_{\sigma(n)}}) F_{\mathcal{O},n}(\sigma(1), \dots, \sigma(n)). \quad (3.3)$$

where L is the length of the operator,¹ $g = \frac{\sqrt{\lambda}}{4\pi}$, and $F_{\mathcal{O},n}$ is called the color-ordered form factor, cf. equation (2.26) for the amplitude case. As for amplitudes, at loop level also multi-trace terms contribute, but are $1/N$ suppressed.

From the perspective of Feynman diagrams, form factors are calculated similarly to amplitudes, but include an additional multi-valent vertex stemming from Wick contraction with the fields inside the operator. The presence of the operator induces UV divergences (which are absent for amplitudes in $\mathcal{N} = 4$ SYM). These are directly related to the renormalization of the operator, and thus to the spectral problem and operator mixing. In fact, the calculation of anomalous dimensions are usually performed by calculating the divergences of form factor integrals, which are simpler than two-point functions. For $\mathcal{N} = 4$ SYM, form factors were first studied in van Neerven (1986).²

From the viewpoint of effective field theory, the vertex induced by the operator models interactions arising from unobserved UV degrees of freedom. A well-known example is the Higgs-to-gluon-gluon amplitude: Since the gluons are massless, the dominant contribution to this process comes from a top quark loop. At low energies, this amplitude is given by the form factor of the operator $\text{tr} F_{SD}^2$, with F_{SD} the self dual field strength.³ In fact, this form factor is a component of the $\mathcal{N} = 4$ SYM form factor which we will study in the following: We will consider the chiral stress-tensor multiplet, which contains the on-shell Lagrangian, including the standard Yang-Mills term.

Furthermore, form factors can appear via the OPE in processes which include nonperturbative, confined states, as is the case in deep inelastic scattering,⁴ and in the calculation of event shapes, for calculations in $\mathcal{N} = 4$ SYM see for example

¹ In the following we will only consider single-trace operators, and the length L is simply the number of fields in the color trace.

² van Neerven, "Infrared Behavior of On-shell Form-factors in a $\mathcal{N} = 4$ Supersymmetric Yang-Mills Field Theory", *Z. Phys.* C30 (1986) 595

³ Wilczek, "Decays of Heavy Vector Mesons Into Higgs Particles", *Phys. Rev. Lett.* 39 (1977) 1304; and Shifman, Vainshtein, Zakharov, "Remarks on Higgs Boson Interactions with Nucleons", *Phys. Lett.* B78 (1978) 443-446

⁴ For an calculation in $\mathcal{N} = 4$ SYM, see Bianchi, Forini, Kotikov, "On DIS Wilson coefficients in $\mathcal{N} = 4$ super Yang-Mills theory", 1304.7252.

Belitsky et al. (2014); Engelund and Roiban (2013).⁵ Finally, form factors play an important role in the description of the universal IR behavior of Yang-Mills amplitudes. Reviews of this topic can be found in Gardi (2014).⁶

In $\mathcal{N}=4$ SYM, the study of form factors has largely focused on tree-level form factors, but recently a lot of progress has been made at loop level, in particular due to the use of the generalized unitarity method (see section 2.3).⁷ A particularly exciting development is the inclusion of composite operators and their form factors in the framework of the twistor space action⁸ which was initiated in the works Koster et al. (2016a,b, 2017).⁹ At strong coupling, form factors have been studied via the AdS/CFT correspondence.¹⁰

3.2 The chiral stress-tensor multiplet

In this chapter, as well as in chapters 4, 5, and partially in chapters 8 and 10, we will consider only form factors of the chiral part of the stress-tensor supermultiplet, which are the ones most widely studied in the literature.

Describing this multiplet in a manifestly supersymmetric way will be a main ingredient for our constructions. Using $\mathcal{N}=4$ harmonic superspace,¹¹ this can be done while staying very close to the formulation of on-shell amplitudes in terms of (super) spinor-helicity variables. In this formulation, the coordinate space Grassmann variables θ_α^A , $\alpha = 1, 2$, $A = 1, \dots, 4$, are projected to + and – components by matrices u_A^{+a} and $u_A^{-a'}$ with $a, a' = 1, 2$:

$$\theta_\alpha^{+a} = \theta_\alpha^A u_A^{+a}, \quad \theta_\alpha^{-a'} = \theta_\alpha^A u_A^{-a'}, \quad (3.4)$$

where the indices a, a' and \pm correspond to the subgroup $SU(2) \times SU(2)' \times U(1)$ of the R symmetry group $SU(4)$. The multiplet can then be written as¹²

$$T(x, \theta^+) = \text{tr}(\phi^{++} \phi^{++}) + \dots + \frac{1}{3}(\theta^+)^4 \mathcal{L}. \quad (3.5)$$

This operator is chiral as it only depends on the θ^+ , and it contains the scalar BPS operator $\text{tr}(\phi^{++} \phi^{++})$ with $\phi^{++} = \frac{1}{2} \epsilon_{ab} u_A^{+a} u_B^{+b} \phi^{AB}$ as the lowest and the on-shell Lagrangian \mathcal{L} as its highest component.

The super form factor of this supermultiplet is defined as

$$F_{n,k}(1, \dots, n; q, \gamma^-) = \int d^4x d^4\theta^+ e^{-iqx - i\theta_\alpha^{+a} \gamma_a^-} \langle 1, \dots, n | T(x, \theta^+) | 0 \rangle_{\text{in}}, \quad (3.6)$$

where γ^{-aa} denotes the supermomentum of the multiplet and k is the super MHV degree, which ranges from $k = 2$ up to $k = n$. For the minimal MHV degree $k = 2$, the form factor of $T(x, \theta^+)$ is given by a Parke-Taylor-type expression which is almost identical to the corresponding formula for MHV amplitudes,

$$F_{n,2}(1, \dots, n; q, \gamma^-) = \frac{\delta^4(P) \delta^4(Q^+) \delta^4(Q^-)}{\langle 12 \rangle \langle 23 \rangle \dots \langle n-1 n \rangle \langle n1 \rangle}, \quad (3.7)$$

where the conserved (super) momenta are defined by

$$P = \sum_{i=1}^n \lambda_i \tilde{\lambda}_i - q, \quad Q^+ = \sum_{i=1}^n \lambda_i \tilde{\eta}_i^+, \quad Q^- = \sum_{i=1}^n \lambda_i \tilde{\eta}_i^- - \gamma^-. \quad (3.8)$$

- 5 Belitsky, Hohenegger, Korchemsky, Sokatchev, Zhiboedov, “From correlation functions to event shapes”, [1309.0769](#); and Engelund, Roiban, “Correlation functions of local composite operators from generalized unitarity”, [1209.0227](#)
- 6 Gardi, “Infrared singularities in multi-leg scattering amplitudes”, [1407.5164](#)
- 7 Gehrmann, Henn, Huber, “The three-loop form factor in $\mathcal{N}=4$ super Yang-Mills”, [1112.4524](#); Nandan, Siegel, Wilhelm, Yang, “Cutting through form factors and cross sections of non-protected operators in $\mathcal{N}=4$ SYM”, [1410.8485](#); Loebbert, Nandan, Siegel, Wilhelm, Yang, “On-Shell Methods for the Two-Loop Dilatation Operator and Finite Remainders”, [1504.06323](#); and Loebbert, Siegel, Wilhelm, Yang, “Two-Loop $SL(2)$ Form Factors and Maximal Transcendentality”, [1610.06567](#)
- 8 Adamo, “Twistor actions for gauge theory and gravity”, PhD thesis, Cambridge U., DAMTP, 2013, [1308.2820](#),
- 9 Koster, Mitev, Staudacher, Wilhelm, “Composite Operators in the Twistor Formulation of $\mathcal{N}=4$ Supersymmetric Yang-Mills Theory”, [1603.04471](#); Koster, Mitev, Staudacher, Wilhelm, “All tree-level MHV form factors in $\mathcal{N}=4$ SYM from twistor space”, [1604.00012](#); and Koster, Mitev, Staudacher, Wilhelm, “On Form Factors and Correlation Functions in Twistor Space”, [1611.08599](#)
- 10 Alday, Maldacena, “Comments on gluon scattering amplitudes via AdS/CFT”, [0710.1060](#); Maldacena, Zhiboedov, “Form factors at strong coupling via a Y-system”, [1009.1139](#); and Gao, Yang, “Y-system for form factors at strong coupling in AdS_5 and with multi-operator insertions in AdS_3 ”, [1303.2668](#)
- 11 Hartwell, Howe, “(N, p, q) harmonic superspace”, [hep-th/9412147](#)
- 12 Our conventions follow the works Eden, Heslop, Korchemsky, Sokatchev, “The super-correlator/super-amplitude duality: Part I”, [1103.3714](#); Brandhuber, Gurdogan, Mooney, Travaglini, Yang, “Harmony of Super Form Factors”, [1107.5067](#); and Bork, “On form factors in $\mathcal{N}=4$ SYM theory and polytopes”, [1407.5568](#). We refer the reader to these articles for details and further references.

Here the Graßmann degrees of freedom of the on-shell particles are again related to the usual ones by a projection,

$$\begin{aligned} Q^{+a\alpha} &= \bar{u}_A^{+a} Q^{A\alpha} & \tilde{\eta}^{+a} &= \bar{u}_A^{+a} \tilde{\eta}^A \\ Q^{-a'\alpha} &= \bar{u}_A^{-a'} Q^{A\alpha} & \tilde{\eta}^{-a'} &= \bar{u}_A^{-a'} \tilde{\eta}^A, \end{aligned} \tag{3.9}$$

and the projectors \bar{u} are the conjugates of the u 's.

From (3.7) we see that for our purposes, using harmonic superspace simply amounts to distinguishing between two types of components of Graßmann variables, and the sole difference will be that the operator T carries supermomentum only in half of the directions, corresponding to the “minus” variables. Otherwise, all the techniques and formulations that rely on spinor-helicity variables λ , $\tilde{\lambda}$ and $\tilde{\eta}$ can straightforwardly be adapted to the current setting.

Note that for brevity and unless otherwise stated, we will often use the term “form factor” to denote a color-ordered tree-level form factor of the chiral part of the stress-tensor multiplet, in what follows.

3.3 From BCFW to on-shell diagrams

Form factors of the chiral stress tensor multiplet obey BCFW recursion relations that express them in terms of their factorization channels as¹³

$$F_{n,k} = \sum_{\substack{n',n'',k',k'' \\ n'+n''=n+2 \\ k'+k''=k+1}} \left(\text{Diagram 1} + \text{Diagram 2} \right). \tag{3.10}$$

Here we already used a diagrammatic language as in section 2.3 implementing the BCFW shift by a “bridge”. We indicate the off-shell kinematics of the operator by a doubled line in these diagrams. The most noteworthy distinction to the amplitude case is that we have to sum over contributions with the operator on either side of the factorization.

For every form factor $F_{n,k}$ we can use these relations recursively to get a representation in terms of a sum of diagrams which only involve amplitudes and form factors with the lowest number of on-shell legs. Apart from the three-point amplitudes $A_{3,2}$ and $A_{3,1}$ which are the only vertices for amplitude on-shell diagrams (cf. section 2.4),

$$\begin{aligned} \text{Diagram 1} &= A_{3,2} = \frac{\delta^4(\lambda_1 \tilde{\lambda}_1 + \lambda_2 \tilde{\lambda}_2 + \lambda_3 \tilde{\lambda}_3) \delta^8(\lambda_1 \tilde{\eta}_1 + \lambda_2 \tilde{\eta}_2 + \lambda_3 \tilde{\eta}_3)}{\langle 12 \rangle \langle 23 \rangle \langle 31 \rangle}, \\ \text{Diagram 2} &= A_{3,1} = \frac{\delta^4(\lambda_1 \tilde{\lambda}_1 + \lambda_2 \tilde{\lambda}_2 + \lambda_3 \tilde{\lambda}_3) \delta^4([\!12\!] \tilde{\eta}_3 + [\!23\!] \tilde{\eta}_1 + [\!31\!] \tilde{\eta}_2)}{[\!12\!] [\!23\!] [\!31\!]}. \end{aligned} \tag{3.11}$$

¹³ See Brandhuber, Spence, Travaglini, Yang, “Form Factors in $\mathcal{N} = 4$ Super Yang–Mills and Periodic Wilson Loops”, 1011.1899, and Brandhuber, Gurdogan, Mooney, Travaglini, Yang, “Harmony of Super Form Factors”, 1107.5067 for the supersymmetric version we use.

the minimal (two-point MHV) form factor appears as a third basic vertex:

$$\begin{array}{c} \parallel \\ \diagup \quad \diagdown \\ 2 \quad \quad 1 \end{array} = F_{2,2} = \frac{\delta^4(\lambda_1 \tilde{\lambda}_1 + \lambda_2 \tilde{\lambda}_2 - q) \delta^4(\lambda_1 \tilde{\eta}_1^+ + \lambda_2 \tilde{\eta}_2^+) \delta^4(\lambda_1 \tilde{\eta}_1^- + \lambda_2 \tilde{\eta}_2^- - \gamma^-)}{\langle 12 \rangle \langle 21 \rangle}. \tag{3.12}$$

In principle, these diagrams can directly be evaluated using the expressions for the MHV subdiagrams and performing the phase-space integration. In chapter 4, however, we will derive a Grassmannian integral representation which greatly facilitates the calculation. Before we turn to these questions of how to evaluate the diagrams, we will discuss some of their properties which manifest themselves on a diagrammatic level. This will also serve to present a range of example diagrams. We will start with the inverse-soft constructibility of certain form factor diagrams.

3.4 Inverse soft limits

Just like MHV amplitudes, MHV form factors can be constructed by attaching so called k -preserving inverse soft factors, shown in figure 3.1, to the diagram with one external leg less.

The inverse soft factor guarantees the correct behavior when particle i becomes soft: for example, when acting on MHV form factors or amplitudes, the inverse soft factor simply multiplies the original expression with a factor $\langle i-1 \ i+1 \rangle / (\langle i-1 \ i \rangle \langle i \ i+1 \rangle)$ while appropriately adjusting the (super) momentum conserving delta functions. Some MHV form factor diagrams exhibiting this structure are shown in figure 3.2.

Note that in the recursion relations, one can choose different positions for the BCFW bridges while recursing to lower and lower point amplitudes; diagrammatically this translates into the statement that the position at which each inverse soft factor is attached can be arbitrary. This can also be understood from the fact that all form factors are cyclicly invariant, in particular the MHV-sub-diagrams appearing in the diagrams of higher point form factors, cf. figure 3.2. Therefore these sub-diagrams can be rotated, keeping the rest of the diagram fixed. This leaves the form factor (3.7) unchanged.

The other extreme are so called N^{\max} MHV form factors, i.e. those with $k = n$. In contrast to $\overline{\text{MHV}}$ amplitudes, these are not related to their MHV counterparts by parity, since the operator itself would transform under such a conjugation. Nevertheless, these form factors have the property that they can be represented by single diagrams. According to the recursion relations (3.10), these are constructed by attaching k -increasing inverse soft factors, shown in figure 3.3, to the minimal form factor. Again, the position at which they placed is arbitrary. As an example, the on-shell diagram of the form factor $F_{4,4}$ is shown in figure 3.4.

We note that it has been shown in Nandan and Wen (2012)¹⁴ – without using the language of on-shell diagrams, that all tree-level amplitudes and form factors can recursively be constructed using only these two types of inverse soft factors.

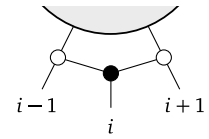


Figure 3.1: k -preserving inverse soft factor.

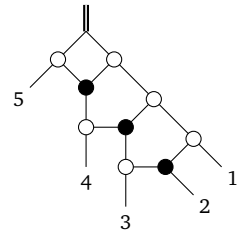
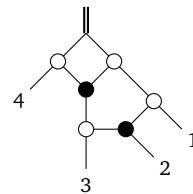
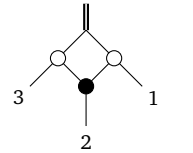


Figure 3.2: The on-shell diagrams for the MHV form factors $F_{3,2}$, $F_{4,2}$ and $F_{5,2}$ (top to bottom).

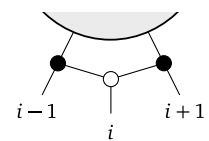


Figure 3.3: k -increasing inverse soft factor.

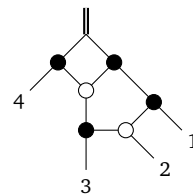


Figure 3.4: The on-shell diagrams for the N^{\max} MHV form factor $F_{4,4}$.

14 Nandan, Wen, “Generating All Tree Amplitudes in $\mathcal{N} = 4$ SYM by Inverse Soft Limit”, 1204.4841

3.5 Cyclicity and equivalence moves

For pure on-shell diagrams, equivalence classes of diagrams are generated by the set of moves presented in figure 2.4 on page 30. While it is clear that these moves can also be applied to form factor on-shell diagrams, yielding diagrams with same analytic expression, the question arises whether these moves are enough to transform any such form factor diagram into any equivalent one.

While we leave the analytic evaluation of these diagrams in terms of Graßmannian integrals to the following chapter, we can use the fact that form factors are cyclicly invariant (i.e. invariant under cyclic relabellings of the external on-shell legs) in order to see that further moves are required. The simplest such cases are the two three-point form factors; their cyclic invariance implies that

$$\begin{aligned}
 & \begin{array}{c} \text{Diagram 1} \\ \text{Diagram 2} \end{array} = \begin{array}{c} \text{Diagram 3} \\ \text{Diagram 4} \end{array} = \begin{array}{c} \text{Diagram 5} \\ \text{Diagram 6} \end{array}, \\
 & \begin{array}{c} \text{Diagram 7} \\ \text{Diagram 8} \end{array} = \begin{array}{c} \text{Diagram 9} \\ \text{Diagram 10} \end{array} = \begin{array}{c} \text{Diagram 11} \\ \text{Diagram 12} \end{array}.
 \end{aligned}
 \tag{3.13}$$

We can consider these identities whenever such three-point form factors appear as subdiagrams of a larger diagram. The fact that the diagrams obtained by rotating these subdiagrams are equivalent is not manifest a priori; we are therefore led to consider the identities (3.13) as new equivalence moves. Note that they appear in a similar way as the box move for amplitudes, which likewise expresses the fact that the “smallest” amplitude with a non-trivial on-shell diagram is cyclicly invariant.

Although we do not have a general proof,¹⁵ we suspect that similar to the case of the box move, the three-point moves (3.13), together with the known ones for amplitude diagrams are complete, in the sense that they are enough to generate all equivalence relations.¹⁶ In figure 3.5, we exemplify this for the case of the four-point MHV form factor, showing its cyclic invariance. We first use the merge/unmerge and box moves, and in the last step rotate the three-point form factor sub-diagram. The same argument applies recursively to all MHV and N^{\max} MHV form factor diagrams, and shows that diagrams obtained by cyclic relabeling are equivalent, on a diagrammatic level.

3.6 A relation to amplitude diagrams

The striking parallels between on-shell diagrams for amplitudes and for form factors suggest to look for a mapping between the two which will allow to recycle known results concerning the former into new results for the latter. Effectively, we are looking for a mapping which replaces the minimal form factor by some amplitude, or vice versa.

¹⁵ Proving this statement is complicated by the fact that the correspondence of diagrams to permutations breaks down for form factors, see section 3.8 below.

¹⁶ In passing we note that the moves (3.13) and the equivalence classes they generate, such as cyclic rotations of any MHV diagrams, can result in diagrams which are nonplanar, in the sense that the minimal form factor is inserted inside the diagram. We will come back to this observation when we discuss the integrability properties of form factors and nonplanar on-shell diagrams in chapters 7, 9 and 10.

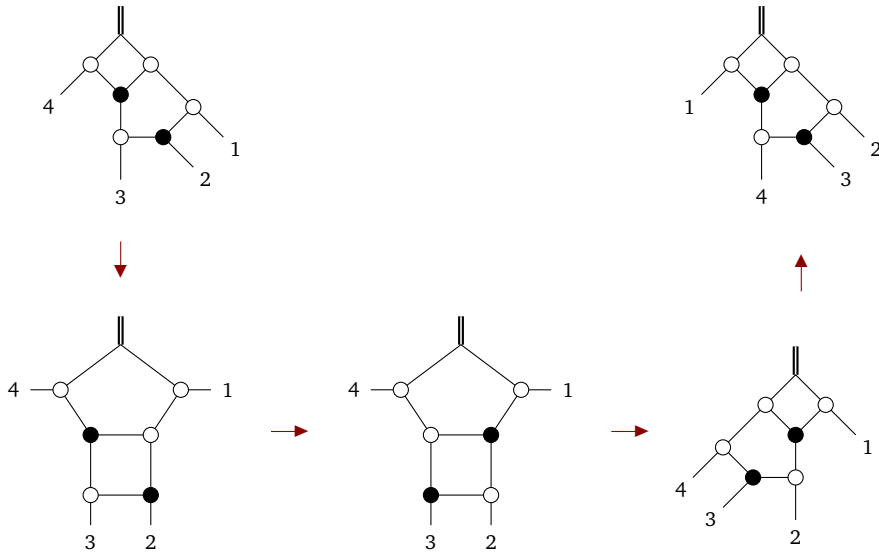


Figure 3.5: Diagrammatic proof of the cyclic invariance of the four-point MHV form factor using the equivalence moves of amplitude on-shell diagrams and rotating the three-point form factor sub-diagram.

In order to preserve the Graßmann degree, the corresponding amplitude should be of MHV type; noting that in contrast to the two three-point amplitudes, the minimal form factor can appear as a factor on both sides of the BCFW factorization in (3.10), we see that the minimal choice is to relate it to the four-point amplitude:

$$(3.14)$$

While (3.14) does not imply a general relation between full amplitudes and full form factors, it will be extremely useful in what follows.

Indeed, recursing the relations (3.10) down to MHV amplitudes and form factors, i.e. to individual on-shell diagrams, we see that every diagram contributing to the form factor $F_{n,k}$, can be turned into a BCFW term of the $n + 2$ point amplitude $A_{n+2,k}$ upon replacing the minimal form factor by a four-point amplitude. This implies that all possible BCFW terms descend from *top-cell diagrams*, which are related to the corresponding amplitude top-cell diagrams by (3.14):

$$(3.15)$$

$\text{TopCell}(A_{n,k})$
 $\text{TopCell}(F_{n,k})$

This relation will allow us to derive the Graßmannian integral representation for form factors in the next chapter, making use of the corresponding representation

for amplitudes. We will see that the relations (3.14) and (3.15) also preserve the number of degrees of freedom in the Grassmannian, motivating the use of the term “top-cell” for these diagrams.¹⁷

Besides making it possible to get the Grassmannian top-form via a shortcut, the correspondence (3.14) will turn out to be a valuable tool also for the determination of the “contour” for form factors – the combination of (multivariable) poles in the Grassmannian top-form that combine into the correct tree-level form factor, which will be explored in chapter 5.

¹⁷ We use the term “top-cell diagram” in a slightly heuristic way. It solely refers to the fact that the Grassmannian form related to the diagram is top dimensional, but does mean that these forms necessarily have an interpretation in terms of some stratification. Due to the relation (3.15), we nevertheless find this nomenclature appropriate.

3.7 Multiple top-cell diagrams

A very important difference to amplitude on-shell diagrams is the fact that there are multiple “top-cell” diagrams, i.e. diagrams that – as we will elaborate in chapter 4 – correspond to top-dimensional integrals in the Grassmannian.

According to the relation (3.15), we can generate such diagrams, for each number of external legs n and MHV degree k , by taking the amplitude top-cell diagram with $n + 2$ legs and the same MHV degree, and replacing a box diagram at two arbitrary neighboring legs by the minimal form factor. The amplitude top-cell diagram is not only unique for given n and k , it is also cyclicly invariant. By replacing $A_{4,2} \rightarrow F_{2,2}$ at two particular, neighboring external legs, we break this cyclicity. This means that there are precisely n top-cell diagrams. They are related to each other by cyclic shifts of the labels of the external on-shell states.

While we leave the analytic evaluation of the diagrams for the next chapter, where we will explicitly see that any single such diagram (except for the cases $k = 2$ and $k = n$ of course) is not cyclic in its on-shell legs, we state already here that also from the current viewpoint, these diagrams are not related by the moves in figure 2.4 and equation (3.13), and therefore the different top-cell diagrams are really inequivalent.

Consider for example the case of the four-point NMHV form factor. Two of its top-cell diagrams are given in figure 3.6 and the other two can be obtained by cyclicly rotating the labels 1, 2, 3 and 4. From (3.10) we see that the actual form factor consists of four terms under the BCFW decomposition:

$$F_{4,3} = A_i + B_i + C_i + D_i . \quad (3.16)$$

Here the terms correspond to the factorization channels

$$\begin{aligned} A_i: & \quad F_{2,2} \times A_{4,2} \\ B_i: & \quad A_{4,2} \times F_{2,2} \\ C_i: & \quad F_{3,3} \times A_{3,1} \\ D_i: & \quad A_{3,2} \times F_{3,2} \end{aligned} \quad (3.17)$$

with BCFW shifts at legs i and $i + 1$.

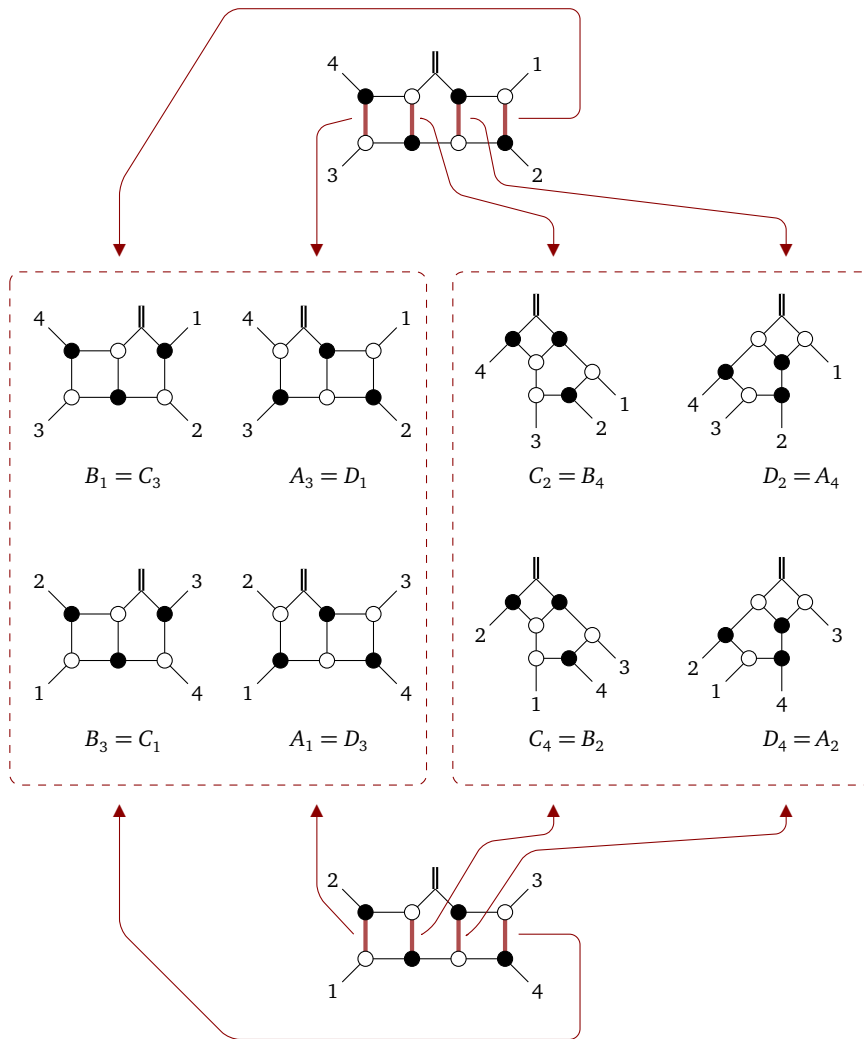


Figure 3.6: Two top-cell diagrams for the form factor $F_{4,3}$. The deletable edges are marked, and the BCFW terms that can be obtained by removing them are shown. The dashed boxes combine terms that together form a BCFW representation of the form factor. There are two more top-cell diagram which generate the same terms in different combinations.

Drawing the corresponding diagrams and using the equivalence moves given in figure 2.4 and equation (3.13) one can see that the following relations between different terms hold:

$$A_i = D_{(i+2) \bmod 4}, \quad B_i = C_{(i+2) \bmod 4}. \quad (3.18)$$

Just as for the six-point NMHV amplitude from which the top-cell diagrams were generated in figure 3.6 using the relation (3.15), the BCFW terms correspond to co-dimension one residues of the top-dimensional Graßmannian integral (which we will present in the next chapter) and can thus be obtained by deleting single edges from the top-cell diagrams. As it turns out, one needs two top-cell diagrams to obtain all four terms; these are shown in figure 3.6, where the deletable edges are marked. Removing them, four possible BCFW terms can be obtained, two of which have to be combined with two other ones from the top-cell diagram with labels shifted by two.

In general, even more top-cell diagrams are needed, and the combinatorics become more intricate; we will present a complete analysis for all NMHV form factors in chapter 5.

3.8 Permutations

Amplitude on-shell diagrams are associated to (decorated) permutations, as we described in section 2.4. The permutation is equivalent to the diagram and encodes the same information. Moreover, it relates the diagram to the positroid stratification and gives a direct link to the geometry of the Graßmannian. Can something similar be said of form factor on-shell diagrams? A priori, one can think of multiple ways of assigning permutations to these diagrams. We will describe them here, and they will all play a role in subsequent chapters.

If we want to read off a permutation from a form factor diagram using the left-right paths of amplitude diagrams as in section 2.4, we need a prescription for the paths running into the minimal form factor. A natural choice is to turn back in this situation:

$$\begin{array}{c} \parallel \\ \swarrow \quad \searrow \\ 2 \quad \quad 1 \end{array} \rightarrow \sigma = (1, 2). \tag{3.19}$$

This rule allows to deduce a permutation for form factor top-cell diagrams. According to (3.15), they are obtained from the amplitude top-cell diagram with two more legs and associated permutation

$$\text{TopCell}(A_{n+2,k}) : \quad \sigma = (k + 1, \dots, n, n + 1, n + 2, 1, 2, \dots, k). \tag{3.20}$$

If we again focus on the case where the minimal form factor is inserted at position $n + 1$ and $n + 2$ using (3.15), then (3.19) leads to the following permutation:

$$\text{TopCell}(F_{n,k}) : \quad \sigma = (k + 1, \dots, n, k - 1, k, 1, 2, \dots, k - 2). \tag{3.21}$$

This type of permutation (not only of top-cell diagrams) will be an important ingredient for the integrability construction in chapter 8, and for the proof of integrability related symmetries.

However, this type of permutation is not enough to specify the diagram. We will describe the construction of diagrams by decomposing permutations into transpositions which then give a sequence of BCFW bridges that result in the diagram in chapter 8. Here we just note that for example, one of the top-cell diagrams of the four-point NMHV form factor shown in figure 3.6 has the permutation $(4, 2, 3, 1)$. The decomposition which leads to the correct diagram is given by $(1, 2) \triangleleft (3, 4) \triangleleft (2, 3) \triangleleft (1, 2) \triangleleft (3, 4)$, which is *not minimal*. A non-minimal decomposition is needed to generate enough degrees of freedom in the Graßmannian. In a way this is similar to the on-shell diagrams of amplitude loop integrands.

Another way of assigning a permutation to a given form factor diagram is to remove the minimal form factor, and then to use the permutation of the resulting on-shell diagram with $n + 2$ legs. Together with the knowledge at which legs the minimal form factor has to be glued in, this is sufficient to construct the diagram. For the top-cell diagram with the minimal form factor at legs $n + 1$ and $n + 2$ the corresponding permutation of the on-shell part of the diagram is given by

$$\text{TopCell}(F_{n,k}) \text{ without } F_{2,2} : \quad \tilde{\sigma} = (k+1, \dots, n, n+2, n+1, 1, 2, \dots, k, k-1). \tag{3.22}$$

The permutation $\tilde{\sigma}$ is furthermore useful, in that it allows to generate a Graßmannian integral representation of this on-shell part, as discussed in section 4.2. This will be very useful for the derivation of the Graßmannian integral for form factors in section 4.3.

3.9 Leading singularities and on-shell functions

Although our focus is on on-shell diagrams for tree-level form factors, it is important to mention that of course, in more generality, on-shell diagrams which include the minimal form factor also represent leading singularities of loop-level form factors.

As an example, consider the diagram in figure 3.7. It is the coefficient of the one-loop triangle integral, when calculating the minimal, i.e. two-point, one-loop form factor. In fact, this integral is the only contribution to this form factor since the stress-tensor is protected, and bubble integrals are UV divergent.¹⁸ By considering the number of delta functions in the constituent parts of this diagram, and the number of phase space integrations, we see that this diagram has one unfixed integration, as is appropriate for a triple cut of a one-loop integral.

Since we now know that all tree-level form factors can be represented via on-shell diagrams, it follows that all leading singularities are given in terms of diagrams which only involve three-point amplitudes and the minimal form factor.

We often will consider arbitrary on-shell diagrams built from the three-point amplitudes (3.11) and the minimal form factor (3.12) without regarding their potential interpretation as (BCFW terms of) tree-level form factors, leading singularities or other cuts of loop integrands, or any other physical quantity. In this context we refer to the analytic expressions they represent as *on-shell functions*.

It is natural to also consider on-shell diagrams which contain the minimal tree-level form factor of other operators, in particular component operators instead of full multiplets. So far, no super BCFW recursion relations have been published for such general operators, and it is very likely that such recursion relations require supermultiplets. While this means that it is unclear whether general tree-level form factors can be represented by on-shell diagrams, some of these diagrams are leading singularities of the respective loop-level form factors, and thus of considerable interest. We will come back to this larger class of on-shell diagrams when we study their relation to integrability in section 8.4.

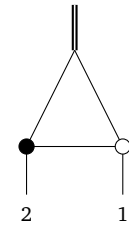


Figure 3.7: Triple cut of the minimal one-loop form factor represented as an on-shell diagram.

¹⁸ Gehrmann, Henn, Huber, “The three-loop form factor in $\mathcal{N} = 4$ super Yang-Mills”, [1112.4524](#)

4

Form factors as Graßmannian integrals

Amplitude on-shell diagrams are deeply connected to the Graßmannian integral representation of scattering amplitudes, as briefly summarized in chapter 2. The strikingly similar diagrammatic structure of form factors we just described raises the question whether there is a corresponding analytic expression for them. The aim of this chapter is to present such an integral formula.

We will first consider the kinematical question of how to accommodate the off-shell momentum q of the operator in the way the Graßmannian integral linearizes momentum conservation, cf. section 2.5. Parametrizing it in terms of two on-shell momenta, we find that the integral will naturally be one over the Graßmannian $G(k, n + 2)$, for MHV degree k and n external on-shell states. After showing how to “glue” the minimal form factor of the chiral stress-tensor multiplet onto arbitrary on-shell diagrams in section 4.2, we will then use the relation (3.15) to do this for the top-forms in section 4.3 obtaining the main result of this chapter: a general expression for the form factor Graßmannian integral, given in equation (4.25), which we furthermore express in twistor, and novel momentum twistor variables. To check our result, and to show that it can indeed be used for the efficient calculation of tree-level form factors, we calculate a variety of examples in section 4.5 and compare them to results in the literature.

The results presented here mark a first step towards a Graßmannian, or geometric, formulation for more general quantities, and in particular to those involving off-shell kinematics. There is some progress in this direction, see for example the papers Bork and Onishchenko (2017a,b),¹ which applied similar arguments as those presented here to obtain a Graßmannian integral representation for amplitudes involving off-shell gluons.

This chapter is based on the author’s publication Frassek, Meidinger, Nandan, Wilhelm, “On-shell diagrams, Graßmannians and integrability for form factors”, 1506.08192.

¹ Bork, Onishchenko, “Wilson lines, Grassmannians and gauge invariant off-shell amplitudes in $\mathcal{N} = 4$ SYM”, 1607.02320; and Bork, Onishchenko, “Grassmannian integral for general gauge invariant off-shell amplitudes in $\mathcal{N} = 4$ SYM”, 1610.09693

4.1 Graßmannian geometry and the off-shell momentum

Before setting out to construct a Graßmannian integral for form factors, it is useful to set up convenient conventions for the kinematics. The Graßmannian integral nicely separates these kinematics, encoded in the delta functions, from the “dynamical” content of the differential form on the Graßmannian. This will allow us to focus on the latter when doing the actual calculations, leading to the Graßmannian integral for form factors.

The Graßmannian integral linearizes momentum (and super momentum) conservation by expressing – schematically – $\delta(P) = \delta(\lambda \cdot \tilde{\lambda})$ as $\delta(C \cdot \tilde{\lambda})\delta(C^\perp \cdot \lambda)$. This means that momentum conservation, which can be regarded as the orthogonality of spinor-helicity variables λ and $\tilde{\lambda}$, seen as two-planes in \mathbb{C}^n , is replaced by the requirement that $\tilde{\lambda}$ is orthogonal to an auxiliary k -plane C , while λ is contained in it, as described in more detail in section 2.5. Note that this geometric picture is only viable for on-shell momenta, which factor into spinors. We therefore propose to parametrize the off-shell momentum in terms of two on-shell momenta,²

$$-q = \lambda_{n+1} \tilde{\lambda}_{n+1} + \lambda_{n+2} \tilde{\lambda}_{n+2}. \quad (4.1)$$

Of course, this parametrization is redundant; the off-shell momentum q has four degrees of freedom, while the two on-shell momenta together have 8, 6 of which are physical, and two corresponding to unfixed little group scaling. Instead of fixing some degrees of freedom, we choose to put the redundancy entirely into the holomorphic spinors λ by setting them to arbitrary non-collinear reference spinors ξ_A and ξ_B . This determines the $\tilde{\lambda}$ in terms of these spinors and the actual momentum q . The full kinematic setup for n on-shell particles and the operator insertion is then given by the following set of variables, which we will distinguish from the original variables by underlining them:

$$\begin{aligned} \underline{\lambda}_i &= \lambda_i, \quad i = 1, \dots, n, \quad \underline{\lambda}_{n+1} = \xi_A, \quad \underline{\lambda}_{n+2} = \xi_B, \\ \underline{\tilde{\lambda}}_i &= \tilde{\lambda}_i, \quad i = 1, \dots, n, \quad \underline{\tilde{\lambda}}_{n+1} = -\frac{\langle \xi_B | q}{\langle \xi_B \xi_A \rangle}, \quad \underline{\tilde{\lambda}}_{n+2} = -\frac{\langle \xi_A | q}{\langle \xi_A \xi_B \rangle}. \end{aligned} \quad (4.2)$$

Analogously, we can decompose the supermomentum as follows

$$\begin{aligned} \underline{\tilde{\eta}}_i^+ &= \tilde{\eta}_i^+, \quad i = 1, \dots, n, \quad \underline{\tilde{\eta}}_{n+1}^+ = 0, \quad \underline{\tilde{\eta}}_{n+2}^+ = 0, \\ \underline{\tilde{\eta}}_i^- &= \tilde{\eta}_i^-, \quad i = 1, \dots, n, \quad \underline{\tilde{\eta}}_{n+1}^- = -\frac{\langle \xi_B | \gamma^-}{\langle \xi_B \xi_A \rangle}, \quad \underline{\tilde{\eta}}_{n+2}^- = -\frac{\langle \xi_A | \gamma^-}{\langle \xi_A \xi_B \rangle}. \end{aligned} \quad (4.3)$$

Note that in these expressions, we introduced the notation $(\langle \xi | q)^{\dot{\alpha}} = \varepsilon_{\beta\alpha} \xi^\beta q^{a\dot{\alpha}}$.

The preceding discussion suggests that the Graßmannian integral for form factors with n external on-shell states should be one over the Graßmannian $G(k, n+2)$. This is in line with the observation (3.14) which relates the minimal form factor to the four-point amplitude (with two more external legs), and in particular with the possible MHV degrees of form factors: While the amplitude A_n has components $A_{n,k}$ with $k = 2, \dots, n-2$, the component with maximal

² Recall that we define the momentum of the operator to be “incoming”, hence the minus sign. See section 3.2 and in particular equation (3.8).

MHV degree is $F_{n,n}$ for an n -point form factor. Integrals over $G(k, n+2)$ are non-singular precisely in this range. We use the underlined variables (4.2) and (4.3) to unambiguously refer to the entire set of on-shell variables for $n+2$ “particles”, and linearize the constraint imposed by (super) momentum conservation by requiring $C \cdot \tilde{\lambda} = 0$, $C \cdot \tilde{\eta} = 0$ and $C^\perp \cdot \lambda = 0$ with $C \in G(k, n+2)$.

4.2 Gluing the operator into on-shell diagrams

To calculate Grassmannian integral representations for form factor on-shell diagrams, we can use the fact that apart from a single insertion of the minimal form factor, they are the same as amplitude on-shell diagrams. Instead of constructing the Grassmannian representation “from scratch”, by gluing together all the Grassmannians corresponding to the three-point vertices and the minimal form factor, we can therefore use the known representation of these parts and combine them. Here, we will develop this procedure for general diagrams; the important case of top-cell diagrams will then be discussed in section 4.3.

Considering some diagram, we start by decomposing it into the minimal form factor $F_{2,2}$ given in (3.12), and the rest of the diagram, which is purely on-shell and has $n+2$ legs, see figure 4.1 For the purpose of the following calculations it is convenient to write the minimal form factor (3.12) as

$$F_{2,2}(1, 2) = \delta^2\left(\tilde{\lambda}_1 - \frac{\langle 2|q\rangle}{\langle 21\rangle}\right) \delta^2\left(\tilde{\eta}_1^- - \frac{\langle 2|\gamma^-}{\langle 21\rangle}\right) \delta^2(\tilde{\eta}_1^+) \delta^2\left(\tilde{\lambda}_2 - \frac{\langle 1|q\rangle}{\langle 12\rangle}\right) \delta^2\left(\tilde{\eta}_2^- - \frac{\langle 1|\gamma^-}{\langle 12\rangle}\right) \delta^2(\tilde{\eta}_2^+) \quad (4.4)$$

which can easily be verified.³

The on-shell part has the following integral representation:

$$I_{\text{on-shell}} = \int \frac{d\alpha_1}{\alpha_1} \dots \frac{d\alpha_m}{\alpha_m} \delta^{k \times 2}(C' \cdot \tilde{\lambda}) \delta^{k \times 4}(C' \cdot \tilde{\eta}) \delta^{(n+2-k) \times 2}(C'^\perp \cdot \lambda). \quad (4.5)$$

Here we expressed the integral in terms of so-called edge variable α_i which are associated to the BCFW bridges the diagram is built of, see section 2.5. There are m such variables and this is the dimension of the corresponding cell in the Grassmannian $G(k, n+2)$ with its representative matrix C' implicitly depending on these variables $C' = C'(\alpha_i)$. Note that this integral depends on the n on-shell momenta of the form factor, as well as two additional on-shell particles which do not correspond to external kinematics; we therefore do not use the underlined variables (4.2) and (4.3).

To obtain an expression for the entire form factor diagram, we now need to glue these pieces, the on-shell part (4.5) and the minimal form factor (4.4), together by performing the phase space integrations. For concreteness we assume that the legs which the minimal form factor attaches to are $n+1$ and $n+2$. Noting that the two on-shell states of the minimal form factor have to be incoming, which we implement by changing the sign of the corresponding λ 's, we can write

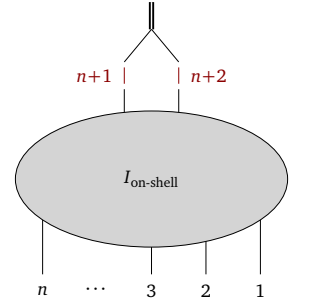


Figure 4.1: Gluing the minimal form factor onto some on-shell diagram with Grassmannian integral representation $I_{\text{on-shell}}$.

³ This representation of the minimal form factor will play another role in the integrability-based construction in chapter 8.

the following expression for the complete diagram:

$$I_F = \int \prod_{i=n+1}^{n+2} \left(\frac{d^2 \lambda_i d^2 \tilde{\lambda}_i}{\text{Vol}[GL(1)]} d^4 \tilde{\eta}_i \right) F_{2,2}(n+1, n+2) \Big|_{\lambda \rightarrow -\lambda} I_{\text{on-shell}}(1, \dots, n+2), \quad (4.6)$$

In order to carry out the phase space integration, we first use the delta functions of the minimal form factor (4.4) to integrate over the variables of type $\tilde{\lambda}$ and $\tilde{\eta}$ which sets

$$\begin{aligned} \tilde{\lambda}_{n+1} &\rightarrow -\frac{\langle n+2|q\rangle}{\langle n+2\ n+1\rangle}, & \tilde{\eta}_{n+1}^- &\rightarrow -\frac{\langle n+2|\gamma^-}{\langle n+2\ n+1\rangle}, & \tilde{\eta}_{n+1}^+ &\rightarrow 0, \\ \tilde{\lambda}_{n+2} &\rightarrow -\frac{\langle n+1|q\rangle}{\langle n+1\ n+2\rangle}, & \tilde{\eta}_{n+2}^- &\rightarrow -\frac{\langle n+1|\gamma^-}{\langle n+1\ n+2\rangle}, & \tilde{\eta}_{n+2}^+ &\rightarrow 0. \end{aligned} \quad (4.7)$$

We parametrize the remaining integrations, i.e. λ_{n+1} and λ_{n+2} modulo the $GL(1)^2$ redundancy, using two variables β_1, β_2 , via

$$\lambda_{n+1} = \xi_A - \beta_1 \xi_B, \quad \lambda_{n+2} = \xi_B - \beta_2 \xi_A, \quad (4.8)$$

It will turn out that the reference spinors ξ_A and ξ_B introduced here correspond exactly to those used in (4.2). Since $\langle n+1\ n+2\rangle = (\beta_1 \beta_2 - 1) \langle \xi_B \xi_A \rangle$ instead of (4.7) we can write

$$\begin{aligned} \tilde{\lambda}_{n+1} &\rightarrow \frac{1}{\beta_1 \beta_2 - 1} \frac{\langle \xi_B | q \rangle}{\langle \xi_B \xi_A \rangle} + \frac{\beta_2}{\beta_1 \beta_2 - 1} \frac{\langle \xi_A | q \rangle}{\langle \xi_A \xi_B \rangle}, \\ \tilde{\eta}_{n+1}^- &\rightarrow \frac{1}{\beta_1 \beta_2 - 1} \frac{\langle \xi_B | \gamma^- \rangle}{\langle \xi_B \xi_A \rangle} + \frac{\beta_2}{\beta_1 \beta_2 - 1} \frac{\langle \xi_A | \gamma^- \rangle}{\langle \xi_A \xi_B \rangle}, \\ \tilde{\lambda}_{n+2} &\rightarrow \frac{1}{\beta_1 \beta_2 - 1} \frac{\langle \xi_A | q \rangle}{\langle \xi_A \xi_B \rangle} + \frac{\beta_1}{\beta_1 \beta_2 - 1} \frac{\langle \xi_B | q \rangle}{\langle \xi_B \xi_A \rangle}, \\ \tilde{\eta}_{n+2}^- &\rightarrow \frac{1}{\beta_1 \beta_2 - 1} \frac{\langle \xi_A | \gamma^- \rangle}{\langle \xi_A \xi_B \rangle} + \frac{\beta_1}{\beta_1 \beta_2 - 1} \frac{\langle \xi_B | \gamma^- \rangle}{\langle \xi_B \xi_A \rangle}. \end{aligned} \quad (4.9)$$

We keep the β integrations as new ‘‘edge variables’’, associated to the operator part of the diagram:

$$\int \frac{d^2 \lambda_{n+1}}{\text{Vol}[GL(1)]} \frac{d^2 \lambda_{n+2}}{\text{Vol}[GL(1)]} = \langle \xi_A \xi_B \rangle \langle \xi_B \xi_A \rangle \int d\beta_1 d\beta_2. \quad (4.10)$$

Combining this measure with (4.9) applied to (4.6), we find the following formula for the form factor diagram:

$$\begin{aligned} I_F &= \langle \xi_A \xi_B \rangle \langle \xi_B \xi_A \rangle \int \frac{d\alpha_1}{\alpha_1} \dots \frac{d\alpha_m}{\alpha_m} \frac{d\beta_1 d\beta_2}{(1 - \beta_1 \beta_2)^2} \\ &\quad \times \delta^{k \times 2}(C(\alpha_i, \beta_i) \cdot \underline{\tilde{\lambda}}) \delta^{k \times 4}(C(\alpha_i, \beta_i) \cdot \underline{\tilde{\eta}}) \delta^{(n+2-k) \times 2}(C^\perp(\alpha_i, \beta_i) \cdot \underline{\lambda}), \end{aligned} \quad (4.11)$$

Because (4.9) is linear in the underlined variables defined in (4.2) and (4.3), we have absorbed the gluing in a new matrix C in this expression, and recovered the Grassmannian picture of the kinematics anticipated in section (4.1).

The explicit form of the matrix C depends on the diagram under consideration, but we can specify how the gluing procedure mixes the entries of the

original matrix C and introduces the dependence on the variables β_1 and β_2 . The columns of $C(\alpha, \beta) = (C_1 \cdots C_{n+2})$ are given in terms of those of $C'(\alpha) = (C'_1 \cdots C'_{n+2})$ by

$$\begin{aligned} C_i &= C'_i \quad \text{for } i = 1, \dots, n, \\ C_{n+1} &= \frac{1}{1 - \beta_1 \beta_2} C'_{n+1} + \frac{\beta_1}{1 - \beta_1 \beta_2} C'_{n+2}, \\ C_{n+2} &= \frac{1}{1 - \beta_1 \beta_2} C'_{n+2} + \frac{\beta_2}{1 - \beta_1 \beta_2} C'_{n+1}. \end{aligned} \quad (4.12)$$

which fixes C^\perp to

$$\begin{aligned} C_i^\perp &= C'^\perp_i \quad \text{for } i = 1, \dots, n, \\ C_{n+1}^\perp &= C'^\perp_{n+1} - \beta_2 C'^\perp_{n+2}, \\ C_{n+2}^\perp &= C'^\perp_{n+2} - \beta_1 C'^\perp_{n+1}. \end{aligned} \quad (4.13)$$

Note that the factor of $(1 - \beta_1 \beta_2)^2$ in (4.11) stems from rewriting the delta functions involving C^\perp , which generates a Jacobian. To see this, write the delta functions in terms of the C' or C matrices as

$$\delta^{(n+2-k) \times 2}(C^\perp \cdot \lambda) = \prod_{K=1}^k \int d^2 \rho_K \delta^{(n+2) \times 2}(\lambda_i - \rho_L C_{Li}), \quad (4.14)$$

with ρ_K^α , $K = 1, \dots, k$. Considering only the columns $n+1$ and $n+2$, the corresponding delta functions need to be rewritten as

$$\begin{aligned} &\delta^2(\lambda_{n+1} - \rho_L C'_{L, n+1}) \delta^2(\lambda_{n+2} - \rho_L C'_{L, n+2}) \\ &\rightarrow \delta^2(\lambda_{n+1} - \rho_L C_{L, n+1} - \beta_1(\lambda_{n+2} - \rho_L C_{L, n+2})) \\ &\quad \delta^2(\lambda_{n+2} - \rho_L C_{L, n+2} - \beta_2(\lambda_{n+1} - \rho_L C_{L, n+1})) \\ &= \frac{1}{(1 - \beta_1 \beta_2)^2} \delta^2(\lambda_{n+1} - \rho_L C_{L, n+1}) \delta^2(\lambda_{n+2} - \rho_L C_{L, n+2}). \end{aligned} \quad (4.15)$$

A remarkable property of the procedure outlined above is the fact that it preserves the degrees of freedom under the mapping between amplitude and form factor diagrams (3.14). Removing a four-point amplitude reduces the number of edge variables by two, which will then be reinstated in form of the variables β_1 and β_2 . This gives further evidence for the usefulness of this mapping, and is the starting point for the calculation of the Graßmannian top-form for form factors, to which we turn now.

4.3 Gluing the top-form

Having established a general scheme for calculating Graßmannian integrals for arbitrary on-shell diagrams (using edge variables), we can now turn to the question of finding the top-forms, expressed in a $GL(k)$ -invariant way using the minors of the C matrix.

The general idea is as follows: Based on the conjectured relation between form factor and amplitude top-cell diagrams given in equation (3.15), we first find the form factor top-cell diagram for a given number of external legs n and MHV degree k . We focus on the diagram where the minimal form factor sits between legs n and 1, and deal with the cyclicly related diagrams later. Having this diagram, we then in particular know the on-shell diagram with the minimal form factor removed; as described in section 3.8, its associated permutation is given by

$$\tilde{\sigma} = (k + 1, \dots, n, n + 2, n + 1, 1, 2, \dots, k, k - 1). \tag{4.16}$$

4 See section 2.5 for details.

5 Bourjaily, "Positroids, Plabic Graphs, and Scattering Amplitudes in Mathematica", 1212.6974

Using this permutation, we can obtain an integral representation in terms of edge variables: we first decompose the permutation into elementary transpositions corresponding to BCFW bridges; one can then use boundary measurements⁴ to generate the C' matrix in terms of these variables. For practical purposes, these steps are conveniently automatized by the Mathematica package `positroid.m`.⁵

We then glue the minimal form factor back onto the diagram, using the formulas derived in section 4.2. Finally, the resulting integral is expressed in a $GL(k)$ invariant way by changing variables to the entries C_{ij} of the matrix C and expressing the integrand in terms of its minors.

We exemplify this approach using the four-point NMHV top-cell diagram. As displayed in figure 4.2, we start from the top-cell diagram of the six-point NMHV amplitude. Removing the box diagram at legs 5 and 6, we obtain the on-shell part of the diagram for the four-point NMHV form factor top-cell. This on-shell diagram is likewise shown in figure 4.2 with the edge variables α_i that can be obtained from decomposing the associated (decorated) permutation of the diagram,

$$\tilde{\sigma} = (4, 6, 5, 7, 9, 8). \tag{4.17}$$

In terms of these variables, the representative matrix in the Graßmannian has the form

$$C'(\alpha) = \begin{pmatrix} 1 & \alpha_2 + \alpha_4 & 0 & -\alpha_2\alpha_3 & -\alpha_2\alpha_3\alpha_6 & 0 \\ 0 & 1 & 0 & -\alpha_3 & -\alpha_3\alpha_6 & -\alpha_1 \\ 0 & 0 & 1 & \alpha_5 + \alpha_7 & \alpha_5\alpha_6 & 0 \end{pmatrix}, \tag{4.18}$$

which can be brought to into the standard gauge fixed form by a $GL(3)$ rotation:⁶

$$C' \sim \begin{pmatrix} 1 & 0 & 0 & \alpha_3\alpha_4 & \alpha_3\alpha_4\alpha_6 & \alpha_1(\alpha_2 + \alpha_4) \\ 0 & 1 & 0 & -\alpha_3 & -\alpha_3\alpha_6 & -\alpha_1 \\ 0 & 0 & 1 & \alpha_5 + \alpha_7 & \alpha_5\alpha_6 & 0 \end{pmatrix}. \tag{4.19}$$

We can now glue the minimal form factor into the diagram. According to (4.12), this gives us a new matrix C which depends on the original edge variables and

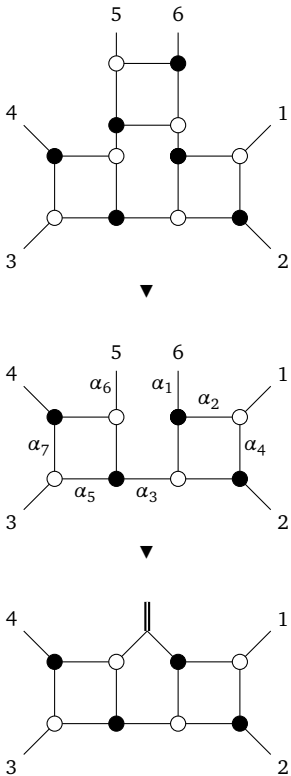


Figure 4.2: Gluing one of the top-cell diagrams for the form factor $F_{4,3}$. We start with the six-point NMHV amplitude top-cell diagram, remove a box, and glue the minimal form factor into this position. We show the edges carrying the edge variables used in the main text.

6 This form of the matrix facilitates the change of variables below.

two new degrees of freedom β_1 and β_2 :

$$C = \begin{pmatrix} 1 & 0 & 0 & \alpha_3 \alpha_4 & -\frac{\alpha_3 \alpha_4 \alpha_6 + \alpha_1 (\alpha_2 + \alpha_4) \beta_1}{-1 + \beta_1 \beta_2} & -\frac{\alpha_1 (\alpha_2 + \alpha_4) + \alpha_3 \alpha_4 \alpha_6 \beta_2}{-1 + \beta_1 \beta_2} \\ 0 & 1 & 0 & -\alpha_3 & \frac{\alpha_3 \alpha_6 + \alpha_1 \beta_1}{-1 + \beta_1 \beta_2} & \frac{\alpha_1 + \alpha_3 \alpha_6 \beta_2}{-1 + \beta_1 \beta_2} \\ 0 & 0 & 1 & \alpha_5 + \alpha_7 & \frac{\alpha_5 \alpha_6}{1 - \beta_1 \beta_2} & \frac{\alpha_5 \alpha_6 \beta_2}{1 - \beta_1 \beta_2} \end{pmatrix}. \quad (4.20)$$

The on-shell form associated with the diagram is then

$$\frac{1}{\alpha_1 \alpha_2 \alpha_3 \alpha_4 \alpha_5 \alpha_6 \alpha_7 (1 - \beta_1 \beta_2)^2}. \quad (4.21)$$

We now want to express this form in a $GL(3)$ invariant way, in terms of the minors of the matrix C . To this end, we note that the Jacobian from this change of variables is

$$\frac{\partial(C_{I_j})}{\partial(\alpha_k, \beta_1, \beta_2)} = \frac{\alpha_1^2 \alpha_2 \alpha_3^2 \alpha_5 \alpha_6}{(1 - \beta_1 \beta_2)^5}. \quad (4.22)$$

One can then check that (4.21) is equivalent to the form

$$\Omega_{4,3} = \frac{1}{(123)(234)(345)(456)(561)(612)} \frac{(345)(612)}{(346)(512) - (345)(612)}. \quad (4.23)$$

Result for all n and k

Directly proving a general formula for the top-form analogous to (4.23) is difficult, since the Jacobian $\partial(C_{I_j})/\partial(\alpha_k, \beta_1, \beta_2)$ can in general be very complicated. Nevertheless, we have repeated the procedure outlined above for a very large number of examples, and invariably found that the top-form with the minimal form factor glued in at the positions $n + 1$ and $n + 2$ (with these kinematical variables encoding the off-shell data as in (4.2)) in the amplitude diagram was given by following expression, which we confidently conjecture to be correct for all n and k :

$$\Omega_{n,k} = \frac{Y(1 - Y)^{-1}}{(1 \cdots k)(2 \cdots k+1) \cdots (n \cdots k-3)(n+1 \cdots k-2)(n+2 \cdots k-1)}, \quad (4.24)$$

$$Y = \frac{(n-k+2 \cdots n \ n+1)(n+2 \ 1 \cdots k-1)}{(n-k+2 \cdots n \ n+2)(n+1 \ 1 \cdots k-1)}.$$

Thus the Grassmannian top-form is given by an amplitude-like form for $G(k, n+2)$ with a product of the consecutive minors, together with a ‘‘correction factor’’ $Y/(1 - Y)$, which involves the labels of the minimal form factor and their neighbors, and accounts for the operator insertion.⁷

As already noted in section 3.7, there are n distinct top-dimensional on-shell diagrams for any k and n , which differ by the position of the minimal form factor and thus are related by a cyclic shift of the external on-shell legs. If we define the shift $s = 0, \dots, n - 1$ such that $s = 0$ means that the minimal form factor comes after leg n and before leg 1, and in general after leg s , we can write the corresponding top-form by either shifting the labels of the kinematical variables or equivalently, by relabeling the columns of the matrix C . We therefore define

⁷ We note that after changing to the edge variables $\{\alpha_i, \beta_1, \beta_2\}$ which are used in the gluing procedure, Y always equals $\beta_1 \beta_2$. Thus the factor $Y(1 - Y)^{-1}$ cancels a factor of $[\beta_1 \beta_2 (1 - \beta_1 \beta_2)]^{-1}$ which is present in the consecutive minors, but not in the gluing formula (4.11).

the Graßmannian integral for a general shift by

$$\mathcal{G}_{n,k}^F = \langle \xi_A \xi_B \rangle^2 \int \frac{d^{k \times (n+2)} C}{\text{Vol}[GL(k)]} \Omega_{n,k} \Big|_{\sigma_s} \delta^{2 \times k}(C \cdot \tilde{\lambda}) \delta^{4 \times k}(C \cdot \tilde{\eta}) \delta^{2 \times (n+2-k)}(C^\perp \cdot \lambda), \quad (4.25)$$

where the shift by s is given as

$$\sigma_s = \begin{pmatrix} 1 & 2 & \cdots & n-1 & n & n+1 & n+2 \\ \downarrow & \downarrow & & \downarrow & \downarrow & \downarrow & \downarrow \\ 1+s & 2+s & & s-1 & s & n+1 & n+2 \end{pmatrix} \quad \text{with } i+n \simeq i \quad (4.26)$$

and the form $\Omega_{n,k}$ is defined in (4.24).

Special case: MHV

Just as MHV amplitudes, MHV form factors are rather special. In particular they can be represented by a single on-shell diagram as discussed in section 3.4, and their Graßmannian integral completely localizes on the delta functions. Here we want to show that the MHV Graßmannian integral can be rewritten in a way that makes the similarities to the amplitude Graßmannian integral manifest, and which allows to directly see that all MHV form factors are given by the simple Parke-Taylor-type formula (3.7).

We again focus on the case where the minimal form factor is attached to legs $n+1$ and $n+2$, although in this case it does not matter, as MHV form factors are represented by a single diagram and are cyclicly invariant (in the external on-shell data). We first note that the unusual factor in the Graßmannian top-form (4.24) can in this case be written as

$$\frac{Y}{1-Y} \Big|_{k=2} = \frac{(n \ n+1)(n+n+2 \ 1)}{(n \ n+2)(n+1 \ 1) - (n \ n+1)(n+2 \ 1)} = \frac{(n \ n+1)(n+2 \ 1)}{(n \ 1)(n+1 \ n+2)}, \quad (4.27)$$

where the last equality follows from a Plücker relation. The Graßmannian form thus simplifies to⁸

$$\Omega_{n,2} = \frac{1}{(12)(23) \cdots (n-1 \ n)(n1)} \frac{1}{(n+1 \ n+2)^2}. \quad (4.28)$$

The Parke-Taylor-type expression for the form factor $F_{n,2}$ is the same as the one for $A_{n,2}$, up to the additional (super) momentum in the delta functions. We can realize this relation on the level of the Graßmannian integral, further simplifying (4.28), and writing it in a way that completely resembles its amplitude counterpart. We present the derivation using an explicit gauge; the final result will be independent of this choice. Let us fix the C matrix to be of the form

$$C = \begin{pmatrix} 1 & 0 & c'_{13} & \cdots & c'_{1n+2} \\ 0 & 1 & c'_{23} & \cdots & c'_{2n+2} \end{pmatrix}, \quad (4.29)$$

using the $GL(2)$ gauge freedom. We furthermore set the reference spinors that parametrize the freedom in representing the off-shell momentum in terms of two

⁸ We note that this form is identical to the integrand of the connected formula for form factors presented in He, Liu, “A note on connected formula for form factors”, 1608.04306 and Brandhuber, Hughes, Panerai, Spence, Travaglini, “The connected prescription for form factors in twistor space”, 1608.03277. We will discuss this representation in chapter 6, cf. equation (6.1).

on-shell momenta as in (4.2) to

$$\xi_A \equiv \underline{\lambda}_{n+1} = \lambda_2 \quad \text{and} \quad \xi_B \equiv \underline{\lambda}_{n+2} = \lambda_1. \quad (4.30)$$

The four delta functions among $\delta(C^\perp \cdot \underline{\lambda})$ which involve the $(n+1)$ th and $(n+2)$ th rows of C then impose

$$-C_{1n+1} \lambda_1^\alpha - C_{2n+1} \lambda_2^\alpha + \lambda_2^\alpha = 0, \quad -C_{1n+2} \lambda_1^\alpha - C_{2n+2} \lambda_2^\alpha + \lambda_1^\alpha = 0. \quad (4.31)$$

Solving these constraints yields a Jacobian $\langle 12 \rangle^{-2}$ which cancels the prefactor in the general expression (4.11), and C is reduced to

$$C = \begin{pmatrix} 1 & 0 & C_{13} & \cdots & C_{1n} & 0 & 1 \\ 0 & 1 & C_{23} & \cdots & C_{2n} & 1 & 0 \end{pmatrix}. \quad (4.32)$$

In particular, note that now $(n+1 \ n+2)^2 = 1$. This already means that the form (4.28) becomes identical to the one for the amplitude $A_{n,2}$.

If we further define the matrix C^* to be C without the last two columns, we can combine coefficients in the delta functions and write the Graßmannian integral as

$$\int \frac{d^{2 \times n} C^*}{\text{Vol}[GL(2)]} \frac{\delta^4(C^* \cdot \underline{\tilde{\lambda}}) \delta^8(C^* \cdot \underline{\tilde{\eta}}) \delta^{2n-4}(C^{*\perp} \cdot \lambda)}{(12)(23) \cdots (n-1 \ n)(n1)}. \quad (4.33)$$

Here we defined the kinematical variables as follows:

$$\begin{aligned} \underline{\tilde{\lambda}}_r &= \tilde{\lambda}_r - \frac{\langle s|q \rangle}{\langle sr \rangle}, & \underline{\tilde{\eta}}_r^- &= \tilde{\eta}_r^- - \frac{\langle s|\gamma^- \rangle}{\langle sr \rangle}, & \underline{\tilde{\eta}}_r^+ &= \tilde{\eta}_r^+, \\ \underline{\tilde{\lambda}}_s &= \tilde{\lambda}_s - \frac{\langle r|q \rangle}{\langle rs \rangle}, & \underline{\tilde{\eta}}_s^- &= \tilde{\eta}_s^- - \frac{\langle r|\gamma^- \rangle}{\langle rs \rangle}, & \underline{\tilde{\eta}}_s^+ &= \tilde{\eta}_s^+. \end{aligned} \quad (4.34)$$

for some r and s and $\underline{\tilde{\lambda}}_i = \tilde{\lambda}_i$, $\underline{\tilde{\eta}}_i = \tilde{\eta}_i$ for all other indices. Note that from our derivation using the choice of gauge and reference spinors as in (4.29) and (4.30), we would get $r = 1$ and $s = 2$, but it can easily be seen that in fact these two indices can be arbitrary. They correspond to “twisted” kinematics, in the sense that the momenta \underline{p}_r and \underline{p}_s together contain the off-shell momentum, $\underline{p}_r + \underline{p}_s = p_r + p_s - q$, and similar for the super momentum.

Since this encoding is done using only the antiholomorphic variables $\tilde{\lambda}$ and $\tilde{\eta}$, it is clear that (4.33) leads to the well-known formula for MHV form factors (3.7): the holomorphic Parke-Taylor prefactor is not changed by the “twisted” kinematics (4.34), and their only effect is to put the kinematics of the operator, q and γ^- into the delta functions.

4.4 Twistor and momentum twistor space

As discussed in chapter 2, twistor and momentum twistor space have played an important role in developing on-shell formulations for amplitudes. The Graßmannian integral and the geometric picture it draws of scattering processes can best be understood in these settings.

In this section we provide such twistor space formulations for form factor Grassmannian integral (4.25) which we derived in spinor-helicity variables. While the transition to twistor space is straightforward, there are new interesting features when going to momentum twistor space. There is a natural ambiguity in the definition of momentum twistors if an off-shell momentum participates in the process; we will see that the Grassmannian integral favors a different convention from the one used in other approaches.

To be definite, we will again only consider the case where the minimal form factor is glued in between the particles n and 1. We therefore assume kinematics as defined in (4.2) and (4.3), and note that all spinor brackets are defined with respect to these variables.

Twistor space

The Grassmannian integral for form factors (4.25), written in terms of the spinor-helicity variables (4.2) and (4.3) can easily be transformed to twistor space

$$\mathcal{W}_i = (\tilde{\underline{\mu}}_i, \tilde{\underline{\lambda}}_i, \tilde{\underline{\eta}}_i), \quad (4.35)$$

where we simply apply Witten's half Fourier transformation⁹ to all the on-shell momenta, including those that parametrize the off-shell momentum:

$$f(\underline{\lambda}, \tilde{\underline{\lambda}}, \tilde{\underline{\eta}}) \rightarrow f(\tilde{\underline{\mu}}, \tilde{\underline{\lambda}}, \tilde{\underline{\eta}}) = \int d^2 \underline{\lambda}_j \exp(-i \tilde{\underline{\mu}}_j^\alpha \underline{\lambda}_{j\alpha}) f(\underline{\lambda}, \tilde{\underline{\lambda}}, \tilde{\underline{\eta}}). \quad (4.36)$$

This is in complete analogy with the amplitude case,¹⁰ see also sections 2.1 and 2.5. Applying this transformation is straightforward; the prefactor in (4.25) becomes

$$\langle \xi_A \xi_B \rangle^2 = \left\langle \frac{\partial}{\partial \tilde{\underline{\mu}}_{n+1}} \frac{\partial}{\partial \tilde{\underline{\mu}}_{n+2}} \right\rangle^2, \quad (4.37)$$

and the integral itself transforms as in the amplitude case. With the delta functions $\delta^{2 \times (n+2-k)}(C^\perp \cdot \underline{\lambda})$ written as in (4.14), we apply the Fourier transform (4.36) and localize the integrals over $\underline{\lambda}_i$ via these delta functions, and find

$$\delta^{2 \times (n+2-k)}(C^\perp \cdot \underline{\lambda}) \rightarrow \prod_{K=1}^k \int d^2 \rho_K \exp\left(-i \sum_{j=1}^{n+2} \sum_{L=1}^k \rho_L^\alpha C_{Lj} \tilde{\underline{\mu}}_{\alpha j}\right) = \delta^{2k}(C \cdot \tilde{\underline{\mu}}). \quad (4.38)$$

Combining everything we can write (4.25) as

$$\left\langle \frac{\partial}{\partial \tilde{\underline{\mu}}_{n+1}} \frac{\partial}{\partial \tilde{\underline{\mu}}_{n+2}} \right\rangle^2 \int \frac{d^{k \times (n+2)} C}{\text{Vol}[GL(k)]} \Omega_{n,k} \delta^{4k|4k}(C \cdot \mathcal{W}), \quad (4.39)$$

where $\Omega_{n,k}$ is the same form as in spinor-helicity variables, and given in (4.24). While the derivatives appearing in (4.39) may seem undesirable, this form of the integral was the most compact expression we could find. It would be interesting to see if this formula can be cast into a more explicit form.

⁹ Witten, "Perturbative gauge theory as a string theory in twistor space", [hep-th/0312171](https://arxiv.org/abs/hep-th/0312171)

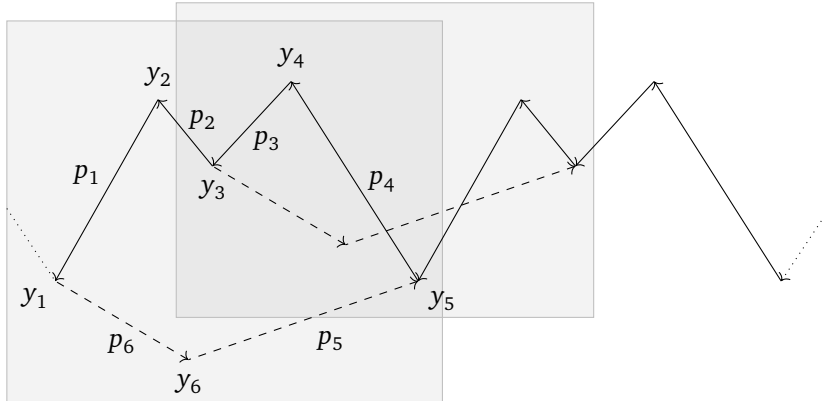
¹⁰ Arkani-Hamed, Cachazo, Cheung, Kaplan, "A Duality For The S Matrix", [hep-th/0712295](https://arxiv.org/abs/hep-th/0712295)

Momentum twistor space

In order to transform the Graßmannian integral (4.25) to momentum twistor space, we first have to define these variables – which are not unique due to the presence of the off-shell momentum of the operator.

In the literature, the dual momenta y_i are set up using only the on-shell momenta of the outgoing particles.¹¹ Since these do not add up to zero, but to the off-shell momentum of the operator $-q$, the dual momenta do not form a closed lightlike polygon; instead a periodic contour (with period q) has to be considered. From these (in principle) infinite points in y space one then defines momentum twistors as described in section 2.1. This construction is illustrated in figure 4.3.

In the same figure, we also show the kinematic picture we use here. The Graßmannian integral forces us to take a different viewpoint: We close the polygon in y space by the two on-shell momenta that parametrize q ; this can be done between any two consecutive momenta, corresponding to the different positions at which the minimal form factor can be glued into the on-shell diagram, and the cyclic shifts in the Graßmannian integral (4.25).



¹¹ Brandhuber, Gurdogan, Mooney, Travaglini, Yang, “Harmony of Super Form Factors”, [1107.5067](#); and Bork, “On form factors in $\mathcal{N} = 4$ SYM theory and polytopes”, [1407.5568](#)

Figure 4.3: The momenta and dual momenta for a four-point form factor. The black arrows correspond to the 4 on-shell momenta p_i of the external states; they are repeated according to the cyclic ordering, to form the periodic contour that is widely used in the literature to define dual momenta and momentum twistors. In this picture the off-shell momentum is implicitly defined as the period of the contour. In contrast, the gray regions indicate two of the closed contours needed for the Graßmannian integral; here the off-shell momentum is decomposed into two on-shell momenta (dashed arrows), which can be inserted between any two consecutive on-shell momenta. The corresponding closed polygons then define the dual momenta y_i used here.

Concretely we define dual momenta y and dual supermomenta ϑ based on the variables defined in (4.2) and (4.3), ordered such that the off-shell data is given in terms of particles $n + 1$ and $n + 2$,

$$\begin{aligned} \underline{\lambda}_i \tilde{\lambda}_i &= y_i - y_{i+1}, \\ \underline{\lambda}_i \tilde{\eta}_i &= \vartheta_i - \vartheta_{i+1}. \end{aligned} \quad (4.40)$$

This corresponds to the first closed polygon in figure 4.3. Using these dual momenta, we define momentum twistor variables

$$\mathcal{X}_i = (\underline{\lambda}_i, \underline{\mu}_i, \underline{\eta}_i), \quad (4.41)$$

via the incidence relations

$$\underline{\mu}_i = \underline{\lambda}_i y_i = \underline{\lambda}_i y_{i+1}, \quad \underline{\eta}_i = \underline{\lambda}_i \vartheta_i = \underline{\lambda}_i \vartheta_{i+1}, \quad (4.42)$$

just as in section 2.1. These relations can be inverted, and give

$$\begin{aligned}\tilde{\lambda}_i &= \frac{\langle i+1 i \rangle \underline{\mu}_{i-1} + \langle i i-1 \rangle \underline{\mu}_{i+1} + \langle i-1 i+1 \rangle \underline{\mu}_i}{\langle i-1 i \rangle \langle i i+1 \rangle}, \\ \tilde{\eta}_i &= \frac{\langle i+1 i \rangle \underline{\eta}_{i-1} + \langle i i-1 \rangle \underline{\eta}_{i+1} + \langle i-1 i+1 \rangle \underline{\eta}_i}{\langle i-1 i \rangle \langle i i+1 \rangle}.\end{aligned}\quad (4.43)$$

Apart from these questions regarding kinematics, the transformation of the integral (4.25) to momentum twistor space is non-trivial because the integrand contains non-consecutive minors. Since this is a new feature, we will present the derivation step-by-step, following the works Arkani-Hamed et al. (2010); Elvang et al. (2014).¹²

We first represent the delta function $\delta^{2 \times (n+2-k)}(C^\perp \cdot \underline{\lambda})$ involving the matrix C^\perp as in (4.14), using an integral over the auxiliary matrix ρ . A part of the $GL(k)$ redundancy can be used to fix this matrix to

$$\rho = \begin{pmatrix} 0 & \cdots & 0 & 1 & 0 \\ 0 & \cdots & 0 & 0 & 1 \end{pmatrix}.\quad (4.44)$$

With this choice, the delta functions in (4.14) can be used to fix the last two rows of C to

$$C_{k-1 i} = \underline{\lambda}_i^1, \quad C_{k i} = \underline{\lambda}_i^2.\quad (4.45)$$

This in turn allows to extract the momentum and super momentum conserving delta functions, such that the Grassmannian integral (4.25) becomes

$$\begin{aligned}\langle \xi_A \xi_B \rangle^2 \delta^4(\underline{\lambda} \cdot \tilde{\lambda}) \delta^8(\underline{\lambda} \cdot \tilde{\eta}) \\ \int \frac{d^{(k-2) \times (n+2)} C}{\text{Vol}[GL(k-2) \times T_{k-2}]} \Omega_{n,k} \delta^{2 \times (k-2)}(C \cdot \tilde{\lambda}) \delta^{4 \times (k-2)}(C \cdot \tilde{\eta}),\end{aligned}\quad (4.46)$$

where both the measure as well as the delta functions refer to the first $k-2$ rows of C only, and T_{k-2} is a residual shift symmetry acting on these rows,

$$C_{Ii} \longrightarrow C_{Ii} + r_{1I} \underline{\lambda}_i^1 + r_{2I} \underline{\lambda}_i^2, \quad I = 1, \dots, k-2,\quad (4.47)$$

with r_{1I}, r_{2I} arbitrary.

Defining a new matrix D , which will be the representative for the Grassmannian $G(k-2, n+2)$ in the momentum twistor Grassmannian integral, as

$$D_{Ii} = \frac{\langle i i+1 \rangle C_{I i-1} + \langle i-1 i \rangle C_{I i+1} + \langle i+1 i-1 \rangle C_{I i}}{\langle i-1 i \rangle \langle i i+1 \rangle},\quad (4.48)$$

we can rewrite the delta functions using

$$\sum_{i=1}^{n+2} C_{Ii} \tilde{\lambda}_i = - \sum_{i=1}^{n+2} D_{Ii} \underline{\mu}_i, \quad \sum_{i=1}^{n+2} C_{Ii} \tilde{\eta}_i = - \sum_{i=1}^{n+2} D_{Ii} \underline{\eta}_i, \quad I = 1, \dots, k-2,\quad (4.49)$$

which follow from (4.43).

We can furthermore relate the minors of the matrices C and D . In the derivation of the amplitude case it was shown that the consecutive minors of C can be express in terms of those of D by

$$(1 \cdots k)_C = - \langle 12 \rangle \cdots \langle k-1 k \rangle (2 \cdots k-1)_D\quad (4.50)$$

¹² Arkani-Hamed, Cachazo, Cheung, "The Grassmannian Origin Of Dual Superconformal Invariance", 0909.0483; and Elvang, Huang, Keeler, Lam, Olsson, Roland, Speyer, "Grassmannians for scattering amplitudes in 4d $\mathcal{N}=4$ SYM and 3d ABJM", 1410.0621

The other consecutive minors follow from cyclic relabeling. Note that in this section, we will indicate the matrix a minor refers to by a subscript.

It is a new feature of Grassmannian integral for form factors that the form (4.24), also contain non-consecutive minors, for which we find

$$\begin{aligned}
 (1 \dots k-1 k+1)_C &= -\langle 12 \rangle \dots \langle k-2 k-1 \rangle \langle k-1 k+1 \rangle (2 \dots k-1)_D \\
 &\quad - \langle 12 \rangle \dots \langle k-2 k-1 \rangle \langle k k+1 \rangle (2 \dots k-2)_D, \\
 (13 \dots k+1)_C &= -\langle 13 \rangle \langle 34 \rangle \dots \langle k k+1 \rangle (3 \dots k)_D \\
 &\quad - \langle 12 \rangle \langle 34 \rangle \dots \langle k k+1 \rangle (24 \dots k)_D.
 \end{aligned} \tag{4.51}$$

From (4.50) we see that the product of consecutive minors in (4.24) becomes

$$\begin{aligned}
 (1 \dots k)_C \dots (n+2 \dots k-1)_C \\
 = (-1)^{n+2} (\langle 12 \rangle \dots \langle n+2 1 \rangle)^{k-1} (1 \dots k)_D \dots (n+2 \dots k-1)_D.
 \end{aligned} \tag{4.52}$$

while for the cross-ratio Y we find using (4.51)

$$\begin{aligned}
 Y &= \frac{(n-k+2 \dots n n+1)_C (n+2 1 \dots k-1)_C}{(n-k+2 \dots n n+2)_C (n+1 1 \dots k-1)_C} \\
 &= \frac{\langle n n+1 \rangle \langle n-k+3 \dots n \rangle_D}{\langle n n+2 \rangle \langle n-k+3 \dots n \rangle_D + \langle n+1 n+2 \rangle \langle n-k+3 \dots n-1 n+1 \rangle_D} \\
 &\quad \frac{\langle n+2 1 \rangle (1 \dots k-2)_D}{\langle n+1 1 \rangle (1 \dots k-2)_D + \langle n+1 n+2 \rangle \langle n+2 2 \dots k-2 \rangle_D}.
 \end{aligned} \tag{4.53}$$

The transformation of the measure is the same as in Elvang et al. (2014).¹³ Using the shift symmetry T_{k-2} to set $C_{I1} = C_{I2} = 0$ we get

$$\frac{d^{(k-2) \times (n+2)}_C}{\text{Vol}[GL(k-2) \times T_{k-2}]} = \langle 12 \rangle^{k-2} \frac{d^{(k-2) \times (n)}_C}{\text{Vol}[GL(k-2)]}. \tag{4.54}$$

The change of variables from C to D yields

$$\frac{d^{(k-2) \times (n)}_C}{\text{Vol}[GL(k-2)]} = \left(\frac{\langle 12 \rangle \dots \langle n+2 1 \rangle}{\langle 12 \rangle^2} \right)^{k-2} \frac{d^{(k-2) \times (n)}_D}{\text{Vol}[GL(k-2)]}. \tag{4.55}$$

Finally, the gauge fixing of the first two columns of the C matrix can be undone, which gives a further factor of

$$\prod_{I=1, \dots, k-2} \langle 12 \rangle \delta^2(D_{Ii} \underline{\lambda}_i) \tag{4.56}$$

The final expression is then

$$\mathcal{G}_{n,k}^F = F_{n,2} \int \frac{d^{(k-2) \times (n+2)}_D}{\text{Vol}[GL(k-2)]} \Omega_{n,k} \delta^{4(k-2)|4(k-2)}(D \cdot \mathcal{Z}), \tag{4.57}$$

where the form $\Omega_{n,k}$ is given by

$$\Omega_{n,k} = \frac{\langle n 1 \rangle \langle n+1 n+2 \rangle Y}{\langle n n+1 \rangle \langle n+2 1 \rangle (1-Y)} \tag{4.58}$$

and Y is given in (4.53).

¹³ Elvang, Huang, Keeler, Lam, Olson, Roland, Speyer, "Grassmannians for scattering amplitudes in 4d $\mathcal{N} = 4$ SYM and 3d ABJM", [1410.0621](#)

Distinguished reference spinors

The Graßmannian integral in momentum twistor space as presented in (4.57) and (4.53) unfortunately – and in contrast to its amplitude counterpart – still depends explicitly on explicit spinor brackets involving the external kinematics. In particular this introduces a nontrivial (but fictitious) dependence on the reference spinors ξ_A and ξ_B . It turns out that this is a consequence of the way momentum twistor variables were introduced, based on dual momenta that assume a (fictitious) cyclic ordering of the external momenta involving the off-shell momentum q .

We can however write the Graßmannian integral in an equivalent much simpler form, which more closely resembles the spinor-helicity version, by a judicious choice of reference spinors. If we set them to

$$\xi_A \equiv \underline{\lambda}_{n+1} = \lambda_1, \quad \xi_B \equiv \underline{\lambda}_{n+2} = \lambda_n, \tag{4.59}$$

the Graßmannian integral (4.57) simply becomes

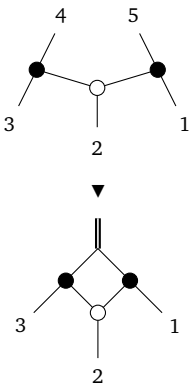
$$F_{n,2} \int \frac{d^{(k-2) \times (n+2)} D}{\text{Vol}[GL(k-2)]} \frac{-\tilde{Y}(1-\tilde{Y})^{-1} \delta^{4(k-2)|4(k-2)}(D \cdot \mathcal{Z})}{(1 \cdots k-2)(2 \cdots k-1) \cdots (n+1 \cdots k-4)(n+2 \cdots k-3)}. \tag{4.60}$$

Here \tilde{Y} is again just a ratio of non-consecutive minors (although no cross-ratio)

$$\tilde{Y} = \frac{(n-k+3 \cdots n)(1 \cdots k-2)}{(n-k+3 \cdots n-1 \ n+1)(n+2 \ 2 \cdots k-2)}. \tag{4.61}$$

4.5 More examples

In section 4.3 we already showed how the Graßmannian integral for form factors in spinor-helicity variables (4.25) reproduces the known MHV form factors. In this section we calculate some further examples, also using the momentum twistor space description derived in the previous section, to show that the Graßmannian indeed is able to reproduce highly non-trivial results for higher MHV degree.



Three-point NMHV

The simplest form factor with higher MHV degree is the three-point NMHV form factor $F_{3,3}$. Like all N^{max} MHV form factors, it can be obtained from k -increasing inverse soft limits of the minimal form factor, in this case a single one, see figure 4.4. The Graßmannian integral representation (4.25) for this form factor is

$$\mathcal{G}_{3,3[0]}^F = \langle \xi_A \xi_B \rangle^2 \int \frac{d^{3 \times 5} C'}{\text{Vol}[GL(3)]} \frac{Y}{1-Y} \frac{\delta^6(C' \cdot \tilde{\lambda}) \delta^{12}(C' \cdot \tilde{\eta}) \delta^4(C'^{\perp} \cdot \lambda)}{(123)(234)(345)(451)(512)}, \tag{4.62}$$

with

$$Y = \frac{(234)(512)}{(235)(412)} \tag{4.63}$$

Figure 4.4: The on-shell part of the form factor $F_{3,3}$, and the complete on-shell diagram. The former is simply a k -increasing inverse soft factor.

and where the off-shell kinematics are encoded in the on-shell variables at position 4 and 5 as in (4.2).

Since the form factor is of N^{\max} MHV type, the integral completely localizes on the delta functions, once the momentum and super momentum conserving delta functions have been pulled out of the integral. We first gauge fix the matrix C by setting the first three columns to the identity matrix,

$$C = \begin{pmatrix} 1 & 0 & 0 & C_{14} & C_{15} \\ 0 & 1 & 0 & C_{24} & C_{25} \\ 0 & 0 & 1 & C_{34} & C_{35} \end{pmatrix}, \quad (4.64)$$

and then solve for the remaining entries by contracting the terms inside $\delta^6(C' \cdot \tilde{\lambda})$ with $\tilde{\lambda}_4$ and $\tilde{\lambda}_5$. This fixes the entries to

$$C_{i4} = -\frac{[i5]}{[45]} = -\frac{\langle \xi_A | q | i \rangle}{q^2}, \quad C_{i5} = -\frac{[i4]}{[54]} = -\frac{\langle \xi_B | q | i \rangle}{q^2}, \quad (4.65)$$

where we have used the definition of the kinematics (4.2) in the second step.

Inserting the solution (4.65) into the delta functions $\delta^4(C'^{\perp} \cdot \lambda)$, we obtain the momentum-conserving delta function contracted with $\tilde{\lambda}_4$ and $\tilde{\lambda}_5$. Rotating them to the usual form gives a Jacobian of $[45]^2$, which, together with the Jacobian $[45]^{-3}$ from the previous contraction with $\tilde{\lambda}_4$ and $\tilde{\lambda}_5$, gives $[45]^{-1}$.

Plugging everything back into the Graßmannian integral (4.62) and applying a Schouten identity, we find

$$F_{3,3} = \mathcal{G}_{3,3[0]}^F = \frac{(q^2)^2}{[12][23][31]} \delta^{12}(C \cdot \tilde{\eta}) \delta^4\left(\sum_{i=1}^3 p_i - q\right), \quad (4.66)$$

where we leave the entries (4.64) and (4.65) of the matrix C implicit. This formula agrees with the result of Brandhuber et al. (2011).¹⁴

Interestingly, the cyclic invariance of the form factor is not manifest in the Graßmannian representation (4.62). The final expression (4.66) obtained from it is nevertheless manifestly invariant under cyclic relabeling of the legs 1, 2 and 3, as can be seen from (4.65).

N^{\max} MHV at 3 and 4 points using momentum twistors

We now turn to the Graßmannian integral in momentum twistor variables, using the convenient choice of reference spinors presented in (4.60). The results will be written in terms of the $SL(4)$ -invariant four-brackets

$$\langle i j k l \rangle = \det(Z_i Z_j Z_k Z_l) = \epsilon_{ABCD} Z_i^A Z_j^B Z_k^C Z_l^D \quad (4.67)$$

using the bosonic components of the super momentum twistors, $Z_i = (\lambda_i, \underline{\mu}_i)$, as well as the five-brackets

$$[i j k l m] = \frac{\delta^4(\langle i j k l \rangle \eta_m + \text{cyclic})}{\langle i j k l \rangle \langle j k l m \rangle \langle k l m i \rangle \langle l m i j \rangle \langle m i j k \rangle}. \quad (4.68)$$

Focusing first on the N^{\max} MHV form factors with $k = n$, the simplest case is again the three-point form factor which we just computed in the spinor-helicity

¹⁴ Brandhuber, Gurdogan, Mooney, Travaglini, Yang, "Harmony of Super Form Factors", 1107.5067

representation. For $k = 3$,

$$D = \begin{pmatrix} d_1 & d_2 & \cdots & d_{n+2} \end{pmatrix}. \quad (4.69)$$

The consecutive minors of D are of course simply given by $\langle i \rangle = d_i$. The “non-consecutive minors” which also appear in the Graßmannian integral for form factors are also given by a single d_i which can be inferred from (4.51). Hence, the Graßmannian integral (4.60) becomes

$$F_{n,2} \int \frac{d^{1 \times (n+2)} D}{\text{Vol}[GL(1)]} \frac{1}{1 - \frac{d_{n+1} d_{n+2}}{d_1 d_n}} \frac{1}{d_1 \cdots d_n} \frac{1}{d_{n+1} d_{n+2}} \delta^{4|4}(D \cdot \mathcal{Z}). \quad (4.70)$$

Specializing to $n = 3$ we can write the form factor $F_{3,3}$ as

$$F_{3,3} = F_{3,2} \int \frac{d^{1 \times 5} D}{\text{Vol}[GL(1)]} \frac{\delta^{4|4}(d_1 \mathcal{Z}_1 + d_2 \mathcal{Z}_2 + d_3 \mathcal{Z}_3 + d_4 \mathcal{Z}_4 + d_5 \mathcal{Z}_5)}{\left(1 - \frac{d_4 d_5}{d_1 d_3}\right) d_1 d_2 d_3 d_4 d_5}. \quad (4.71)$$

The $GL(1)$ redundancy can be used to fix $d_5 = \langle 1234 \rangle$, and the other integration variables are completely determined by the delta functions:

$$d_1 = \langle 2345 \rangle, \quad d_2 = \langle 3451 \rangle, \quad d_3 = \langle 4512 \rangle, \quad d_4 = \langle 5123 \rangle. \quad (4.72)$$

Thus,

$$F_{3,3} = F_{3,2} \frac{[12345]}{1 - \frac{\langle 5123 \rangle \langle 1234 \rangle}{\langle 2345 \rangle \langle 4512 \rangle}}, \quad (4.73)$$

While we use a different definition of the momentum twistor variable compared to Bork (2014),¹⁵ the result numerically agrees with the one from this paper.¹⁶

For the next case, the form factor $F_{4,4}$, the Graßmannian matrix D can be gauge-fixed to

$$D = \begin{pmatrix} 1 & 0 & d_{13} & d_{14} & d_{15} & d_{16} \\ 0 & 1 & d_{23} & d_{24} & d_{25} & d_{26} \end{pmatrix}. \quad (4.74)$$

Solving the constraints imposed by the delta functions we find for the remaining entries

$$d_{i3} = -\frac{\langle i456 \rangle}{\langle 3456 \rangle}, \quad d_{i4} = +\frac{\langle i356 \rangle}{\langle 3456 \rangle}, \quad d_{i5} = -\frac{\langle i346 \rangle}{\langle 3456 \rangle}, \quad d_{i6} = +\frac{\langle i345 \rangle}{\langle 3456 \rangle}, \quad (4.75)$$

where $i = 1, 2$. Plugging this into the integral (4.60) we find

$$F_{4,4} = F_{4,2} \frac{\langle 1345 \rangle \langle 1346 \rangle \langle 1356 \rangle \langle 2346 \rangle \langle 2356 \rangle \langle 2456 \rangle [13456] [23456]}{\langle 1234 \rangle \langle 1236 \rangle \langle 3456 \rangle^2 (\langle 1246 \rangle \langle 1345 \rangle + \langle 1256 \rangle \langle 3456 \rangle)}. \quad (4.76)$$

We have successfully compared components of this expression against the results presented in Brandhuber et al. (2011).¹⁷

¹⁵ Bork, “On form factors in $\mathcal{N} = 4$ SYM theory and polytopes”, 1407.5568

¹⁶ Recall that we use the “cyclic” contour for the dual momenta instead of the periodic one, see section 4.4 and in particular figure 4.3.

¹⁷ Brandhuber, Gurdogan, Mooney, Travaglini, Yang, “Harmony of Super Form Factors”, 1107.5067

Four- and five-point NMHV using momentum twistors

Starting from the four-point NMHV form factor, the Graßmannian integral has free integration variables, and we have to evaluate it by calculating suitable residues. In particular, we have to consider multiple, cyclicly related top-forms as discussed in section 4.3. We will come back to the question of how to determine the set of residues which yield the tree-level form factor in chapter 5; here we will pick the residues simply “by hand” and focus on their actual calculation.

For arbitrary n , the form in (4.70) has poles for

$$d_i = 0, \quad i = 2, \dots, n-1, n+1, n+2, \\ d_1 = \frac{d_{n+1}d_{n+2}}{d_n}, \quad d_n = \frac{d_{n+1}d_{n+2}}{d_1}, \quad d_{n+1} = \frac{d_1d_n}{d_{n+2}}, \quad d_{n+2} = \frac{d_1d_n}{d_{n+1}}. \quad (4.77)$$

Because of the additional factor in the form (4.70) compared to the amplitude integral, we could already encounter more complicated and in particular composite residues. We find, however, that the only residues needed to reconstruct the tree-level form factors are those where a subset of the d_i 's are zero, and these can be thought of as sequentially taking residues in a single complex variable. As for amplitudes,¹⁸ these poles can be specified by the five d_i 's which remain non-zero. In contrast to the amplitude case, these always have to include d_1 and d_n , since otherwise the $\tilde{Y}/(1-\tilde{Y})$ part in (4.70) blows up.

We can distinguish two types of residues, depending on whether they involve the columns associated to the operator or not. In the first case, no residues are taken with respect to d_{n+1} and d_{n+2} . The corresponding residue then reads

$$\text{Res}_i = \frac{1}{1 - \frac{\langle n+2 \ 1 \ n \ i \rangle \langle 1 \ n \ i \ n+1 \rangle}{\langle n \ i \ n+1 \ n+2 \rangle \langle i \ n+1 \ n+2 \ 1 \rangle}} [i \ n+1 \ n+2 \ 1 \ n], \quad (4.78)$$

where $i \in \{2, \dots, n-1\}$. In the second case, at least one residue is taken with respect to either d_{n+1} or d_{n+2} . The resulting expressions are

$$\widetilde{\text{Res}}_{i,j,k} = [i \ j \ k \ 1 \ n], \quad (4.79)$$

where $i, j, k \in \{2, \dots, n-1, n+1, n+2\}$. Analogous expressions hold for the shifted top-forms, with kinematics as in figure 4.3.

Numerically comparing with the results of Bork (2014),¹⁹ we find

$$F_{4,3} = F_{4,2} \left(\text{Res}_3 + \widetilde{\text{Res}}_{2,3,5} + \text{Res}_3^{s=2} + \widetilde{\text{Res}}_{2,3,5}^{s=2} \right), \\ F_{5,3} = F_{5,2} \left(\text{Res}_4 + \widetilde{\text{Res}}_{3,4,6} + \widetilde{\text{Res}}_{2,3,6}^{s=3} + \text{Res}_3^{s=3} - \widetilde{\text{Res}}_{2,3,4} \right. \\ \left. + \widetilde{\text{Res}}_{2,3,6} + \widetilde{\text{Res}}_{3,4,7}^{s=3} - \widetilde{\text{Res}}_{2,3,4}^{s=3} + \text{Res}_5^{s=1} \right), \quad (4.80)$$

where the superscript s specifies the shift.

The previous examples show that the Graßmannian integral formulation can be used to compute form factors efficiently; we now turn to the question of determining the correct combination of residues systematically.

¹⁸ Elvang, Huang, Keeler, Lam, Olson, Roland, Speyer, “Grassmannians for scattering amplitudes in 4d $\mathcal{N} = 4$ SYM and 3d ABJM”, [1410.0621](#)

¹⁹ Bork, “On form factors in $\mathcal{N} = 4$ SYM theory and polytopes”, [1407.5568](#)

5

The BCFW contour for NMHV

As its amplitude counterpart, the Graßmannian integral for form factors (4.25) has to be considered as a contour integral. After extracting the momentum and super momentum conserving delta functions one can use the remaining delta functions to eliminate some of the integrations over the entries of the representative matrix C parametrizing the Graßmannian $G(k, n + 2)$. The remaining integrations can then be localized on the multi-variable poles of the integrand, and each such pole gives rise to a different BCFW term or leading singularity; global residue theorems¹ generate non-trivial relations between these quantities. The correct contour, i.e. the combination of residues which gives the BCFW decomposition of the tree-level amplitude or form factor, is independent data that needs to be specified. In section 4.5, we calculated some form factors by manually picking the correct combination of residues; in this chapter we want to show how to systematically determine the contour for all NMHV form factors from recursion relations and the geometries in the Graßmannian encoded by on-shell diagrams.

In order to construct this “contour”, which will be presented in equation (5.21), we need to specify the location of all poles contributing to the BCFW representation. This location is expressed as a set of minors of the Graßmannian matrix C which vanish at that point. The corresponding configuration of points can be expressed in different ways. We will see that there is a particularly convenient choice, which allows to see the general structure.

A major new challenge compared to the amplitude Graßmannian is the fact that we have to deal with multiple top-forms, i.e. top-dimensional forms on the Graßmannian, each corresponding to a diagram related to the amplitude top-cell diagram as discussed in section 3.7. Any form factor is given in terms of a sum of residues of these top-forms. For each such contributing term, we therefore not only have to specify the location of the pole, but also the top-form from which the residue is taken. This poses some interesting questions: Are the residues at a given point the same for all top-forms which contain such a pole? Can the “contour” really be interpreted as a contour, by summing multiple top-forms into a single integrand for which a single contour can be specified? Or can we merely give a prescription for taking certain terms of the BCFW sum from particular

This chapter is based on the author's publication Meidinger, Nandan, Penante, Wen, “A note on NMHV form factors from the Graßmannian and the twistor string”, 1707.00443.

¹ Griffiths, Harris, “Principles of algebraic geometry”, Wiley, New York, NY, 1994.

top-forms individually? These questions render the form factor Grassmannian integral more intricate compared to its amplitude counterpart. We think that much can be learned from this preliminary study of the NMHV case which will be of importance for higher MHV degrees, the investigation of which we leave for future work.

5.1 The NMHV top-forms

Before deriving the contour, we introduce some useful notation, which also allows to write the Grassmannian integral (4.25) for the NMHV in a compact way. Since we will have to deal with multiple top-forms, we first want to make the cyclic structure of external on-shell states (excluding the states representing the operator) more explicit. To this end, we label the columns of the C matrix corresponding to the operator (the two columns which get modified by gluing in the minimal form factor, see section 4.2) with x and y . Likewise we will label the two on-shell momenta that parametrize the off-shell momentum q in this way, in particular we call the reference spinors simply λ_x and λ_y .

Extending a widely used notation,² we denote consecutive minors by a single label, and write minors which contain both columns x and x using the single remaining label and underlining it,

$$\begin{aligned} (i) &:= (i \ i+1 \ i+2), \\ \underline{(i)} &:= (ixy). \end{aligned} \tag{5.1}$$

This notation is useful in order to express the contour in a way which respects the actual ordering of the external states, in which x and y do not participate. Here and in the rest of this chapter, we therefore also cyclicly identify the labels of the external on-shell states.

For NMHV, we can represent the $Y/(1-Y)$ part of the Grassmannian form (4.24) using intersections of lines in \mathbb{CP}^2 . Interpreting the columns C_i of the matrix C as homogeneous coordinates of points in \mathbb{CP}^2 , we write the intersection of lines (ij) and (kl) as

$$(ij) \cap (kl) := C_i(jkl) - C_j(ikl), \tag{5.2}$$

and thus define the intersection “minor”

$$(rs(ij) \cap (kl)) = (rsi)(jkl) - (rsj)(ikl). \tag{5.3}$$

It is zero if the three lines (rs) , (ij) and (kl) intersect, and only depends on the orientation of these lines,

$$\begin{aligned} (rs(ij) \cap (kl)) &= (kl(rs) \cap (ij)) = (ij(kl) \cap (rs)) \\ &= -(kl(ij) \cap (rs)) = -(ij(rs) \cap (kl)) = -(rs(kl) \cap (ij)), \end{aligned} \tag{5.4}$$

which can be shown using Plücker relations.

² See for example Arkani-Hamed, Bourjaily, Cachazo, Trnka, “Unification of Residues and Grassmannian Dualities”, 0912.4912 and Bourjaily, Trnka, Volovich, Wen, “The Grassmannian and the Twistor String: Connecting All Trees in $\mathcal{N} = 4$ SYM”, 1006.1899.

Using these notations, we can write the Graßmannian integral for NMHV form factors, with arbitrary shifts s , i.e. insertion positions of the operators, as

$$\mathcal{G}_{n,3[s]}^F = \langle xy \rangle^2 \int \frac{d^{3 \times (n+2)} C}{\text{Vol}[GL(k)]} \frac{\delta^{2 \times 3}(C \cdot \tilde{\lambda}) \delta^{4 \times 3}(C \cdot \tilde{\eta}) \delta^{2 \times (n-1)}(C^\perp \cdot \underline{\lambda})}{[(1) \cdots (n-2) (\underline{1})(\underline{n}) (xy(n-1 \ n) \cap (12))]_{\sigma_s}} \quad (5.5)$$

where σ_s is a cyclic shift by s in the on-shell labels,

$$\sigma_s = \begin{pmatrix} 1 & 2 & \cdots & n-1 & n & x & y \\ \downarrow & \downarrow & & \downarrow & \downarrow & \downarrow & \downarrow \\ 1+s & 2+s & & n-1+s & n+s & x & y \end{pmatrix} \quad \text{with } i+n \simeq i \quad (5.6)$$

which permutes these labels in the integrand of (5.5). Note that the only non-consecutive minors in this expression (in the sense of the color ordering, see (5.1)) stem from the “minor” of type (5.3) that contains the intersection of lines.

5.2 Extracting the geometry from diagrams

Given an (amplitude) on-shell diagram, with an associated decorated permutation $\sigma(i) \geq i$, we can determine the corresponding constraints on the representative matrix C in the Graßmannian as follows:³ If we interpret the columns of C as points in \mathbb{CP}^{k-1} , then the permutation $\sigma(i)$ labels the first column (in cyclic order) such that

$$C_i \in \text{span} \{C_{i+1}, \dots, C_{\sigma(i)}\}. \quad (5.7)$$

For NMHV this means that

$$\sigma(i) = i+2 \implies (i \ i+1 \ i+2) = 0, \quad (5.8)$$

and this is enough to specify a contour of integration in the Graßmannian as a torus around a point where a set of minors vanishes.⁴ We will denote a residue at a pole where the minors (i_1) up to (i_{n-3}) vanish by $\{(i_1), \dots, (i_{n-3})\}$. Any combination of such residues simultaneously define a contour in the Graßmannian.

For form factor diagrams we adopt a strategy which makes use of the relation with amplitude diagrams discussed in section 3.6 and the gluing procedure of section 4.2: We will simply replace the minimal form factor in the diagram by a box diagram, and then read off the permutation and the configuration in the Graßmannian. This works, because any constraints which do not involve the two columns corresponding to the operator insertion are also present in the purely on-shell part of the form factor diagram, with the minimal form factor removed. This smaller diagram however has more such constraints, since it corresponds to a cell in the Graßmannian with two degrees of freedom less. Gluing in the box precisely removes these spurious restrictions.

³ Arkani-Hamed, Bourjaily, Cachazo, Goncharov, Postnikov, Trnka, “Scattering Amplitudes and the Positive Grassmannian”, Cambridge University Press, 2016, [1212.5605](#)

⁴ For higher k degree, it is necessary to consider so-called composite residues, for which minors factorize on the zero locus of others.

The BCFW recursion relations (3.10) for NMHV take the following form:

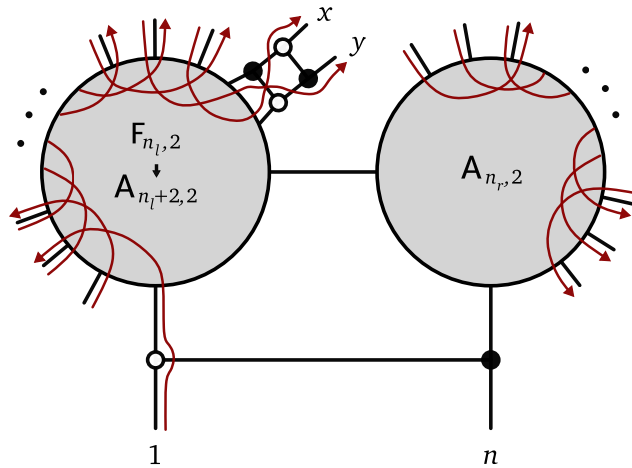
$$F_{n,3} = \sum_{n_l=2}^{n-2} \left[\text{Diagram 1} \right] + \sum_{n_l=3}^n \left[\text{Diagram 2} \right] + \left[\text{Diagram 3} \right] \quad (5.9)$$

where $n_r = n - n_l + 2$. Without loss of generality, and in order to make a comparison with amplitudes easier, we choose to use the common BCFW shift at legs n and 1 . We will discuss these three types of terms separately, reading off the configuration of points and thus obtaining the set of poles which have to be included in the contour. Of course, the last term in (5.9) is recursive, and we will give an explicit solution to this recursion afterwards.

MHV form factor \times MHV amplitude

We first consider the diagrams in (5.9) which have an MHV form factor on the left side of the factorization and an MHV amplitude on the right. If we replace the minimal form factor by a four-point amplitude, we can read off the permutation as shown in figure 5.1.

Figure 5.1: A type of on-shell diagram contributing to the NMHV form factor with n external legs. The form factor factorizes into a lower point MHV form factor and an MHV amplitude with $n_r = n - n_l + 2$ external legs. The minimal form factor has been replaced by a box, with on-shell legs x and y parametrizing the kinematics of the operator. Left-right paths indicating the associated permutation are sketched in red. Only paths going from i to $i + 2$ are shown.



Because the permutations associated to the two MHV subdiagrams are given by $\sigma_{l/r}(i) = i + 2$, each forces the C_i connected to its external states to lie on a line. More concretely, we see from the left part of figure 5.1 that C_1 up to C_{n_l-1} lie all on the line (xy) , which enforces the vanishing of the minors $(\underline{1})$ to $(\underline{n_l - 1})$:

$$\begin{array}{c} x & y & 1 & \cdots & n_l - 1 \\ \hline \bullet & \bullet & \bullet & & \bullet \end{array} \longrightarrow (\underline{1}), \dots, (\underline{n_l - 1}) = 0 \quad (5.10)$$

From the right hand side of figure 5.1, we can read off the collinearity of C_{n_l} to

C_{n-1} which implies that the following minors vanish:

$$\begin{array}{ccccccc} n_l & n_l + 1 & \cdots & n-2 & n-1 & & \\ \bullet & \bullet & & \bullet & \bullet & & \end{array} \longrightarrow (n_l), \dots, (n-3) = 0 \quad (5.11)$$

This gives $n - 3$ residues of the form

$$\{(\underline{1}), \dots, (\underline{n_l - 1}), (n_l), \dots, (n-3)\}, \quad \text{for } n_l = 2, \dots, n-2. \quad (5.12)$$

Since the MHV form factor is cyclicly invariant, for each term we can take the residue from any top-form with a shift of

$$s = 0, 1, \dots, n_l - 1. \quad (5.13)$$

Strictly speaking, the cyclicity of the MHV form factor only implies possible shifts from 1 to $n_l - 1$;⁵ we nevertheless have checked that a shift of zero also produces the correct result. This follows from the consistency of the set of all possible BCFW shifts. Moreover, we note that the top-forms with these shifts are exactly those which contain a pole of the given form.

⁵ A shift of 0 has the minimal form factor between particle n and particle 1 which is – diagrammatically – incompatible with our choice of BCFW shift.

MHV amplitude \times MHV form factor

We can repeat this analysis for the diagrams where the MHV amplitude is on the left and the MHV form factor on the right side of the factorization. These diagrams and their left-right path structure are displayed in figure 5.2.

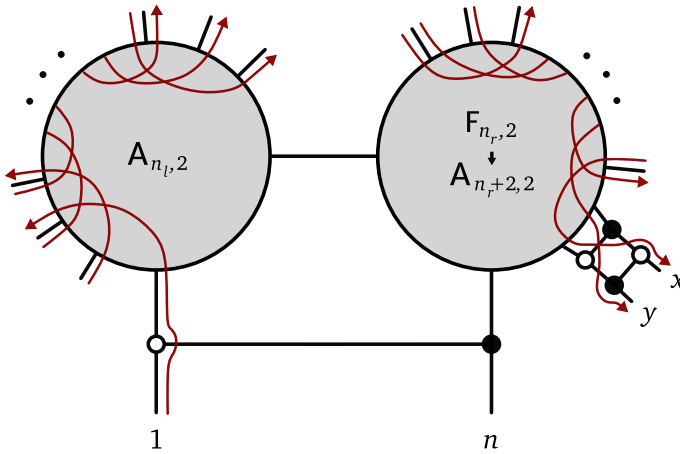


Figure 5.2: The on-shell diagrams of factorization channels of the form factor $F_{n,3}$ with a lower point MHV amplitude on the left and an MHV form factor on the right, with $n_r = n - n_l + 2$. The minimal form factor has been replaced by a box, with on-shell legs x and y parametrizing the kinematics of the operator. Left-right paths indicating the associated permutation are sketched in red. Only paths going from i to $i + 2$ are shown.

Similar to the form factor \times amplitude case, the subdiagrams force the points C_i to lie on two lines, each corresponding to one of the subdiagrams:

$$\begin{array}{ccccccc} 1 & 2 & \cdots & n_l - 1 & & & \\ \bullet & \bullet & & \bullet & & & \end{array} \longrightarrow (1), \dots, (n_l - 3) = 0 \quad (5.14)$$

for the amplitude and

$$\begin{array}{ccccccc} x & y & n_l & \cdots & n-1 & & \\ \bullet & \bullet & \bullet & & \bullet & & \end{array} \longrightarrow (n_l), \dots, (n-1) \quad (5.15)$$

for the form factor. This give $n - 2$ terms with poles

$$\{(1), \dots, (n_l - 3), (\underline{n_l}), \dots, (\underline{n-1})\}, \quad \text{for } n_l = 3, \dots, n, \quad (5.16)$$

and possible shifts

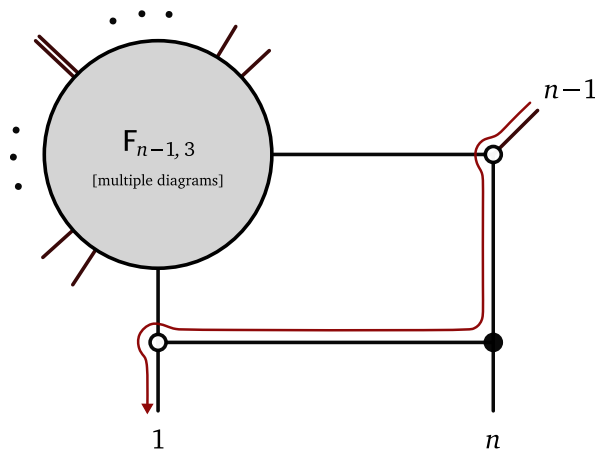
$$s = \begin{cases} n_l - 1, \dots, n - 1 & \text{for } n_l = 3, \dots, n - 1 \\ 0, n - 1 & \text{for } n_l = n \end{cases}, \quad (5.17)$$

which again follow from the cyclicity of the sub form factor. We also note that the shift $s = 0$ does not follow from these diagrammatic considerations, but was checked in a number of cases to also work. Furthermore these shifts give again *all* top-forms which contain the respective pole.

Lower point NMHV form factor

The last term in (5.9) is the most interesting one, since it contains the lower point form factor $F_{n-1,3}$, which itself will be given in terms of a sum of diagrams. Diagrammatically, it is just the inverse soft limit of the $n - 1$ point NMHV form factor, with the k -preserving inverse soft factor, introduced in section 3.4, attached. See figure 5.3 for a sketch of the diagrams.

Figure 5.3: The recursive on-shell diagram contributing to the form factor $F_{n,3}$. The lower point NMHV form factor $F_{n-1,3}$, which itself is given in terms of multiple diagrams, is extended by an inverse soft factor, which contributes an additional vanishing minor $(n - 1)$ to the configuration of the subdiagrams.



For each term in the sub form factor $F_{n-1,3}$, this additional inverse soft factor imposes $(n - 1) = 0$, in addition to the vanishing minors of the lower point form factor:

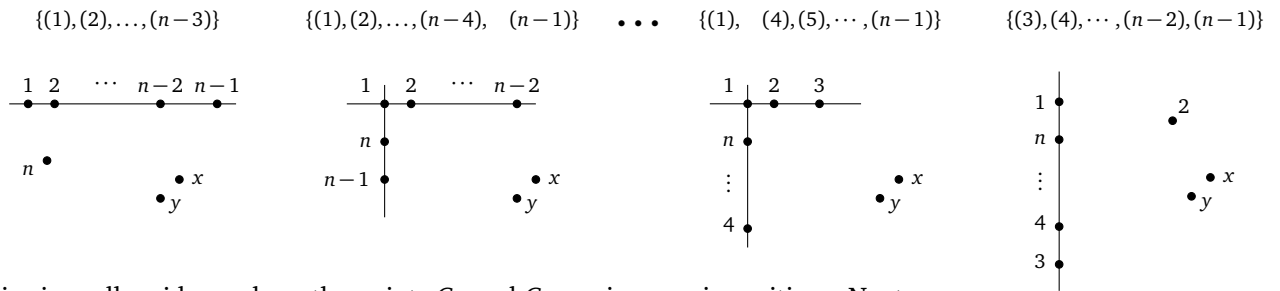
$$\sum_{\text{subdiagrams}} \{\text{poles of subdiagram}\} \cup \{(n - 1)\} \quad (5.18)$$

Note that the possible shifts are inherited from the subdiagram.

5.3 The contour in closed form

Because of the recursive nature of the terms corresponding to a sub NMHV form factor, we haven't obtained a closed expression for the "contour" yet. We can however solve this recursion, as we explain now, by enumerating all configurations which contribute. For this, take the set of numbers $1, \dots, n-1$. These are the labels that can appear either as (i) or (\underline{i}) , since (n) and (\underline{n}) never appear. Now sum over all possibilities to remove two consecutive labels; this splits the set into two, $\{1, \dots, k\}$ and $\{k+3, \dots, n-1\}$, and gives the residues shown in figure 5.4 together with the corresponding configurations of points C_i .

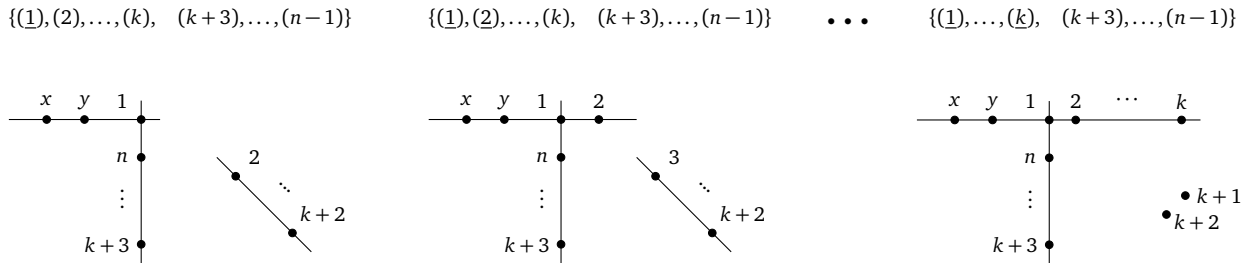
Figure 5.4: All residues contributing to $F_{n,3}$, with poles not involving the columns x and y , and the configurations they represent.



This gives all residues where the points C_x and C_y are in generic positions. Next, for each of these terms, we add further residues, which all impose restrictions on these two columns, by replacing poles (i) by (\underline{i}) .

We first sum over all sets of minors which have the first minors of the set $\{1, \dots, k\}$, those below the gap of two missing labels, replaced by their underlined versions, as shown in figure 5.5:

Figure 5.5: Set of residues and corresponding configuration where the points C_x and C_y align with the points with labels $\leq k$.



Then we do the same for the second subset of labels, those above the gap, again changing the (i) minors to (\underline{i}) one at a time, see figure 5.6:

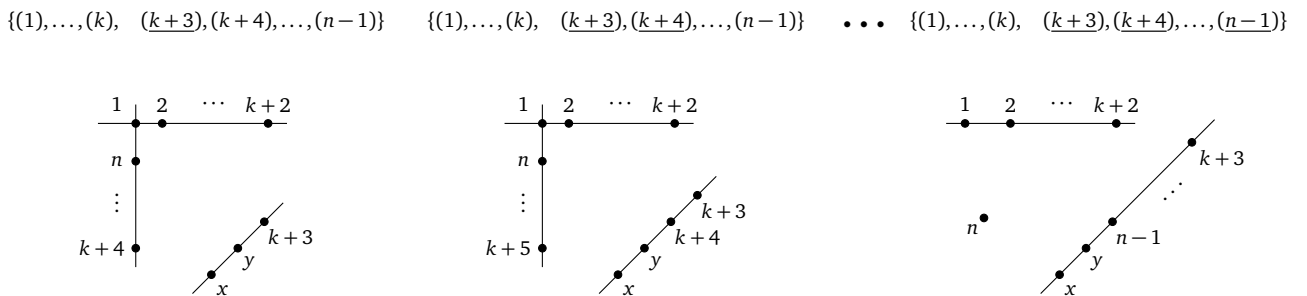


Figure 5.6: Set of residues and corresponding configuration where the points C_x and C_y align with the points with labels $\geq k+3$.

In total, this gives all $(n-2)^2$ terms. Note that all configurations belong to the inverse soft term in (5.9), unless no constraints are imposed on the point n .

$F_{4,3}$	$\{\underline{(1)}\}$ $s = 0, 1$ $F_{2,2} \times A_{4,2}$	$\{(1)\}$ $s = 0, 3$ $A_{4,2} \times F_{2,2}$		
	$\{(3)\}$ $s = 1, 2$ $F_{3,3} \times A_{3,1}$	$\{\underline{(3)}\}$ $s = 2, 3$ $A_{3,2} \times F_{3,2}$		
$F_{4,3}$	$\{(1), (2)\}$ $s = 0, 1, 2$ $F_{3,2} \times A_{4,2}$	$\{(1), (2)\}$ $s = 0, 1$ $F_{2,2} \times A_{5,2}$	$\{(1), (2)\}$ $s = 0, 4$ $A_{5,2} \times F_{2,2}$	
	$\{(1), (4)\}$ $s = 0, 1$	$\{(1), (4)\}$ $s = 0, 3$	$\{(1), (4)\}$ $s = 3, 4$ $A_{4,2} \times F_{3,2}$	
	$\{(3), (4)\}$ $s = 1, 2$	$\{(3), (4)\}$ $s = 2, 3$	$\{(3), (4)\}$ $s = 2, 3, 4$ $A_{3,2} \times F_{4,2}$	
	$F_{4,3} \times A_{3,1}$			
$F_{6,3}$	$\{(1), (2), (3)\}$ $s = 0, 1, 2, 3$ $F_{4,2} \times A_{4,2}$	$\{(1), (2), (3)\}$ $s = 0, 1, 2$ $F_{3,2} \times A_{5,2}$	$\{(1), (2), (3)\}$ $s = 0, 1$ $F_{2,2} \times A_{6,2}$	$\{(1), (2), (3)\}$ $s = 0, 5$ $A_{6,2} \times F_{2,2}$
	$\{(1), (2), (5)\}$ $s = 0, 1, 2$	$\{(1), (2), (5)\}$ $s = 0, 1$	$\{(1), (2), (5)\}$ $s = 0, 4$	$\{(1), (2), (5)\}$ $s = 4, 5$ $A_{5,2} \times F_{3,2}$
	$\{(1), (4), (5)\}$ $s = 0, 1$	$\{(1), (4), (5)\}$ $s = 0, 3$	$\{(1), (4), (5)\}$ $s = 3, 4$	$\{(1), (4), (5)\}$ $s = 3, 4, 5$ $A_{4,2} \times F_{4,2}$
	$\{(3), (4), (5)\}$ $s = 1, 2$	$\{(3), (4), (5)\}$ $s = 2, 3$	$\{(3), (4), (5)\}$ $s = 2, 3, 4$	$\{(3), (4), (5)\}$ $s = 2, 3, 4, 5$ $A_{3,2} \times F_{5,2}$
	$F_{5,3} \times A_{3,1}$			

Figure 5-7:

Poles contributing to the four, five and six-point NMHV form factor. The corresponding factorization channels are indicated in blue, and we list all possible values of the shift s , which labels the Grassmannian top-forms featuring the respective pole. The blue boxes contain the poles from the inverse soft limit of the lower-point form factor, which share the vanishing minor $(n-1)$, and otherwise are given by the contour of $F_{n-1,3}$.

We can specify this set of residues, or “contour”, in a more compact way if we define the individual residues as

$$R_k^{i_1 i_2} := \left\{ \underbrace{(1), \dots, (i_1)}_{i_1}, \underbrace{(i_1 + 1), \dots, (k)}_k, \right. \\ \left. \underbrace{(k + 3), \dots, (k + i_2 + 2)}_{i_2}, \underbrace{(k + i_2 + 3), \dots, (n - 1)}_{n-k-3} \right\} \quad (5.19)$$

For each term, one can take the residue from any top-form (using any shift), as long as this form has a pole at the desired configuration. To be explicit, we can summarize these possible choices as follow:

$$\begin{aligned} R_k^{i_1 0} &: s = 0, 1, \dots, i_1 \\ R_k^{0 i_2} &: s = k + 2, \dots, k + 2 + i_2 \\ R_0^{00} &: s = 1, 2 \\ R_{n-3}^{00} &: s = 0, n - 1 \\ R_k^{00} &: s = k + 2 \end{aligned} \quad (5.20)$$

We then find the following BCFW representation of NMHV form factors, which simultaneously defines the contour in the Graßmannian:

$$F_{n,3} = \sum_{k=0}^{n-3} \left[R_k^{00} + \sum_{i_1=1}^k R_k^{i_1 0} + \sum_{i_2=1}^{n-k-3} R_k^{0 i_2} \right]. \quad (5.21)$$

The fact that this set of poles solves the recursive structure imposed by the diagrams can best be understood by sorting the poles into an $(n-2) \times (n-2)$ grid as exemplified in figure 5.7. In each row we collect the residues with the same labels for the poles. These are sorted starting from the residue with all poles in the first set $1, \dots, k$ of type (\cdot) and ending with those where all poles in the second set $k + 3, \dots, n - 1$ are of this type. The rows are sorted according to the labels they do not contain, the first row omits the labels $n - 2$ and $n - 1$, the last row comes without 1 and 2. In this way, one can identify all the MHV \times MHV factorization channels (the upper row and the right column of the grid), as well as the recursive, inverse soft terms: residues coming from sub NMHV form factors form a sub-grid in the lower left, with the poles from this subdiagram combined with the new constraint $(n - 1) = 0$. This sub-grid has the same structure and in turn contains the MHV \times MHV row and column, as well as a sub-grid corresponding to $F_{n-2,3}$, and so on. We also note that this contour bears some similarity to the “even-odd” contour for NMHV amplitudes.⁶

We can also answer one of the questions posed at the beginning of this chapter: Is the “contour” for the form factor Graßmannian integral really a contour, i.e. can we combine multiple top-forms (4.24) under a single integral, and specify the contour as picking out certain poles? It turns out that this not possible. Consider the examples shown in figure 5.7. Whatever sum of top-forms we use,

⁶ See Arkani-Hamed, Cachazo, Cheung, Kaplan, “A Duality For The S Matrix”, 0907.5418; note that due to our choice of BCFW bridge, the contour is actually more akin to the (P)BCFW “odd-even” contour.

we cannot make all poles appear the same number of times, starting from five points. We are thus forced to conclude that in order to get tree-level form factors from the Grassmannian integral, we have to manually pick different residue from different, cyclicly related top-forms.

To summarize, we have shown that the contour for the form factor Grassmannian integral is much more involved compared to its amplitude counterpart. Beyond NMHV, the strategy used here could be pursued, using the BCFW recursion relations and reading off the configuration in the Grassmannian, but the combinatorics will be more complicated, and as discussed above, one will have to deal with composite residues. For amplitudes a different strategy was more successful: the Grassmannian integral was related to the connected formula coming from the twistor string formulation of particle scattering, which directly provides a description of the contour.⁷ Recently, a connected formula was proposed for form factors; in the next chapter we will investigate the connection to the Grassmannian integral in detail.

⁷ Nandan, Volovich, Wen, “A Grassmannian Étude in NMHV Minors”, [0912.3705](#); Arkani-Hamed, Bourjaily, Cachazo, Trnka, “Unification of Residues and Grassmannian Dualities”, [0912.4912](#); and Bourjaily, Trnka, Volovich, Wen, “The Grassmannian and the Twistor String: Connecting All Trees in $\mathcal{N} = 4$ SYM”, [1006.1899](#)

6

The Grassmannian and the connected prescription

In the last chapter, we determined the contour, i.e. the correct combination of residues, which allows to calculate NMHV form factors from the Grassmannian integral representation developed in chapter 4. It can in principle be obtained for any form factor, employing the same strategy as for NMHV: drawing all on-shell diagrams which are generated from the BCFW recursion relations, and subsequently finding the respective configuration in the Grassmannian. Starting from N^2 MHV, this method however becomes very tedious. The number of terms in the recursion rapidly grows, and the configurations become more involved, as composite residues start to appear. From a formal perspective, it would furthermore be desirable to have a closed form of the contour, from which the BCFW representation simply follows.

For scattering amplitudes, the contour for any tree-level amplitude was determined from representations of the amplitudes based on Witten's twistor string.¹ While Witten only considered MHV amplitudes in generality, the construction was soon generalized to all NMHV amplitudes and beyond in Roiban et al. (2004); Roiban and Volovich (2004); Roiban et al. (2004).² These works in particular derived formulas which expressed the localization of amplitudes in twistor space in terms of momentum space spinor-helicity variables. So-called link variables then allowed to write these connected prescription formulas as integrals over Grassmannians.³ Contrary to the Grassmannian integral, this representation came with an explicit contour, enforced by delta functions, which left no free integration variables. On the other hand, the integrand of this formula was superficially very different. The contour for the NMHV case was already known however. This was used in Nandan et al. (2010)⁴ to relate the two formulations for this MHV degree by a one-parameter deformation. Finally, generalizing this strategy then allowed to write down the contour for all amplitudes.⁵

Very recently a connected formula for the form factors of the chiral stress-tensor multiplet in $\mathcal{N} = 4$ SYM has been conjectured in He and Liu (2016); Brandhuber et al. (2016).⁶ An attempt in the latter work to relate this formula to the Grassmannian integral representation failed for all but the simplest cases, despite the fact that both representations lead to the correct results.

This chapter is based on the author's publication Meidinger, Nandan, Penante, Wen, "A note on NMHV form factors from the Grassmannian and the twistor string", 1707.00443.

- 1 Witten, "Perturbative gauge theory as a string theory in twistor space", [hep-th/0312171](#)
- 2 Roiban, Spradlin, Volovich, "A Googly amplitude from the B model in twistor space", [hep-th/0402016](#); Roiban, Volovich, "All conjugate-maximal-helicity-violating amplitudes from topological open string theory in twistor space", [hep-th/0402121](#); and Roiban, Spradlin, Volovich, "On the tree level S matrix of Yang-Mills theory", [hep-th/0403190](#)
- 3 Dolan, Goddard, "Gluon Tree Amplitudes in Open Twistor String Theory", [0909.0499](#); and Spradlin, Volovich, "From Twistor String Theory To Recursion Relations", [0909.0229](#)
- 4 Nandan, Volovich, Wen, "A Grassmannian Étude in NMHV Minors", [0912.3705](#)
- 5 Arkani-Hamed, Bourjaily, Cachazo, Trnka, "Unification of Residues and Grassmannian Dualities", [0912.4912](#); and Bourjaily, Trnka, Volovich, Wen, "The Grassmannian and the Twistor String: Connecting All Trees in $\mathcal{N} = 4$ SYM", [1006.1899](#)
- 6 He, Liu, "A note on connected formula for form factors", [1608.04306](#); and Brandhuber, Hughes, Panerai, Spence, Travaglini, "The connected prescription for form factors in twistor space", [1608.03277](#)

In this chapter we investigate the relation between the two Graßmannian formulations of form factors in more detail. The NMHV contour from the last chapter provides important input data for this program, which aims both at a better understanding of the various representations of form factors, as well as making progress towards a general contour. After reviewing the connected prescription for form factors in section 6.1, we consider the NMHV case and lift the formula to a $GL(3)$ invariant Graßmannian integral in section 6.2. Subsequently we show that this integral can be rewritten in a way which closely mirrors the integral for amplitudes, giving the formula a recursive structure which makes its origin in terms of inverse soft factors manifest. Section 6.3 then investigates the relation between the two approaches, considering some low-point examples in detail. Remarkably, these examples show that the methods which were used for amplitudes do not allow to relate the integral for form factors. Since we can pinpoint where problems arise, the results of this chapter provide a good starting point to investigate the different representation in more detail; this should enable a better understanding of both formulations, and for on-shell representations of partially off-shell quantities more generally.

6.1 Brief review of the connected prescription for form factors

In analogy with the amplitude connected prescription, Brandhuber et al. (2016)⁷ and He and Liu (2016)⁸ obtained a similar formula for form factors of the chiral part of the stress tensor multiplet. This representation was given an ambitwistor string interpretation in Bork and Onishchenko (2017).⁹ Our notation here will follow chapter 5: we add to the set of n on-shell states two additional particles labeled by x and y . Then, for a helicity sector with Graßmann degree $4k$ one chooses k labels from the set $\{1, \dots, n\}$ to form the set m , indexed by upper case letters $I = \{i_1, \dots, i_k\}$. The remaining $n + 2 - k$ labels (which always contain x and y) form the set \bar{p} , labeled by lower case letters i . The set p is the same as \bar{p} with x and y removed. Using this notation, the form factor connected formula reads

$$F_{n,k} = \langle xy \rangle^2 \int \frac{1}{\text{Vol}(GL(2))} \frac{d^2\sigma_x d^2\sigma_y}{(xy)^2} \prod_{a=1}^n \frac{d^2\sigma_a}{(a a + 1)} \\ \times \prod_{i \in \bar{p}} \delta^2(\lambda_i - \lambda(\sigma_i)) \prod_{I \in m} \delta^2(\tilde{\lambda}_I - \tilde{\lambda}(\sigma_I)) \delta^4(\tilde{\eta}_I - \tilde{\eta}(\sigma_I)), \quad (6.1)$$

where (σ_a^1, σ_a^2) are homogeneous coordinates in \mathbb{CP}^1 , $(ab) = \epsilon_{\alpha\beta} \sigma_a^\alpha \sigma_b^\beta$, and

$$\lambda(\sigma_I) = \sum_{i \in \bar{p}} \frac{1}{(Ii)} \lambda^i, \quad \tilde{\lambda}(\sigma_I) = - \sum_{I \in m} \frac{1}{(Ii)} \tilde{\lambda}^I, \quad \tilde{\eta}(\sigma_I) = - \sum_{I \in m} \frac{1}{(Ii)} \tilde{\eta}^I. \quad (6.2)$$

As is the case with scattering amplitudes, one can go from the connected prescription to the link representation by introducing link variables¹⁰ c_{Ij} , and imposing $c_{Ij} = \frac{1}{(Ij)}$ as additional equations.¹¹ The advantage of using these vari-

7 Brandhuber, Hughes, Panerai, Spence, Travaglini, “The connected prescription for form factors in twistor space”, 1608.03277

8 He, Liu, “A note on connected formula for form factors”, 1608.04306

9 Bork, Onishchenko, “Four dimensional ambitwistor strings and form factors of local and Wilson line operators”, 1704.04758

10 Arkani-Hamed, Cachazo, Cheung, Kaplan, “The S-Matrix in Twistor Space”, 0903.2110

11 Spradlin, Volovich, “From Twistor String Theory To Recursion Relations”, 0909.0229; and Dolan, Goddard, “Gluon Tree Amplitudes in Open Twistor String Theory”, 0909.0499

ables is that the equations (6.2) become linear. For form factors this results in the expression

$$F_{n,k} = \langle xy \rangle^2 \int \prod_{I \in \mathfrak{m}, j \in \bar{\mathfrak{p}}} dc_{Ij} U(c_{Ij}) \prod_{i \in \bar{\mathfrak{p}}} \delta^2(\lambda_i - c_{Ii} \lambda_i) \prod_{I \in \mathfrak{m}} \delta^2(\tilde{\lambda}_I + c_{Ii} \tilde{\lambda}_i) \delta^4(\tilde{\eta}_I + c_{Ii} \tilde{\eta}_i), \quad (6.3)$$

with the integrand given by

$$U(c_{Ii}) = \int \frac{1}{\text{Vol}(GL(2))} \frac{d^2\sigma_x d^2\sigma_y}{(xy)^2} \prod_{a=1}^n \frac{d^2\sigma_a}{(a a + 1)} \prod_{I \in \mathfrak{m}, i \in \bar{\mathfrak{p}}} \delta\left(c_{Ii} - \frac{1}{(Ii)}\right). \quad (6.4)$$

Note that although (6.3) carries the degrees of freedom of a $G(k, n+2)$ Graßmannian formula, all integration variables are fixed by the delta functions. Similarly to what was done for scattering amplitudes in, we will now lift this formulation in the NMHV case to a fully $GL(3)$ invariant Graßmannian formulation by performing the σ integrations.

6.2 Graßmannian integrals from the connected prescription

In the following we will focus on NMHV form factors with $k=3$, and write (6.3) with the integrand (6.4) in the form of a $GL(3)$ invariant Graßmannian integral, with no free integration variables. Indeed, while the explicit delta functions of (6.3) can only fix $2n$ out of the $3(n-1)$ integration variables c_{Ii} , the function $U(c_{Ij})$ provides precisely the additional $n-3$ constraints required to solve for all c_{Ij} . After solving $2n$ out of the $3n-3$ constraints imposed by the delta functions of (6.4), there are no integrations over the variables σ_a left. It is then straightforward to restore $GL(3)$ invariance, simply by replacing the link variables in the resulting integrand by corresponding 3×3 minors. A dependence on the minor involving the three gauge fixed columns cannot be restored in this way, but it can be inferred by requiring the correct scaling of the formula under $GL(3)$ transformations.

The $n-3$ remaining delta functions in $U(c_{Ij})$, evaluated on the support of the delta functions involving the kinematics, generate constraints depending on six points each. These equations, when written in terms of $GL(3)$ minors, have the general form $\delta(S_{i_1 i_2 i_3 i_4 i_5 i_6})$, where

$$S_{i_1 i_2 i_3 i_4 i_5 i_6} \equiv (i_1 i_2 i_3)(i_3 i_4 i_5)(i_5 i_6 i_1)(i_2 i_4 i_6) - (i_2 i_3 i_4)(i_4 i_5 i_6)(i_6 i_1 i_2)(i_3 i_5 i_1). \quad (6.5)$$

The equations $S=0$ are the same that feature for scattering amplitudes, and are in general polynomials of degree four in the link variables. Their geometric meaning was discussed in Arkani-Hamed et al. (2011);¹² the localization of N^k MHV scattering amplitudes on degree $(k-1)$ -curves in twistor space, as in Witten's twistor string theory, has a counterpart as a localization in the Graßmannian. Namely, by viewing each column in the matrix $C \in G(k, n+2)$ as a point in

¹² Arkani-Hamed, Bourjaily, Cachazo, Trnka, "Unification of Residues and Grassmannian Dualities", 0912.4912

$\mathbb{C}\mathbb{P}^{k-1}$, each column must be the image of a map $\mathbb{C}\mathbb{P}^1 \mapsto \mathbb{C}\mathbb{P}^{k-1}$, generally given by the Veronese map

$$(\sigma^1, \sigma^2) \mapsto ((\sigma^1)^{k-1}, (\sigma^1)^{k-2}\sigma^2, \dots, \sigma^1(\sigma^2)^{k-2}, (\sigma^2)^{k-1}). \quad (6.6)$$

For $k = 3$ this corresponds to a map of degree two, and the constraints must ensure that all $n + 2$ points lie on the same curve. This is achieved by a combination of equations of the form (6.5), which impose that a sixth point lies on the degree-two curve generated by the other five. For this reason, we refer to these equations as conic constraints. It is straightforward to see that, if a matrix $C \in G(3, n + 2)$ has all columns as in (6.6), all equations (6.5) trivially vanish since the 3×3 minors factorize in terms of 2×2 minors formed of the σ coordinates as $(abc) = (ab)(bc)(ca)$.

Performing an explicit lift of (6.3) from the link representation to an integral over $GL(3)$ for low values of n reveals a recursive structure in which the n -point form factor is obtained from the $(n - 1)$ -point one as follows:

$$\begin{aligned} F_{n,3} &= \langle xy \rangle^2 \int \frac{d^{3 \times (n+2)} C}{\text{Vol}(GL(3))} I_{n,3} \delta^{2 \times 3}(C \cdot \tilde{\lambda}) \delta^{4 \times 3}(C \cdot \tilde{\eta}) \delta^{2 \times (n-1)}(C^\perp \cdot \lambda), \\ I_{4,3} &= \frac{(13x)(13y)}{(123)(134)(1xy)(3xy)} \delta(S_{1234xy}), \\ I_{n,3} &= I_{n-1,3} \times \left[(-1)^{n-1} \frac{(12n-1)(13n-1)(1xy)(23x)(23y)}{(1n-1n)(23n-1)} \delta(S_{123nxy}) \right], \end{aligned} \quad (6.7)$$

Note that the conic constraints imposed by the delta functions ensure the cyclic invariance of these expressions.

There are several ways of representing the integrand of (6.7), all coinciding on the support of the conic constraints. Likewise, the choice of equations appearing inside the delta functions is not unique as the geometric constraint that the $n + 2$ points lie on the same degree-two curve can be represented in various distinct ways. For the particular representation in (6.7), we consider the conic defined by the five points $\{1, 2, 3, x, y\}$ and each conic constraint imposes that one of the other points $\{4, \dots, n\}$ lie on the same curve, as can be seen from the additional constraints present in each recursive factor. The minors appearing in the numerator of the recursive factor are responsible for annihilating spurious solutions of the conic constraints. For instance, a configuration where four out of the points in the set $\{1, 2, 3, x, y\}$ are collinear would set to zero all conic constraints, but would not imply that all points lie on the same curve. The numerator factor $(13x)(13y)(23x)(23y)(1xy)$ precisely vanishes for every configuration of this sort. A special case where the cancellation of spurious singularities does not happen is for $n = 5$, since the factor of $(1xy)$ cancels between $I_{4,3}$ and the recursive factor in (6.7). In this case, one needs to ensure that only the physical solutions of the conic constraints are taken into account. This situation is discussed in further detail in section 6.3.

Formulation with inverse soft interpretation

For scattering amplitudes, it is possible to interpret the recursive factors I_n/I_{n-1} as the addition of a particle via an inverse soft factor.¹³ The same should be true for form factors, as they are inverse soft constructible.¹⁴ In particular, we will now show that for form factors with sufficiently many on-shell legs, namely six, the effect of the operator may be omitted and it is possible to write the recursive factor of (6.7) in the same way as for amplitudes. This is achieved by rewriting (6.7) by means of the identity

$$\delta(S_{ijk_rst})\delta(S_{ijk_rsu}) = \frac{(jkt)(irt)}{(jks)(irs)} \delta(S_{ijk_rst})\delta(S_{ijk_rtu}). \quad (6.8)$$

We start by considering the ratio $I_{5,3}/I_{4,3}$, and trade $S_{123xy5} \rightarrow S_{123x45}$ on the support of $S_{1234xy} = 0$ using (6.8). This results in

$$I_{5,3}/I_{4,3} = \frac{(124)(134)(23x)(1x4)}{(145)} \delta(S_{123x45}). \quad (6.9)$$

This factor is already much more similar to the amplitude “soft factor”, but it is clear that either x or y , representing the kinematics of the operator, has to participate in each conic constraints. Next we consider $I_{6,3}/I_{5,3}$. We first trade y in S_{123xy6} for 4 using S_{1234xy} , then we can use S_{123x45} from the last step to trade $x \rightarrow 5$. Thus we get

$$I_{6,3}/I_{5,3} = \frac{(125)(135)(234)(145)}{(156)} \delta(S_{123456}), \quad (6.10)$$

which is precisely the recursive factor which maps $A_{5,3}$ to $A_{6,3}$.

We can now proceed recursively, and find that also for higher point form factors the recursive structure of the integrand can be written in exactly the same way as for amplitudes,

$$I_{n,3}/I_{n-1,3} = \frac{(12n-1)(13n-1)(1n-2n-1)(23n-2)}{(1n-1n)} \delta(S_{123n-2n-1n}), \quad n \geq 6. \quad (6.11)$$

This form of the recursive factor is the same as the one used in Arkani-Hamed et al. (2011),¹⁵ where it was shown that this factor ensures the correct soft limit for particle n . This representation was also important for matching the connected formula with the Grassmannian integral via deformations of the constraints and applications of the global residue theorem. In the next section we will investigate this strategy for form factors.

6.3 Relating the formulations

At this point, we studied two different Grassmannian representations of form factors. On one hand, there is the integral derived from on-shell diagrams in chapter 4. For NMHV form factors this integral is given explicitly in equation (5.5),

13 Arkani-Hamed, Bourjaily, Cachazo, Trnka, “Unification of Residues and Grassmannian Dualities”, [0912.4912](#); and Bourjaily, Trnka, Volovich, Wen, “The Grassmannian and the Twistor String: Connecting All Trees in $\mathcal{N} = 4$ SYM”, [1006.1899](#)

14 Nandan, Wen, “Generating All Tree Amplitudes in $\mathcal{N} = 4$ SYM by Inverse Soft Limit”, [1204.4841](#)

15 Arkani-Hamed, Bourjaily, Cachazo, Trnka, “Unification of Residues and Grassmannian Dualities”, [0912.4912](#)

and is equipped with the contour (5.21), derived from the BCFW recursion relations in the last chapter. On the other hand we have the formula that arises from the connected prescription, given in (6.7) and (6.11). This integral features a different integrand, and comes with a contour prescription involving the conic constraints.

These formulations are the form factor analogues of corresponding expressions for scattering amplitudes, whose NMHV Graßmannian formulas are related as follows,

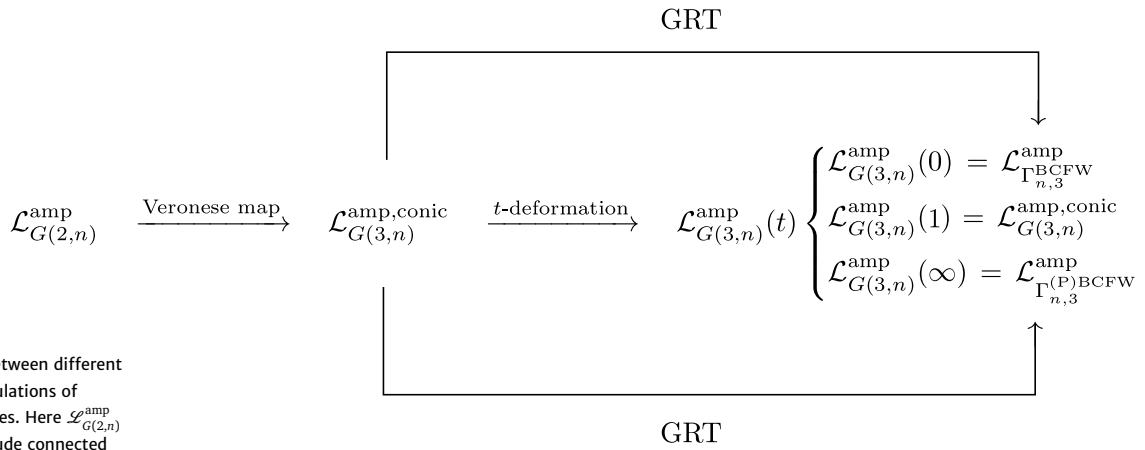


Figure 6.1: Relation between different Graßmannian formulations of scattering amplitudes. Here $\mathcal{L}_{G(2,n)}^{\text{amp}}$ denotes the amplitude connected formula, which can be understood as an integral over the Graßmannian $G(2, n)$. The Veronese map leads to a $G(3, n)$ Graßmannian integral with conic constraints $\mathcal{L}_{G(3,n)}^{\text{amp,conic}}$. There are different ways in which the Graßmannian integral with BCFW or (P)BCFW integration contour, $\mathcal{L}_{G(3,n),\Gamma}^{\text{amp}}$, can be obtained from this representation: either via the smooth deformations of the conic constraints $\mathcal{L}_{G(3,n)}^{\text{amp,conic}}(t)$, or via applications of the global residue theorem (GRT).

Here the Veronese map is given in (6.6) and the t -deformation amounts to introducing $n - 5$ parameters t_j into the conic constraints in a systematic way, namely

$$S_{i_1 i_2 i_3 i_4 i_5 i_6}(t) \equiv (i_1 i_2 i_3)(i_3 i_4 i_5)(i_5 i_6 i_1)(i_2 i_4 i_6) - t_j (i_2 i_3 i_4)(i_4 i_5 i_6)(i_6 i_1 i_2)(i_3 i_5 i_1). \tag{6.12}$$

Note in particular that the BCFW contour can be recovered both from taking limits of the deformation parameters t_j or through applications of the global residue theorem starting from the formula with the conic constraints.

The aim of this section is to investigate whether similar relations exist for the corresponding form-factor formulas. A preliminary attempt to use the Veronese map to relate the Graßmannian integral based on on-shell diagrams directly to the connected formula was made in Brandhuber et al. (2016),¹⁶ and found to be impossible. We can understand this now, based on the BCFW contour derived in chapter 5: the contour contains poles from different top-forms in such a way that no linear combination of top-forms gives the tree-level form factor with a single contour of integration. Such a single integral however would be necessary to directly apply the Veronese map.

In this section, we explore the possibility of relating the Graßmannian formulations directly using the GRT, focusing on low-point examples. Specifically, already at four points we find that there is no naive analogue to the t -deformation for the form-factor formulas. Moreover, we show that while for four and five points successive applications of the GRT lead from the Graßmannian formula with conic constraints to that with the BCFW contour, this is no longer the case

¹⁶ Brandhuber, Hughes, Panerai, Spence, Travaglini, “The connected prescription for form factors in twistor space”, 1608.03277

starting at six points. We furthermore highlight subtleties involved in the computation of the BCFW residues which do not appear for scattering amplitudes.

Four points

Consider the integral given in (6.7), which we repeat here for clarity:

$$I_{4,3} = \frac{(13x)(13y)}{(123)(134)(1xy)(3xy)} \delta(S_{1234xy}).$$

The contour is defined by the equation $S_{1234xy} = 0$. Applying the residue theorem one obtains the new contour given by

$$\{S_{1234xy}\} \rightarrow -\{(123)\} - \{(341)\} - \{(1xy)\} - \{(3xy)\}. \quad (6.13)$$

The location of these poles are the same as the four-point contour which can be read off figure 5.7. For each of the factors on the right-hand-side of (6.13), the left over S_{1234xy} factorizes into a product of four minors. It is straightforward to check that the value of each residue is the same as that of the Graßmannian formula.

A major difference to scattering amplitudes can be observed already from this simple case. Consider the analogous example of the six-point scattering amplitude:

$$I_{6,3}^{\text{amp}} = \frac{(135)}{(123)(345)(561)} \delta(S_{123456}) = \frac{(246)}{(234)(456)(612)} \delta(S_{123456}). \quad (6.14)$$

In this situation S_{123456} always factorizes in the same way for all three poles present in the amplitude integrand, both in the BCFW or (P)BCFW representations. This means that one can introduce a parameter t to the term that vanishes, $S_{123456}(t) = t(123)(345)(561)(246) - (234)(456)(612)(351)$, and the amplitude will be independent of the value of t .¹⁷ In particular, a one-parameter family of Graßmannian integrals is defined in this fashion, with the particular cases of the twistor string formula for $t = 1$ and the BCFW and (P)BCFW cases for $t = 0$ or $t = \infty$, respectively.

For form factors this is not possible: in the four-point example we see that S_{1234xy} always factorizes, but differently on each pole:

$$S_{1234xy} = \begin{cases} (341)(4xy)(23x)(12y) & \text{on } \{(123)\} \\ (123)(2xy)(34x)(14y) & \text{on } \{(341)\} \\ (234)(3xy)(12x)(41y) & \text{on } \{(1xy)\} \\ (1xy)(412)(23x)(34y) & \text{on } \{(3xy)\} \end{cases}. \quad (6.15)$$

This means that there is no deformation – or at least no naive one – of S_{1234xy} which could interpolate between the on-shell diagram Graßmannian integral and the one based on the connected prescription.

¹⁷ Arkani-Hamed, Bourjaily, Cachazo, Trnka, “Unification of Residues and Grassmannian Dualities”, [0912.4912](#); and Nandan, Volovich, Wen, “A Grassmannian Étude in NMHV Minors”, [0912.3705](#)

Five points

We now consider the five-point form factor, for which the integrand in the inverse soft formulation (6.9) reads

$$I_{5,3} = \frac{(13x)(13y)(23x)(124)(14x)}{(123)(1xy)(3xy)(145)} \delta(S_{1234xy}) \delta(S_{123x45}) \quad (6.16)$$

Note that, as mentioned in section 6.1, the integrand is finite for a spurious solution of $S_{1234xy} = S_{123x45} = 0$, namely that with particles 1, 2, 3 and 4 collinear, as the ratio $\frac{(124)}{(123)}$ does not vanish.

Consider first the fact, following from the GRT, that $\{f_1, f_2\} = 0$ with $f_1 \equiv S_1$ and $f_2 \equiv S_2(123)(1xy)(3xy)(145)$. For simplicity, we denote $S_1 \equiv S_{1234xy}$ and $S_2 \equiv S_{123x45}$. The residue theorem then implies:

$$\{S_1, S_2\} = -\{S_1, (123)\} - \{S_1, (1xy)\} - \{S_1, (3xy)\} - \{S_1, (145)\} = 0. \quad (6.17)$$

Note further that for $(123) = 0$, S_1 factorizes and thus

$$\{S_1, (123)\} = \{(234), (123)\} + \{(4xy), (123)\} + \{(y12), (123)\} + \{(3x1), (123)\}. \quad (6.18)$$

Plugging (6.18) back into (6.17), we get

$$\begin{aligned} \{S_1, S_2\} = & -\{(234), (123)\} - \{(4xy), (123)\} - \{(y12), (123)\} \\ & - \{(3x1), (123)\} - \{S_1, (1xy)\} - \{S_1, (3xy)\} - \{S_1, (145)\} = 0 \end{aligned} \quad (6.19)$$

Note the subtlety here: the left hand side and the first term on the right hand side appear not to be entirely distinct, since the configuration where $(123) = (234) = 0$ is also a (spurious) solution of $S_1 = S_2 = 0$. The fact that such a configuration appears after the application of a GRT follows from the requirement that the constraint $S_1 = S_2 = 0$ in (6.16) only includes non-spurious solutions, which for five points is not enforced by the numerator.

Interestingly, this term also highlights another phenomenon which does not occur for amplitudes. Indeed, for the term $\{(234), (123)\}$ the integrand is

$$\frac{(13y)(23x)(124)(14x)}{(1xy)(3xy)(145)(4xy)(y12) S_2} \delta((234)) \delta((123)), \quad (6.20)$$

and both the minor (124) in the numerator as well as S_2 in the denominator approach zero linearly. If one parametrizes this limit, one finds that the direction in which the limit is taken changes the result. To calculate the correct residue, we have to take the limit in way which ensures that S_1 is vanishing along the limiting path. We do so by setting $(123) = \varepsilon$ and $(234) = \frac{(34x)(xy1)(24y)}{(4xy)(y12)(3x1)} \varepsilon$, and then letting $\varepsilon \rightarrow 0$. Note that this term arises from factorizing S_1 in $\{S_1, (123)\}$; the limit ensures that $(123) = 0$ is approached precisely from the surface $S_1 = 0$.

The other residues coming from (6.19) can be calculated straightforwardly. Note that S_1 factorizes for the terms $\{S_1, (1xy)\}$ and $\{S_1, (3xy)\}$; the resulting terms, together with those not involving S_1 in (6.19) are in one-to-one correspondence with the MHV×MHV factorization poles of the BCFW contour (5.21).

For the term $\{S_1, (145)\}$ one applies the GRT again, after which the calculation is identical to the four-point case, and results in all inverse soft contributions to the form factor. For all terms, (6.16) gives the same residues as the corresponding poles of the Graßmannian integral.

Six points

For the six-point form factor, we find that it is impossible to reproduce all BCFW poles from (6.11) by applying the GRT, despite the fact that this formula reproduces the form factor when evaluating the conic constraints, which we checked numerically. We furthermore collected evidence that even by using the identity (6.8), one cannot generate other representations which have all BCFW poles.

The integrand in the inverse-soft-like representation (6.11) is given for the six-point form factor by

$$I_{6,3} = \frac{(13x)(13y)(23x)(124)(14x)(125)(135)(234)}{(123)(1xy)(3xy)(156)} \times \delta(S_{1234xy})\delta(S_{12345x})\delta(S_{123456}), \quad (6.21)$$

and the poles contributing to the BCFW representation of the form factor can be found in figure 5.7. Most of these poles can be recovered by successively applying the GRT to (6.21), in particular all poles with $(156) = 0$, corresponding to the inverse soft limit of $F_{5,3}$.

It is however impossible to find the poles $\{(1), (2), (3)\}$ and $\{(1), (2), (5)\}$, corresponding to the factorization channels $A_{6,2} \times F_{2,2}$ and $A_{5,2} \times F_{3,2}$. To see that these poles can never appear it is sufficient to realize that, in the vicinity of these configurations, the integrand (6.21) is not singular enough to produce a finite residue. Regarding the delta functions $\delta(S)$ as $\frac{1}{S}$ (with an appropriate contour), and letting each of the vanishing minors at those poles approach zero as $\varepsilon \sim 0$, we find that for the respective configurations the integrand behaves as

$$\begin{aligned} \{(1), (2), (3)\}: & \quad \frac{(124)(125)(135)(234)}{(123) S_{1234xy} S_{12345x} S_{123456}} \sim \frac{1}{\varepsilon^2}, \\ \{(1), (2), (5)\}: & \quad \frac{(124)(234)}{(123) S_{1234xy} S_{12345x} S_{123456}} \sim \frac{1}{\varepsilon^2}, \end{aligned} \quad (6.22)$$

while in order for a residue to exist, the integrand would have to scale as ε^{-3} . Since the GRT does not change this power counting, potential poles at these locations would be canceled by numerator factors. We furthermore note that the minor $(5xy)$ which vanishes for the second configuration does not even appear in (6.21).

The identity (6.8) can change degree of divergence at configurations away from the support of the conic constraints, i.e. at positions reached by the GRT. To see if other representations of the integrand with the correct singularities at the all BCFW poles exist, we generated around half a million different representations of the integrand with a computer program, using the identity (6.8) and cyclic symmetry, and taking both (6.21) and (6.7) as starting points. We then

checked that none of these representations has the correct degree of divergence at all BCFW poles. This result is not conclusive, since we could only generate a finite number of representations due to computational constraints. In principle, the identity (6.8) can be applied over and over again. Nevertheless, our result is a very strong indication that no $G(3, 8)$ representation based on the connected formula exists, which reproduces all BCFW terms.

A possibility which we cannot exclude is to apply a GRT to (6.21), and then to apply different identities to each resulting terms, effectively combining different representations. Of course there is a proliferation of such possibilities, and several attempts did not lead to the correct residues. We note that in this case there is also no clearly preferred choice with a physical motivation, and it would be hard to apply such a strategy systematically to generalize beyond NMHV.

These examples show that the relation between the connected formula and the Graßmannian integral is much more subtle for form factors than for amplitudes, despite the fact that both formulations lead to correct expressions for tree-level form factors. As already noted in Brandhuber et al. (2016),¹⁸ the Veronese map (6.6) is not enough to relate the formulations; we have seen that this is due to the fact that different top-cells contribute a different number of residues to the BCFW representation, and therefore a joint contour for a linear combination of top-forms cannot work. Furthermore, the deformations of the conic constraints $S_{i_1 i_2 i_3 i_4 i_5 i_6} = 0$ which allowed to introduce a parameter smoothly linking both Graßmannian formulations cannot be introduced in the case of form factors, since for different BCFW terms the $S_{i_1 i_2 i_3 i_4 i_5 i_6}$ factor in different ways. Finally, using the most basic way of relating the formulations by reproducing the BCFW terms explicitly using global residue theorems, also seems to be problematic: besides subtleties regarding spurious solutions of the geometric constraints coming from the RSV equations and residues which depend on the path taken towards the singular point, we also find mismatches. The inverse soft factor formulation seems to be necessary to recover the recursive structure stemming from exactly such inverse soft limits of lower point form factors. On the other hand this formulation does not recover all factorization channels which contribute to the BCFW form of the form factor. We conclude that that in addition to the GRT, further identities such as (6.8) are required to map the formulations into each other. This will likely make it difficult to use the contour data from the connected prescription to obtain the BCFW contour for the Graßmannian integral in closed form for higher MHV degree.

¹⁸ Brandhuber, Hughes, Panerai, Spence, Travaglini, “The connected prescription for form factors in twistor space”, 1608.03277

II

**ON-SHELL METHODS
AND INTEGRABILITY**

Yangian invariants and R-operators

On-shell diagrams for amplitudes are directly related to their symmetries, and to the spin chain picture of $\mathcal{N}=4$ SYM at weak coupling. Such integrable spin chain models can be characterized as possessing an infinite-dimensional symmetry algebra. For so-called rational models this algebra is the Yangian. While the symmetry is usually reduced to ordinary $\mathfrak{su}_{n|m}$ invariance for the observables of finite size systems, the corresponding Yangian $\mathcal{Y}(\mathfrak{su}_{n|m})$ still underlies the entire integrable structure of the model and its solution via the Bethe Ansatz.

Scattering amplitudes in $\mathcal{N}=4$ SYM are invariant under the action of the superconformal algebra $\mathfrak{psu}_{2,2|4}$ as a consequence of Ward identities which follow from the invariance of the action. For tree-level amplitudes, it was first observed in Drummond et al. (2010); Brandhuber et al. (2008)¹ that, apart from being superconformally invariant in the original momentum space, they are also covariant with respect to a superconformal algebra defined in the dual space described in section 2.1. The closure of these two algebras then was shown to be the Yangian of $\mathfrak{psu}_{2,2|4}$.²

The Grassmannian integral representation is intimately linked to this Yangian invariance. While the Grassmannian integral in twistor variables (2.59) makes superconformal symmetry manifest, the integral in the momentum twistor version (2.60) does so for dual superconformal symmetry. Indeed it can directly be shown that the integral and all its residues are Yangian invariants, and that the top-form is uniquely determined by this symmetry.³

Apart from scattering amplitudes, Yangian symmetry plays an important role for other aspects of $\mathcal{N}=4$ SYM integrability. Noteworthy examples are smooth Maldacena-Wilson loops,⁴ as well as recent attempts to understand these symmetries field-theoretically on the level of the Lagrangian or action.⁵ For an overview of Yangian symmetry in the AdS₅/CFT₄ correspondence we refer the reader to Beisert (2011)⁶ for the field theory side of the correspondence and to Dolan et al. (2004)⁷ for a view on the algebra from a string perspective.

This chapter serves to introduce many integrability related concepts used in the following. We first review the RTT realization of the Yangian in section 7.1, relate it to the transfer matrices used in the Quantum Inverse Scattering method

- 1 Drummond, Henn, Korchemsky, Sokatchev, “Dual superconformal symmetry of scattering amplitudes in $\mathcal{N}=4$ super-Yang-Mills theory”, [0807.1095](#); and Brandhuber, Heslop, Travaglini, “A Note on dual superconformal symmetry of the $\mathcal{N}=4$ super Yang-Mills S-matrix”, [0807.4097](#)
- 2 Drummond, Henn, Plefka, “Yangian symmetry of scattering amplitudes in $\mathcal{N}=4$ super Yang-Mills theory”, [0902.2987](#)
- 3 Drummond, Ferro, “Yangians, Grassmannians and T-duality”, [1001.3348](#); and Drummond, Ferro, “The Yangian origin of the Grassmannian integral”, [1002.4622](#)
- 4 Müller, Minkler, Plefka, Pollok, Zarembo, “Yangian Symmetry of smooth Wilson Loops in $\mathcal{N}=4$ super Yang-Mills Theory”, [1309.1676](#); and Beisert, Müller, Plefka, Vergu, “Integrability of smooth Wilson loops in $\mathcal{N}=4$ superspace”, [1509.05403](#)
- 5 Beisert, Garus, Rosso, “Yangian Symmetry and Integrability of Planar $\mathcal{N}=4$ Supersymmetric Yang-Mills Theory”, [1701.09162](#)
- 6 Beisert, “On Yangian Symmetry in Planar $\mathcal{N}=4$ SYM”, [1004.5423](#)
- 7 Dolan, Nappi, Witten, “Yangian symmetry in D = 4 superconformal Yang-Mills theory”, [hep-th/0401243](#)

in section 7.2, and discuss the invariants of the Yangian in section 7.3. We then turn to certain deformations recently introduced in the context of scattering amplitudes, which can naturally be accommodated in the RTT realization as discussed in section 7.4, and play a major role in the integrability construction of Yangian invariants via so-called R-operators. We introduce this construction in section 7.5, and show that it leads to Yangian invariants in section 7.6.

7.1 The RTT realization of the Yangian

The Yangian invariance of scattering amplitudes is often discussed using Drinfeld’s first realization⁸, which extends the simple Lie superalgebra $\mathfrak{psu}_{2,2|4}$, expressed in terms of generators and structure constants by further generators, imposing additional commutation and Serre relations. Here however, we will be working with the RTT realization of the Yangian,⁹ which is intimately related to integrable spin chains and the Algebraic Bethe Ansatz.¹⁰

Strictly speaking, the RTT realization defines the Yangian of the algebra $\mathfrak{gl}_{n|m}$ while Drinfeld’s realizations give the Yangian of $\mathfrak{sl}_{n|m}$, which is a subalgebra. Since we will be concerned only with algebraic aspects of $\mathcal{N} = 4$ SYM at weak coupling, this distinction will not play a role here, and we will work with the algebra $\mathfrak{gl}_{4|4}$ and its Yangian instead of the actual superconformal algebra $\mathfrak{psu}_{2,2|4}$ and the corresponding Yangian algebra.¹¹

We begin by defining the fundamental representation of $\mathfrak{gl}_{4|4}$, generated by the elementary $(4|4) \times (4|4)$ supermatrices e^{AB} , with indices taking values $A, B = 1, \dots, 8$. These generators have matrix elements

$$(e^{AB})_{CD} = \delta_C^A \delta_D^B, \tag{7.1}$$

and satisfy the $\mathfrak{gl}_{4|4}$ commutation relations

$$[e^{AB}, e^{CD}] = \delta^{BC} e^{AD} - (-1)^{(|A|+|B|)(|C|+|D|)} \delta^{AD} e^{CB}; \tag{7.2}$$

here and in what follows, all commutators are graded,

$$[A, B] := AB - (-1)^{|A||B|} BA \tag{7.3}$$

where $|\cdot|$ denotes the degree of an index, state or operator, and is $|\cdot| = 0$ for bosons and $|\cdot| = 1$ for fermions. We will generally use a grading where $|1| = \dots = |4| = 0$ and $|5| = \dots = |8| = 1$.

The most basic quantity for integrability and the Yangian is the fundamental R-matrix

$$\mathcal{R}_{ij}(u) = \begin{array}{c} | \\ \vdots \\ i \text{ --- } \vdots \text{ ---} \\ | \\ j \end{array} = u + (-1)^{|B|} e_i^{AB} e_j^{BA} = u + \mathbb{P}_{ij}, \tag{7.4}$$

acting on the i ’th and j ’th factor in the tensor product $\dots \otimes (\mathcal{V}_\square)_i \otimes \dots \otimes (\mathcal{V}_\square)_j \otimes \dots$, of n $(4|4)$ -dimensional representation spaces \mathcal{V}_\square corresponding to the fundamental representation. The complex variable u is called the spectral parameter, and is

8 Drinfeld, ‘‘Hopf algebras and the quantum Yang–Baxter equation’’, *Sov. Math. Dokl.* 32 (1985) 254–258, [Dokl. Akad. Nauk Ser. Fiz.283,1060(1985)]; and Drinfeld, ‘‘Quantum groups’’, *J. Sov. Math.* 41 (1988) 898–915

9 Molev, Nazarov, Olshansky, ‘‘Yangians and classical Lie algebras’’, [hep-th/9409025](#); Molev, ‘‘Yangians and their applications’’, [math/0211288](#); and Nazarov, ‘‘Quantum Berezinian and the classical Capelli identity’’, *Letters in Mathematical Physics* 21 (1991), no. 2, 123–131

10 Faddeev, ‘‘Algebraic aspects of Bethe Ansatz’’, [hep-th/9404013](#); and Faddeev, ‘‘How algebraic Bethe ansatz works for integrable model’’, [hep-th/9605187](#)

11 We refer the reader to Marboe, Volin, ‘‘The full spectrum of AdS5/CFT4 I: Representation theory and one-loop Q-system’’, [1701.03704](#) for a nice introduction on the subtleties concerning the symmetries of $\mathcal{N} = 4$ SYM at weak coupling.

of fundamental importance both to the various Bethe Ansätze, as well as the definition of the Yangian algebra, which we will discuss shortly. In equation (7.4), we already presented a widely used graphical notation for the quantities appearing in the integrability description.¹² In particular, we draw (“inputs” or “outputs”) of maps acting on the fundamental representation space \mathcal{V}_\square as a dashed line, ----. As indicated in (7.4), the R-matrix can be written in terms of the graded permutation operator $\mathbb{P}_{ij} = (-1)^{|B|} e_i^{AB} e_j^{BA}$, which swaps vectors in the tensor product, $\mathbb{P}v_1 \otimes v_2 = (-1)^{|v_1||v_2|} v_2 \otimes v_1$. Its defining property is the Yang-Baxter equation it satisfies,

$$\mathcal{R}_{12}(u_1 - u_2)\mathcal{R}_{13}(u_1 - u_3)\mathcal{R}_{23}(u_2 - u_3) = \mathcal{R}_{23}(u_2 - u_3)\mathcal{R}_{13}(u_1 - u_3)\mathcal{R}_{12}(u_1 - u_2). \tag{7.5}$$

This is an equation in the triple tensor product $\mathcal{V}_\square \otimes \mathcal{V}_\square \otimes \mathcal{V}_\square$, and the tensor factors on which the individual R-matrices act are indicated by subscripts. The Yang-Baxter equation can be represented graphically,

$$\tag{7.6}$$

and this way of representing it allows to think of it in terms of scattering particles. The Yang-Baxter equation then is the consistency condition for the factorization of the scattering of three particles into consecutive two-particle scattering events, the order of which is unimportant. This is the basis of integrable two-dimensional field theories¹³, and the appearance of the Yangian in such theories.¹⁴

To describe amplitudes and form factors, and the Yangian relevant to them, we need a second representation, which expresses the superconformal algebra in terms of the spinor-helicity variables introduced in section 2.1 and used throughout the last chapters.¹⁵ We will denote maps acting on the corresponding representation space by —. This “physical” representation is of factorized, or Jordan-Schwinger¹⁶ form. We define it in terms of 8 creation operators x^A and 8 annihilators p^A , which can be decomposed into the different spinor-helicity variables and their derivatives as

$$x^A = \left(\lambda^\alpha, -\frac{\partial}{\partial \tilde{\lambda}^{\dot{\alpha}}}, \frac{\partial}{\partial \tilde{\eta}^A} \right), \quad p^A = \left(\frac{\partial}{\partial \lambda^\alpha}, \tilde{\lambda}^{\dot{\alpha}}, \tilde{\eta}^A \right). \tag{7.7}$$

Note that we now regard the $\mathfrak{gl}_{4|4}$ indices as multi-indices $A = (\alpha, \dot{\alpha}, A)$, where the usual spinor-helicity indices range over $\alpha = 1, 2$, $\dot{\alpha} = 1, 2$ and $A = 1, \dots, 4$. The non-compactness of the superconformal group is already visible here, by the fact that the variables $\tilde{\lambda}$ appear in a particle-hole transformed manner, with variables and derivatives exchanged.¹⁷

The operators x and p satisfy the commutation relations of independent graded harmonic oscillators

$$[x^A, p^B] = (-1)^{|A|} \delta^{AB} \tag{7.8}$$

12 This graphical notation is also highlighted the one-to-one relation between integrable quantum mechanical spin chains and integrable lattice models in statistical physics, see e.g. Baxter, “Exactly solved models in statistical mechanics”, 1982. Via the perimeter Bethe Ansatz developed in Baxter, “Perimeter Bethe ansatz”, *Journal of Physics A: Mathematical and General* **20** (1987), no. 9, 2557, these statistical models are closely related to Yangian invariance, see Frassek, Kanning, Ko, Staudacher, “Bethe Ansatz for Yangian Invariants: Towards Super Yang–Mills Scattering Amplitudes”, **1312.1693**.

13 Dorey, “Exact S matrices”, [hep-th/9810026](https://arxiv.org/abs/hep-th/9810026)

14 MacKay, “Introduction to Yangian symmetry in integrable field theory”, [hep-th/0409183](https://arxiv.org/abs/hep-th/0409183)

15 In section 8.4 we will see that this representation is actually the same as the one used to describe composite operators in terms of oscillators.

16 Jordan, “Der Zusammenhang der symmetrischen und linearen Gruppen und das Mehrkörperproblem”, *Zeitschrift für Physik* **94** (1935), no. 7, 531–535

17 The variables $\tilde{\eta}$ are similarly particle-hole transformed; since they are fermionic, this however does not affect the compactness or non-compactness.

which implies that the generators defined by

$$\mathcal{G}^{AB} = x^A p^B \tag{7.9}$$

form a representation of $\mathfrak{gl}_{4|4}$:

$$[\mathcal{G}^{AB}, \mathcal{G}^{CD}] = \delta^{BC} \mathcal{G}^{AD} - (-1)^{(|A|+|B|)(|C|+|D|)} \delta^{AD} \mathcal{G}^{CB} \tag{7.10}$$

The algebra contains the central charge \mathbf{c} and the hypercharge \mathbb{B} defined by¹⁸

$$\mathbf{c} = \mathcal{G}^{AA}, \quad \mathbb{B} = (-1)^{|A|} \mathcal{G}^{AA}. \tag{7.11}$$

To get the algebra $\mathfrak{sl}_{4|4}$, we would remove the supertrace, defined by

$$\text{str } U = (-1)^{|A|} U_{AA}, \tag{7.12}$$

for an arbitrary supermatrix U , to obtain generators $\mathcal{G}_{AB} - \frac{(-1)^{|A|}}{8} \mathbb{B} \delta_{AB}$, and by requiring $\mathbf{c} \sim 0$ we obtain $\mathfrak{psl}_{4|4}$.

We can now define the Lax operator, which will be the central object in the definition of the Yangian. It acts on the tensor product $\mathcal{V}_{\square} \otimes \mathcal{V}_{\text{sh}}$ and is given by

$$\mathcal{L}_i(u) = \begin{array}{c} | \\ \hline \text{---} \\ | \\ i \end{array} = u + (-1)^{|B|} e^{AB} \mathcal{G}_i^{BA}. \tag{7.13}$$

It satisfies an equation similar to the Yang-Baxter equation (7.5), but in the tensor product $\mathcal{V}_{\square} \otimes \mathcal{V}_{\square} \otimes \mathcal{V}_{\text{sh}}$ of one particles in the spinor-helicity representation and two ‘‘auxiliary particles’’ in the fundamental,

$$\mathcal{R}(u-v) (\mathcal{L}_i(u) \otimes \mathbb{1}) (\mathbb{1} \otimes \mathcal{L}_i(v)) = (\mathbb{1} \otimes \mathcal{L}_i(v)) (\mathcal{L}_i(u) \otimes \mathbb{1}) \mathcal{R}(u-v). \tag{7.14}$$

If we consider the Lax operator as a matrix in the fundamental space with operator valued entries acting on the ‘‘physical space’’, we can define its matrix elements by

$$\mathcal{L}_i(u) = e^{AB} \mathcal{L}_i^{AB}(u) = e^{AB} (u \delta^{AB} + (-1)^B \mathcal{G}_i^{BA}). \tag{7.15}$$

As we will shortly see, the Lax operator (7.13) generates the Yangian for one-particle states; for multi-particle states we take a product of these Lax operators, which defines the so called monodromy matrix¹⁹

$$\mathcal{M}_n(u) = \begin{array}{c} | \\ \hline \text{---} \\ | \\ n \end{array} \begin{array}{c} \vdots \\ \text{---} \\ \vdots \\ 2 \end{array} \begin{array}{c} | \\ \hline \text{---} \\ | \\ 1 \end{array} = \mathcal{L}_n(u) \cdots \mathcal{L}_2(u) \mathcal{L}_1(u), \tag{7.16}$$

This matrix combines all the generators of the Yangian into a single object. To get the individual generators, we have to expand the monodromy matrix in the spectral parameter

$$\mathcal{M}_n(u) = \sum_{k=0}^n u^{n-k} \mathcal{M}_{n[k]}, \tag{7.17}$$

18 Here and in what follows we always sum over repeated indices.

19 This just means that the coproduct in this realization of the Yangian is given by the tensor product in the physical, and the matrix product in the auxiliary space.

and look at individual matrix elements again defined by

$$\mathcal{M}_n(u) = e^{AB} \mathcal{M}_n^{AB}(u) = e^{AB} \sum_{k=0}^n u^{n-k} \mathcal{M}_{n[k]}^{AB}. \quad (7.18)$$

The operators $\mathcal{M}_{n[k]}^{AB}$ are the generators of the Yangian; A and B are just ordinary $\mathfrak{gl}_{4|4}$ indices while the subscript $[k]$ refers to the so-called level.²⁰ Indeed, the first few of these levels in the expansion in the spectral parameter are given by

$$\begin{aligned} \mathcal{M}_{n[0]}^{AB} &= \delta^{AB}, \\ \mathcal{M}_{n[1]}^{AB} &= (-1)^B \sum_{i=1}^n \mathcal{G}_i^{BA}, \\ \mathcal{M}_{n[2]}^{AB} &= (-1)^B \sum_{i < j} (-1)^C \mathcal{G}_i^{BC} \mathcal{G}_j^{CA}. \end{aligned} \quad (7.19)$$

The fact that the lowest level $\mathcal{M}_{n[0]}^{AB} = \delta^{AB}$ is just the identity is actually important for the commutation relations of the Yangian which will be derived shortly.²¹ We see furthermore that the first level generators are simply the $\mathfrak{gl}_{4|4}$ generators defined in (7.9), and acting on the tensor product in the usual way. The higher levels consist of non-local combinations of these generators, i.e. appropriate sums over products of \mathcal{G} 's acting on different particles at the same time.

The commutation relations of the Yangian algebra follow from the so-called RTT²² or fundamental commutation relation

$$\mathcal{R}(u-v)(\mathcal{M}_n(u) \otimes \mathbb{1})(\mathbb{1} \otimes \mathcal{M}_n(v)) = (\mathbb{1} \otimes \mathcal{M}_n(v))(\mathcal{M}_n(u) \otimes \mathbb{1})\mathcal{R}(u-v), \quad (7.20)$$

which can be derived by repeatedly applying (7.14) to the left hand side. In components this equation reads

$$\begin{aligned} (u-v)[\mathcal{M}_n^{AB}(u), \mathcal{M}_n^{CD}(v)] \\ = (-1)^{|A||C|+|A||D|+|C||D|} (\mathcal{M}_n^{CB}(v)\mathcal{M}_n^{AD}(u) - \mathcal{M}_n^{CB}(u)\mathcal{M}_n^{AD}(v)), \end{aligned} \quad (7.21)$$

and if we expand in the spectral parameter we get

$$\begin{aligned} [\mathcal{M}_{n[k+1]}^{AB}, \mathcal{M}_{n[\ell]}^{CD}] - [\mathcal{M}_{n[k]}^{AB}, \mathcal{M}_{n[\ell+1]}^{CD}] \\ = (-1)^{|A||C|+|A||D|+|C||D|} (\mathcal{M}_{n[\ell]}^{CB}\mathcal{M}_{n[k]}^{AD} - \mathcal{M}_{n[k]}^{CB}\mathcal{M}_{n[\ell]}^{AD}). \end{aligned} \quad (7.22)$$

While this equation can be taken as the defining relations of the Yangian of $\mathfrak{gl}_{4|4}$, one can obtain a more enlightening representation if we bring the factor of $(u-v)$ in (7.21) to the right hand side and expand afterwards. This yields the commutation relations for the Yangian generators²³

$$\begin{aligned} [\mathcal{M}_{n[k]}^{AB}, \mathcal{M}_{n[\ell]}^{CD}] \\ = (-1)^{|A||C|+|A||D|+|C||D|} \sum_{q=0}^{\min(k,\ell)-1} (\mathcal{M}_{n[k+\ell-q-1]}^{CB}\mathcal{M}_{n[q]}^{AD} - \mathcal{M}_{n[q]}^{CB}\mathcal{M}_{n[k+\ell-q-1]}^{AD}). \end{aligned} \quad (7.23)$$

These relations contain the $\mathfrak{gl}_{4|4}$ commutation relations (7.10). To see this set $k = \ell = 1$ in (7.23), which fixes $q = 0$, and plug in the explicit form of the zeroth

²⁰ Note that in the literature on Drinfeld's first realization, the ordinary algebra generators are usually referred to as the zeroth level, the bilocal generators as the first etc. Despite not commonly used in the RTT literature, we employ this terminology here, but for convenience shift the counting of levels by one.

²¹ Representations of the Yangian where this condition is violated form the basis for the oscillator construction of Q-operators as we will see in chapter 12.

²² In many works the monodromy matrix \mathcal{M} is denoted by T , hence the name.

²³ While we derived these relations from the explicit form of the monodromy matrix (7.16), they can of course be taken as a definition of the algebra, with abstract generators and an infinite number of levels.

and first level given in (7.19); this yields

$$[\mathcal{J}_n^{BA}, \mathcal{J}_n^{DC}] = (-1)^{|B|+|D|} (-1)^{|A||C|+|A||D|+|C||D|} \left((-1)^{|B|} \delta^{AD} \mathcal{J}_n^{BC} - (-1)^{|D|} \delta^{CB} \mathcal{J}_n^{DA} \right), \quad (7.24)$$

and noting that the signs of the terms are given by

$$\begin{aligned} (-1)^{|D|+|A||C|+|A||D|+|C||D|} \delta^{AD} &= \delta^{AD}, \\ -(-1)^{|B|+|A||C|+|A||D|+|C||D|} \delta^{BC} &= -(-1)^{(|A|+|B|)(|C|+|D|)} \delta^{BC}, \end{aligned} \quad (7.25)$$

we recover (7.10). The Yangian extends these relations to the whole tower of levels defined above.

7.2 Transfer matrices and Hamiltonians

Before we turn to the question of understanding the invariants of the Yangian, let us discuss another important operator, which will allow us to make more direct contact with integrable spin chains, and which will play an important role in the following chapters. Given a monodromy matrix (7.16), we can define a so-called transfer matrix \mathcal{T} by taking the supertrace over the fundamental space

$$\mathcal{T}_n(u) = \left(\begin{array}{c|c|c} \cdots & \cdots & \cdots \\ \cdots & \cdots & \cdots \\ \cdots & \cdots & \cdots \end{array} \right) = \text{str } \mathcal{M}_n(u). \quad (7.26)$$

$\begin{array}{ccc} n & 2 & 1 \end{array}$

Since the fundamental space is traced out, it is called auxiliary; the other spaces, on which the transfer matrix acts, are called physical, and constitute the Hilbert space of the spin chain model. An important property of the transfer matrix is its $\mathfrak{gl}_{4|4}$ invariance,

$$[\mathcal{T}(u), \sum_{i=1}^n \mathcal{J}_i^{AB}] = 0. \quad (7.27)$$

Taking the supertrace on both sides of the RTT relation (7.20) and using the expression for the R-matrix (7.4), one can furthermore derive the most important property of the transfer matrix: it commutes with itself at different values of the spectral parameter,

$$[\mathcal{T}_n(u), \mathcal{T}_n(v)] = 0 \quad (7.28)$$

Therefore an expansion of the transfer matrix in the spectral parameter,

$$\mathcal{T}_n(u) = \sum_{k=0}^n u^{n-k} \mathcal{T}_{n[k]}, \quad (7.29)$$

generates a set of mutually commuting charges. These charges can be regarded as special linear combinations of the Yangian generators (7.18). On the other hand, in the context of spin chain models, they really can be considered as higher conserved charges of the corresponding model, which exist due to integrability.

We note in passing that in our case, the level $\mathcal{T}_{n[0]} = 0$ because the supertrace $\text{str } \mathbb{1} = 0$, and likewise $\mathcal{T}_{n[1]} = 0$ due to the vanishing of the central charge of physical states.

The spin chain Hamiltonian itself is not among the operators generated by the transfer matrix $\mathcal{T}(u)$, with the fundamental representation in the auxiliary space. Rather, it can be obtained from a transfer matrix which is constructed with the same representation in the auxiliary and the tensor factors of the physical space. The corresponding R-matrix, which we denote by \mathbf{R} , from which this transfer matrix can be constructed was found in Kulish et al. (1981)²⁴ and contains the Hamiltonian density $\mathcal{H}_{i,i+1}$ when expanded in the spectral parameter

$$\mathbf{R}_{i,i+1}(u) = \mathbb{P}_{i,i+1}(\mathbb{1} + u\mathcal{H}_{i,i+1} + \dots), \quad (7.30)$$

see e.g. Sklyanin (1991).²⁵ This so-called harmonic action Hamiltonian was first studied, in the context of $\mathcal{N} = 4$ SYM in Beisert (2004).²⁶ The full Hamiltonian is then defined as

$$\mathbf{H} = \sum_{i=1}^n \mathcal{H}_{i,i+1} \quad (7.31)$$

with periodic boundary conditions.

The \mathbf{R} matrix satisfies the following Yang-Baxter equation

$$\mathbf{R}_{i,i+1}(u)\mathcal{L}_i(u+u')\mathcal{L}_{i+1}(u') = \mathcal{L}_{i+1}(u')\mathcal{L}_i(u+u')\mathbf{R}_{i,i+1}(u) \quad (7.32)$$

which for the representations at hand was investigated in Ferro et al. (2014).²⁷ If we take the derivative with respect to u of this equation and multiply by the permutation operator, we arrive at the Sutherland criterion²⁸

$$[\mathcal{H}_{i,i+1}, \mathcal{L}_i(u')\mathcal{L}_{i+1}(u')] = \mathcal{L}_i(u') - \mathcal{L}_{i+1}(u'). \quad (7.33)$$

It is easy to see that this implies, by telescopic cancelation, that the charges generated by the transfer matrix \mathcal{T} commute with the Hamiltonian, and are thus conserved.

Although we will not go into any detail concerning this technique, we want to point out that the (nested) Algebraic Bethe Ansatz, or Quantum Inverse Scattering method, is based entirely on this observation. It diagonalizes the Hamiltonian \mathbf{H} by finding the eigenstates of the transfer matrix $\mathcal{T}(u)$, using matrix elements of the monodromy matrix (7.16) as lowering operators acting on a highest-weight state that serves as a vacuum. The RTT relations (7.20) can then be used to find consistency relations for the Ansatz, the Bethe equations.²⁹

7.3 Yangian invariance

We can now define precisely what we mean by Yangian invariance in the RTT formulation of the Yangian. Naively, an invariant should be annihilated by all generators (7.18) of the Yangian. This would indeed be the case in Drinfeld's first realization of the Yangian. Here however we see that this cannot be true.

24 Kulish, Reshetikhin, Sklyanin, "Yang-Baxter Equation and Representation Theory. 1.", *Lett. Math. Phys.* 5 (1981) 393–403

25 Sklyanin, "Quantum inverse scattering method. Selected topics", [hep-th/9211111](https://arxiv.org/abs/hep-th/9211111)

26 Beisert, "The complete one loop dilatation operator of $\mathcal{N} = 4$ Super Yang-Mills theory", [hep-th/0307015](https://arxiv.org/abs/hep-th/0307015)

27 Ferro, Łukowski, Meneghelli, Plefka, Staudacher, "Spectral Parameters for Scattering Amplitudes in $\mathcal{N} = 4$ Super Yang-Mills Theory", [1308.3494](https://arxiv.org/abs/1308.3494)

28 Sutherland, "Exact Solution of a Two-Dimensional Model for Hydrogen-Bonded Crystals", *Phys. Rev. Lett.* 19 Jul (1967) 103–104

29 For an introduction see Faddeev, "How algebraic Bethe ansatz works for integrable model", [hep-th/9605187](https://arxiv.org/abs/hep-th/9605187); a complete and systematic treatment can be found in the paper Belliard, Ragoucy, "Nested Bethe ansatz for 'all' closed spin chains", [0804.2822](https://arxiv.org/abs/0804.2822).

First of all, the lowest level of the Yangian is the identity and cannot annihilate any state; furthermore we cannot require that the diagonal generators $\mathcal{M}_{n[\ell]}^{AA}$ annihilate the invariant, since we work with $\mathfrak{gl}_{4|4}$ generators and don't impose a vanishing supertrace. We have however to require that these generators act diagonally.

We thus arrive at the following definition of Yangian invariants

$$\mathcal{M}_{n[\ell]}^{AB} |\Omega\rangle = f_{n,\ell} \delta^{AB} |\Omega\rangle , \tag{7.34}$$

where the coefficients $f_{n,\ell}$ may depend on the state. A powerful feature of the RTT realization is that these conditions can be combined into an elegant eigenvalue equation³⁰

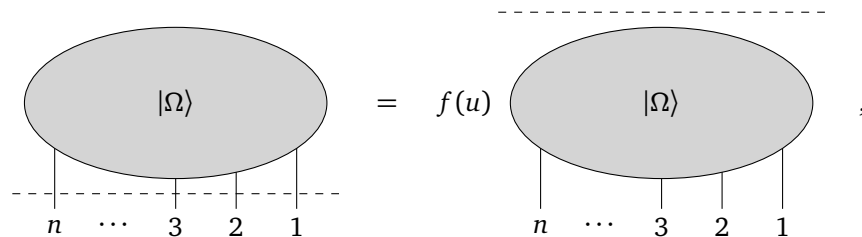
$$\mathcal{M}_n(u) |\Omega\rangle = f(u) |\Omega\rangle . \tag{7.35}$$

This simply states that Yangian invariants are the eigenstates of the monodromy matrix. In particular this implies that they are special eigenstate of the transfer matrix

$$\mathcal{T}_n(u) |\Omega\rangle = f(u) (-1)^{|\Lambda|} \delta^{AA} |\Omega\rangle = 0 . \tag{7.36}$$

Here the last equality is a consequence of the fact that there are as many fermionic as bosonic indices for $\mathfrak{gl}_{4|4}$. Being eigenstates of the transfer matrix, the invariants can in principle be constructed using Bethe Ansatz methods, as suggested in Frassek et al. (2014).³¹ We will however shortly see that there is more direct way of writing them down.

The graphical notation outlined above will play an important role in this development, and we note that in this language, the Yangian invariance condition (7.35) can be represented as the possibility to “pull” the monodromy matrix “through” the invariant state, as shown in figure 7.1.



Here the state is represented by a “blob” with n outgoing lines in the spinor-helicity representation; the monodromy matrix is drawn as in in equation (7.16), with the dashed line representing the space in the fundamental representation crossing the physical space. If the state is invariant, the fundamental line can be pulled through the blob, and becomes the identity matrix (since no crossings remain). The subsequent sections will show that these invariant blobs are precisely given by on-shell diagrams.

30 Chicherin, Kirschner, “Yangian symmetric correlators”, 1306.0711; and Chicherin, Derkachov, Kirschner, “Yang-Baxter operators and scattering amplitudes in $\mathcal{N} = 4$ super-Yang-Mills theory”, 1309.5748

31 Frassek, Kanning, Ko, Staudacher, “Bethe Ansatz for Yangian Invariants: Towards Super Yang-Mills Scattering Amplitudes”, 1312.1693

Figure 7.1: Yangian invariance, depicted graphically as pulling the line corresponding to the auxiliary space of the monodromy matrix through the state.

7.4 Deformations

While Yangian invariance as described above is the actual invariance of physical on-shell functions, the integrability-based formulation of the problem allows for certain deformations of these states, which preserve Yangian invariance with adjustments to the representation of the Yangian. These deformations are not only interesting in themselves, but also serve to motivate a purely integrability-based construction of invariants. We will first describe these deformations, then discuss their interpretation, and finally provide an overview of the development of this subject.

The main idea is to allow for different spectral parameters of the Lax operators which build up the monodromy matrix; as is customary, we separate these parameters into a shared value, the spectral parameter u , and local shifts, the inhomogeneities v_i ,

$$\mathcal{M}_n(u, \{v_i\}) = \mathcal{L}_n(u - v_n) \cdots \mathcal{L}_2(u - v_2) \mathcal{L}_1(u - v_1). \quad (7.37)$$

From this monodromy matrix we can construct a transfer matrix depending on both the spectral parameter as well as the inhomogeneities by taking the supertrace

$$\mathcal{T}_n(u, \{v_i\}) = \text{str } \mathcal{M}_n(u, \{v_i\}). \quad (7.38)$$

We note that this transfer matrix is still $\mathfrak{gl}_{4|4}$ invariant,

$$[\mathcal{T}(u, \{v_i\}), \sum_{i=1}^n \mathcal{J}_i^{\text{AB}}] = 0. \quad (7.39)$$

The Yangian invariance condition takes the same form as before, but the eigenvalue can now depend on the inhomogeneities:

$$\mathcal{M}_n(u, \{v_i\})|\Omega\rangle = f(u, \{v_i\})|\Omega\rangle \quad (7.40)$$

We will also use the same graphical language for the deformed as for the undeformed case.

There are different perspectives on these deformations: From a spin chain point of view, they correspond to inhomogeneities, local shifts of the spectral parameter, which can be interpreted as local defects. Regarding the Yangian, this corresponds to using different representations at each site: a single Lax operator itself constitutes a representation of the Yangian in RTT language (it satisfies the RTT relation (7.20) which in this case is nothing else than the Yang-Baxter equation (7.14)); it is constructed from a representation of $\mathfrak{gl}_{4|4}$ by adding the spectral parameter dependent term – this is called the evaluation map; having different spectral parameters at each site thus amounts to using different representations of the Yangian (based on the same representations of $\mathfrak{gl}_{4|4}$ though) in the tensor product representation. Finally, the invariants of this representation of the Yangian will have non-zero central charges at each site. These are determined by the inhomogeneities, as we will see shortly. The total central charge is

- 32 Faddeev, “How algebraic Bethe ansatz works for integrable model”, [hep-th/9605187](#)
- 33 Beisert, Dippel, Staudacher, “A Novel long range spin chain and planar $\mathcal{N} = 4$ super Yang–Mills”, [hep-th/0405001](#)
- 34 Ferro, Łukowski, Meneghelli, Plefka, Staudacher, “Harmonic R–matrices for Scattering Amplitudes and Spectral Regularization”, [1212.0850](#); and Ferro, Łukowski, Meneghelli, Plefka, Staudacher, “Spectral Parameters for Scattering Amplitudes in $\mathcal{N} = 4$ Super Yang–Mills Theory”, [1308.3494](#)
- 35 Frassek, Kanning, Ko, Staudacher, “Bethe Ansatz for Yangian Invariants: Towards Super Yang–Mills Scattering Amplitudes”, [1312.1693](#)
- 36 Beisert, Broedel, Rosso, “On Yangian-invariant regularization of deformed on-shell diagrams in $\mathcal{N} = 4$ super-Yang–Mills theory”, [1401.7274](#)
- 37 Broedel, de Leeuw, Rosso, “Deformed one-loop amplitudes in $\mathcal{N} = 4$ super-Yang–Mills theory”, [1406.4024](#)
- 38 Bargheer, Huang, Loebbert, Yamazaki, “Integrable Amplitude Deformations for $\mathcal{N} = 4$ Super Yang–Mills and ABJM Theory”, [1407.4449](#); and Ferro, Łukowski, Staudacher, “ $\mathcal{N} = 4$ scattering amplitudes and the deformed Grassmannian”, [1407.6736](#)
- 39 Kanning, Ko, Staudacher, “Grassmannian integrals as matrix models for non-compact Yangian invariants”, [1412.8476](#)
- 40 Chicherin, Kirschner, “Yangian symmetric correlators”, [1306.0711](#); and Chicherin, Derkachov, Kirschner, “Yang–Baxter operators and scattering amplitudes in $\mathcal{N} = 4$ super-Yang–Mills theory”, [1309.5748](#)
- 41 Broedel, de Leeuw, Rosso, “A dictionary between R-operators, on-shell graphs and Yangian algebras”, [1403.3670](#)
- 42 Kanning, Łukowski, Staudacher, “A shortcut to general tree-level scattering amplitudes in $\mathcal{N} = 4$ SYM via integrability”, [1403.3382](#)
- 43 Formally, the operator can also be written as $\Gamma(-z)(x_j \cdot p_i)^z$, which simplifies some calculations; the complex power of operators should be interpreted in terms of fractional derivatives, see Lovoie, Osler, Tremblay, “Fractional derivatives and special functions”, *SIAM review* **18** (1976), no. 2, 240–268.

still imposed to be zero, but we can regard the individual central charges as new physical properties of the particles participating in the scattering process.

While inhomogeneous spin chains have been considered for a long time in the literature,³² and in the context of $\mathcal{N} = 4$ SYM have been used as approximate models for the spectrum,³³ their application to scattering amplitudes is a very recent development. It was first found that certain inhomogeneities result in Yangian invariants which can be given an integrability interpretation. In particular, the deformation of the four-point amplitude can be regarded as an R-matrix, and other on-shell diagrams as generalizations thereof,³⁴ with the inhomogeneities playing the role of a spectral parameter. This idea was then related to integrable vertex models and usual Bethe Ansatz techniques.³⁵ Another development which makes use of these deformations is the R-operator formalism. It will be the focus of the next sections, and can be adapted to the case of form factors, as we will show in chapter 8. We note that the deformations usually prevent the consistent addition of different diagrams, both for tree-level amplitudes³⁶ as well as for loop level integrands³⁷. This makes it difficult to give a “physical” interpretation to the deformations, despite the fact that they can be considered as complex superhelicities of the participating particles. Finally, the deformation where directly lifted to the Grassmannian top-form,³⁸ which interestingly relates these developments to matrix models.³⁹

7.5 Construction of on-shell functions via R-operators

The papers Chicherin and Kirschner (2013); Chicherin et al. (2014)⁴⁰ introduced a purely integrability-based method of constructing Yangian invariants using so-called Yang-Baxter operators, or R-operators. This approach was further developed and related to on-shell diagrams in Broedel et al. (2014),⁴¹ and to the Bethe Ansatz construction in Kanning et al. (2014).⁴² The construction naturally leads to the deformations of scattering amplitudes we just discussed.

The basic object in this approach is the R-operator which we define as⁴³

$$R_{ij}(z) = \begin{array}{c} | \\ \circ \\ | \\ j \end{array} \begin{array}{c} | \\ \bullet \\ | \\ i \end{array} = \int \frac{d\alpha}{\alpha^{1+z}} e^{-\alpha(x_j \cdot p_i)} . \quad (7.41)$$

Here the operators x_i^A and p_i^A are the Jordan-Schwinger oscillators defined in (7.7). The exponential in this definition of the R-operator acts as a shift operator on the spinor-helicity variables, with an action given by

$$R_{ij}(z) f(\lambda_i, \tilde{\lambda}_i, \tilde{\eta}_i, \lambda_j, \tilde{\lambda}_j, \tilde{\eta}_j) = \int \frac{d\alpha}{\alpha^{1+z}} f(\lambda_i - \alpha\lambda_j, \tilde{\lambda}_i, \tilde{\eta}_i, \lambda_j, \tilde{\lambda}_j + \alpha\tilde{\lambda}_i, \tilde{\eta}_j + \alpha\tilde{\eta}_j) . \quad (7.42)$$

This is just the familiar BCFW shift (2.35), and explains the graphical notation: the R-operator is simply a BCFW bridge, with the noteworthy distinction that it

does not simply add a dlog integration over the shift, corresponding to an edge variable, but instead comes with a scaling factor z , the spectral parameter. We have left the integration contour in (7.41) unspecified. Indeed, all manipulations we will perform with these operators are purely algebraic and do not depend on the contour. It suffices to say that in the context of amplitudes, where the parameters z are taken to zero the contour is always closed, either localizing a holomorphic delta function or setting the edge variable α to zero.

The R-operator is $\mathfrak{gl}_{4|4}$ invariant

$$\begin{aligned} [R_{ij}(z), \mathcal{G}_i^{AB}] &= -x_j^A p_i^B R_{ij}(z-1) \\ [R_{ij}(z), \mathcal{G}_j^{AB}] &= +x_j^A p_i^B R_{ij}(z-1) \\ \implies [R_{ij}(z), \mathcal{G}_i^{AB} + \mathcal{G}_j^{AB}] &= 0 \end{aligned} \tag{7.43}$$

and has the following commutators with the central charge (7.11)

$$\begin{aligned} [R_{ij}(z), \mathbf{c}_i] &= z R_{ij}(z) \\ [R_{ij}(z), \mathbf{c}_j] &= -z R_{ij}(z) \end{aligned} \tag{7.44}$$

These equations imply that the R-operator changes the local central charges $\propto z$, while keeping the total central charge constant, $[R_{ij}(z), \mathbf{c}_i + \mathbf{c}_j] = 0$.

The “deformation” z introduced by (7.41) plays an important role in the integrability perspective on the construction of Yangian invariants. Indeed the R-operators satisfy the following Yang-Baxter equation

$$R_{12}(z_{12})R_{23}(z_{13})R_{12}(z_{23}) = R_{23}(z_{23})R_{12}(z_{13})R_{23}(z_{12}) \tag{7.45}$$

This is the same as the Yang-Baxter equation (7.5), if a permutation operator is factored out of the R-matrix.⁴⁴

If we take one space in the fundamental representation, and two in the spinor-helicity representation, we get a different Yang-Baxter equation involving both the R-operators (7.41) as well as the Lax operators (7.13).

$$R_{ij}(u_j - u_i) \mathcal{L}_j(u_j) \mathcal{L}_i(u_i) = \mathcal{L}_j(u_i) \mathcal{L}_i(u_j) R_{ij}(u_j - u_i), \tag{7.46}$$

which can be depicted as



$$\tag{7.47}$$

This equation will eventually guarantee the Yangian invariance of states constructed from R-operators: Given appropriate values for the spectral parameters z , it shows that the monodromy matrix commutes with chains of R-operators. Therefore they can be used to create new invariants starting from other ones, simply by acting on them. We now turn to the details of this construction.

The simplest invariants are the so-called vacua, which are states on a single site of the spin chain, i.e. they depend on only one set of spinor-helicity variables:⁴⁵

⁴⁴ In the literature, such reduced R-matrices are usually called \check{R} .

⁴⁵ In the diagrammatic language of on-shell diagrams, they correspond to white and black “lollipop” diagrams, see e.g. Arkani-Hamed, Bourjaily, Cachazo, Goncharov, Postnikov, Trnka, “Scattering Amplitudes and the Positive Grassmannian”, Cambridge University Press, 2016, 1212.5605.

$$\begin{array}{c} \oplus \\ | \\ i \end{array} = \delta_i^+ = \delta^2(\lambda_i), \quad \begin{array}{c} \ominus \\ | \\ i \end{array} = \delta_i^- = \delta^2(\tilde{\lambda}_i)\delta^4(\tilde{\eta}_i). \quad (7.48)$$

To construct an invariant for n particles and MHV degree k , one takes a product of n such vacua, one for each particle, k of which have to be of type δ^- .

Any such state is Yangian invariant as defined in (7.40), since the Lax operators act diagonally on the vacua

$$\mathcal{L}_i(u) \delta_i^+ = (u-1) \mathbb{I} \delta_i^+, \quad \mathcal{L}_i(u) \delta_i^- = u \mathbb{I} \delta_i^-, \quad (7.49)$$

which can be depicted as

$$\begin{array}{c} \oplus \\ -| \\ i \end{array} = (u-1) \begin{array}{c} \oplus \\ | \\ i \end{array}, \quad \begin{array}{c} \ominus \\ -| \\ i \end{array} = u \begin{array}{c} \ominus \\ | \\ i \end{array}. \quad (7.50)$$

To obtain further invariants, we can act with sequences of R-operators on these products of vacuum states. An ansatz for a general invariant is then given by

$$|\mathcal{A}\rangle = R_{i_1 j_1}(z_1) \cdots R_{i_m j_m}(z_m) \prod_{j \in \mathcal{J}^+} \delta_j^+ \prod_{j \in \mathcal{J}^-} \delta_j^-, \quad (7.51)$$

where \mathcal{J}^+ is the set of positions of “+” vacua and \mathcal{J}^- those of the “-” vacua; m is simply the number of BCFW bridges of the diagram, which can be arbitrary.

Since the R-operators are essentially (deformed) BCFW bridges, we can associate a permutation to this state, in accordance with the left-right paths of on-shell diagrams:

$$\sigma = (i_1, j_1) \triangleleft \cdots \triangleleft (i_m, j_m), \quad (7.52)$$

where the product \triangleleft is the composition defined in (2.49). As noted above, the number of plus and minus vacua fixes the MHV degree of the state

$$|\mathcal{J}^+| = n - k, \quad |\mathcal{J}^-| = k. \quad (7.53)$$

Furthermore, a given chain of R-operators fixes the positions of the “+” and “-” vacua. For each site, consider the first R-operator which acts on this site; if the site appears as the first index of the operator, it is of type δ^+ , and if it corresponds to the second index, of type δ^- . According to (7.42), this ensures that all R-operators act non-trivially.⁴⁶

As an example, we consider the deformed three-point MHV amplitude. The associated permutation can be decomposed into adjacent transpositions as

$$(3, 1, 2) = (2, 3) \triangleleft (1, 2). \quad (7.54)$$

This translates into the following expression in terms of R-operators and vacua

$$A_{3,2}^{\text{deformed}} = R_{23}(v_{32})R_{12}(v_{31})\delta_1^+\delta_2^-\delta_3^-, \quad (7.55)$$

⁴⁶ In principle one can of course use a different distribution of the vacua, but this would generate integrations over variables which do not appear in any delta functions, i.e. “bubbles” in the sense of figure 2.5.

where we already set the deformations to the values imposed by Yangian invariance, to be discussed shortly, and use the abbreviation $v_{ij} = v_i - v_j$.

We can draw the state using the diagrammatic language outlined above; this is shown in figure 7.2. Note that graphically, one obtains the standard on-shell diagram by removing the vacua, and subsequently deleting all two-valent vertices. It is easy to evaluate the action of the R-operators on the vacua, such that one finds

$$A_{3,2}^{\text{deformed}} = \frac{\delta^4(\sum_{i=1}^3 \lambda_i \tilde{\lambda}_i) \delta^4(\sum_{i=1}^3 \lambda_i \tilde{\eta}_i^+) \delta^4(\sum_{i=1}^3 \lambda_i \tilde{\eta}_i^-)}{\langle 12 \rangle^{1-v_{23}} \langle 23 \rangle^{1-v_{31}} \langle 31 \rangle^{1-v_{12}}}. \quad (7.56)$$

It is evident that the undeformed amplitude $A_{3,2}$ will be recovered setting $v_i \rightarrow 0$.

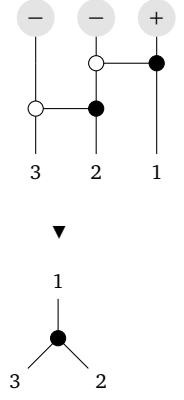


Figure 7.2: Integrability construction for the deformed three-point MHV amplitude.

7.6 Yangian invariance of R-operator states

The construction based on R-operators allows to immediately deduce the Yangian invariance of the states, making use of the Yang-Baxter equation (7.46).

We first consider the undeformed case, where the spectral parameters of the R-operators are set to zero, i.e. states of the form

$$|\mathcal{A}\rangle = R_{i_1 j_1}(0) \cdots R_{i_m j_m}(0) \prod_{j \in \mathcal{J}^+} \delta_j^+ \prod_{j \in \mathcal{J}^-} \delta_j^-. \quad (7.57)$$

These states correspond to normal on-shell diagrams, representing (BCFW terms of) scattering amplitudes, leading singularities and so forth. Specializing equation (7.46) to this case, we see that the monodromy matrix defined in (7.16) commutes with the sequence of R-operators; then it acts diagonally on the vacua according to (7.49):

$$\begin{aligned} \mathcal{M}_n(u) |\mathcal{A}\rangle &= \mathcal{M}_n(u) R_{i_1 j_1}(0) \cdots R_{i_m j_m}(0) \prod_{j \in \mathcal{J}^+} \delta_j^+ \prod_{j \in \mathcal{J}^-} \delta_j^- \\ &= R_{i_1 j_1}(0) \cdots R_{i_m j_m}(0) \mathcal{M}_n(u) \prod_{j \in \mathcal{J}^+} \delta_j^+ \prod_{j \in \mathcal{J}^-} \delta_j^- \\ &= (u-1)^{|\mathcal{J}^+|} (u)^{|\mathcal{J}^-|} \mathbb{1} |\mathcal{A}\rangle. \end{aligned} \quad (7.58)$$

This shows that the states are Yangian invariants as defined in (7.35), and the eigenvalues are simply the products of those of the vacua δ_i^\pm , the numbers of which are given in (7.53). Graphically, this argument can be represented as in figure 7.3; the monodromy can successively be pulled through all BCFW bridges, as well as through the vacua, given that they are eigenstates.

The deformed case is more subtle. The states defined in (7.51) have to be considered only as an ansatz for Yangian invariants, with the parameters z_i to be determined in a suitable way. To fix them, we determine under which circumstances the inhomogeneous monodromy matrix (7.37) commutes with the sequence of R-operators in (7.51). Using (7.46), one finds that

$$\mathcal{M}(u, \{v_i\}) R_{i_1 j_1}(z_1) \cdots R_{i_m j_m}(z_m) = R_{i_1 j_1}(z_1) \cdots R_{i_m j_m}(z_m) \mathcal{M}(u, \{v_{\sigma(i)}\}), \quad (7.59)$$

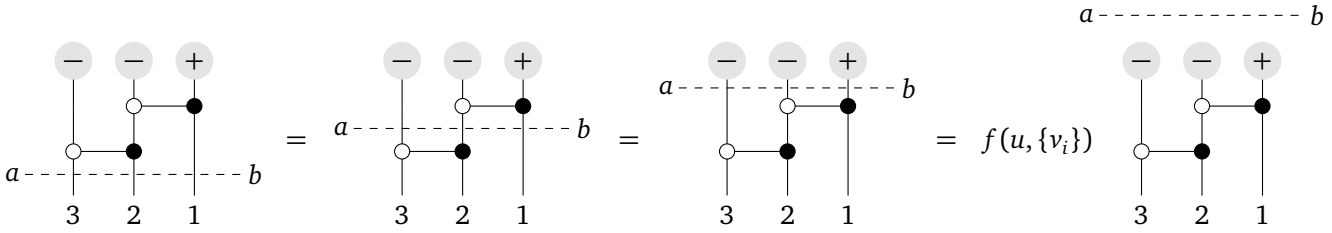


Figure 7.3: Steps to show the Yangian invariance of the three-point MHV amplitude using R-operators.

provided that the parameters z_ℓ satisfy

$$z_\ell = v_{\tau_\ell(i_\ell)} - v_{\tau_\ell(j_\ell)} \quad \text{with} \quad \tau_\ell = (i_1, j_1) \triangleleft \cdots \triangleleft (i_\ell, j_\ell), \quad \ell = 1, \dots, m, \quad (7.60)$$

We see that the monodromy matrix does not really commute with the sequence of R-operators, but given these constraints, it commutes up to a reshuffling of the inhomogeneities: v_i is replaced by $v_{\sigma(i)}$, where σ is the permutation associated to the state as in (7.52), which is the same as the one which can be read off from the on-shell diagram using left-right paths as discussed in section 2.4.

Using the commutators (7.44), and the fact that the vacua δ^\pm carry no central charge, one finds that the state (7.51), upon fixing the parameters z_i as in (7.60) carries the following local central charges

$$\mathbf{c}_i = v_i - v_{\sigma(i)}. \quad (7.61)$$

Due to this difference property the total central charge $\mathbf{c} = \mathbf{c}_1 + \cdots + \mathbf{c}_n$ vanishes.

Finally, since each Lax operator in the monodromy matrix acts diagonally on the corresponding site, we find that the Yangian invariance condition is satisfied in the following form

$$\begin{aligned} & \mathcal{M}_n(u, \{v_i\}) | \cdot \mathcal{A} \rangle \\ &= \mathcal{M}_n(u, \{v_i\}) R_{i_1 j_1}(v_{\tau_1(i_1)} - v_{\tau_1(j_1)}) \cdots R_{i_m j_m}(v_{\tau_m(i_m)} - v_{\tau_m(j_m)}) \prod_{j \in \mathcal{J}^+} \delta_j^+ \prod_{j \in \mathcal{J}^-} \delta_j^- \\ &= R_{i_1 j_1}(v_{\tau_1(i_1)} - v_{\tau_1(j_1)}) \cdots R_{i_m j_m}(v_{\tau_m(i_m)} - v_{\tau_m(j_m)}) \mathcal{M}_n(u, \{v_i\}) \prod_{j \in \mathcal{J}^+} \delta_j^+ \prod_{j \in \mathcal{J}^-} \delta_j^- \\ &= \prod_{j \in \mathcal{J}^+} (u - v_j - 1) \prod_{j \in \mathcal{J}^-} (u - v_j) \mathbb{1} | \cdot \mathcal{A} \rangle. \end{aligned} \quad (7.62)$$

We see that the proof of the Yangian invariance of on-shell diagrams is purely algebraic, if the corresponding on-shell functions are expressed in terms of R-operators. In the next chapter we will use these operators to derive similar statements in the case of form factors.

8

Integrability construction for form factors

The integrability-based construction of amplitudes and on-shell functions explored in the last chapter did not only provide a convenient and algebraic way of writing these quantities, it also allowed to interpret them as spin chain states, introduced deformations, and made their integrability properties – namely their Yangian invariance – manifest.

On-shell diagrams for form factors, as explored in chapter 3, mark a starting point for an adaptation of this approach to form factors, and their related on-shell functions. This is the aim of this chapter. We will see that the minimal form factor can be interpreted as a new kind of entangled vacuum state. We can then build up more complex diagrams using the R-operator construction, leading to deformed form factor on-shell functions.

Far from being a purely formal exercise, the integrability-based construction enables the derivation of novel properties of these on-shell functions: we will show that they are eigenstates of the integrable transfer matrix defined in equation (7.26). We furthermore show that this is not only the case for on-shell diagrams involving the chiral stress energy tensor, but that similar identities hold for all on-shell functions with arbitrary operator insertions. These identities can be regarded as symmetries constraining the on-shell functions, but also properly account for them as states in the integrable model behind $\mathcal{N}=4$ SYM, maybe opening up further possibilities to calculate them purely based on integrability. Furthermore, while integrability can be used to calculate amplitudes, the state of the art for the spectral problem is considerably more advanced; we hope that form factors may provide a link in this context.

This chapter is based on the author's publication Frassek, Meidinger, Nandan, Wilhelm, "On-shell diagrams, Grassmannians and integrability for form factors", 1506.08192.

8.1 The minimal form factor as a vacuum state

In chapter 3, we saw that the minimal, i.e. the two-point form factor (3.12) was the essential new building block for form factor on-shell diagrams. Here we want to leverage this fact to describe an integrability-based construction in terms of R-operators. For this construction we adapt the formalism described in section 7.5

to harmonic superspace; this merely amounts to replacing the four Graßmann variables $\tilde{\eta}^A$, $A = 1, 2, 3, 4$ by $\tilde{\eta}^{+a}$ and $\tilde{\eta}^{-a'}$, which have two components each. This applies to the entire Schwinger representation defined in (7.7), and both to the R-operators (7.41) as well as the vacua (7.48).

The starting point of our construction is the observation that the minimal form factor can be written purely in terms of delta functions,

$$F_{2,2}(1,2) = \delta^2(\underline{\tilde{\lambda}}_1) \delta^4(\underline{\tilde{\eta}}_1) \delta^2(\underline{\tilde{\lambda}}_2) \delta^4(\underline{\tilde{\eta}}_2) \equiv \delta_{12}^F, \quad (8.1)$$

if we define kinematic variables as

$$\begin{aligned} \underline{\tilde{\lambda}}_1 &= \tilde{\lambda}_1 - \frac{\langle 2|q}{\langle 21 \rangle}, & \underline{\tilde{\eta}}_1^- &= \tilde{\eta}_1^- - \frac{\langle 2|\gamma^-}{\langle 21 \rangle}, & \underline{\tilde{\eta}}_1^+ &= \tilde{\eta}_1^+, \\ \underline{\tilde{\lambda}}_2 &= \tilde{\lambda}_2 - \frac{\langle 1|q}{\langle 12 \rangle}, & \underline{\tilde{\eta}}_2^- &= \tilde{\eta}_2^- - \frac{\langle 1|\gamma^-}{\langle 12 \rangle}, & \underline{\tilde{\eta}}_2^+ &= \tilde{\eta}_2^+. \end{aligned} \quad (8.2)$$

These variables are “twisted” in such a way that they not only encode the original on-shell kinematics, but also the off-shell momentum and supermomentum of the operator; we encountered them already when we discussed the MHV Graßmannian integral, see equation (4.34).

We use the notation $\delta_{i\ i+1}^F$ to stress the remarkable fact that the minimal form factor (8.1), expressed in these variables, looks precisely like the product of two R-operator vacua defined in (7.48):

$$\delta_{12}^F = \delta_1^- \delta_2^- |_{\lambda \rightarrow \underline{\lambda}, \tilde{\lambda} \rightarrow \underline{\tilde{\lambda}}, \tilde{\eta} \rightarrow \underline{\tilde{\eta}}}. \quad (8.3)$$

This strongly suggests that in order to construct form factor on-shell functions using the integrability approach presented in section 7.5, we have to use the minimal form factor as an additional vacuum state. While the two sites with this “vacuum” are clearly entangled, the factorized form (8.1) implies that the action of the R-operators is very similar to the amplitude case.

8.2 Permutations, bridges and R-operators

Using the minimal form factor as given in (8.1) as a vacuum state, together with the amplitude vacua $\delta_i^+ \delta_i^-$ defined in (7.48), we can construct general form factor on-shell functions for any planar on-shell diagram containing the minimal form factor, including top-cell diagrams, individual BCFW terms, factorization channels etc. using R-operators as in section 7.5. Note that both the R-operators as well as the vacua have been adapted to harmonic superspace by replacing occurrences of the Graßmann variables $\tilde{\eta}$ by $\tilde{\eta}^+$ and $\tilde{\eta}^-$. For example, in the definition of the vacuum state $\delta_i^- = \delta^2(\tilde{\lambda}_i) \delta^4(\tilde{\eta}_i)$ we interpret $\delta^4(\tilde{\eta}_i) = \tilde{\eta}_i^{+1} \tilde{\eta}_i^{+2} \tilde{\eta}_i^{-1} \tilde{\eta}_i^{-2}$.

A general form factor on-shell function $|\mathcal{F}\rangle$ of the chiral stress-tensor multiplet with n particles and MHV degree k can then be written as

$$|\mathcal{F}\rangle = R_{i_1 j_1}(z_1) \cdots R_{i_m j_m}(z_m) |\Omega_{\mathcal{F}}\rangle, \quad (8.4)$$

where we separated the vacuum states by defining

$$|\Omega_{\mathcal{S}}\rangle = \delta_{ll+1}^F \prod_{j \in \mathcal{S}^+} \delta_j^+ \prod_{j \in \mathcal{S}^-} \delta_j^- . \quad (8.5)$$

The set \mathcal{S}^+ contains the position of the $n - k$ δ^+ vacua, and \mathcal{S}^- those of the δ^- ones, the number of which is $k - 2$. The minimal form factor serves as the vacuum at sites l and $l + 1$.

The number m of R-operators is determined by the diagram under consideration. The precise sequence can be obtained from the permutation that can be read off the diagram as described in section 3.8, by decomposing it into transpositions. However, as already noted there, this decomposition has to be non-minimal in most cases. In the following we will consider only sequences of R-operators that correspond to planar diagrams. Some examples of this construction are presented in figure 8.1, which also serves to illustrate the graphical notation of section 7.5, adapted to form factor on-shell functions.

If we keep the parameters z_i of the R-operators non-zero, the resulting on-shell functions will be central-charge-deformed, similar to the amplitude case considered in the previous chapter. We will now calculate these deformations in the case of MHV form factors.

8.3 Deformed MHV form factors

The states constructed in the last section can be evaluated explicitly using the action of the R-operators (7.42) on the vacuum states, including the minimal form factor in the factorized representation (8.1). In this way, we can find deformations of form factor on-shell functions. Here we provide the derivation of these deformations for all MHV form factors both as deformed versions of the Parke-Taylor-type formula (3.7), as well as deformed Graßmannian integrals.¹

For these MHV form factors, we take the minimal form factor to be the vacuum for sites $n - 1$ and n . All other vacua are of type δ^+ :

$$\text{Vacuum}(F_{n,2}) = \delta_1^- \cdots \delta_{n-2}^- \delta_{n-1}^+ \delta_n^+ . \quad (8.6)$$

The chain of R-operators is the same as for the MHV amplitudes with the same number of particles, and given by²

$$(R_{23}R_{12}) \cdots (R_{n-1}R_{n-2}R_{n-1}) . \quad (8.7)$$

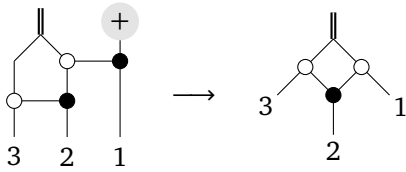
We start by considering the three-point case; acting with the appropriate sequence of R-operators as in (7.42) by shifting the arguments of the delta function in the vacuum states, we get

$$\begin{aligned} & \mathbf{F}_{3,2}^{\text{def.}}(1, 2, 3) \\ &= R_{23}(v_{32})R_{12}(v_{31})\delta_1^+ \delta_{23}^F \\ &= \int \frac{d\alpha_2}{\alpha_2^{1+v_{32}}} \int \frac{d\alpha_1}{\alpha_1^{1+v_{31}}} \delta^4(C(\alpha_1, \alpha_2) \cdot \underline{\tilde{\lambda}}) \delta^8(C(\alpha_1, \alpha_2) \cdot \underline{\tilde{\eta}}) \delta^2(C^\perp(\alpha_1, \alpha_2) \cdot \lambda) . \end{aligned} \quad (8.8)$$

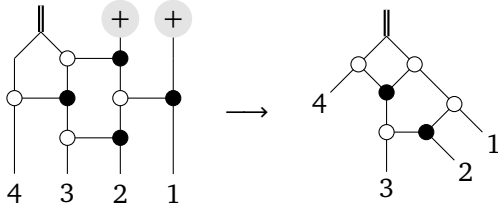
¹ Bargheer, Huang, Loebbert, Yamazaki, “Integrable Amplitude Deformations for $\mathcal{N} = 4$ Super Yang–Mills and ABJM Theory”, 1407.4449; and Ferro, Łukowski, Staudacher, “ $\mathcal{N} = 4$ scattering amplitudes and the deformed Graßmannian”, 1407.6736

² This is of course just one possible choice, cf. figure 8.1. Many more decompositions are possible, corresponding to different positions of the inverse soft factors, see section 3.4.

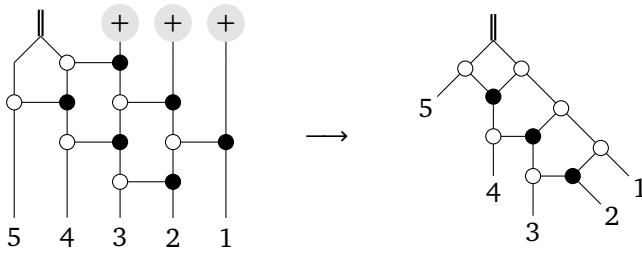
$F_{3,2} \quad \sigma = (3, 1, 2) = (2, 3) \triangleleft (1, 2)$



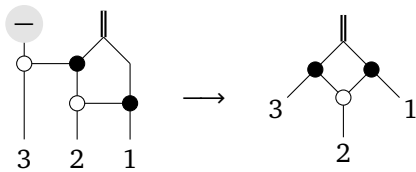
$F_{4,2} \quad \sigma = (3, 4, 1, 2) = (2, 3) \triangleleft (3, 4) \triangleleft (1, 2) \triangleleft (2, 3)$



$F_{5,2} \quad \sigma = (3, 4, 5, 1, 2) = (2, 3) \triangleleft (3, 4) \triangleleft (4, 5) \triangleleft (1, 2) \triangleleft (2, 3) \triangleleft (3, 4)$



$F_{3,3} \quad \sigma = (2, 3, 1) = (1, 2) \triangleleft (2, 3)$



$\text{TopCell}(F_{4,3}) \quad \sigma = (4, 2, 3, 1) = (1, 2) \triangleleft (3, 4) \triangleleft (2, 3) \triangleleft (1, 2) \triangleleft (3, 4)$

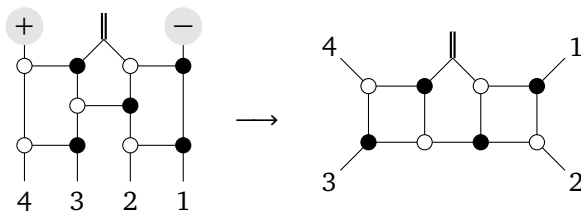


Figure 8.1: Integrability construction for several form factor on-shell diagrams. The permutation is determined from the diagram, and decomposed into adjacent transpositions. This decomposition corresponds to the sequence of R-operators acting on the vacuum states.

Here the kinematic variables for particles 2 and 3 are “twisted” as in (8.1) while those for particle 1 remain unchanged. We also set the parameters of the R-operators to specific values, with $v_{ij} = v_i - v_j$, for reasons that will be explained later. The matrices C and C^\perp contain the information of the BCFW shifts

$$C(\alpha_1, \alpha_2) = \begin{pmatrix} \alpha_1 & 1 & 0 \\ 0 & \alpha_2 & 1 \end{pmatrix}, \quad C^\perp(\alpha_1, \alpha_2) = \begin{pmatrix} 1 & -\alpha_1 & \alpha_1\alpha_2 \end{pmatrix}. \quad (8.9)$$

and parametrize the Grassmannian $G(2, 3)$.

We can transform this Grassmannian integral in edge variables to the usual form by a change of variables to the entries of the C matrix, in order to make the $GL(2)$ invariance manifest:

$$F_{3,2}^{\text{def}}(1, 2, 3) = \int \frac{d^{2 \times 3} C}{(12)^{1-v_{23}}(23)^{1-v_{31}}(31)^{1-v_{12}}} \delta^4(C \cdot \tilde{\lambda}) \delta^8(C \cdot \tilde{\eta}) \delta^2(C^\perp \cdot \lambda), \quad (8.10)$$

Without going through the details of the derivation, we can immediately generalize this formula to any number of particles:

$$F_{n,2}^{\text{def}}(1, \dots, n) = \int \frac{d^{2 \times n} C}{\prod_{i=1}^n (i \ i+1)^{1-v_{i+1 \ i+2}}} \delta^4(C \cdot \tilde{\lambda}) \delta^8(C \cdot \tilde{\eta}) \delta^{2n-4}(C^\perp \cdot \lambda). \quad (8.11)$$

The twisted kinematic variables (8.2) can be placed at any two sites in this formula. In order to prove this equation, one merely has to note that the sequence of R-operators (8.7) is the same as for amplitudes, and that it acts in such a way on the vacua that the final dependence on the kinematic variables $\tilde{\lambda}, \tilde{\eta}$ is not spoiled.³ We note the resulting deformed Grassmannian integral (8.11) is the same as its amplitude counterpart derived in the papers Bargheer et al. (2015); Ferro et al. (2014).⁴ All information on the operator insertion is contained in the twisted kinematics (8.2).

It is easy to evaluate the integral. The twisted kinematics only changes the variables $\tilde{\lambda}$ and $\tilde{\eta}$ and therefore does not affect the Parke-Taylor prefactor, while adjusting the momentum and supermomentum conserving delta functions in the correct way, by shifting $P \rightarrow P - q$ and $Q^- \rightarrow Q^- - \gamma^-$. This is a consequence of the identity

$$\lambda_i^\alpha \left(\tilde{\lambda}_i^{\dot{\alpha}} - \frac{\langle j | q^{\dot{\alpha}}}{\langle ji \rangle} \right) + \lambda_j^\alpha \left(\tilde{\lambda}_j^{\dot{\alpha}} - \frac{\langle i | q^{\dot{\alpha}}}{\langle ij \rangle} \right) = \lambda_i^\alpha \tilde{\lambda}_i^{\dot{\alpha}} + \lambda_j^\alpha \tilde{\lambda}_j^{\dot{\alpha}} - \underbrace{\frac{\varepsilon_{\gamma\beta} (\lambda_i^\alpha \lambda_j^\gamma - \lambda_j^\alpha \lambda_i^\gamma)}{\langle ji \rangle}}_{=\delta_\beta^\alpha} q^{\beta\dot{\alpha}}, \quad (8.12)$$

and a similar identity for the supermomentum, obtained by replacing q with γ in the (8.12). Thus we see that (8.11) gives a deformed version of the Parke-Taylor-type expression (3.7),

$$F_{n,2}^{\text{def}}(1, \dots, n) = \frac{\delta^4(\sum_{i=1}^n \lambda_i \tilde{\lambda}_i - q) \delta^4(\sum_{i=1}^n \lambda_i \tilde{\eta}_i^+) \delta^4(\sum_{i=1}^n \lambda_i \tilde{\eta}_i^- - \gamma^-)}{\prod_{i=1}^n \langle i \ i+1 \rangle^{1-v_{i+1 \ i+2}}}. \quad (8.13)$$

Note that in the preceding derivations, we have chosen the parameters z in a specific way in terms of variables v_i ; this was to ensure that the resulting deformed form factors are eigenstates of the integrable transfer matrix (7.38), as we will now show.

³ In principle, the BCFW shifts could affect the denominators in (8.2). This does not happen.

⁴ Bargheer, Huang, Loebbert, Yamazaki, “Integrable Amplitude Deformations for $\mathcal{N} = 4$ Super Yang-Mills and ABJM Theory”, 1407.4449; and Ferro, Łukowski, Staudacher, “ $\mathcal{N} = 4$ scattering amplitudes and the deformed Grassmannian”, 1407.6736

8.4 Form factor on-shell functions as spin chain eigenstates

One of the properties of the R-operator formalism is that it reduces the proof of Yangian invariance of amplitude on-shell functions to some simple algebraic computations. While the Yangian invariance of amplitudes was known prior to the development of this construction, it can be used to derive novel integrability properties, or symmetries, in the context of form factor on-shell functions. In this section we will show that these functions are eigenstates of integrable transfer matrices. The corresponding eigenvalue equations can be regarded as symmetries, in the same sense as Yangian invariance, since the expansion of the transfer matrix contains linear combinations of the Yangian generators.

We will first consider on-shell functions of the chiral stress tensor multiplet, which we discussed exclusively so far. Finally, we will also consider on-shell functions of generic component operators, and show that they have similar integrability properties.

On-shell functions of the chiral stress tensor multiplet

Consider the general on-shell function defined in (8.4) in terms of vacua and R-operators. We want to investigate the action of the inhomogeneous monodromy matrix (7.37) on this state, to test whether it is Yangian invariant.

Since – compared to the amplitude states (7.51) – only the vacuum part is different, while the sequence of R-operators is of the same form, we can still use the commutation relations (7.59) between the monodromy matrix and a chain of R-operators as in (8.4), which we repeat here for the reader's convenience,

$$\mathcal{M}(u, \{v_i\}) R_{i_1 j_1}(z_1) \cdots R_{i_m j_m}(z_m) = R_{i_1 j_1}(z_1) \cdots R_{i_m j_m}(z_m) \mathcal{M}(u, \{v_{\sigma(i)}\}), \quad (8.14)$$

under the condition that

$$z_\ell = v_{\tau_\ell(i_\ell)} - v_{\tau_\ell(j_\ell)} \quad \text{with} \quad \tau_\ell = (i_1, j_1) \triangleleft \cdots \triangleleft (i_\ell, j_\ell), \quad \ell = 1, \dots, m. \quad (8.15)$$

The central charges induced by the inhomogeneities, under these constraints, are the same as for amplitudes and given by $\mathbf{c}_i = v_i - v_{\sigma(i)}$.

A first noteworthy observation is that the permutation σ that shuffles the inhomogeneities in the relation (8.14), thereby determining the parameters of the R-operators in terms of them, is the one obtained from the on-shell diagram using the rule (3.19) to turn back at the minimal form factor. This can be understood as follows: One can use left-right paths as discussed in section 3.8 to determine permutations from the type of diagrams we use in the integrability construction, consisting of BCFW bridges and vacua. Even for amplitude diagrams, one then has to use the further rule to turn back when the path arrives at a δ^\pm vacuum. One can easily convince oneself of this fact, if one compares both types of diagrams as for example shown in figure 7.2. This justifies our rule (3.19) to turn back if a path hits the minimal form factor: this simply mirrors the behavior of the

amplitude vacua, and ensures that we get the correct permutation required for the commutation relation between the monodromy matrix and the R-operators (8.14). For completeness, we summarize the rules to determine the permutation σ using left-right paths in the integrability diagrams in figure 8.2.

We can now use (8.14) to commute the monodromy matrix through the sequence of R-operators in the state (8.4) under the conditions (8.15):

$$\mathcal{M}_n(u, \{v_i\}) |\mathcal{F}\rangle = R_{i_1 j_1}(z_1) \cdots R_{i_m j_m}(z_m) \mathcal{M}_n(u, \{v_{\sigma(i)}\}) |\Omega_{\mathcal{F}}\rangle. \quad (8.16)$$

Now most of the Lax operators in the monodromy act on the δ^\pm vacua, and we can use the equations (7.49) to replace them by the corresponding eigenvalues. What remains is a small monodromy matrix of length two,

$$\mathcal{M}_2(u, \{v_{\sigma(i)}\}) = \mathcal{L}_l(u - v_{\sigma(l)}) \mathcal{L}_{l-1}(u - v_{\sigma(l-1)}), \quad (8.17)$$

acting on the minimal form factor $\delta_{l-1 l}^F$ at sites $l-1$ and l . We thus have

$$\mathcal{M}_n(u, \{v_{\sigma(i)}\}) |\mathcal{F}\rangle = f(u, \{v_{\sigma(i)}\}) \prod_{j \in \mathcal{J}^+} \delta_j^+ \prod_{j \in \mathcal{J}^-} \delta_j^- [\mathcal{M}_2(u, \{v_{\sigma(i)}\}) \delta_{l-1 l}^F], \quad (8.18)$$

where

$$f(u, \{v_{\sigma(i)}\}) = \prod_{i \in \mathcal{J}^+} (u - v_{\sigma(i)} - 1) \prod_{i \in \mathcal{J}^-} (u - v_{\sigma(i)}). \quad (8.19)$$

The calculation so far can be depicted as in figure 8.3: the monodromy acts on the state, but we can pull it through the R-operators / BCFW bridges; then most of the Lax operators act on the amplitude vacua and the remaining two Lax operators form a smaller monodromy matrix.

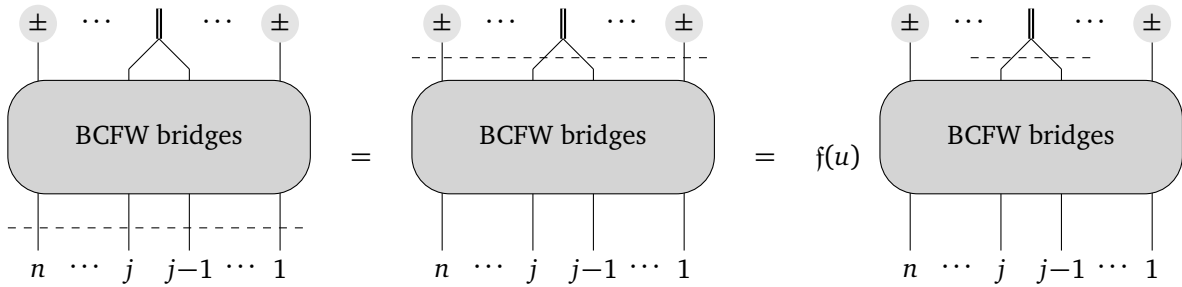


Figure 8.3: Action of the monodromy on a form factor on-shell function.

After the steps taken so far, we have to consider the action of the length two monodromy matrix (8.17) on the minimal form factor. If it was an eigenstate, the entire on-shell function would be Yangian invariant, as defined in (7.40). It is easy to see that this is not the case. We can ignore the deformations for a moment, since they do not change the argument. Consider the momentum generators $\sum_i \lambda_i^\alpha \tilde{\lambda}_i^{\dot{\alpha}}$, which constitute some of the off-diagonal generators of the

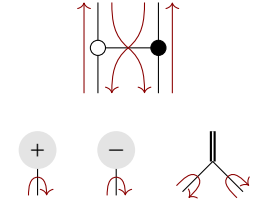


Figure 8.2: Rules to determine the permutation from the R-operator diagrams.

first level of the Yangian, cf. (7.18). The action of these generators on the minimal form factor is proportional to

$$(\lambda_{k-1}\tilde{\lambda}_{k-1} + \lambda_k\tilde{\lambda}_k) \delta^4(\lambda_{k-1}\tilde{\lambda}_{k-1} + \lambda_k\tilde{\lambda}_k - q), \quad (8.20)$$

which clearly is non-zero, since the on-shell monodromy does not have any information on the off-shell momentum q (for $q = 0$, the expression would be of the form $x\delta(x) = 0$). Invariance under these lowest level generators would be a prerequisite for general Yangian invariance.⁵ This implies that form factor on-shell functions are not Yangian invariant.⁶

However, it turns out that we can prove an interesting statement about the integrability properties of form factor on-shell functions by taking the supertrace on both sides of equation (8.18). The supertrace replaces the monodromy matrices by the respective transfer matrices (7.38), and we get

$$\mathcal{T}_n(u, \{v_{\sigma(i)}\}) | \mathcal{F} \rangle = f(u, \{v_{\sigma(i)}\}) \prod_{j \in \mathcal{J}^+} \delta_j^+ \prod_{j \in \mathcal{J}^-} \delta_j^- [\mathcal{T}_2(u, \{v_{\sigma(i)}\}) \delta_{l-1l}^F], \quad (8.21)$$

with the length two transfer matrix defined by

$$\mathcal{T}_2(u, \{v_{\sigma(i)}\}) = \text{str } \mathcal{L}_l(u - v_{\sigma(l)}) \mathcal{L}_{l-1}(u - v_{\sigma(l-1)}). \quad (8.22)$$

Remarkably, this transfer matrix annihilates the minimal form factor! We show this considering the $\text{tr}(\phi^{++}\phi^{++})$ component

$$\tilde{\eta}_{l-1}^{+1} \tilde{\eta}_{l-1}^{+2} \tilde{\eta}_l^{+1} \tilde{\eta}_l^{+2} (\gamma^-)^4 \delta^4(\lambda_{l-1}\tilde{\lambda}_{l-1} + \lambda_l\tilde{\lambda}_l - q). \quad (8.23)$$

The $\text{gl}(4|4)$ invariance of the transfer matrix (7.39) then extends the result to the full form factor. First note that the transfer matrix is independent of γ^- , and that it annihilates the momentum conserving delta function:

$$\mathcal{T}_2(u, \{v_{\sigma(i)}\}) \delta^4(\lambda_1\tilde{\lambda}_1 + \lambda_2\tilde{\lambda}_2 - q) = 0. \quad (8.24)$$

Therefore, it only acts on the product of $\tilde{\eta}$'s, and an explicit computation shows that

$$\mathcal{T}_2(u, \{v_{\sigma(i)}\}) \tilde{\eta}_{l-1}^{+1} \tilde{\eta}_{l-1}^{+2} \tilde{\eta}_l^{+1} \tilde{\eta}_l^{+2} = 0. \quad (8.25)$$

This can also be understood from the map between spinor-helicity variables and the oscillator representation of operators, to be discussed shortly: It is the state that $\text{tr}(\phi^{++}\phi^{++})$ is a vacuum Bethe state of the spin chain, both in the homogeneous as well as the inhomogeneous case.

We thus found that the minimal form factor is an eigenstate of the integrable transfer matrix (8.22), with eigenvalue zero,

$$\mathcal{T}_2(u, \{v_{\sigma(i)}\}) \delta_{l-1l}^F = 0. \quad (8.26)$$

Plugging this into (8.21), we see that the same is true for the entire on-shell function:

$$\mathcal{T}_n(u, \{v_i\}) | \mathcal{F} \rangle = 0, \quad (8.27)$$

⁵ It would be an interesting avenue for future research to consider the off-shell data as another site of the spin chain, in a different representation.

⁶ It turns out, however, that a part of the Yangian invariance persists, as we will show in chapter 10.

under the constraints on the inhomogeneities (8.15). In particular the statement is true for vanishing inhomogeneities, i.e. undeformed form factor on-shell functions such as tree-level form factors:

$$\mathcal{T}_n F_{n,k} = 0. \quad (8.28)$$

This identity is very similar to the Yangian invariance condition (7.35). Indeed, taking the supertrace of (7.35), we see that a consequence of Yangian invariance is that the corresponding states are also eigenstates of the transfer matrix with eigenvalue zero. Form factors, and their on-shell functions are not Yangian invariant but satisfy the latter condition. We can also regard the identities (8.27) or (8.28) as symmetries, with the states annihilated by certain linear combinations of Yangian generators.

Generic operators

We just showed that on-shell functions of the chiral part of the stress tensor multiplet are eigenstates of integrable transfer matrices (7.38), and that their eigenvalue turns out to be zero. Since most of the derivation did not depend on the specific operator under consideration, one may suspect that this may be a general phenomenon. We will now indeed extend the result to on-shell functions with an insertion of an arbitrary operator.

The discussion will focus on the undeformed case. We will construct planar on-shell functions by attaching BCFW bridges or R-operators to states constructed out of amplitude vacua and the minimal form factors of arbitrary operators. The operators will be defined in terms of component fields, without introducing supermultiplets. Provided that the operator under consideration is itself an eigenstate of a transfer matrix, i.e. a solution to the 1-loop spectral problem, the on-shell function will also be an eigenstate.

As is well known, the single trace operators of $\mathcal{N} = 4$ SYM theory can be described in terms of oscillators.⁷ Conventionally, the bosonic oscillators are called $\bar{\mathbf{a}}_i^\alpha$ and $\bar{\mathbf{b}}_i^{\dot{\alpha}}$ and the fermionic ones \mathbf{d}_i^A . States are constructed by acting with these oscillators on a Fock vacuum. The oscillators transform under the superconformal algebra $\mathfrak{psu}(2, 2|4)$ in the same way as the super spinor-helicity variables λ_i^α , $\tilde{\lambda}_i^{\dot{\alpha}}$ and $\tilde{\eta}_i^A$. We can therefore identify the representations via

$$\begin{aligned} \bar{\mathbf{a}}_i^\alpha &\leftrightarrow \lambda_i^\alpha, & \bar{\mathbf{b}}_i^{\dot{\alpha}} &\leftrightarrow \tilde{\lambda}_i^{\dot{\alpha}}, & \bar{\mathbf{d}}_i^A &\leftrightarrow \tilde{\eta}_i^A, \\ \mathbf{a}_{i,\alpha} &\leftrightarrow \partial_{i,\alpha} = \frac{\partial}{\partial \lambda_i^\alpha}, & \mathbf{b}_{i,\dot{\alpha}} &\leftrightarrow \partial_{i,\dot{\alpha}} = \frac{\partial}{\partial \tilde{\lambda}_i^{\dot{\alpha}}}, & \mathbf{d}_{i,A} &\leftrightarrow \partial_{i,A} = \frac{\partial}{\partial \tilde{\eta}_i^A}. \end{aligned} \quad (8.29)$$

This identification, following from the fact that both realizations describe the free on-shell fields of $\mathcal{N} = 4$ SYM, is described in detail in Beisert (2011);⁸ it was used to connect the one-loop dilatation operator to the tree-level four-point scattering amplitude based on symmetry considerations.⁹

The relation between oscillators and spinor-helicity variables becomes most evident when considering minimal tree-level form factors of arbitrary operators. In Wilhelm (2015)¹⁰ it was shown via an explicit Feynman diagram calculation

7 Günaydin, Minic, Zagermann, “4D doubleton conformal theories, CPT and IIB string on $\text{AdS}_5 \times S^5$ ”, [hep-th/9806042](#), [Erratum: Nucl. Phys.B538,531(1999)]; and Beisert, “The complete one loop dilatation operator of $\mathcal{N} = 4$ Super Yang-Mills theory”, [hep-th/0307015](#)

8 Beisert, “On Yangian Symmetry in Planar $\mathcal{N} = 4$ SYM”, [1004.5423](#)

9 Zwiebel, “From Scattering Amplitudes to the Dilatation Generator in $\mathcal{N} = 4$ SYM”, [1111.0083](#)

10 Wilhelm, “Amplitudes, Form Factors and the Dilatation Operator in $\mathcal{N} = 4$ SYM Theory”, [1410.6309](#)

that the color-ordered minimal tree-level super form factors of generic single-trace operators \mathcal{O} can be obtained from their representation in the oscillator picture as¹¹

$$F_{\mathcal{O},L}(1, \dots, L; q) = L \delta^4 \left(\sum_{i=1}^L \lambda_i \tilde{\lambda}_i - q \right) \left[\mathcal{O} \left| \begin{array}{l} \bar{\mathbf{a}}_i^\alpha \rightarrow \lambda_i^\alpha \\ \bar{\mathbf{b}}_i^{\dot{\alpha}} \rightarrow \tilde{\lambda}_i^{\dot{\alpha}} \\ \bar{\mathbf{d}}_i^A \rightarrow \tilde{\eta}_i^A \end{array} \right. \right], \quad (8.30)$$

where L is the number of fields in the single-trace operator which has been translated according to (8.29).

Let us first show that this structure of the minimal form factors imply that they are eigenstates of the homogeneous transfer matrix of length $n = L$, if the operator is a solution of the 1-loop spectral problem, i.e. it renormalizes multiplicatively.

Since the transfer matrix (7.26) is $\mathfrak{gl}_{4|4}$ invariant, see (7.39), it commutes with any function $f(\sum_{i=1}^L \mathcal{G}_i^{AB})$. In particular this is the case for the momentum-conserving delta function in (8.30), which is easy to see by writing the delta functions as Fourier integrals,

$$\delta^4 \left(\sum_{i=1}^L \lambda_i \tilde{\lambda}_i - q \right) = \int d^4 x e^{2\pi i (\sum_{i=1}^L \lambda_i \tilde{\lambda}_i - q) \cdot x}, \quad (8.31)$$

and noting that the sum of the momenta correspond to the momentum generators $\mathcal{G}^{\alpha\dot{\alpha}}$, while for that matter q can be regarded as a constant. Therefore, the transfer matrix only acts on the polynomial in spinor-helicity variables, which represents the operator:

$$\mathcal{T}_L(u) F_{\mathcal{O},L} = L \delta^4 \left(\sum_{i=1}^L \lambda_i \tilde{\lambda}_i - q \right) \mathcal{T}_L(u) \left[\mathcal{O} \left| \begin{array}{l} \bar{\mathbf{a}}_i^\alpha \rightarrow \lambda_i^\alpha \\ \bar{\mathbf{b}}_i^{\dot{\alpha}} \rightarrow \tilde{\lambda}_i^{\dot{\alpha}} \\ \bar{\mathbf{d}}_i^A \rightarrow \tilde{\eta}_i^A \end{array} \right. \right] \quad (8.32)$$

Now note that using the relations (8.29), the transfer matrix can be translated into the fundamental oscillator transfer matrix which we call \mathbf{T} :

$$\mathbf{T}(u) = \text{str} \mathbf{L}_L(u) \cdots \mathbf{L}_1(u) \quad \text{with} \quad \mathbf{L}_i(u) = \mathcal{L}_i(u) \left| \begin{array}{l} \partial_{i,\alpha}, \lambda_i^\alpha \rightarrow \mathbf{a}_{i,\alpha}, \bar{\mathbf{a}}_i^\alpha \\ \partial_{i,\dot{\alpha}}, \tilde{\lambda}_i^{\dot{\alpha}} \rightarrow \mathbf{b}_{i,\dot{\alpha}}, \bar{\mathbf{b}}_i^{\dot{\alpha}} \\ \partial_{i,A}, \tilde{\eta}_i^A \rightarrow \mathbf{d}_{i,A}, \bar{\mathbf{d}}_i^A \end{array} \right. . \quad (8.33)$$

We can therefore write

$$\mathcal{T}_L(u) F_{\mathcal{O},L} = F_{\mathbf{T}_L(u)\mathcal{O},L}, \quad (8.34)$$

where

$$F_{\mathbf{T}_L(u)\mathcal{O},L} = L \delta^4 \left(\sum_{i=1}^L \lambda_i \tilde{\lambda}_i - q \right) \left[(\mathbf{T}_L(u) \mathcal{O}) \left| \begin{array}{l} \bar{\mathbf{a}}_i^\alpha \rightarrow \lambda_i^\alpha \\ \bar{\mathbf{b}}_i^{\dot{\alpha}} \rightarrow \tilde{\lambda}_i^{\dot{\alpha}} \\ \bar{\mathbf{d}}_i^A \rightarrow \tilde{\eta}_i^A \end{array} \right. \right]. \quad (8.35)$$

This can be interpreted as the minimal form factor of the operator which results from the action of the transfer matrix $\mathbf{T}(u)$ on the operator \mathcal{O} .

If the operator \mathcal{O} renormalizes multiplicatively, i.e. is a solution of the one-loop spectral problem with a well-defined anomalous dimension, it is an eigenstate of $\mathbf{T}(u)$.¹² Let its eigenvalue be $t(u)$: we then find that the minimal form

¹¹ Note that we do not restrict the operator \mathcal{O} in any way; it may be a monomial or a sum of terms, and does not need to have a well-defined anomalous dimension.

¹² This follows from the discussion in section 7.2, which shows that the Hamiltonian (in our case the one-loop dilatation operator) commutes with the fundamental transfer matrix.

factor is likewise an eigenstate, of the transfer matrix $\mathcal{T}(u)$, with the same eigenvalue:

$$\mathcal{T}_L(u)F_{\theta,L} = F_{T_L(u)\theta,L} = F_{t(u)\theta,L} = t(u)F_{\theta,L}. \quad (8.36)$$

We can now define a general form factor on-shell function of the operator, with n external on-shell fields. Diagrammatically, they are on-shell diagrams with the minimal form factors $F_{\theta,L}$ glued in by on-shell phase space integrations, similar to form factors of the chiral stress tensor multiplet. This can be achieved by constructing a vacuum state using the amplitude vacua δ^\pm and the minimal form factor, and then acting with a sequence of R-operators (7.41) on this state. The only restriction we make is that the resulting diagram has to be planar. We thus define the state

$$|\mathcal{F}_{\theta,n}\rangle = R_{i_1 j_1}(0) \cdots R_{i_m j_m}(0) F_{\theta,L}(l, \dots, l+L-1) \prod_{j \in \mathcal{S}^+} \delta_j^+ \prod_{j \in \mathcal{S}^-} \delta_j^-, \quad (8.37)$$

where there are $|\mathcal{S}^+| = n - k$ vacua of type δ^+ and $|\mathcal{S}^-| = k - L$ vacua of type δ^- , and we define the ‘‘MHV’’ degree k such that the minimal form factor has $k = L$.

This state is a transfer matrix eigenstate as well. Acting with the transfer matrix \mathcal{T}_n of length n on the state, we can first use (8.14) to commute it through the R-operators. Then the Lax operators acting on the amplitude vacua can be replaced by their eigenvalues, which combine into the factor $f(u)$ as defined in (8.19), and we are left with the transfer matrix of length L acting on the minimal form factor as in (8.36); we assume the operator to renormalize multiplicatively, and therefore find

$$\mathcal{T}_n(u) |\mathcal{F}_{\theta,n}\rangle = f(u) |\mathcal{F}_{T_L(u)\theta,n}\rangle = f(u)t(u) |\mathcal{F}_{\theta,n}\rangle \quad (8.38)$$

This calculation is represented in figure 8.4.

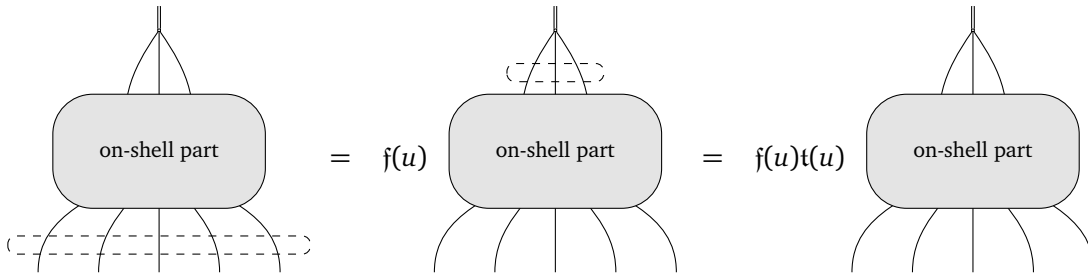


Figure 8.4: Action of the transfer matrix on an on-shell diagram with an insertion of the minimal form factor of the operator θ .

We would like to point out that we only considered undeformed on-shell functions here, since using an inhomogeneous transfer matrix (7.38) would require that the operators have to be eigenstates of the inhomogeneous spin chain as well; while this would be interesting to consider, the physical interpretation of such states would be unclear.

The preceding discussion casts a new light on the role of R-operators. They are more than a means to construct Yangian invariants – one should rather consider them as operators which allow to obtain further eigenstates from any eigenstate of the integrable model.

Given that the R-operators can be defined for any rational spin chain with a representation that allows a Jordan-Schwinger form¹³, it seems plausible that for each such spin chain they allow to map transfer matrix eigenstates to other ones, possible at a different length. To our knowledge, this potentially interesting structure has never been investigated in other contexts.¹⁴

¹³ Kanning, Lukowski, Staudacher,
“A shortcut to general tree-level
scattering amplitudes in $\mathcal{N} = 4$ SYM
via integrability”, [1403.3382](#)

¹⁴ We strongly suspect that for compact
spin chains one has to consider the
inhomogeneous case.

9

Yangian symmetries of nonplanar on-shell diagrams

Nonplanar on-shell diagrams, i.e. diagram constructed from three-point amplitudes by fusing them via on-shell phase space integrations, in such way that they cannot be embedded on a disk, have recently gained a lot of attention. They are interesting for a variety of reasons: firstly, it is natural to wonder whether they share the rich mathematical structure and the simplicity of their planar counterparts; furthermore, they appear as leading singularities when calculating general higher-loop amplitudes and are thus of practical interest.

Here we want to investigate these quantities from an integrability perspective. It is fair to say that Yangian invariance can be considered the defining property of planar on-shell diagrams and the on-shell functions they represent. Yangian symmetry is a hallmark feature of integrability; while $\mathcal{N} = 4$ SYM is generally thought to be integrable only in the planar limit, we want to answer the following question: can Yangian, or Yangian-like, symmetries persist in the nonplanar regime, at least systematically in the $1/N$ expansion?

This chapter is structured as follows: We begin by summarizing the recent work on nonplanar on-shell diagrams, mainly pointing to the relevant literature in section 9.1, and describe the reasons to suspect that these diagrams – despite being nonplanar – still enjoy symmetries based on integrability, and how these could be useful, in section 9.2. Then we turn to the actual derivations of our results. After setting up some notation and basic definitions in section 9.3, we show that higher-level Yangian generators which act independently on the boundaries of nonplanar on-shell diagrams still annihilate them, and are thus unbroken symmetries. The first levels are broken depending on the degree of nonplanarity, which is parametrized by the number of internal edges which need to be “cut open” in order to make the diagram planar. This is the main result of section 9.4, and given in equation (9.16). In section 9.5, we turn to similar identities involving transfer matrices. We first derive an identity for diagrams on cylinders, given in (9.21), which can be interpreted as a conservation law or an intertwining relation. Based on this identity, we can derive further symmetries

This chapter is based on the author's publication Frassek, Meidinger, “Yangian-type symmetries of non-planar leading singularities”, 1603.00088.

for general diagrams, which are given in equation (9.24). Finally, we will apply our results to a simple nonplanar example diagram in section 9.6, in order to make the symmetries more explicit.

9.1 Nonplanar on-shell diagrams

Nonplanar on-shell diagrams were first considered, for the special case of the annulus or cylinder, by Gekhtman et al. (2012),¹ following the work Postnikov (2006),² even before such diagrams were related to scattering processes. In the context of $\mathcal{N} = 4$ SYM, their study was initiated by a complete description of general MHV on-shell functions in Arkani-Hamed et al. (2015).³ The general case however is much more intricate; in Franco et al. (2015),⁴ among other results, a generalization of the boundary measurement procedure was developed which applies to any on-shell diagram. A first step towards a classification of general on-shell diagrams was taken in Bourjaily et al. (2016).⁵ For the Grassmannian $G(3, 6)$, this work enumerates all top-cell diagrams together with their forms on the Grassmannian, and discusses their lower dimensional residues.

A further domain where nonplanar on-shell diagrams are naturally encountered is scattering in theories of gravity.⁶

9.2 Motivation

There are three major reasons which motivate us to study the integrability related symmetries of nonplanar on-shell diagrams. First, nonplanar contributions to loop integrands of scattering amplitudes were recently studied and compared to the rich structure present in the planar case in Bern et al. (2015); Arkani-Hamed et al. (2014); Bern et al. (2016).⁷ For the examples that were studied, it was observed that the integrands have several properties which have been shown to be consequences of dual conformal symmetry – and thereby of the Yangian and integrability – in the case of planar integrands. While dual superconformal symmetry surely is not present for nonplanar integrands, as the dual momenta y_i cannot even be defined, it is a pressing question whether some form of integrability is behind the observations. In this chapter, we look for such symmetries in the case of nonplanar on-shell functions; since these appear as leading singularities of the full integrand, novel symmetries of the former are at least plausible candidate symmetries of the latter, and it might be possible to show that they are responsible for the special structure of general integrands in $\mathcal{N} = 4$ SYM.

Furthermore, on-shell diagrams are extremely simple quantities, compared to other data of $\mathcal{N} = 4$ SYM. Thus we may hope to get some general insights into integrability beyond the planar limit. Indeed, previous investigations into this issue focused on the spectral problem,⁸ see Kristjansen (2012)⁹ for a review. It was found that the dilatation operator, once subleading contribution in the $1/N$ expansion are taken into account, cannot be interpreted as an integrable

1 Gekhtman, Shapiro, Vainshtein, “Poisson Geometry of Directed Networks in an Annulus”, [0901.0020](#)

2 Postnikov, “Total positivity, Grassmannians, and networks”, [math/0609764](#)

3 Arkani-Hamed, Bourjaily, Cachazo, Postnikov, Trnka, “On-Shell Structures of MHV Amplitudes Beyond the Planar Limit”, [1412.8475](#)

4 Franco, Galloni, Penante, Wen, “Non-Planar On-Shell Diagrams”, [1502.02034](#)

5 Bourjaily, Franco, Galloni, Wen, “Stratifying On-Shell Cluster Varieties: the Geometry of Non-Planar On-Shell Diagrams”, [1607.01781](#)

6 Heslop, Lipstein, “On-shell diagrams for $\mathcal{N} = 8$ supergravity amplitudes”, [1604.03046](#); and Herrmann, Trnka, “Gravity On-shell Diagrams”, [1604.03479](#)

7 Bern, Herrmann, Litsey, Stankowicz, Trnka, “Logarithmic Singularities and Maximally Supersymmetric Amplitudes”, [1412.8584](#); Arkani-Hamed, Bourjaily, Cachazo, Trnka, “Singularity Structure of Maximally Supersymmetric Scattering Amplitudes”, [1410.0354](#); and Bern, Herrmann, Litsey, Stankowicz, Trnka, “Evidence for a Nonplanar Amplituhedron”, [1512.08591](#)

8 Beisert, Kristjansen, Staudacher, “The Dilatation operator of conformal $\mathcal{N} = 4$ Super Yang-Mills theory”, [hep-th/0303060](#); Beisert, “The complete one loop dilatation operator of $\mathcal{N} = 4$ Super Yang-Mills theory”, [hep-th/0307015](#); Peeters, Plefka, Zamaklar, “Splitting spinning strings in AdS/CFT”, [hep-th/0410275](#); and Bellucci, Casteill, Morales, Sochichiu, “Spin bit models from nonplanar $N = 4$ SYM”, [hep-th/0404066](#)

9 Kristjansen, “Review of AdS/CFT Integrability, Chapter IV.1: Aspects of Non-Planarity”, [1012.3997](#)

spin chain Hamiltonian. Work on three-point functions¹⁰ however suggests that quantities with nonplanar topologies can indeed be calculated using integrability, if the topology is properly taken into account. In particular it turned out that a successful strategy is to cut nonplanar objects into planar parts, to use planar integrability, and then to glue the pieces back together. In this chapter we pursue such a strategy in order to prove that at least a part of the Yangian symmetry is present in nonplanar on-shell diagrams.

Finally, after having discussed on-shell diagrams for form factors in the previous chapters, we note that these diagrams are inherently nonplanar in the sense that the color structure implies an ordering of the external on-shell states, in which the operator does not participate. Hence, if one removes the minimal form factor from the diagram, the two legs at which it is glued in can be considered as a second boundary. We will discuss this in more detail in the next chapter, but already here it allows us to understand the integrability properties of form factor on-shell function investigated in chapter 8 as special cases of a more general phenomenon.

9.3 Setup & notation

In this chapter we will work exclusively using the super twistor variables \mathcal{W}_i^a which are obtained from the spinor-helicity variables by Fourier transforming the λ variables, see chapter 2.1 for details. The derivatives with respect to these variables will be denoted by $\partial_i^a = \partial / \partial \mathcal{W}_i^a$.

Our proofs of Yangian symmetries rely heavily on “cutting” and “gluing” the on-shell diagrams. By gluing we simply refer to identifying external state of a diagram using a projective delta function

$$\Delta_{ij} = \int \frac{d\alpha}{\alpha} \delta^{4|4}(\mathcal{W}_i + \alpha \mathcal{W}_j), \quad (9.1)$$

and then to perform the on-shell phase space integration over the newly created internal state,

$$\int d^{3|4} \mathcal{W} = \int \frac{d^{4|4} \mathcal{W}}{\text{Vol}[GL(1)]}. \quad (9.2)$$

We call the reverse operation cutting, since it opens up an internal edge of the diagram into two external particle states.

It is known that not only any planar, but also any nonplanar on-shell diagram A has an analytic expression in terms of a Grassmannian integral

$$A = \int \frac{d^{k \times n} C}{\text{Vol}[GL(k)]} \Omega \delta^{4k|4k}(C \cdot \mathcal{W}). \quad (9.3)$$

The form Ω can be written as function of the $k \times k$ minors of the matrix C . For planar diagrams this was discussed in section 2.5, and the form is presented in equation (2.59) and is given by the inverse of the product of all consecutive minors.

¹⁰ Vieira, Wang, “Tailoring Non-Compact Spin Chains”, 1311.6404; and Escobedo, Gromov, Sever, Vieira, “Tailoring Three-Point Functions and Integrability”, 1012.2475

11 Franco, Galloni, Penante, Wen, “Non-Planar On-Shell Diagrams”, 1502.02034; and Penante, “On-shell methods for off-shell quantities in $\mathcal{N} = 4$ Super Yang-Mills: from scattering amplitudes to form factors and the dilatation operator”, PhD thesis, Queen Mary, U. of London, 2016, 1608.01634,

12 Bourjaily, Franco, Galloni, Wen, “Stratifying On-Shell Cluster Varieties: the Geometry of Non-Planar On-Shell Diagrams”, 1607.01781

13 In the notation of section 7.1, we have $x_i^a = \mathcal{W}_i^a$ and $p_i^a = \partial_i^a$.

For nonplanar diagrams, one can obtain the form – for example – using a generalization of boundary measurements.¹¹ The form has to be calculated anew for any diagram, as no general formula is known at the moment. In particular, there are multiple such top dimensional forms for given k and n , which have only been classified for the case $k = 3$ and $n = 6$ so far.¹²

In the following, we want to show that these integrals – while generally not Yangian invariant in the strict sense presented in section 7.3 – still exhibit a wealth of Yangian-like symmetries. These symmetries severely constrain the forms Ω and can hopefully be used to classify or construct them.

As throughout this thesis, we will work with the RTT realization of the Yangian of $\mathfrak{gl}_{4|4}$ as described in section 7.1. The basic building block will thus be the Lax operator

$$\mathcal{L}_i(u) = u + (-1)^b e^{ab} \mathcal{W}_i^b \partial_i^a \tag{9.4}$$

where the generators $\mathcal{G}_i^{ab} = \mathcal{W}_i^a \partial_i^b$ of $\mathfrak{gl}_{4|4}$ acting on the particles are given in terms of the Jordan-Schwinger realization.¹³ The elementary matrices e^{ab} again form the fundamental representation of $\mathfrak{gl}_{4|4}$ and u is the spectral parameter. Using these Lax operators, we can define monodromy and transfer matrices as discussed above in the spinor-helicity representation, see equations (7.16) and (7.26). The nonplanar setting however requires that we explicitly specify the particles on which the Lax operators in these monodromy and transfer matrices act, and we will often need to relate different such objects. We therefore introduce the notation for these quantities when they are needed in the following arguments.

Finally, let us note that once general nonplanar diagrams are considered, the embedding of a given diagram, i.e. its embedding on a two-dimensional surface of some topology, is not unique. This is already the case for planar diagrams, which allow (trivial) nonplanar embeddings. An example of this is shown in figure 9.1. Our discussions will always consider a digram in a given embedding, which makes some symmetries manifest. The set of all embeddings then determines the full set of symmetries of the on-shell function.

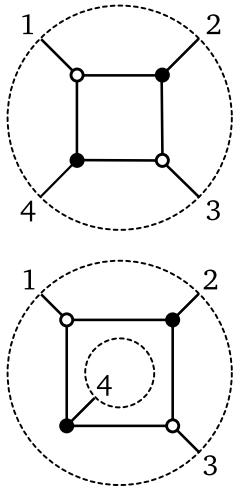


Figure 9.1: The on-shell diagram for the four-point amplitude, and one of its nonplanar embeddings.

9.4 Monodromy matrix identities

We consider an arbitrary nonplanar on-shell diagram A_{np} , with n_{np} external states and MHV degree k_{np} . Diagrammatically, we can “cut” internal edges of the diagram open, until the resulting diagram is planar, see figure 9.2. Which edges have to be cut depends on the diagram and the topology of the embedding, likewise the total number of cut edges that is necessary to obtain a planar diagram. Furthermore, the set of cut edges is generally not unique and neither is the planar diagram. We focus on one particular way of performing this cutting procedure, and call the number of cut lines n_{cut} . This will give us a planar diagram A_p with more external states and higher MHV degree,

$$n_p = n_{np} + 2n_{cut}, \quad k_p = k_{np} + n_{cut}. \tag{9.5}$$

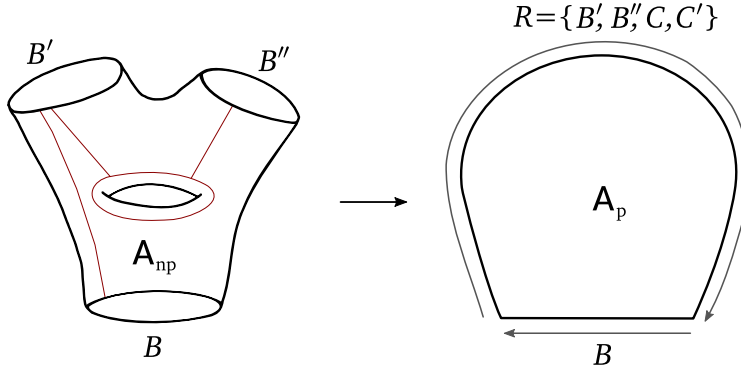


Figure 9.2: Cutting a nonplanar into a planar on-shell diagram. We only show the surface on which the diagram is embedded, indicating possible cuts. For the planar diagram we combine the states on boundaries B' and B'' together with the cut lines C and C' into the ordered set R . The arrows indicate the ordering of these labels.

The cutting procedure gives us a particular way of writing the on-shell function of the nonplanar diagram, by gluing together the cut edges via on-shell phase space integrations (9.1) and (9.2),

$$A_{\text{np}} = \int_{C, C'} \Delta_{CC'} A_{\text{p}}. \quad (9.6)$$

Here and in the following, we label ordered subsets of the external on-shell states using capital letters, such that $\int_{C, C'}$ in this equation is a shorthand notation for the projective integrations (9.2) over all the states C_i, C'_i with $i = 1, \dots, n_{\text{cut}}$ of A_{p} which are internal to A_{np} . Likewise, we abbreviate the projective delta functions (9.1) which identify the states

$$\Delta_{CC'} = \Delta_{C_1 C'_1} \cdots \Delta_{C_{n_{\text{cut}}} C'_{n_{\text{cut}}}}. \quad (9.7)$$

Since the Yangian acts nonlocally, it requires the states on which they act to be ordered. For nonplanar diagrams this is the case for particles on a single boundary. Therefore we distinguish among the particles on one of the boundaries of A_{np} which we call B , and the remaining external particles of A_{p} which we label by R . They include the particles on other boundaries of A_{np} as well as the $2n_{\text{cut}}$ particles that become external when cutting the diagram open, see figure 9.2.

As described in section 7.3, see in particular equation (7.35), the Yangian invariance of the planar on-shell diagram A_{p} can be compactly expressed as a set of 8×8 eigenvalue equations¹⁴ involving a monodromy matrix:

$$\mathcal{M}_{RB}^{ab}(u) A_{\text{p}} = (u - 1)^{k_{\text{p}}} u^{n_{\text{p}} - k_{\text{p}}} \delta^{ab} A_{\text{p}}, \quad (9.8)$$

Here the subscript on the monodromy matrix labels the ordered set of states it acts on, here on the set $R \cup B$ in that order. Therefore the monodromy matrix \mathcal{M}_{RB} can be written as the product of two monodromy matrices acting on B and R respectively,

$$\mathcal{M}_{RB}(u) = \mathcal{M}_R(u) \mathcal{M}_B(u). \quad (9.9)$$

Each of the monodromies yields a realization of the Yangian separately. They are defined in terms of the Lax operators as

$$\mathcal{M}_B(u) = \mathcal{L}_{B_1}(u) \cdots \mathcal{L}_{B_{n_B}}(u), \quad (9.10)$$

with $\mathcal{M}_R(u)$ correspondingly.

14 The eigenvalues of planar diagrams can be obtained by adapting the R-operator formalism described in section 7.5 to twistor space by using the definition of the Schwinger oscillators x_i^a and p_i^a given above. The eigenvalues can then simply be obtained by acting with the Lax operators (9.4) on the vacua $\delta_i^- = \delta^{4|4}(\mathcal{W}_i)$ and $\delta_i^+ = 1$.

We now show that identities similar to the Yangian invariance of the planar on-shell diagram A_p in (9.8) also hold for the nonplanar diagram A_{np} . In order to derive those identities we note that the product of two Lax operators \mathcal{L}_i for a certain choice of the spectral parameters is proportional to the identity

$$\mathcal{L}_i(u)\mathcal{L}_i(1-u-c_i) = u(1-u-c_i). \quad (9.11)$$

In the context of integrable models this property is also known as unitarity.¹⁵ Note that (9.11) is an operator statement, and in practice we can set the central charges $c_i = \mathcal{W}_i^a \partial_i^a$ to zero when acting on an on-shell diagram. Using the inversion relation in (9.11), the planar Yangian invariance condition (9.8) can be rewritten as

$$\mathcal{M}_B(u)A_p = \frac{(-1)^{k_p} u^{n_B - k_p}}{(1-u)^{n_R - k_p}} \mathcal{M}_{\bar{R}}(1-u)A_p. \quad (9.12)$$

Here the Lax operators in $\mathcal{M}_{\bar{R}}(u) = \mathcal{L}_{R_{n_R}}(u) \cdots \mathcal{L}_{R_1}(u)$ are multiplied in the opposite order compared to (9.10), which we indicate by the bar in the label. The monodromy matrix on the left-hand side of this equation does not depend on the cut lines, and only acts on the boundary for which we want to find Yangian symmetries. Thus we can glue the diagram back together using (9.6), and can pull the monodromy matrix out of the integral to obtain an equation for the nonplanar on-shell function A_{np} ,

$$\mathcal{M}_B(u)A_{np} = \frac{(-1)^{k_p} u^{n_B - k_p}}{(1-u)^{n_R - k_p}} \int_{C, C'} \Delta_{CC'} \mathcal{M}_{\bar{R}}(1-u)A_p. \quad (9.13)$$

As described in section 7.1, we have to expand the monodromy matrix in the spectral parameter u to obtain the Yangian generators, see equation (7.18). For the action of the Yangian on the boundary B , this yields the generators

$$\mathcal{M}_B^{ab}(u) = u^{n_B} \delta^{ab} + u^{n_B - 1} \mathcal{M}_{B[1]}^{ab} + \cdots + \mathcal{M}_{B[n_B]}^{ab}, \quad (9.14)$$

where the number in the brackets indicates the level of the generators and n_B is the number of particles on boundary B . The analogous expansion holds for the monodromy $\mathcal{M}_{\bar{R}}(u)$. Thus we can expand both sides of (9.13) around $u = 0$ to obtain the action of the Yangian generators $\mathcal{M}_{B[i]}^{ab}$ on the boundary B . We find that the action of the first k_p levels is rather complicated

$$\mathcal{M}_{B[i]}^{ab} A_{np} = \sum_{j=0}^{n_R} \frac{(j - k_p)_{k_p - i}}{(k_p - i)!} \int_{C, C'} \Delta_{CC'} \mathcal{M}_{\bar{R}[j]}^{ab} A_p, \quad i = 0, \dots, k_p. \quad (9.15)$$

Here $\mathcal{M}_{\bar{R}[j]}^{ab}$ denote the Yangian generators of the monodromy $\mathcal{M}_{\bar{R}}(u)$ involving superconformal generators acting on internal particles of the diagram and $(a)_n = \Gamma(a+n)/\Gamma(a)$ is the Pochhammer symbol.

However, we find that the remaining higher levels of Yangian generators that act on the boundary B annihilate the nonplanar on-shell diagram A_{np} , and generate unbroken symmetries,

$$\mathcal{M}_{B[i]}^{ab} A_{np} = 0, \quad i = k_p + 1, \dots, n_B. \quad (9.16)$$

¹⁵ This nomenclature stems from integrable field theories, see for example Dorey, ‘‘Exact S matrices’’, [hep-th/9810026](https://arxiv.org/abs/hep-th/9810026).

This is the main result of this section, and shows that nonplanar on-shell functions still exhibit partial Yangian symmetries.

Note that the number of unbroken symmetries in (9.16) depends in an interesting way on the degree of nonplanarity and is given by $n_B - k_p$. The number of external states n_B fixes the number of levels of the Yangian generators in the expansion (9.14), and $k_p = k_{np} + n_{\text{cut}}$ can be regarded as a measure of nonplanarity, as each additional boundary or handle requires further internal lines to be cut. If $k_p \leq n_B$, no unbroken symmetries remain.

Here we did not specify any particular embedding of the diagram, nor any specific way of cutting it into a planar one. The preceding discussion shows that the actual symmetries are determined by the minimal way to cut the diagram, and that one should consider all possible embeddings of the diagram to identify as many symmetries as possible. We will discuss an example in section 9.6 which clarifies this point.

9.5 Transfer matrix identities

The supertrace of monodromy matrices defines transfer matrices as discussed in section 7.2. For a boundary B this matrix is defined by

$$\mathcal{T}_B(u) = \text{str } \mathcal{M}_B(u). \quad (9.17)$$

It generates a set of mutually commuting operators $\mathcal{T}_{B[i]} = \text{str } \mathcal{M}_{B[i]}$ with $i = 1, \dots, n_B$, cf. (9.14). We already encountered symmetries of on-shell functions involving transfer matrices in chapter 8. Now we show that such symmetries also exist for nonplanar on-shell diagrams.

We will first focus on diagrams that are embedded on a cylinder. For this special case we derive exact conservation laws, which can also be interpreted as intertwining relations. These can subsequently be used to derive symmetries involving the operators $\mathcal{T}_{B[i]}$ for general nonplanar on-shell function which extend the results in (9.16).

Intertwining relation for diagrams on cylinders

First, we specialize (9.13) to the case of a diagram with two boundaries. Then the supertrace yields

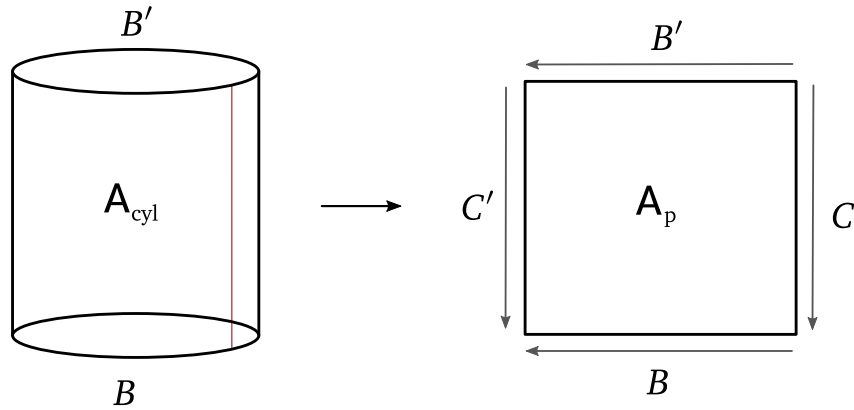
$$\mathcal{T}_B(u) \mathbf{A}_{\text{cyl}} = \frac{(-1)^{k_p} u^{n_B - k_p}}{(1-u)^{n_{B'} + 2n_{\text{cut}} - k_p}} \int_{C, C'} \Delta_{CC'} \mathcal{T}_{\tilde{C}B'C'}(1-u) \mathbf{A}_p, \quad (9.18)$$

where \mathbf{A}_{cyl} denotes an on-shell diagram on a cylinder, cf. figure 9.3.

At first sight we have not gained anything in comparison to (9.13). However, when acting with the transfer matrix on \mathbf{A}_{cyl} we can evaluate the integral over the internal lines on the right-hand side. We first integrate by parts using

$$\int d^{3|4} \mathcal{W} g(\mathcal{W}) \mathcal{L}(u) f(\mathcal{W}) = - \int d^{3|4} \mathcal{W} [\mathcal{L}(1-u) g(\mathcal{W})] f(\mathcal{W}), \quad (9.19)$$

Figure 9.3: Cutting an on-shell diagram on a cylinder into a planar on-shell diagram. We only show the surface on which the diagram is embedded. The gray line indicates a possible cut. The external states C and C' arise from cutting internal lines of A_{cyl} . Arrows indicate the ordering of labels.



which holds for arbitrary functions f and g . Now the Lax operators \mathcal{L}_{C_i} and $\mathcal{L}_{C'_i}$ act on the Δ 's instead of A_p . The special feature of diagrams on cylinders is that here, the cyclicity of the supertrace allows to bring the Lax operators \mathcal{L}_{C_i} and $\mathcal{L}_{C'_i}$ into a consecutive order, $\mathcal{T}_{\tilde{C}B'C'} = \mathcal{T}_{C'\tilde{C}B'}$. We can now use the identity

$$\mathcal{L}_{C'_i}(u)\mathcal{L}_{C_i}(u)\Delta_{C_iC'_i} = u(u-1)\Delta_{C_iC'_i}, \tag{9.20}$$

which is equivalent to the inversion relation in (9.11). This removes these Lax operators entirely from the right-hand side, and the transfer matrix becomes simply $\mathcal{T}_{B'}(1-u)$ and can be pulled out of the integral. The integral is then the original diagram on the cylinder, $A_{\text{cyl}} = \int_{CC'} \Delta_{CC'} A_p$, and we finally find

$$u^{k_{\text{cyl}}} \frac{\mathcal{T}_B(u)}{u^{n_B}} A_{\text{cyl}} = (u-1)^{k_{\text{cyl}}} \frac{\mathcal{T}_{B'}(1-u)}{(1-u)^{n_{B'}}} A_{\text{cyl}}, \tag{9.21}$$

The steps of the proof of equation (9.21) can be understood graphically and are shown in figure 9.4.

The result (9.21) can be understood as a conservation law of charges that flow between the two boundaries of the cylinder. Equivalently, one could consider to use the on-shell function of a given cylinder diagram as the kernel of an integral operator mapping from states on B to states on B' or vice versa.¹⁶ Equation (9.21) would then turn into an intertwining relation, stating that this operator would “commute” with the transfer matrix, in the sense that it turns the transfer matrix \mathcal{T}_B into the transfer matrix $\mathcal{T}_{B'}$.

Comparing with (9.12), we see that equation (9.21) plays a similar role as an exact identity for the cylinder as the Yangian invariance does for planar diagrams. Note in particular that there is no dependence on the number of cut lines.

General transfer matrix symmetries

Similar to the case of the monodromy in Section 9.4, we use (9.21) to obtain further identities for general nonplanar on-shell diagrams. Again we consider an arbitrary on-shell diagram A_{np} . This time we cut internal lines until the diagram can be embedded on a cylinder, such that

$$A_{\text{np}} = \int_{C,C'} \Delta_{CC'} A_{\text{cyl}}. \tag{9.22}$$

¹⁶ This use of on-shell diagrams would be in the same spirit as the R-matrix construction in Ferro, Łukowski, Meneghelli, Plefka, Staudacher, “Harmonic R-matrices for Scattering Amplitudes and Spectral Regularization”, 1212.0850.

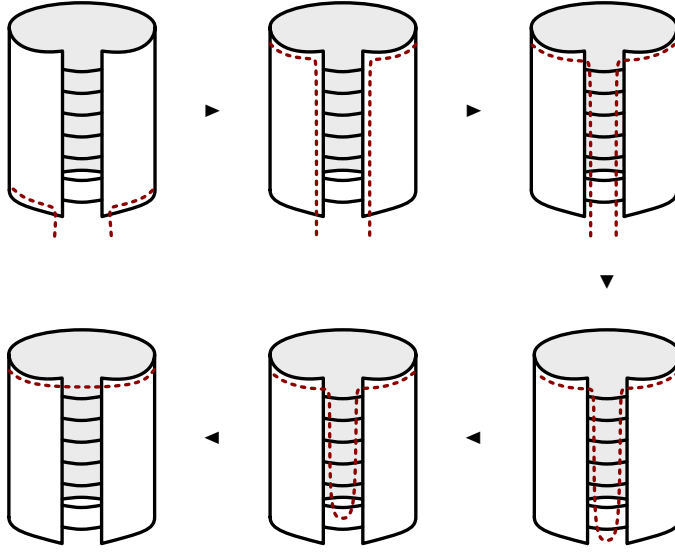


Figure 9.4: Graphical representation of the proof of the identity (9.21). We first act with the monodromy matrix on the lower boundary of the cylinder and use (9.13). After integrating by parts as in (9.19) the Lax operators act on the cut lines. After taking the trace we can successively apply the identity (9.20).

The on-shell diagram on the cylinder A_{cyl} satisfies (9.21). Here we take B to be an actual boundary of A_{np} . The other boundary B' of A_{cyl} contains the other boundaries of the initial diagram as well as the cut lines C_i, C'_i . Integrating this identity over the cut lines as in (9.22) we get

$$\mathcal{T}_B(u)A_{\text{np}} = \frac{(-1)^{k_{\text{cyl}}}u^{n_B-k_{\text{cyl}}}}{(1-u)^{n_{B'}-k_{\text{cyl}}}} \int_{C,C'} \Delta_{CC'} \mathcal{T}_{B'}(1-u)A_{\text{cyl}}. \quad (9.23)$$

By arguments identical to those used in Section 9.4, we can expand in the spectral parameter and identify powers where the right-hand side of (9.23) vanishes:

$$\mathcal{T}_{B[i]}A_{\text{np}} = 0, \quad i = k_{\text{cyl}} + 1, \dots, n_B. \quad (9.24)$$

Note that although (9.24) looks like the supertrace of (9.16), the crucial difference lies in the number of broken levels: Here k_{cyl} refers to the MHV degree after cutting to a cylinder, which is smaller than k_p , the MHV degree after continuing to cut the diagram to a planar one. Thus (9.24) provides additional identities not obtained from the supertrace of (9.16).

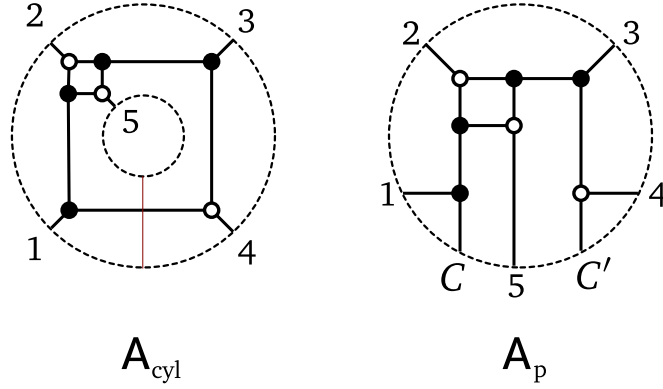
9.6 Example: Five-point MHV on a cylinder

In this section we exemplify and validate the symmetries derived in Section 9.4 and 9.5 for a five-point MHV diagram with $k_{\text{np}} = 2$ on a cylinder as depicted in figure 9.5.

In the embedding of the nonplanar diagram A_{cyl} shown in this figure, particle “5” belongs to one boundary $B' = (5)$, while the remaining particles are placed on the other boundary $B = (1, 2, 3, 4)$. The form for the Grassmannian integral (9.3) was given in Franco et al. (2015),¹⁷ and can be written as

¹⁷ Franco, Galloni, Penante, Wen, “Non-Planar On-Shell Diagrams”, 1502.02034

Figure 9.5: A five-point MHV diagram on a cylinder, and the planar diagram obtained after cutting along the indicated line.



$$\Omega_{\text{cyl}} = \frac{1}{(12)(23)(34)(41)} \frac{(13)}{(35)(51)}. \quad (9.25)$$

Here (ij) denotes the 2×2 minor with respect to the i th and j th column of the $k \times n$ matrix C , cf. (9.3), and the form is written in a way that makes manifest that particle 5 is added to the four-point amplitude via a nonplanar inverse soft factor between particles 1 and 3, cf. the discussion in section 3.4.

First we note that there are no Yangian-like symmetries as in (9.16) associated to boundary B' , since these are never present for less than two particles on the boundary. For boundary B however, we can consider the action of the Yangian generators $\mathcal{M}_{B[i]}^{ab}$, generated by the monodromy

$$\mathcal{M}_B(u) = \mathcal{L}_1(u)\mathcal{L}_2(u)\mathcal{L}_3(u)\mathcal{L}_4(u). \quad (9.26)$$

As discussed in Section 9.4, we can decompose the nonplanar diagram A_{cyl} using the cutting procedure (9.6). When minimally cut, the planar diagram A_p has $n_p = 7$ external particles and MHV degree $k_p = 3$, as a single line has to be cut, i.e. $n_{\text{cut}} = 1$. This is shown on the right-hand side of figure 9.5. Note that other possibilities to cut the diagram via a single edge are equivalent due to cyclic symmetry on the boundary, while cutting two edges does not yield any identity. As we have $n_B = 4$ and $k_p = 3$, we find from (9.16) that the fourth level of Yangian generators has to annihilate the nonplanar on-shell function A_{cyl} . These generators of this level read

$$\mathcal{M}_{B[4]}^{ab} = (-1)^{ab+c+d+e} (\mathcal{W}_4^a \partial_4^c) (\mathcal{W}_3^c \partial_3^d) (\mathcal{W}_2^d \partial_2^e) (\mathcal{W}_1^e \partial_1^b). \quad (9.27)$$

In order to show that A_{cyl} is annihilated by the operator above we proceed in analogy to Drummond and Ferro (2010a)¹⁸ noting that a general method to evaluate such symmetries of Grassmannian integrals will be presented in chapter 11. After commuting the variables and derivatives in (9.27) and acting on the delta function we obtain

$$\mathcal{M}_{B[4]}^{ab} A_{\text{cyl}} = (-1)^{ab} \sum_{i=1}^4 \int \frac{d^{2 \times 5} C}{\text{Vol}[GL(2)]} \Omega g(i) \mathcal{W}_4^b \partial_i^a \delta^{8|8}(C \cdot \mathcal{W}), \quad (9.28)$$

with $g(1) = \partial_{12} \partial_{23} \partial_{34}$, $g(2) = -\partial_{23} \partial_{34}$, $g(3) = \partial_{34}$, $g(4) = -1$ and $\partial_{ij} = C_{Ii} \frac{\partial}{\partial C_{Ij}}$, where we sum over the index $I = 1, 2$. Integrating by parts such that the

¹⁸ Drummond, Ferro, ‘‘Yangians, Grassmannians and T-duality’’, 1001.3348

operators $g(i)$ act only on Ω , we find

$$\mathcal{M}_{B[4]}^{ab} \mathbf{A}_{\text{cyl}} = 0, \quad (9.29)$$

which agrees with (9.16).

We will now discuss the symmetries as derived in Section 9.5. Since the diagram \mathbf{A}_{np} is embedded on a cylinder, the exact transfer matrix identity (9.21) holds. In order to check this identity, we note that in our particular case there is only one particle on the boundary B' . Thus, due to the vanishing central charge constraint we trivially find

$$\mathcal{T}_{B'}(u) \mathbf{A}_{\text{cyl}} = \text{str } \mathcal{L}_5(u) \mathbf{A}_{\text{cyl}} = 0. \quad (9.30)$$

The evaluation of the action of the transfer matrix on the particles at the boundary B is more involved, but can be done straightforwardly using a similar method as in (9.28), and shows that

$$\mathcal{T}_B(u) \mathbf{A}_{\text{cyl}} = \sum_{i=0}^4 u^{4-i} \underbrace{\sum_{j_1 > \dots > j_i} (\mathcal{W}_{j_1}^{a_1} \partial_{j_1}^{a_2}) \dots (\mathcal{W}_{j_i}^{a_i} \partial_{j_i}^{a_1})}_{\mathcal{T}_{B[i]}} \mathbf{A}_{\text{cyl}} = 0. \quad (9.31)$$

Note that (9.31) yields three independent identities when expanded in the spectral parameter u for the action of $\mathcal{T}_{B[i]}$ with $i = 2, 3, 4$, cf. (9.24). Here we did not include the case $i = 0$ which identically vanishes as well as $i = 1$ which trivially holds when acting on a function with vanishing central charge. The only identity that can be obtained from (9.27) by taking the supertrace is the case $i = 4$.

Note that in the diagram of \mathbf{A}_{cyl} in figure 9.5, another embedding on the cylinder is obtained by simply exchanging particles “2” and “5”. The integrand (9.25) is invariant under this replacement. Therefore the invariance relations (9.27) and (9.31) also hold with the labels “2” and “5” interchanged. This shows that even for this simple example one has to consider all possible embeddings in order to find all symmetries, as briefly discussed at the end of Section 9.4.

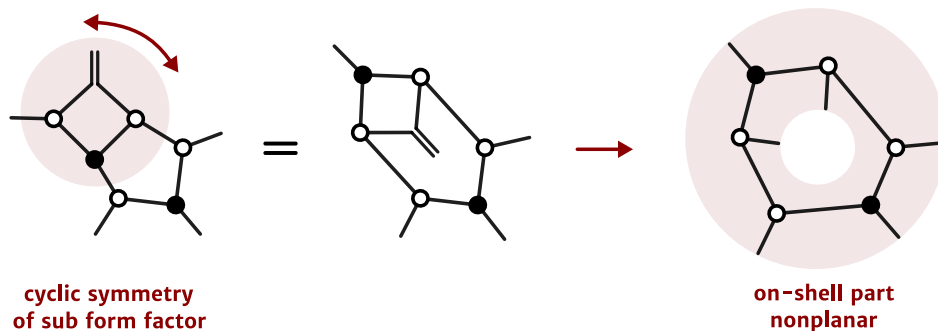
Having established that nonplanar on-shell diagrams possess symmetries that they inherit from the Yangian invariance of planar diagrams will now allow us to take a fresh look at the symmetries of form factor on-shell functions.

Partial Yangian invariance of form factors

In the last chapters, we have derived a variety of results related to the integrability properties of on-shell diagrams. First we found in chapter 8, using the language of R-operators, that form factors of the chiral stress tensor multiplet, as well as planar on-shell functions of arbitrary single trace operators, are eigenstates of integrable transfer matrices. Then we saw in chapter 9, that nonplanar on-shell diagrams (without operator insertions) enjoy both a partial Yangian invariance, as well as certain symmetries related to transfer matrices.

In this chapter we return to form factor on-shell functions and show that apart from being transfer matrix eigenstates, they also exhibit a “partial Yangian invariance”: they are annihilated by the higher levels of Yangian generators, in complete analogy to nonplanar on-shell diagrams.

Heuristically, this can be understood from the fact that the equivalence moves (3.13) which cyclicly rotate sub form factors in these diagrams can be used to move the minimal form factor into the interior of the diagram, such that the pure on-shell part is embedded on a cylinder or annulus. This is shown in figure 10.1.



This chapter presents unpublished results.

Figure 10.1: Form factor on-shell diagrams give rise to nonplanar on-shell diagrams. Here we show the 4 point MHV form factor. Using the move (3.13) to rotate the $F_{3,2}$ subdiagram, it can be converted into an equivalent diagram, where the on-shell part is nonplanar. Note that in this example, the on-shell part can of course be embedded in a planar way. For larger diagrams this is not the case.

In order to prove these symmetries, we will adapt the ideas developed in chapter 9 using twistor variables to the spinor-helicity variables in which form factor on-shell functions can best be described, and combine them with the R-operator construction developed in chapter 8. Since the arguments are identical, we will not consider on-shell functions of the chiral stress tensor multiplet separately, and instead consider on-shell functions with arbitrary operator insertion.

10.1 Dual Jordan–Schwinger realization

To make this idea more precise, we have to change conventions slightly, in order to adapt the arguments and results that we derived in chapter 9 using twistor variables to the spinor-helicity setup we used for the integrability description of form factor on-shell functions in chapter 8.

As it turns out, to directly apply the ideas of chapter 9 we will need to use the dual of the $\mathfrak{gl}_{4|4}$ representation given in (7.7) and (7.9), which can be generated by a particle-hole transformation. This allows to make the spinor-helicity language more similar to the twistor representation. To see this, recall that in both cases, we used a Jordan-Schwinger realization $\mathcal{J}^{AB} = x^A p^B$ with $[p^A, x^B] = \delta^{AB}$. The components of the operators x^A and p^A were respectively given by

$$x_{\text{tw}}^A = \left(\tilde{\mu}^{\dot{\alpha}} \quad , \quad \tilde{\lambda}^{\dot{\alpha}} \quad , \quad \tilde{\eta}^A \quad \right) \quad p_{\text{tw}}^A = \left(\frac{\partial}{\partial \tilde{\mu}^{\dot{\alpha}}} \quad , \quad \frac{\partial}{\partial \tilde{\lambda}^{\dot{\alpha}}} \quad , \quad \frac{\partial}{\partial \tilde{\eta}^A} \quad \right) \quad (10.1)$$

$$x_{\text{sh}}^A = \left(\lambda^\alpha \quad , \quad -\frac{\partial}{\partial \tilde{\lambda}^{\dot{\alpha}}} \quad , \quad \frac{\partial}{\partial \tilde{\eta}^A} \quad \right) \quad p_{\text{sh}}^A = \left(\frac{\partial}{\partial \lambda^\alpha} \quad , \quad \tilde{\lambda}^{\dot{\alpha}} \quad , \quad \tilde{\eta}^A \quad \right) \quad (10.2)$$

where for clarity, $x_{\text{tw}}^A = \mathcal{W}^A$ and $p_{\text{tw}}^A = \frac{\partial}{\partial \mathcal{W}^A}$ are expressed in terms of their constituent spinors. As can be seen from equation (10.1), to relate the generators in this form, we need to apply the half Fourier transform¹ which relates λ and $\tilde{\mu}$, but also a particle-hole transformation on all variables which exchanges raising and lowering operators (variables and their derivative):

$$x^A \rightarrow -(-1)^{|A|} p^A, \quad p^A \rightarrow x^A. \quad (10.3)$$

We therefore want to work – in this chapter – with generators that differ from the ones in (10.1) by this particle-hole transformation:

$$x_{\text{sh}}^A = \left(-\frac{\partial}{\partial \lambda^\alpha} \quad , \quad -\tilde{\lambda}^{\dot{\alpha}} \quad , \quad \tilde{\eta}^A \quad \right) \quad p_{\text{sh}}^A = \left(\lambda^\alpha \quad , \quad -\frac{\partial}{\partial \tilde{\lambda}^{\dot{\alpha}}} \quad , \quad \frac{\partial}{\partial \tilde{\eta}^A} \quad \right) \quad (10.4)$$

These Jordan-Schwinger oscillators generate the dual representation

$$\tilde{\mathcal{J}}^{AB} := x_{\text{sh}}^A p_{\text{sh}}^B = -(-1)^{|A|+|B|} x_{\text{sh}}^B p_{\text{sh}}^A - (-1)^{|A|} \delta^{AB} \quad (10.5)$$

which is the supertranspose of the original representation, up to a diagonal term. For the algebraic purposes that we pursue here, this can be considered as just a different repackaging of the symmetry generators.

10.2 Construction with R-operators

We now move on to define all the objects that are necessary for the integrability construction using the dual representation. The Lax operators are given by

$$\tilde{\mathcal{L}}_i(u) = u + (-1)^B e_{AB} \tilde{\mathcal{J}}_i^{BA} \quad (10.6)$$

and can be used to build up a monodromy matrix

$$\tilde{\mathcal{M}}_n(u) = \tilde{\mathcal{L}}_n(u) \cdots \tilde{\mathcal{L}}_1(u). \quad (10.7)$$

¹ Note that the half-Fourier transform can itself be interpreted as a particle-hole transformation.

We do not consider inhomogeneities, or deformations in this chapter, so the Lax operators carry the same spectral parameter at each sites.

For the R-operator construction we use the same vacua as before,

$$\begin{aligned}\delta_i^+ &= \delta^2(\lambda_i), \\ \delta_i^- &= \delta^2(\tilde{\lambda}_i)\delta^4(\tilde{\eta}_i).\end{aligned}\tag{10.8}$$

Due to the use of the dual representation the two types of vacua exchange their eigenvalues under the action of the Lax operators:

$$\begin{aligned}\bar{\mathcal{L}}_i(u)\delta_i^+ &= u\delta_i^+, \\ \bar{\mathcal{L}}_i(u)\delta_i^- &= (u-1)\delta_i^-.\end{aligned}\tag{10.9}$$

We define new R-operators, which are related to those previously defined in (7.41) by the particle-hole transformation (10.3),

$$\bar{R}_{ij}(z) = \int \frac{d\alpha}{\alpha^{1+z}} e^{-\alpha(x_{\text{sh},j}^- p_{\text{sh},i}^-)} = \int \frac{d\alpha}{\alpha^{1+z}} e^{+\alpha(x_{\text{sh},i}^+ p_{\text{sh},j}^+)} = (-1)^{-z} R_{ji}(z) = \begin{array}{c} \bullet \text{---} \circ \\ | \qquad | \\ j \qquad i \end{array}.\tag{10.10}$$

It is evident that these R-operators simply correspond to parity conjugated BCFW bridges (in the limit $z \rightarrow 0$). We use these R-operators rather than the ones defined in (7.41), since the particle hole transformation (10.3) preserves the commutation relations between x and p . Therefore the Lax and R-operators in the dual representation obey the Yang-Baxter equation

$$\bar{R}_{ij}(u_j - u_i) \bar{\mathcal{L}}_j(u_j) \bar{\mathcal{L}}_i(u_i) = \bar{\mathcal{L}}_j(u_i) \bar{\mathcal{L}}_i(u_j) \bar{R}_{ij}(u_j - u_i).\tag{10.11}$$

Finally we can define the same general (undeformed) form factor on-shell functions as in chapter 8, corresponding to on-shell diagrams where the color-ordered minimal form factor of some length L single trace operator \mathcal{O} is glued in planarly,

$$|\mathcal{F}_{\mathcal{O},n}\rangle = \bar{R}_{i_1 j_1}(0) \cdots \bar{R}_{i_m j_m}(0) F_{\mathcal{O},L}(l, \dots, l+L-1) \prod_{j \in \mathcal{J}^+} \delta_j^+ \prod_{j \in \mathcal{J}^-} \delta_j^-, \tag{10.12}$$

The minimal form factor $F_{\mathcal{O},L}$ can be obtained from the oscillator content of the operator using (8.30). The state (10.12) can be compared to (8.37). Again there are $|\mathcal{J}^+| = n - k$ vacua of type δ^+ and $|\mathcal{J}^-| = k - L$ vacua of type δ^- , for a k such that the minimal form factor defines the minimal MHV degree $k = L$.

10.3 Yangian symmetries

We now proceed to the derivation of Yangian symmetries for form factor on-shell functions of arbitrary operators. The argument closely mirrors the corresponding calculation of transfer matrix identities for these quantities in section 8.4, but is heavily informed on the results for nonplanar diagrams in section 9.4.

We start by taking the general on-shell function (10.12), and act with the monodromy matrix (10.7) on it. Using the Yang-Baxter equation (10.11), we can commute the monodromy through the sequence of R-operators to obtain

$$\begin{aligned}
 \tilde{\mathcal{M}}_n(u) |\mathcal{F}_{\theta,n}\rangle &= \\
 \bar{R}_{i_1 j_1}(0) \cdots \bar{R}_{i_m j_m}(0) \tilde{\mathcal{M}}_n(u) F_{\theta,L}(l, \dots, l+L-1) \prod_{j \in \mathcal{J}^+} \delta_j^+ \prod_{j \in \mathcal{J}^-} \delta_j^- &= \\
 u^{|\mathcal{J}^+|} (u-1)^{|\mathcal{J}^-|} \bar{R}_{i_1 j_1}(0) \cdots \bar{R}_{i_m j_m}(0) \prod_{j \in \mathcal{J}^+} \delta_j^+ \prod_{j \in \mathcal{J}^-} \delta_j^- \left[\tilde{\mathcal{M}}_L(u) F_{\theta,L}(l, \dots, l+L-1) \right]. &
 \end{aligned} \tag{10.13}$$

In the third line, we used the eigenvalue equations the Lax operators and the vacua given in (10.9), such that the only Lax operators left are those acting on the minimal form factor of the operator θ , forming a smaller monodromy $\tilde{\mathcal{M}}_L(u) = \tilde{\mathcal{L}}_{l+L-1}(u) \cdots \tilde{\mathcal{L}}_1(u)$. Note that in contrast to the transfer matrix considered in equation (8.34), we cannot “translate” this monodromy via (8.29) into the corresponding oscillator monodromy to act directly on the operator in its oscillator representation. The reason for this is that the monodromy matrix is not $\mathfrak{gl}_{4|4}$ invariant, and therefore does not commute with the momentum conserving delta function in the minimal form factor (8.30).

Instead we note that similar to equation (9.13) which served as a starting point to derive the Yangian symmetries of nonplanar on-shell diagrams, the last line in (10.13) has an expansion in the spectral parameter u which start at least from $u^{|\mathcal{J}^+|}$, the number of δ^+ vacua. The monodromy acting on the minimal form factor could raise this power by at most L , but we make no assumptions regarding the state.

If we expand both sides in u , the left hand sides gives the Yangian generators

$$\tilde{\mathcal{M}}_n^{AB}(u) = \sum_{\ell=0}^n u^{n-\ell} \tilde{\mathcal{M}}_{n[\ell]}^{AB}, \tag{10.14}$$

analogous to (7.18). By comparing powers of u , we see that for low enough powers the right hand side vanishes as just discussed, and we get the following invariance statements:

$$\tilde{\mathcal{M}}_{n[\ell]}^{AB} |\mathcal{F}_{\theta,n}\rangle = 0, \quad \ell = n - |\mathcal{J}^+| + 1, \dots, n. \tag{10.15}$$

This is a partial Yangian invariance similar to the results for nonplanar on-shell diagrams in section 9.4. We note that (10.15) is in complete agreement with the corresponding result for a nonplanar on-shell diagram with a boundary of length n . For example, form factor on-shell functions of the chiral stress tensor multiplet have $|\mathcal{J}^+| = n - k$, which implies that the levels $k + 1$ up to n are unbroken symmetries. Regardless of the type of the operator insertion, one level of Yangian symmetries is gained for each on-shell particle that is added to the diagram without increasing the MHV degree, starting from the minimal form factor.

10.4 Symmetries from the original representation

We can now see why we needed to use the dual representation (10.4): comparing the action of the Lax operators in the original and in the dual representation (given respectively in equations (7.49) and (10.9)) it is evident that using the original representation (7.7), the right hand side in (10.13) would be proportional to $u^{|\mathcal{G}^-|}$ instead of $u^{|\mathcal{G}^+|}$. This would imply that we would find more symmetries for on-shell functions with a higher MHV degree, in contrast to the results of chapter 9, where there were more unbroken symmetries the closer the on-shell function was to being MHV. Concretely we would have

$$\mathcal{M}_{n[\ell]}^{\text{AB}} |\mathcal{F}_{\mathcal{O},n}\rangle = 0, \quad \ell = n - |\mathcal{G}^-| + 1, \dots, n. \quad (10.16)$$

with the monodromy matrix defined in equation (7.16).

This shows that one should really consider both representations; depending on the MHV degree, we can recover more symmetries using the appropriate one of them. This restores the approximate parity symmetry: only the operator insertion prevents the form factor on-shell function to transform simply under parity, while the on-shell part does so under an exchange of black and white vertices. We see this comparing (10.15) and (9.15): since the minimal form factor effectively replaces $L \delta^-$ vacua, these relations are not symmetric under exchanging $k \leftrightarrow n - k$.

It would be very interesting to see if a similar argument applies to the nonplanar on-shell functions discussed in the last chapter; if both the on-shell functions as well as the Yangian generators are expressed in terms of spinor-helicity variables, we suspect that the number of unbroken Yangian levels is the same for a given diagram and the diagram obtained by exchanging black and white vertices, if one simultaneously particle-hole transforms the symmetry generators.

The Grassmannian integral as a map between spin chains

In this short chapter we present an observation that allows to interpret the *integrand*s of general Grassmannian integrals, such as those appearing for amplitudes, nonplanar on-shell functions or for form factors, as spin chain states. The corresponding models are non-compact \mathfrak{gl}_k spin chains – where k refers to the MHV degree – which are a priori unrelated to the $\mathcal{N}=4$ SYM spin chain.

The previously unpublished results presented in this chapter were obtained in joint work with Rouven Frassek.

The fact that other integrable spin chains describe the Grassmannian integrands is based on a relation which shows that the Grassmannian integral maps the $\mathfrak{gl}_{4|4}$ transfer matrix of $\mathcal{N}=4$ SYM into the corresponding \mathfrak{gl}_k transfer matrix and vice versa. While we currently do not understand whether this mapping indicates any deeper relation between the models, either from the viewpoint of $\mathcal{N}=4$ SYM or from a general integrable models perspective, it is a useful tool to investigate and check the symmetries discussed in the previous chapters, directly on the level of the form on the Grassmannian.

11.1 A formula for transfer matrices in terms of rotations in the space of particles

As in chapter 7, we represent the $\mathfrak{gl}_{4|4}$ generators $\mathcal{J}_i^{AB} = x_i^A p_i^B$, which satisfy the commutation relations (7.10), via Schwinger oscillators with $[p_i^A, x_j^B] = \delta_{ij} \delta^{AB}$. To make some calculations easier, we use twistor variables

$$x_i^A = \mathcal{W}_i^A, \quad p_i^A = \frac{\partial}{\partial \mathcal{W}_i^A} = \partial_i^A, \quad (11.1)$$

but all conclusions in this chapter also hold for spinor-helicity variables. From these generators, one can construct Lax operators (7.13) as well as monodromy (7.16) and transfer matrices (7.26) as described in detail in chapter 7. Our aim now is to derive representations for the monodromy and transfer matrices using operators which act on the indices labeling the particle instead of the $\mathfrak{gl}_{4|4}$ indices. This will then be the basis for proving the mapping between transfer matrices.

We first consider the matrix elements appearing in the expansion of the monodromy matrix in the spectral parameter (7.18). A general level is given in terms of the generators \mathcal{G}^{AB} by

$$\mathcal{M}_{n[\ell]}^{BA} = (-1)^{|A|} \sum_{i_1 < \dots < i_\ell} (-1)^{\sum_{j=1}^{\ell-1} |C_j|} \mathcal{G}_{i_1}^{AC_{i_1}} \mathcal{G}_{i_2}^{C_{i_1} C_{i_2}} \dots \mathcal{G}_{i_{\ell-1}}^{C_{i_{\ell-2}} C_{i_{\ell-1}}} \mathcal{G}_{i_\ell}^{C_{i_{\ell-1}} B}, \quad (11.2)$$

which follows from the definition of the Lax operators. Using the fact that the generators of $\mathfrak{gl}_{4|4}$ have Jordan-Schwinger form, we can transform this into

$$\mathcal{M}_{n[\ell]}^{BA} = (-1)^{|A|} \sum_{i_1 < \dots < i_\ell} x_{i_1}^A \mathcal{O}_{i_2 i_1} \mathcal{O}_{i_3 i_2} \dots \mathcal{O}_{i_\ell i_{\ell-1}} p_{i_\ell}^B \quad (11.3)$$

where we defined the \mathfrak{gl}_n generators (acting in “particle space”)

$$\mathcal{O}_{ij} = x_i \cdot p_j = x_i^A p_j^A. \quad (11.4)$$

They obey the commutation relations of \mathfrak{gl}_n ,

$$[\mathcal{O}_{ij}, \mathcal{O}_{kl}] = \delta_{jk} \mathcal{O}_{il} - \delta_{il} \mathcal{O}_{kj}. \quad (11.5)$$

Note that these operators also appear in the R-operators (7.41).¹ The operators x^A and p^A transform as follows under the action of the \mathfrak{gl}_n generators:

$$\begin{aligned} [\mathcal{O}_{ij}, x_i^A] &= 0, & [\mathcal{O}_{ij}, x_j^A] &= +x_i^A, \\ [\mathcal{O}_{ij}, p_i^A] &= -p_j^A, & [\mathcal{O}_{ij}, p_j^A] &= 0. \end{aligned} \quad (11.6)$$

By taking the supertrace of (11.3) and using these commutators to bring the remaining x and p operators next to each other, we can write the operators in the expansion (7.29) of the transfer matrix entirely in terms of these \mathfrak{gl}_n rotations:

$$\begin{aligned} \mathcal{T}_{n[\ell]} = \sum_{i_1 < \dots < i_\ell} \left\{ + \mathcal{O}_{i_1 i_\ell} \mathcal{O}_{i_2 i_1} \dots \mathcal{O}_{i_{\ell-1} i_{\ell-2}} \mathcal{O}_{i_\ell i_{\ell-1}} - \mathcal{O}_{i_1 i_{\ell-1}} \mathcal{O}_{i_2 i_1} \dots \mathcal{O}_{i_{\ell-2} i_{\ell-3}} \mathcal{O}_{i_{\ell-1} i_{\ell-2}} \right. \\ \left. \dots + (-1)^\ell \mathcal{O}_{i_1 i_2} \mathcal{O}_{i_2 i_1} + (-1)^{\ell+1} \mathcal{O}_{i_1 i_1} \right\}. \end{aligned} \quad (11.7)$$

Note that this form of the transfer matrix is not special for $\mathfrak{gl}_{4|4}$, but is valid for any rational $\mathfrak{gl}_{n|m}$ spin chain with a representation of Jordan-Schwinger form.

11.2 Action on Graßmannian integrals

The representation of the transfer matrix given in equation (11.7) allows to derive its action on Graßmannian integrals. We write a general such integral – with arbitrary integrand – as

$$\int [dC] \Omega \Delta \quad \text{with} \quad [dC] = \frac{dC^{k \times n}}{\text{Vol}[GL(k)]} \quad \text{and} \quad \Delta = \delta^{4k|4k}(C \mathcal{W}). \quad (11.8)$$

We first consider the action of the \mathcal{O}_{ij} operators on the delta functions, which are the only factors in the integral involving the external kinematics. One finds

¹ See also footnote 43 on page 96; essentially the R-operators are powers of the operators \mathcal{O}_{ij} .

that this action can be expressed in terms of operators acting on the entries of the matrix C as follows:

$$\mathcal{O}_{ij} \Delta = c_j^a \partial_i^a \Delta. \quad (11.9)$$

Here c_j^a is the matrix element in the a 'th row and j 'th column of the matrix C and $\partial_i^a = \frac{\partial}{\partial c_i^a}$. This equation implies that the operator \mathcal{O}_{ij} has the following action on the full Grassmannian integral:

$$\mathcal{O}_{ij} \int [dC] \Omega \Delta = \int [dC] \Omega \mathcal{O}_{ij} \Delta = \int [dC] \Omega c_j^a \partial_i^a \Delta = \int [dC] \{ \mathbb{O}_{ij} \Omega \} \Delta, \quad (11.10)$$

where the last equality follow from partial integration, assuming a closed contour. The operators \mathbb{O}_{ij} are another set of \mathfrak{gl}_n generators, expressed in terms of Jordan-Schwinger operators acting on the Grassmannian integrand,

$$\mathbb{O}_{ij} = -\partial_i^a c_j^a. \quad (11.11)$$

As the operators \mathcal{O}_{ij} , they also satisfy the commutation relations given (11.5).² Now we can consider the individual terms in the expansion of the transfer matrix as written in (11.7). From (11.10) it follows that

$$\mathcal{O}_{i_1 i_r} \mathcal{O}_{i_2 i_1} \cdots \mathcal{O}_{i_{r-1} i_{r-2}} \mathcal{O}_{i_r i_{r-1}} \int [dC] \Omega \Delta = \int [dC] \{ \mathbb{O}_{i_1 i_r} \mathbb{O}_{i_2 i_1} \cdots \mathbb{O}_{i_{r-1} i_{r-2}} \mathbb{O}_{i_r i_{r-1}} \Omega \} \Delta. \quad (11.12)$$

Note that the order of the operators is preserved because it reverses twice: when acting on the delta functions and when performing the partial integration.

Equation (11.12) can be applied to any term in (11.7) and to any level of the expansion of the transfer matrix. Since the structure of the resulting operators remains identical, we can act with the full transfer matrix on the Grassmannian integral, and – remarkably – reassemble a transfer matrix acting on the *integrand* of the Grassmannian integral. We therefore find that

$$\mathcal{T}_n(u) \int [dC] \Omega \Delta = \int [dC] \{ (\mathbb{T}_n(u) - ku^n) \Omega \} \Delta, \quad (11.13)$$

which is the main result of this chapter. In this equation we defined the fundamental \mathfrak{gl}_k transfer matrix, with k the MHV degree, in terms of Lax operators as

$$\mathbb{T}_n(u) = \text{tr} \mathbb{L}_n(u) \cdots \mathbb{L}_2(u) \mathbb{L}_1(u), \quad \mathbb{L}_i(u) = u + e^{ab} \mathbb{J}_i^{bc}. \quad (11.14)$$

The matrices e^{ab} are the fundamental generators of \mathfrak{gl}_k , and

$$\mathbb{J}_i^{ab} = -\partial_i^a c_i^b \quad (11.15)$$

the \mathfrak{gl}_k generators in Jordan-Schwinger form acting on the sites of the ‘‘Grassmannian spin chain’’. Note that the term $-ku^n$ in (11.13) arises because the

² Note that equation (11.10) was used in Drummond, Ferro, ‘‘Yangians, Grassmannians and T-duality’’, 1001.3348, to show the invariance of the Grassmannian integral (with the standard amplitude top-form) under the first level of the Yangian.

lowest level of the $\mathfrak{gl}_{4|4}$ transfer matrix is $u^n \text{str } \mathbb{1} = 0$, while for the \mathfrak{gl}_k transfer matrix it is $u^n \text{tr } \mathbb{1} = ku^n$.

The action of the Yangian generators can be derived by a similar argument and is given by

$$\mathcal{M}_{n[\ell]}^{\text{BA}} \int [\text{dC}] \Omega \Delta = \int [\text{dC}] \left\{ (-1)^{|\text{A}|} \sum_{i_1 < \dots < i_\ell} x_{i_1}^{\text{A}} \circ_{i_2 i_1} \circ_{i_3 i_2} \dots \circ_{i_\ell i_{\ell-1}} c_{i_\ell}^{\text{B}} \Omega \Delta_{,b,\text{B}} \right\} \quad (11.16)$$

Here the notation $\Delta_{,b,\text{B}}$ indicates which of the $k \times (4|4)$ of the delta functions is to be replaced by the derivative δ' . We see that in contrast to the transfer matrix, the Yangian generators $\mathcal{M}_{n[\ell]}^{\text{BA}}$ are not mapped into the Yangian generators of the \mathfrak{gl}_k spin chain.

Equation (11.13) shows that the Grassmannian integral can be viewed as a map between the $\mathfrak{gl}_{4|4}$ and a \mathfrak{gl}_k spin chain, in particular transforming eigenstates into eigenstates. The Yangian generators do not transform into the \mathfrak{gl}_k Yangian generators under this map, but one can still calculate their action, given in (11.16), purely on the level of the Grassmannian form. The relations derived here are still valid when the monodromy and transfer matrices do not involve all particles, as was the case for the symmetries derived in the previous chapters for form factor on-shell functions (where two additional sites carry the information of the operator insertion) and for nonplanar on-shell diagrams. Therefore the relations (11.13) and (11.16) provide a very efficient way to check and investigate these symmetries, which in the \mathfrak{gl}_k picture are realized by differential operators acting on the Grassmannian form Ω .

11.3 The \mathfrak{gl}_k spin chain

Since we consider the map between spin chains as an interesting fact in itself, we investigate the \mathfrak{gl}_k spin chain in more detail now.

The MHV Grassmannian and the Faddeev–Korchemsky model

We first show that the \mathfrak{gl}_2 spin chain for the MHV Grassmannian integral is identical to a model which appeared in the context of high energy scattering in QCD. Lipatov proposed that in the leading log approximation and at large N , the partial waves for hadron scattering can be described by an integrable noncompact spin 0 Heisenberg model.³ The transverse coordinates (x_j, y_j) of the reggeized gluons can be combined into the light-cone variables $z_j = x_j + iy_j$, $\bar{z}_j = x_j - iy_j$ which are used to describe the n -gluon states. These wavefunctions are eigenstates of a Hamiltonian, which at large N decouples into a holomorphic and an antiholomorphic component, and their energies are related to the angular momentum of the states.

Subsequently, Faddeev and Korchemsky showed that the spin chain model

³ Lipatov, “Asymptotic behavior of multicolor QCD at high energies in connection with exactly solvable spin models”, [hep-th/9311037](https://arxiv.org/abs/hep-th/9311037), [Pisma Zh. Eksp. Teor. Fiz.59,571(1994)]

is equivalent to a spin -1 model, for which the algebraic Bethe Ansatz can be applied.⁴ Further work, investigating the model using Q-operators and the separation of variables approach can be found in the papers Korchemsky (1995); Derkachov et al. (2001, 2002, 2003); Maassarani and Wallon (1995).⁵ For a review see also Korchemsky (2012).⁶

Returning the Graßmannian integral, we now consider the MHV case with $k = 2$. The symmetry generators (11.15) acting on the Graßmannian integrand define the following \mathfrak{sl}_2 generators,

$$S^+ = \mathbb{J}^{12} = -\partial^1 c^2, \quad S^- = \mathbb{J}^{21} = -\partial^2 c^1, \quad S^3 = \frac{1}{2}(\mathbb{J}^{11} - \mathbb{J}^{22}) = c^2 \partial^2 - c^1 \partial^1, \quad (11.17)$$

with $[S^+, S^-] = 2S^3$. The Graßmannian integral requires that the form Ω is of homogeneous degree $-k$ in the elements of the matrix C . This fixes the highest-weight state to be

$$|hws\rangle = \frac{1}{(c^2)^2} \implies S^+ |hws\rangle = 0 \quad \text{and} \quad S^3 |hws\rangle = -|hws\rangle, \quad (11.18)$$

and shows that the spin chain carries the same spin -1 representation as the model for high energy QCD. To make the relation more concrete, we can write the generators in Holstein-Primakoff form, by restricting the Fock space to the spin -1 representation. If we consider the columns of the matrix C as homogeneous coordinates on \mathbb{CP}^1 , this can be understood as choosing a chart, see for example Fuksa and Kirschner (2017),⁷ and can be realized by parametrizing the variables c as

$$c^2 \rightarrow z, \quad c^1 \rightarrow 1, \quad (11.19)$$

which implies for the derivatives

$$\partial^1 = \frac{\partial}{\partial z} = \partial, \quad \partial^2 = -z\partial - 2, \quad (11.20)$$

where $\partial = \frac{\partial}{\partial z}$. To arrive at these expressions one uses the central charge constraint for the representation, $c^1 \partial^1 + c^2 \partial^2 = -2$, and solves for ∂^2 . The symmetry generators are then given by⁸

$$S^+ = z^2 \partial + 2z, \quad S^- = -\partial, \quad S^3 = z\partial + 1, \quad (11.21)$$

which coincide with the ones used in Faddeev and Korchemsky (1995) for the spin -1 model. The highest-weight state for a chain of length n is then given by

$$\frac{1}{z_1^2 z_2^2 \cdots z_{n-1}^2 z_n^2}, \quad (11.22)$$

and the Graßmannian top-form for scattering amplitudes is the entangled state

$$\frac{(-1)^n}{(z_1 - z_2)(z_2 - z_3) \cdots (z_{n-1} - z_n)(z_n - z_1)}. \quad (11.23)$$

Note that this state corresponds to the trivial constant state in the spin 0 model.

4 Faddeev, Korchemsky, “High-energy QCD as a completely integrable model”, [hep-th/9404173](#)

5 Korchemsky, “Bethe ansatz for QCD pomeron”, [hep-ph/9501232](#); Derkachov, Korchemsky, Manashov, “Noncompact Heisenberg spin magnets from high-energy QCD: 1. Baxter Q operator and separation of variables”, [hep-th/0107193](#); Derkachov, Korchemsky, Kotanski, Manashov, “Noncompact Heisenberg spin magnets from high-energy QCD. 2. Quantization conditions and energy spectrum”, [hep-th/0204124](#); Derkachov, Korchemsky, Manashov, “Noncompact Heisenberg spin magnets from high-energy QCD. 3. Quasiclassical approach”, [hep-th/0212169](#); and Maassarani, Wallon, “Baxter equation for the QCD odderon”, [hep-th/9507056](#)

6 Korchemsky, “Review of AdS/CFT Integrability, Chapter IV.4: Integrability in QCD and $N < 4$ SYM”, [1012.4000](#)

7 Fuksa, Kirschner, “Correlators with \mathfrak{sl}_2 Yangian symmetry”, [1608.04912](#)

8 Note that when performing this change of variables on the generators, one first has to commute all derivative ∂^a to the right.

Representation for other k

For the general \mathfrak{gl}_k case, we can find the representation at the spin chain sites by noting that the Grassmannian integral fixes the integrand Ω to be a homogeneous function of degree $-k$ in the entries of the C matrix. Consider the generators defined in (11.15). The highest-weight state is annihilated by the generators \mathbb{J}^{ab} with $b > a$. It is easy to see that it is given by

$$|\text{hws}\rangle = \frac{1}{(c^k)^k}. \quad (11.24)$$

We can read off the representation labels by acting with the diagonal generators on the highest-weight state,

$$\mathbb{J}^{11} |\text{hws}\rangle = \dots = \mathbb{J}^{k-1, k-1} |\text{hws}\rangle = -|\text{hws}\rangle \quad \mathbb{J}^{kk} |\text{hws}\rangle = (k-1) |\text{hws}\rangle \quad (11.25)$$

Therefore the \mathfrak{gl}_k weights are $(-1, \dots, -1, k-1)$ and the Dynkin labels are therefore given by $(0, \dots, 0, -k)$.

Importantly, not all states on the \mathfrak{gl}_k spin chain can be mapped via the Grassmannian integral to $\mathfrak{gl}_{4|4}$ states; for it to be a well-defined integral, the form Ω needs to be \mathfrak{gl}_k invariant. Therefore the mapping only works for singlets, such as the amplitude top-form $[(1 \cdots k) \cdots (n \cdots k-1)]^{-1}$. It remains an open question how to find the other invariant eigenstates, and to see what they correspond to in $\mathcal{N}=4$ SYM. The form factor Grassmannian integral given in equations (4.24) and (4.25) provides examples of states which are entangled via additional sites $n+1$ and $n+2$ on which the transfer matrix does not act. We leave the investigation of these questions for future work.

Nevertheless, we have used the results presented here for practical checks of the results of the last chapters, especially using (11.16) and (11.13). The fact that these equations allow to calculate the action of transfer matrices and Yangian generators on the level of the Grassmannian integrand means that no integrals or distributions are involved, such that all calculations can easily be automatized in Mathematica. We hope that they can thus be used as a powerful tool, in particular for the classification of nonplanar on-shell functions.⁹

⁹ Bourjaily, Franco, Galloni, Wen, "Stratifying On-Shell Cluster Varieties: the Geometry of Non-Planar On-Shell Diagrams", 1607.01781

III

**TOWARDS STATES
AT HIGHER LOOPS**

The Quantum Spectral Curve & Baxter Q-operators

After having discussed form factors and other on-shell functions as states of the $\mathcal{N}=4$ SYM spin chain, we will now consider states which are more widely studied from the spin chain perspective, namely gauge invariant composite operators. These can be described at the level of their eigenvalues (their energy and higher conserved charges), by the Quantum Spectral Curve, a concise set of equations governing this spectral problem. This formulation however carries no information on the structure of the state vectors, i.e. the perturbative expansion of the eigenstates in terms of trace operators. While these vectors carry some amount of renormalization scheme dependence, a better understanding of them, or even a way of determining them from integrability, is clearly desirable. Having a solid picture of these states, and the operatorial form of the commuting transfer matrices and conserved charges at higher loop order could be a stepping stone for a better understanding of how integrability emerges from the field theory.

The aim of this and the next chapters is to provide a definition, and tools for the explicit calculation, of the perturbative, operatorial Q-system of $\mathcal{N}=4$ SYM. We consider the Q-operators at the one-loop level and show how to calculate explicit representations as finite matrices in each magnon sector. The reason for considering these explicit matrices is that they can be used as input data for perturbative calculations based on the Quantum Spectral Curve, lifting it to the operatorial level. While nonperturbative Q-operators for $\mathcal{N}=4$ SYM certainly exist, this strategy circumvents the problems of formulating $\mathcal{N}=4$ SYM as a spin chain at higher loops, where the length of states ceases to be a good quantum number and the QISM constructions are no longer available. The following chapters describe the first steps of this program.

This chapter serves as an introduction to both the Quantum Spectral Curve as well as the Q-operators of integrable spin chain models. In section 12.1 we review the oscillator representation of fields and composite operators in $\mathcal{N}=4$ SYM, which is essential to the spin chain description. We then give a brief summary of the QSC as a system of Q-functions, including some notes on its weak coupling expansion in section 12.2. Finally we introduce the oscillator construction of Q-operators, which builds them as traces over monodromy matrices, sim-

ilar to the other commuting transfer matrices of the integrable model, which we already encountered in chapter 7. This construction will play a key role in the next chapter, where we apply it to the cases relevant to $\mathcal{N}=4$ SYM.

12.1 Composite operators in $\mathcal{N}=4$ SYM

The fundamental fields in $\mathcal{N}=4$ SYM can conveniently be described in terms of an oscillator representation, first introduced in Bars and Günaydin (1983); Günaydin and Marcus (1985).¹ This representation uses four bosonic and four fermionic pairs of creation and annihilation operators, with commutation relations

$$\begin{aligned} [\mathbf{a}_\alpha, \bar{\mathbf{a}}_\beta] &= \delta_{\alpha\beta}, & \alpha, \beta &= 1, 2, \\ [\mathbf{b}_{\dot{\alpha}}, \bar{\mathbf{b}}_{\dot{\beta}}] &= \delta_{\dot{\alpha}\dot{\beta}}, & \dot{\alpha}, \dot{\beta} &= 1, 2, \\ \{\mathbf{d}_a, \bar{\mathbf{d}}_b\} &= \delta_{ab}, & a, b &= 1, 2, 3, 4. \end{aligned} \quad (12.1)$$

These operators act on a Fock vacuum $|0\rangle$ with $\mathbf{a}_\alpha |0\rangle = \mathbf{b}_{\dot{\alpha}} |0\rangle = \mathbf{d}_a |0\rangle = 0$. We also define the number operators $\mathbf{N}_{\mathbf{a}_\alpha} = \bar{\mathbf{a}}_\alpha \mathbf{a}_\alpha$ and similarly for the other oscillators. The symmetry generators will likewise be given in terms of bilinears of the raising and lowering operators; we will discuss them in more detail in section 13.3. The singleton representation under which the fields of $\mathcal{N}=4$ SYM transform is obtained by restricting the Fock space to states with vanishing central charge,

$$\mathbf{c} = \sum_{\alpha=1}^2 \mathbf{N}_{\mathbf{a}_\alpha} - \sum_{\dot{\alpha}=1}^2 \mathbf{N}_{\mathbf{b}_{\dot{\alpha}}} - \sum_{a=1}^4 \mathbf{N}_{\mathbf{d}_a} + 2 = 0. \quad (12.2)$$

Note that this description of fields is the same we already introduced when form factor on-shell functions of general operators were discussed in section 8.4.

The correspondence with the fields of $\mathcal{N}=4$ SYM is then as follows:

ϕ_{ab}	$\psi_{a\alpha}$	$\bar{\psi}_{\alpha\dot{a}}$	$\mathcal{F}_{\alpha\beta}$	$\bar{\mathcal{F}}_{\dot{\alpha}\dot{\beta}}$	$\mathcal{D}_{\alpha\dot{\alpha}}$
$\bar{\mathbf{d}}_a \bar{\mathbf{d}}_b 0\rangle$	$\varepsilon^{abcd} \bar{\mathbf{d}}_b \bar{\mathbf{d}}_c \bar{\mathbf{d}}_d \bar{\mathbf{a}}_\alpha 0\rangle$	$\bar{\mathbf{d}}_a \bar{\mathbf{b}}_{\dot{\alpha}} 0\rangle$	$\bar{\mathbf{d}}_1 \bar{\mathbf{d}}_2 \bar{\mathbf{d}}_3 \bar{\mathbf{d}}_4 \bar{\mathbf{a}}_\alpha \bar{\mathbf{a}}_\beta 0\rangle$	$\bar{\mathbf{b}}_{\dot{\alpha}} \bar{\mathbf{b}}_{\dot{\beta}} 0\rangle$	$\bar{\mathbf{a}}_\alpha \bar{\mathbf{b}}_{\dot{\alpha}}$

(12.3)

Here we denote the six scalars by $\phi_{ab} = -\phi_{ba}$, the eight fermions are $\psi_{a\alpha}$ and their conjugates, and the self-dual and anti-self-dual field strengths are written as $\mathcal{F}_{\alpha\beta}$ and $\bar{\mathcal{F}}_{\dot{\alpha}\dot{\beta}}$. Finally, \mathcal{D} denotes a covariant derivative. The lowest-weight state of the representation is the scalar $|\mathcal{L}\rangle = \bar{\mathbf{d}}_1 \bar{\mathbf{d}}_2 |0\rangle$. Note that the state space is infinite-dimensional since an arbitrary number of covariant derivatives can act on the fields. This is a general property of unitary representations of non-compact groups. Using oscillators to represent the fields has the advantage that due to the automatic (anti-)symmetrization, the equations of motions are already factored out.

The states of planar, weakly coupled $\mathcal{N}=4$ SYM are gauge-invariant composite operators, which are color traces of products of the fundamental fields,

¹ Bars, Günaydin, “Unitary Representations of Noncompact Supergroups”, *Commun. Math. Phys.* 91 (1983) 31; and Günaydin, Marcus, “The Spectrum of the S^5 Compactification of the Chiral $N=2, D=10$ Supergravity and the Unitary Supermultiplets of $U(2, 2/4)$ ”, *Class. Quant. Grav.* 2 (1985) L11

evaluated at the same point in space-time, which we can take to be the origin:

$$\mathcal{O} = \text{tr} \left(\Phi_1(0) \cdots \Phi_L(0) \right). \quad (12.4)$$

Here each Φ_i can be any of the fields given in (12.3) with an arbitrary number of derivatives. In terms of the oscillators, these single trace operators are given in terms of graded-cyclic tensor products of the field representations.

These operators are subject to renormalization, and operators with the same classical charges can mix in this process, such that the Z -factors have a matrix structure, $\mathcal{O}_{i,\text{ren}} = Z_i^j \mathcal{O}_{j,\text{bare}}$. The dilatation operator measures the dependence of the renormalized operators on the renormalization scale μ , $\mathcal{D} = \mu \frac{d}{d\mu} Z$. Since $\mathcal{N}=4$ SYM is conformal, its eigenvalues, i.e. the scaling dimensions of operators which renormalize multiplicatively, are observables. In the following, we decompose the scaling dimension into the classical dimension Δ_0 , and the anomalous dimension $\gamma(g)$ which depends on the coupling $g = \frac{\sqrt{\lambda}}{4\pi}$, with the 't Hooft coupling λ

$$\mathcal{D}|\mathcal{O}\rangle = \Delta(g)|\mathcal{O}\rangle, \quad \Delta(g) = \Delta_0 + \gamma(g). \quad (12.5)$$

The classical dimension of the operator is just the sum of the dimensions of the constituent fields, which is given in terms of the oscillators by

$$\Delta_0 = \frac{1}{2} \sum_{\alpha=1}^4 \mathbf{N}_{\mathbf{d}_\alpha} + \sum_{\alpha=1}^2 \mathbf{N}_{\mathbf{a}_\alpha}, \quad (12.6)$$

where we used the central charge constraint, which likewise determines the length L of the operator, i.e. the number of factors in the tensor product, via the oscillator numbers,

$$L = \frac{1}{2} \left(\sum_{\alpha=1}^2 \mathbf{N}_{\mathbf{b}_\alpha} + \sum_{\alpha=1}^4 \mathbf{N}_{\mathbf{d}_\alpha} - \sum_{\alpha=1}^2 \mathbf{N}_{\mathbf{a}_\alpha} \right). \quad (12.7)$$

Due to length-changing effects at higher loop order, L is only a good quantum number at tree-level and one-loop.

A state at weak coupling is determined by these eight oscillator numbers (up to degeneracies), or equivalently by the $\mathfrak{gl}_{4|4}$ weights

$$\lambda_a = L - \mathbf{N}_{\mathbf{d}_a}, \quad \nu_i = (\mathbf{N}_{\mathbf{a}_1}, \mathbf{N}_{\mathbf{a}_2}, -L - \mathbf{N}_{\mathbf{b}_1}, -L - \mathbf{N}_{\mathbf{b}_2}), \quad (12.8)$$

Then the six numbers $r_a = \lambda_a - \lambda_{a+1}$ and $q_i = \nu_i - \nu_{i+1}$ define the representation of $\mathfrak{psu}_{2,2|4}$ the state transforms in.

While the eigenstates of the dilatation operators carry some scheme dependence, the conformal dimensions are well-defined properties of the theory, and via the state-operator map can be regarded as the energies of the states of the theory. Determining these quantities constitutes the spectral problem. Note that the scaling dimensions completely determine the two-point correlation functions of composite operators; together with the structure constants of the OPE, they in principle determine all correlators of the theory.

12.2 The Quantum Spectral Curve

The Quantum Spectral Curve (often abbreviated as QSC in the following), a remarkably concise formulation of the spectral problem in $\mathcal{N} = 4$ SYM at finite coupling, was announced in Gromov et al. (2014)² and derived³ from the Thermodynamic Bethe Ansatz equations in Gromov et al. (2015).⁴ It allows to find the scaling dimension of any state, taking its integer charges as an input, and then bootstrapping a system of Q-functions from known analytic properties. The QSC is generally considered the “final” formulation of the spectral problem, in the sense that no simpler formulation appears to be possible. During the last years, it allowed to derive a wealth of novel results, see for example Alfimov et al. (2015); Gromov and Levkovich-Maslyuk (2016a,b).⁵ Here we give a brief overview of the QSC, with an emphasis on its weak coupling limit and its interpretation as a Q-system in order to motivate the developments of the next chapters.

Q-system

The basis of the Quantum Spectral Curve is an algebraic Q-system. We will discuss the Q-system for general integrable models with $\mathfrak{gl}_{N|M}$ invariance; the case relevant to $\mathcal{N} = 4$ SYM is recovered by specializing to $\mathfrak{gl}_{4|4}$. Note that all algebraic properties of this system depend only on the symmetry algebra, but not on the representation.

For each state of the model, i.e. for each eigenstate of the family of commuting operators,⁶ there exist 2^{N+M} so called Q-functions, which are indexed by ordered subsets of the $N + M$ $\mathfrak{gl}_{N|M}$ indices, and depend on the spectral parameter u . In accordance with the Quantum spectral curve literature, we separate the bosonic indices and the fermionic indices and write the Q-functions as $Q_{A|I}$, where capital letters are used to denote ordered sets of indices, and the A are bosonic, while the I are fermionic.⁷ We denote the empty set by \emptyset and the full set by $\bar{\emptyset} = 123 \cdots N$ or $\bar{\emptyset} = 123 \cdots M$. The notation \bar{A} means the complement of A . The Q-functions are anti-symmetric in their indices.

While the total number of Q-functions is very large, there are only $N+M+1$ independent ones, since the Q-functions satisfy the following functional relations, often called QQ-relations:

$$\begin{aligned} Q_{A|I} Q_{Aab|I} &= Q_{Aa|I}^+ Q_{Ab|I}^- - Q_{Aa|I}^- Q_{Ab|I}^+, \\ Q_{A|I} Q_{A|Iij} &= Q_{A|Ii}^+ Q_{A|Ij}^- - Q_{A|Ii}^- Q_{A|Ij}^+, \\ Q_{Aa|I} Q_{A|Ii} &= Q_{Aa|Ii}^+ Q_{A|I}^- - Q_{Aa|Ii}^- Q_{A|I}^+. \end{aligned} \tag{12.9}$$

Together with the requirement that $Q_{\emptyset|\emptyset} = 1$, these relations allow to determine all functions from e.g. those with a single index. The set of all Q-functions can be visualized on hypercubic Hasse diagrams, representing the partial order induced by the inclusion of indices.⁸ An example diagram for $\mathfrak{gl}_{2|1}$ is given in figure 12.1.⁹ The three types of functional relations in (12.9) correspond to the three different types of quadrilaterals occurring in the Hasse diagrams, as shown in figure 12.2.

² Gromov, Kazakov, Leurent, Volin, “Quantum Spectral Curve for Planar $\mathcal{N} = 4$ Super-Yang-Mills Theory”, 1305.1939

³ We remark that this derivation ultimately rest on the Asymptotic Bethe Ansatz and hence on the assumption of integrability. Despite a wealth of evidence – a proof that the integrable model discussed here really describes $\mathcal{N} = 4$ SYM and/or the type IIB superstring on $\text{AdS}_5 \times S^5$ remains an outstanding research problem.

⁴ Gromov, Kazakov, Leurent, Volin, “Quantum spectral curve for arbitrary state/operator in $\text{AdS}_5/\text{CFT}_4$ ”, 1405.4857

⁵ Alfimov, Gromov, Kazakov, “QCD Pomeron from AdS/CFT Quantum Spectral Curve”, 1408.2530; Gromov, Levkovich-Maslyuk, “Quark-anti-quark potential in $\mathcal{N} = 4$ SYM”, 1601.05679; and Gromov, Levkovich-Maslyuk, “Quantum Spectral Curve for a cusped Wilson line in $\mathcal{N} = 4$ SYM”, 1510.02098

⁶ The transfer matrices discussed in section 7.2 are prominent examples of such operators.

⁷ Given this notation, we will use indices $A \ni a = 1, \dots, N$ and $I \ni i = 1, \dots, M$.

⁸ Tsuboi, “Solutions of the T-system and Baxter equations for supersymmetric spin chains”, 0906.2039

⁹ The Hasse diagram for $\mathcal{N} = 4$ SYM can be found on the title page of this work.

The Q-system can be used to solve the integrable model, provided that further data on the analytic structure of the Q-functions is known. This data is determined by the representation of the real form $u_{p,q|r+s}$ under which the states transform. For ordinary spin chain models, the Q-functions are either polynomials for compact representations, or rational functions and functions with ladders of poles in the non-compact case. The value of $Q_{\bar{0}|\bar{0}}$ is independent of the state and only determined by the representation at each site of the spin chain. Each state has a characteristic asymptotic behavior, determined by its charges. Bootstrapping the Q-system from this data, one can use readily available formulas to determine the energy and the higher conserved charges of the state.¹⁰

For $\mathcal{N}=4$ SYM at finite coupling, the Q-functions with empty and full index sets are fixed to be (up to normalization),

$$Q_{\emptyset|\emptyset} = Q_{\bar{0}|\bar{0}} = 1, \quad (12.10)$$

but the analytic structure of the remaining Q-functions is more involved compared to simple spin chains. In particular, the functions are multi-valued and depend on the coupling constant g . Their precise structure is determined by the $P\mu$ and $Q\omega$ systems, which we describe next.

$P\mu$ and $Q\omega$ systems

The Quantum Spectral Curve is formulated in terms of $4 + 4$ functions P_a and Q_i and their counterparts with upper indices, which correspond to some of the functions of the Q-system:

$$P_a = Q_{a|\emptyset}, \quad Q_i = Q_{\emptyset|i}, \quad P^a = (-1)^a Q_{\bar{a}|\emptyset}, \quad Q^i = (-1)^i Q_{\emptyset|\bar{i}}. \quad (12.11)$$

Furthermore there are six functions $\mu_{ab} = -\mu_{ba}$ and six functions $\omega_{ij} = -\omega_{ji}$, which are related to the central Q-functions $Q_{ab|ij}$, satisfying

$$\mu_{ab} = \frac{1}{2} Q_{ab|ij}^- \omega^{ij}. \quad (12.12)$$

All of these functions are multi-valued, having branch points of square-root type, but no other singularities. The branch points occur only at the positions $\pm 2g \pm \frac{ni}{2}$ for integer n . For the branch cuts connecting these points there are two convenient choices: the cuts can be “short”, in which case they are placed on the interval $[-2d \pm \frac{in}{2}, +2g \pm \frac{in}{2}]$, or they can be “long”, connecting the branch points to infinity, $[-\infty, -2g \pm \frac{ni}{2}] \cup [2g \pm \frac{ni}{2}, \infty]$.

The structure of cuts of the functions used to define the QSC are shown in figure 12.3. The functions P_a have a single short cut on the real axis of their first Riemann sheet, and their analytic continuation to the second sheet which are denoted by \tilde{P}_a have an infinite ladder of short cuts, as do the functions μ_{ab} . The cut structure of Q_i , \tilde{Q}_i and ω_{ij} is identical, except that all cuts are long. Also note that the functions with upper indices have the same cut structure as those with lower indices. The functions μ_{ab} and ω_{ij} furthermore satisfy the following

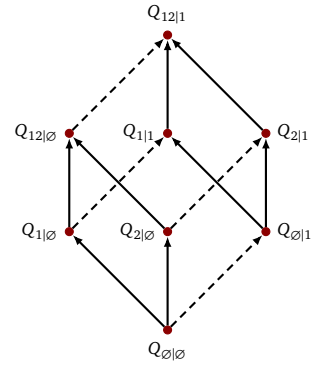


Figure 12.1: Example Hasse diagram for $\mathfrak{gl}_{2|1}$. The inclusion of the fermionic index is represented by a dashed line.

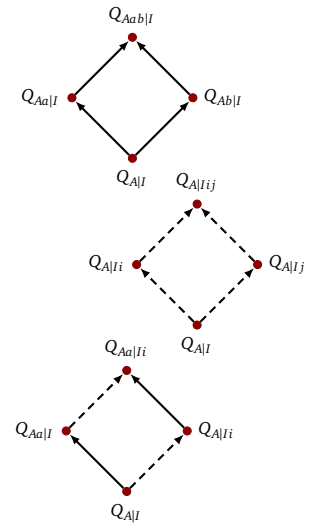
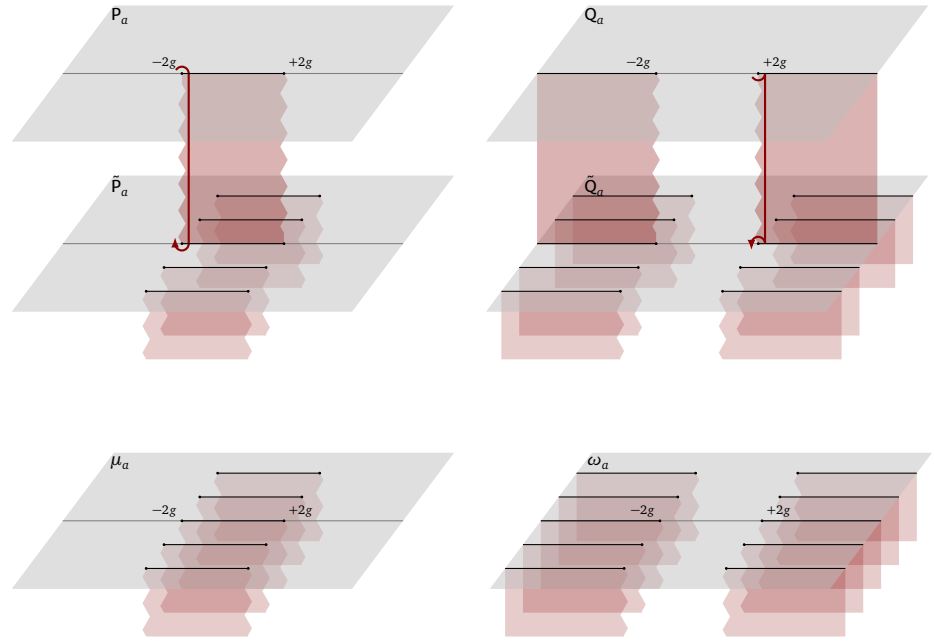


Figure 12.2: The three types of quadrilaterals which can appear in the Hasse diagrams for $\mathfrak{gl}_{N|M}$, corresponding to the QQ-relations given in equation (12.9).

¹⁰ We note that the investigation of Q-systems has recently also led to some new ideas for solving the Bethe equations of the model, see Marboe, Volin, “Fast analytic solver of rational Bethe equations”, 1608.06504 and Marboe, Volin, “The full spectrum of AdS5/CFT4 I: Representation theory and one-loop Q-system”, 1701.03704.

Figure 12.3: The analytic structure of the $P\mu$ and $Q\omega$ systems. The red arrows indicate possible paths for the analytic continuation to the second Riemann sheets.



pseudo-periodicity conditions,

$$\tilde{\mu}_{ab}(u) = \mu_{ab}(u + i), \quad \tilde{\omega}_{ij} = \omega_{ij}(u + i), \quad (12.13)$$

which means that the functions are periodic for the opposite choice of long and short cuts.

The Quantum Spectral Curve can be formulated either in terms of P_a and μ_{ab} or in terms of Q_i and ω_{ij} . These $P\mu$ and $Q\omega$ systems are coupled systems of equations which relate the analytic continuations of the functions on the second Riemann sheet to their values on the defining sheet,

$$\begin{aligned} \tilde{P}_a &= \mu_{ab} P^b, & \tilde{\mu}_{ab} - \mu_{ab} &= P_a \tilde{P}_b - P_b \tilde{P}_a, \\ \tilde{Q}_i &= \omega_{ij} Q^j, & \tilde{\omega}_{ij} - \omega_{ij} &= Q_i \tilde{Q}_j - Q_j \tilde{Q}_i. \end{aligned} \quad (12.14)$$

The functions are further constrained by algebraic relations which follow from the Q-system:

$$\begin{aligned} P_a P^a &= 0, & \text{Pf}(\mu) &= 1, \\ Q_i Q^i &= 0, & \text{Pf}(\omega) &= 1. \end{aligned} \quad (12.15)$$

Here, Pf denotes the Pfaffian.

Finally, to fully specify the system of equations for a particular state, the asymptotic behavior of the P and Q functions has to be imposed,

$$\begin{aligned} P_a &\simeq A_a u^{-\lambda_a - n_a}, & P^a &\simeq A^a u^{\lambda_a - \tilde{n}_a}, \\ Q_i &\simeq B_i u^{-\nu_i - \tilde{n}_i}, & Q^i &\simeq B^i u^{\nu_i - n_i}. \end{aligned} \quad (12.16)$$

Here, the coefficients A and B can be determined from the Q-system, and the power-like asymptotics are determined by the charges λ_a and ν_i of the state, which are defined in (12.8) for the weakly coupled theory.¹¹ We furthermore defined the integer shifts $(n_a) = (n_i) = (1, 0, 1, 0)$ and $(\tilde{n}_a) = (\tilde{n}_i) = (0, 1, 0, 1)$.

¹¹ Note that compared to the oscillator construction, where indices a are fermionic and indices $i = \alpha, \dot{\alpha}$ are bosonic as in equation (12.8), the QSC literature conventionally uses the opposite grading, which is equivalent.

For finite coupling, the charges ν_i receive quantum corrections proportional to the anomalous dimension,

$$\nu_i = \nu_i(g=0) + \frac{\gamma(g)}{2}(1, 1, -1, -1); \quad (12.17)$$

this allows to extract the dimension from solutions of the QSC.

The asymptotic structure shows that the $P\mu$ system is related to the S^5 or R part of the symmetry, while the $Q\omega$ system reflects the isometries of AdS_5 , or the conformal symmetry. It also explains why the P_a have short and the Q_i long cuts: the R symmetry charges λ_a are integers protected from quantum corrections, and therefore the functions P_a have trivial monodromy around infinity, according to equation (12.16); the charges ν_i however correspond to the non-compact part of the symmetry algebra and – being real numbers – induce a non-trivial monodromy around infinity.

The Quantum Spectral Curve equations may very likely be the simplest formulation of the spectral problem, but nevertheless they are far from being trivially solvable. While it is possible to obtain solutions for finite coupling in numerical form,¹² analytic results can be derived by perturbative methods.

The QSC at weak coupling

We conclude this section with some notes on the weak coupling expansion of the Quantum Spectral Curve, in order to make contact with the operatorial description of the Q -system developed in the next chapters. Such perturbative methods were first explored in Marboe and Volin (2015)¹³ and subsequently used to obtain many results at high loop order.¹⁴

To apply an perturbative expansion in the coupling g , the analytic structure at $g=0$ of all functions has to be known. For P_a , P^a and μ_{ab} , as well as their analytic continuations, the short cuts will collapse into poles at weak coupling. The functions with long cuts however do not behave properly in this limit, so their sheets have to be glued together differently first, in such a way that all cuts are short. This can be done by combining the upper half plane of Q_i with the lower half plane of \tilde{Q}_i into a new function \mathcal{Q}_i , and vice versa for $\tilde{\mathcal{Q}}_i$. The functions with upper indices can be treated similarly. For vanishing coupling, all these functions then have poles at $+i\mathbb{N}$ or $-i\mathbb{N}$. On a sheet with short cuts, the functions ω_{ij} become i -periodic, and have poles at $\pm i\mathbb{N}$. The analytic structure of all these functions is shown in figure 12.4.

Although the analytic continuation of the functions cannot be accessed at weak coupling, the $P\mu$ system still provides “gluing conditions” that relate these functions. These conditions can be derived by resolving the branch cuts using the Zhukovsky variable $x = x(u)$ defined by

$$\frac{u}{g} = x + \frac{1}{x}, \quad (12.18)$$

which obeys $\tilde{x} = \frac{1}{x}$. The equations (12.14) then turn into constraints on the coefficients of the Laurent expansions of the respective functions in x at weak

¹² Gromov, Levkovich–Maslyuk, Sizov, “Quantum Spectral Curve and the Numerical Solution of the Spectral Problem in AdS_5/CFT_4 ”, [1504.06640](#)

¹³ Marboe, Volin, “Quantum spectral curve as a tool for a perturbative quantum field theory”, [1411.4758](#)

¹⁴ Marboe, Velizhanin, Volin, “Six-loop anomalous dimension of twist-two operators in planar $\mathcal{N} = 4$ SYM theory”, [1412.4762](#); and Marboe, Velizhanin, “Twist-2 at seven loops in planar $\mathcal{N} = 4$ SYM theory: full result and analytic properties”, [1607.06047](#)

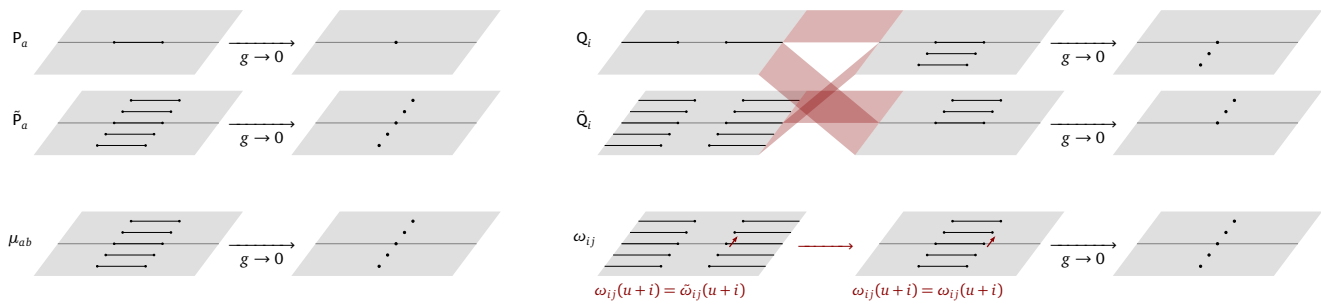


Figure 12.4: The analytic structure of the Quantum Spectral Curve at weak coupling.

coupling. Using further constraints from the other properties of the Quantum Spectral Curve, this allows to completely fix Ansätze for the functions P_a and for \tilde{P}_a in a small neighborhood around the origin. Importantly, the one-loop Q-functions provide the input data for this iterative procedure.

12.3 Q-operators

The Q-functions discussed above are known to be the eigenvalues of Q-operators. These operators belong to the commuting family of transfer matrices of the integrable model, and satisfy the same functional relations as their eigenvalues. They were introduced in Baxter’s seminal work on the eight vertex model¹⁵ and applied to two-dimensional field theories with quantum group symmetry.¹⁶

Surprisingly, for the simplest integrable model, the spin $\frac{1}{2}$ Heisenberg magnet solved by Hans Bethe in 1931,¹⁷ Q-operators were constructed only recently.¹⁸ We give a very brief overview of the Q-operators of this model, to motivate the oscillator construction for more general cases in the following. The Heisenberg model has ℓ spin $\frac{1}{2}$ particles at the sites of a periodic chain, which couple only via nearest-neighbor exchange interactions. The Hamiltonian of this model is therefore given by

$$H = -2 \sum_{i=1}^{\ell} \left(\mathbf{s}_i \cdot \mathbf{s}_{i+1} - \frac{1}{4} \right) = \sum_{i=1}^{\ell} (\mathbb{1} - \mathbb{P}_{i,i+1}), \quad \ell + 1 \sim 1. \quad (12.19)$$

Here the spin operators can be expressed using the Pauli matrices, $\mathbf{S}^a = \frac{\sigma^a}{2}$, and \mathbb{P}_{ij} is the operator which permutes the spins at site i and site j .

The oscillator construction for the Q-operators of this model is based on the following Lax matrices, indexed by subsets $I \subset \{1, 2\}$:¹⁹

$$L_{\emptyset}(z) = \begin{pmatrix} 1 & 0 \\ 0 & 1 \end{pmatrix}, \quad L_{\{1\}}(z) = \begin{pmatrix} z - \bar{\xi}\xi - \frac{1}{2} & \bar{\xi} \\ -\xi & 1 \end{pmatrix}, \quad (12.20)$$

$$L_{\{2\}}(z) = \begin{pmatrix} z & 0 \\ 0 & z \end{pmatrix}, \quad L_{\overline{\{2\}}}(z) = \begin{pmatrix} 1 & \bar{\xi} \\ \xi & z + \bar{\xi}\xi + \frac{1}{2} \end{pmatrix}.$$

The Lax-matrices are degenerate solutions of the Yang-Baxter equation, and form representations of the Yangian where the lowest level is not proportional to the

15 Baxter, “Partition function of the eight vertex lattice model”, *Annals Phys.* 70 (1972) 193–228, [*Annals Phys.*281,187(2000)]

16 Bazhanov, Lukyanov, Zamolodchikov, “Integrable structure of conformal field theory. 2. Q operator and DDV equation”, [hep-th/9604044](#); Bazhanov, Lukyanov, Zamolodchikov, “Integrable structure of conformal field theory. 3. The Yang-Baxter relation”, [hep-th/9805008](#); Bazhanov, Hibberd, Khoroshkin, “Integrable structure of $W(3)$ conformal field theory, quantum Bousinesq theory and boundary affine Toda theory”, [hep-th/0105177](#); Bazhanov, Tsuboi, “Baxter’s Q-operators for supersymmetric spin chains”, [0805.4274](#); and Kojima, “Baxter’s Q-operator for the W -algebra WN ”, [0803.3505](#)

17 Bethe, “Zur Theorie der Metalle”, *Zeitschrift für Physik* 71 (1931), no. 3, 205–226

18 Bazhanov, Łukowski, Meneghelli, Staudacher, “A Shortcut to the Q-Operator”, [1005.3261](#)

19 This indexing by subsets is commonly used in the Q-operator literature, and is equivalent to using the multi-indices as used in section 12.2 above, see also section 13.2 below.

identity, cf. equation (7.19). The operators ξ and $\bar{\xi}$ obey the standard oscillator algebra $[\xi, \bar{\xi}] = 1$, and the corresponding Fock space constitutes the auxiliary space of the L_I .²⁰ The Q-operators of the model can be defined as normalized and twisted traces over this space of monodromies built from products of ℓ Lax-matrices,

$$\mathbf{Q}_I(z) = e^{i \sum_{a \in I} \phi_a z} \widehat{\text{tr}} \left(L_I(z)^{[1]} \otimes \cdots \otimes L_I^{[\ell]}(z) \right), \quad (12.21)$$

for $I = \emptyset, \{1\}, \{2\}, \{1, 2\}$. We defer a discussion of the subtleties involved when taking these traces to section 13.2, where a more general case will be explained. Both the trace as well as the normalization factor involve the twist angles $\phi_1 = -\phi_2$, which can be understood as a magnetic flux. This flux breaks the \mathfrak{su}_2 invariance of the model without spoiling integrability. This is necessary for the convergence of the trace, but also prevents diverging Q-functions for descendant states.²¹ The four Q-operators satisfy a relation, which can easily be seen to be a special case of (12.9),

$$2i \sin \left(\frac{\phi_1 - \phi_2}{2} \right) \mathbf{Q}_{\emptyset}(z) \mathbf{Q}_{\emptyset}(z) = \mathbf{Q}_{\{1\}} \left(z + \frac{1}{2} \right) \mathbf{Q}_{\{2\}} \left(z - \frac{1}{2} \right) - \mathbf{Q}_{\{1\}} \left(z - \frac{1}{2} \right) \mathbf{Q}_{\{2\}} \left(z + \frac{1}{2} \right). \quad (12.22)$$

The prefactor arises from the specific normalization used in (12.21) and will be discussed in more generality in section 13.2.

The oscillator construction for Q-operators has been generalized subsequently to many other models, which are invariant under higher rank or super algebras, and transform in other representations, or have open boundary conditions.²² It was furthermore shown, at least for the Heisenberg spin chain, that the eigenfunctions of the Q-operators indeed give the polynomials appearing in the Bethe Ansatz.²³ For all these models, the Q-operators are in a sense the most fundamental operators among the family of commuting transfer matrices, and they allow to calculate both the Hamiltonian as well as the higher conserved charges in operatorial form without referring to any other transfer matrices.²⁴

We note that there are other approaches for the construction of Q-operators, see for example Belitsky et al. (2007); Derkachov and Manashov (2006, 2011, 2009); Kazakov et al. (2012).²⁵

The discussion here is only meant as a brief introduction; we will revisit most of the ideas discussed here in the next chapters, where we investigate the Q-operators for supersymmetric non-compact spin chains, in particular those of $\mathcal{N}=4$ SYM.

20 Note that in contrast to what is usually done for the standard Lax operator, (12.20) shows the matrix structure of the Lax operators in the *physical* space; it is in this sense, with the physical and auxiliary spaces swapped, that these Lax operators form a representation of the Yangian.

21 In the context of the QSC, twists have been described in some detail in Kazakov, Leurent, Volin, “T-system on T-hook: Grassmannian Solution and Twisted Quantum Spectral Curve”, 1510.02100.

22 Bazhanov, Frassek, Łukowski, Meneghelli, Staudacher, “Baxter Q-Operators and Representations of Yangians”, 1010.3699; Frassek, Łukowski, Meneghelli, Staudacher, “Oscillator Construction of $\mathfrak{su}(n|m)$ Q-Operators”, 1012.6021; Frassek, Łukowski, Meneghelli, Staudacher, “Baxter Operators and Hamiltonians for ‘nearly all’ Integrable Closed $\mathfrak{gl}(n)$ Spin Chains”, 1112.3600; and Frassek, Szecsenyi, “Q-operators for the open Heisenberg spin chain”, 1509.04867

23 Frassek, “Algebraic Bethe ansatz for Q-operators: The Heisenberg spin chain”, 1504.04501

24 Frassek, Meneghelli, “From Baxter Q-Operators to Local Charges”, 1207.4513

25 Belitsky, Derkachov, Korchemsky, Manashov, “Baxter Q-operator for graded $\text{SL}(2|1)$ spin chain”, hep-th/0610332; Derkachov, Manashov, “R-matrix and baxter Q-operators for the noncompact $\text{SL}(N, C)$ invariant spin chain”, nlin/0612003; Derkachov, Manashov, “Noncompact $\mathfrak{sl}(N)$ spin chains: BGG-resolution, Q-operators and alternating sum representation for finite dimensional transfer matrices”, 1008.4734; Derkachov, Manashov, “Factorization of R-matrix and Baxter Q-operators for generic $\mathfrak{sl}(N)$ spin chains”, 0809.2050; and Kazakov, Leurent, Tsuboi, “Baxter’s Q-operators and operatorial Backlund flow for quantum (super)-spin chains”, 1010.4022

Q-operators for non-compact super spin chains

We have seen that the integrable model behind $\mathcal{N} = 4$ SYM can be described by a Q-system at finite coupling, and that at least for spin chain models, such Q-systems exist in operatorial form. Although there are many works on a variety of cases, the Q-operators of non-compact supersymmetric spin chains have not been investigated in detail. In this chapter we describe these operators for non-compact representations of Jordan-Schwinger type, the prime example of which is $\mathcal{N} = 4$ SYM at weak coupling, as discussed in section 12.1. We first give a derivation of the relevant Lax operators in section 13.1, starting from a Yang-Baxter equation they solve.¹ These Lax operators allow to define Q-operators satisfying the functional relations of the Q-system, which we describe in section 13.2. All these constructions only depend on the symmetry algebra of the model, and make no reference to the representation in the quantum space. In section 13.3 we show how to specialize to the infinite-dimensional unitary representations of the non-compact algebras $u_{p,q|r+s}$ of oscillator type. Concretely evaluating the Q-operators for these representations is difficult, since the matrix elements involve many infinite sums over the state spaces of the representation. To showcase these difficulties and to motivate the methods we will develop in the next chapter, we consider spin $-s$ Heisenberg spin chains in section 13.4. Finally, many of the properties of such non-compact Q-systems, such as the analytic structure of the operators in terms of the spectral parameter, can be understood on general grounds; we provide an overview in section 13.5.

This chapter is based on the author's publication Frassek, Marboe, Meidinger, "Evaluation of the operatorial Q-system for non-compact super spin chains", 1706.02320.

¹ A more general case of these Lax operators can be found in Frassek, "Q-operators, Yangian invariance and the quantum inverse scattering method", PhD thesis, Humboldt University Berlin, 2014, 1412.3339, which follows from an unpublished derivation by R. Frassek, T. Łukowski, C. Meneghelli and M. Staudacher.

13.1 Lax operators for the Q-system from Yang-Baxter equations

In this section we derive the Lax operators which allow to construct the Q-operators of $\mathfrak{gl}_{N|M}$ spin chains with representations realized via Schwinger oscillators as traces of monodromy matrices, similar to the example considered in section 12.3. The derivation closely follows the bosonic case in Frassek et al. (2013)² but incorporates the supersymmetric Lax matrices derived in Frassek et al. (2011).³ The more general derivation of the Lax operators for generalized rectangular representations is unpublished,⁴ but expressions for the resulting operators can be found in Frassek (2014).⁵ We will see however that the Lax operators take a particularly simple form for the type of representations we consider.

The basis of the derivation is a Yang-Baxter equation involving three representations: the oscillator representation that will constitute the physical space of the spin chain model $\mathcal{V}_{\text{phys}}$, the fundamental representation \mathcal{V}_{\square} , and a Fock space of auxiliary oscillators \mathcal{V}_{osc} , similar to the example of the Heisenberg spin chain discussed in section 12.3. The operators we want to define intertwine $\mathcal{V}_{\text{phys}}$ and \mathcal{V}_{osc} , and we therefore need the Lax operators which intertwine the other pairs of representations, in order to solve the Yang-Baxter equation for the operators of interest.

The Lax operators intertwining arbitrary representations of $\mathfrak{gl}_{N|M}$ with \mathcal{V}_{\square} , which already played a key role in Part II of this thesis, see (7.13), were introduced by Kulish (1986)⁶ and are given by

$$\mathcal{L}(z) = z + \sum_{a,b=1}^{N+M} (-1)^{|b|} e_{ab} E_{ba}. \quad (13.1)$$

Here the indices take the values $a, b = 1, \dots, N+M$ while $|a|$ denotes the grading $|\text{fermion}| = 1$ and $|\text{boson}| = 0$. The $\mathfrak{gl}_{N|M}$ generators E_{ab} satisfy the commutation relations

$$[E_{ab}, E_{cd}] = \delta_{bc} E_{ad} - (-1)^{(|a|+|b|)(|c|+|d|)} \delta_{da} E_{cb}, \quad (13.2)$$

where we defined the graded commutator as $[X, Y] = XY - (-1)^{|X||Y|} YX$. The generators e_{ab} in (13.1) denote the defining fundamental generators of $\mathfrak{gl}_{N|M}$ satisfying $e_{ab} e_{cd} = \delta_{bc} e_{ad}$. In the following we restrict to realizations in terms of Schwinger oscillators, acting on $\mathcal{V}_{\text{phys}}$

$$E_{ab} = \bar{\chi}_a \chi_b, \quad (13.3)$$

where $[\chi_a, \bar{\chi}_b] = \delta_{ab}$. Note that these Lax operators are the same as those considered in chapter 7, defining the Yangian of $\mathfrak{gl}_{N|M}$.

Q-operators with the defining representation of $\mathfrak{gl}_{N|M}$ at each site (the so-called quantum space) are based on another set of Lax operators intertwining \mathcal{V}_{osc} and \mathcal{V}_{\square} , which were derived in Frassek et al. (2011), and are given by

$$L_I(z) = \begin{pmatrix} (z - s_I) \delta_{ab} - (-1)^{|b|} \bar{\xi}_{a\bar{a}} \xi_{\bar{a}b} & \bar{\xi}_{\bar{a}b} \\ -(-1)^{|b|} \xi_{\bar{a}b} & \delta_{\bar{a}\bar{b}} \end{pmatrix}. \quad (13.4)$$

² Frassek, Łukowski, Meneghelli, Staudacher, “Baxter Operators and Hamiltonians for ‘nearly all’ Integrable Closed $\mathfrak{gl}(n)$ Spin Chains”, [1112.3600](#)

³ Frassek, Łukowski, Meneghelli, Staudacher, “Oscillator Construction of $\mathfrak{su}(n|m)$ Q-Operators”, [1012.6021](#)

⁴ Frassek, Łukowski, Meneghelli, Staudacher, “unpublished”

⁵ Frassek, “Q-operators, Yangian invariance and the quantum inverse scattering method”, PhD thesis, Humboldt University Berlin, 2014, [1412.3339](#)

⁶ Kulish, “Integrable graded magnets”, *J. Sov. Math.* 35 (1986) 2648–2662, [Zap. Nauchn. Semin.145,140(1985)]

Here we sum over repeated indices. There are 2^{N+M} such Lax operators labeled by the subset $I \subseteq \{1, \dots, N+M\}$. The indices without a bar take values $a, b \in I$ while the barred ones take values in its complement, $\bar{a}, \bar{b} \in \bar{I}$. The $(N|M) \times (N|M)$ matrix in (13.4) is written in terms of the sub-blocks under this decomposition.⁷ The shift s_I in the spectral parameter z is introduced for convenience and reads

$$s_I = \frac{\sum_{\bar{a} \in \bar{I}} (-1)^{|\bar{a}|}}{2}. \quad (13.5)$$

The oscillators $(\xi_{\bar{a}a}, \bar{\xi}_{a\bar{a}})$ satisfy the graded Heisenberg algebra

$$[\xi_{\bar{a}a}, \bar{\xi}_{b\bar{b}}] = \xi_{\bar{a}a} \bar{\xi}_{b\bar{b}} - (-1)^{(|a|+|\bar{a}|)(|b|+|\bar{b}|)} \bar{\xi}_{b\bar{b}} \xi_{\bar{a}a} = \delta_{ab} \delta_{\bar{a}\bar{b}}. \quad (13.6)$$

We can now write down the defining Yang-Baxter equation for the Lax operators \mathcal{R}_I which are the building blocks for Q-operators when the sites of the quantum space are in the representation space \mathcal{V}_{sh} . As in the bosonic case⁸ this relation is given by

$$\mathcal{L}(x-y) L_I(x) \mathcal{R}_I(y) = \mathcal{R}_I(y) L_I(x) \mathcal{L}(x-y). \quad (13.7)$$

The \mathcal{R} -operators were obtained by R. Frassek, T. Łukowski, C. Meneghelli and M. Staudacher, and can be found in Frassek (2014).⁹ The derivation follows Meneghelli (2011); Frassek et al. (2013)¹⁰ and, as we will discuss in the following, simplifies significantly in the case which we are interested in. As for \mathfrak{gl}_N one takes a factorized Ansatz,

$$\mathcal{R}_I(z) = e^{(-1)^{|c|+|c|} \bar{\xi}_{c\bar{c}} E_{c\bar{c}}} \mathcal{R}_0^I(z) e^{(-1)^{|d|+|\bar{d}|+|d|} \xi_{\bar{d}d} E_{\bar{d}d}}. \quad (13.8)$$

This turns the Yang-Baxter equation (13.7) into a difference equation for the middle part $\mathcal{R}_0^I(z)$. The solution to the difference equation simplifies significantly for the choice of generators (13.3). Specifically, one finds that $\mathcal{R}_0^I(z)$ can be written in terms of a single Gamma function which only depends on a subset of the quantum space oscillators

$$\mathcal{R}_0^I(z) = \rho_I(z) \Gamma(z+1-s_I - \bar{\mathcal{X}}_{\bar{a}} \mathcal{X}_{\bar{a}}). \quad (13.9)$$

Here ρ_I denotes a normalization not fixed by the Yang-Baxter equation (13.7). As we will see a good choice for it is given by

$$\rho_I(z) = \frac{1}{\Gamma(z+1-s_I - \mathbf{c})}, \quad (13.10)$$

which depends on the central charge \mathbf{c} that can be expressed in terms of the number operators $\mathbf{N}_a = \bar{\mathcal{X}}_a \mathcal{X}_a$ as

$$\mathbf{c} = \sum_{a=1}^{N+M} \mathbf{N}_a. \quad (13.11)$$

We conclude that

$$\mathcal{R}_I(z) = e^{(-1)^{|c|+|c|} \bar{\xi}_{c\bar{c}} \bar{\mathcal{X}}_c \mathcal{X}_c} \frac{\Gamma(z+1-s_I - \bar{\mathcal{X}}_{\bar{a}} \mathcal{X}_{\bar{a}})}{\Gamma(z+1-s_I - \mathbf{c})} e^{(-1)^{|d|+|\bar{d}|+|d|} \xi_{\bar{d}d} \bar{\mathcal{X}}_{\bar{a}} \mathcal{X}_d} \quad (13.12)$$

solves the Yang-Baxter equation in (13.7). The normalization (13.10) ensures that for the empty set $\mathcal{R}_{\emptyset}(z) = 1$, and renders $\mathcal{R}_I(z)$ a polynomial in z for compact representations. As we will see now, these properties are inherited by the Q-operators.

⁷ We remark that quantities labeled by the set I depend on the partition $I \cup \bar{I} = \{1, \dots, N+M\}$. We leave the dependence on this “full set” implicit.

⁸ Frassek, Łukowski, Meneghelli, Staudacher, “Baxter Operators and Hamiltonians for ‘nearly all’ Integrable Closed $\mathfrak{gl}(n)$ Spin Chains”, [1112.3600](#)

⁹ Frassek, “Q-operators, Yangian invariance and the quantum inverse scattering method”, PhD thesis, Humboldt University Berlin, 2014, [1412.3339](#)

¹⁰ Meneghelli, “Superconformal Gauge Theory, Yangian Symmetry and Baxter’s Q-Operator”, PhD thesis, Humboldt University Berlin, 2011; and Frassek, Łukowski, Meneghelli, Staudacher, “Baxter Operators and Hamiltonians for ‘nearly all’ Integrable Closed $\mathfrak{gl}(n)$ Spin Chains”, [1112.3600](#)

13.2 Monodromy construction of Q-operators

We can now construct Q-operators as traces over monodromy matrices which are products of the \mathcal{R} -operators. For $\mathfrak{gl}_{N|M}$ invariant spin chains in the fundamental representation, these Q-operators were introduced in Frassek et al. (2011),¹¹ using the Lax operators $L_I(z)$ defined in (13.4). We are interested in more general representations of oscillators type, cf. (13.3). However, the construction of the Q-operators and the functional relations among them are independent of the representation in the quantum space.¹² We therefore define the operators as

$$\mathbf{Q}_I(z) = e^{iz \sum_{a \in I} (-1)^{|a|} \phi_a} \widehat{\text{str}} \mathcal{M}_I(z). \quad (13.13)$$

Here the monodromy \mathcal{M}_I is built from the tensor product of the \mathcal{R} -operators in (13.12) in the space of oscillators $(\chi, \bar{\chi})$ and multiplication in the auxiliary space of oscillators $(\xi, \bar{\xi})$ as

$$\mathcal{M}_I(z) = \mathcal{R}_I^{[1]}(z) \otimes \mathcal{R}_I^{[2]}(z) \otimes \dots \otimes \mathcal{R}_I^{[L]}(z). \quad (13.14)$$

The normalized supertrace $\widehat{\text{str}}$ is defined by

$$\widehat{\text{str}} X = \frac{\text{str} e^{-i \sum_{a,b} (\phi_a - \phi_b) N_{ab}} X}{\text{str} e^{-i \sum_{a,b} (\phi_a - \phi_b) N_{ab}}}, \quad (13.15)$$

where str denote the ordinary supertrace over the auxiliary Fock space spanned by the states generated by the operators $\bar{\xi}_{a\bar{a}}$ acting on the Fock vacuum which satisfies $\bar{\xi}_{a\bar{a}} |0\rangle = 0$. These states are labeled by the values of the number operators

$$N_{ab} = \bar{\xi}_{ab} \xi_{ba}, \quad (13.16)$$

where no summation over the indices a and b is implied. The twist parameters ϕ_a can be interpreted as Aharonov-Bohm phases and break the $\mathfrak{gl}_{N|M}$ invariance down to its diagonal subalgebra. They are required for the convergence of the supertraces, and by breaking the symmetry, they prevent diverging Q-functions for descendant states. Note that a regularization procedure is needed to make some of the traces converge, even in the presence of twists; one can use an $i\epsilon$ prescription for the twist phases, such that $\text{Re}(\exp(-i \sum_{a,b} (\phi_a - \phi_b))) < 1$, see Bazhanov et al. (2011).¹³

As a consequence of the Yang-Baxter equation (13.7), the Q-operators defined in (13.13) commute with the transfer matrix built from the Lax operators \mathcal{L} realized via (13.3), and with each other, $[\mathbf{Q}_I(z), \mathbf{Q}_I(z')] = 0$. Depending on the grading the Q-operators satisfy either the bosonic QQ-relations

$$\Delta_{ab} \mathbf{Q}_{I \cup \{a,b\}} \mathbf{Q}_I = \mathbf{Q}_{I \cup \{a\}}^+ \mathbf{Q}_{I \cup \{b\}}^- - \mathbf{Q}_{I \cup \{a\}}^- \mathbf{Q}_{I \cup \{b\}}^+, \quad (13.17)$$

if $|a| = |b| = 0$ or $|a| = |b| = 1$ or the fermionic QQ-relations

$$\Delta_{ab} \mathbf{Q}_{I \cup \{a\}} \mathbf{Q}_{I \cup \{b\}} = \mathbf{Q}_{I \cup \{a,b\}}^+ \mathbf{Q}_I^- - \mathbf{Q}_{I \cup \{a,b\}}^- \mathbf{Q}_I^+, \quad (13.18)$$

¹¹ Frassek, Łukowski, Meneghelli, Staudacher, "Oscillator Construction of $\mathfrak{su}(n|m)$ Q-Operators", [1012.6021](#)

¹² Frassek, Łukowski, Meneghelli, Staudacher, "Baxter Operators and Hamiltonians for 'nearly all' Integrable Closed $\mathfrak{gl}(n)$ Spin Chains", [1112.3600](#)

¹³ Bazhanov, Frassek, Łukowski, Meneghelli, Staudacher, "Baxter Q-Operators and Representations of Yangians", [1010.3699](#)

whenever $|a| \neq |b|$. Here we used the notation $\mathbf{Q}^\pm = \mathbf{Q}(z \pm \frac{1}{2})$ and defined the trigonometric prefactor

$$\Delta_{ab} = (-1)^{|a|} 2i \sin\left(\frac{\phi_a - \phi_b}{2}\right). \quad (13.19)$$

The set of all Q-operators can be visualized on a hypercubic Hasse diagram, as discussed in section 12.2. The relations (13.17) and (13.18) then constrain the operators on each quadrilateral of this diagram.

It is straightforward to compute the Q-operators for the empty set $I = \emptyset$ and the full set $I = \{1, \dots, N+M\} = \overline{\emptyset}$. Explicitly, using the normalization in (13.10), one finds

$$\mathbf{Q}_{\emptyset}(z) = 1, \quad \mathbf{Q}_{\overline{\emptyset}}(z) = \left(\frac{\Gamma(z+1)}{\Gamma(z+1-\mathbf{c})}\right)^L, \quad (13.20)$$

where we imposed the constraint

$$\sum_{a=1}^{N+M} (-1)^{|a|} \phi_a = 0. \quad (13.21)$$

This relation is needed for $\mathbf{Q}_{\overline{\emptyset}}$ to be a rational function of the spectral parameter. Note that in the case of $\mathfrak{gl}_{N|M}$, one has the additional constraint $\sum_{a=1}^{2N} \phi_a = 0$.

Aside: different normalizations

Before we continue our investigation of operatorial Q-systems, we briefly want to discuss different conventions for the functional relations of Q-operators and twisted Q-functions which have been used in the literature, with the aim of facilitating comparisons between the oscillator construction of Q-operators and the literature on the Quantum Spectral Curve. These forms of the functional relations follow from different choices for the normalization of the Q-operators. To make the notation more compact, the twists will be parametrized by $\tau_a = e^{-i\phi_a}$.

In this work, we use the normalization that is typically employed in the literature on the oscillator construction of Q-operators. The operators are defined as in (13.13), and the normalization can be written as $\prod_{a \in I} \tau_a^{-(-1)^{|a|} z}$. The functional equations were just given in (13.17) and (13.18), with $\Delta_{ab} = (-1)^{|a|} \frac{\tau_b - \tau_a}{\sqrt{\tau_a \tau_b}}$ in terms of the variables τ_a . Note that this normalization is compatible with indexing the operators by sets (which is natural for the oscillator construction), since it does not impose an ordering of the $\mathfrak{gl}_{N|M}$ indices. Other possible choices induce such an ordering. This can be reflected by indexing the Q-operators with antisymmetric multi-indices, as we did in section 12.2; here we will instead label the Q-operators with sets, and keep track of the ordering in the functional relations.

One possibility, described for example in Kazakov et al. (2016)¹⁴ on the eigenvalue level, uses Q-operators without exponential scaling factors:

$$\mathbf{Q}_I(z) = \prod_{\substack{a, b \in I \\ a < b}} (\tau_a - \tau_b)^{(-1)^{|a|+|b|}} \widehat{\text{str}} \mathcal{M}_I(z), \quad (13.22)$$

¹⁴ Kazakov, Leurent, Volin, “T-system on T-hook: Grassmannian Solution and Twisted Quantum Spectral Curve”, 1510.02100

which gives functional relations

$$\begin{aligned} \mathbf{Q}_{I \cup \{a,b\}} \mathbf{Q}_I &= \tau \mathbf{Q}_{I \cup \{a\}}^+ \mathbf{Q}_{I \cup \{b\}}^- - \tilde{\tau} \mathbf{Q}_{I \cup \{a\}}^- \mathbf{Q}_{I \cup \{b\}}^+ & |a| = |b| \\ \mathbf{Q}_{I \cup \{a\}} \mathbf{Q}_{I \cup \{b\}} &= \tau \mathbf{Q}_{I \cup \{a,b\}}^+ \mathbf{Q}_I^- - \tilde{\tau} \mathbf{Q}_{I \cup \{a,b\}}^- \mathbf{Q}_I^- & |a| \neq |b| \end{aligned} \quad (13.23)$$

where $\tau = \tau_a$ and $\tilde{\tau} = \tau_b$ if $a < b$ or $\tau = \tau_b$ and $\tilde{\tau} = \tau_a$ if $b < a$.

Another relevant normalization is given by

$$\mathbf{Q}_I(z) = \prod_{a \in I} \tau_a^{(-1)^{|a|}(z+s_I)} \prod_{\substack{a,b \in I \\ a < b}} (\tau_a - \tau_b)^{(-1)^{|a|+|b|}} \widehat{\text{str}} \mathcal{M}_I(z). \quad (13.24)$$

Here the shift s_I is defined in (13.5). The functional relations for these operators are identical to those of untwisted Q-functions:

$$\begin{aligned} \mathbf{Q}_{I \cup \{a,b\}} \mathbf{Q}_I &= \mathbf{Q}_{I \cup \{a\}}^+ \mathbf{Q}_{I \cup \{b\}}^- - \mathbf{Q}_{I \cup \{a\}}^- \mathbf{Q}_{I \cup \{b\}}^+ & |a| = |b| \\ \mathbf{Q}_{I \cup \{a\}} \mathbf{Q}_{I \cup \{b\}} &= \mathbf{Q}_{I \cup \{a,b\}}^+ \mathbf{Q}_I^- - \mathbf{Q}_{I \cup \{a,b\}}^- \mathbf{Q}_I^- & |a| \neq |b| \end{aligned} \quad (13.25)$$

In the first equation, we have to assume that $a < b$ if $|a| = |b| = 0$, or $b < a$ if $|a| = |b| = 1$; otherwise, the left hand side changes its sign.

13.3 Non-compact representations

So far we did not specify a representation in the quantum space. Most of our derivations will be independent of the concrete representation, but calculations of explicit matrix elements of course require a concrete knowledge of the representation space. Here we show how to apply our construction to unitary representations of $u_{p,q|r+s}$ of oscillator type which were first investigated in Bars and Günaydin (1983).¹⁵ To specialize to a real form of the algebra, we have to indicate, in addition to the grading $|a| = 0, 1$, which directions have opposite sign under conjugation. This can be realized via a particle-hole transformation. We indicate these using the variables

$$\omega_a = \begin{cases} +1 & \text{if oscillator } a \text{ is not transformed} \\ -1 & \text{if oscillator } a \text{ is transformed} \end{cases}. \quad (13.26)$$

Then the generators $E_{ab} = \bar{\chi}_a \chi_b$ can be realized by the oscillators

$$(\chi_a, \bar{\chi}_a) = \begin{cases} (\mathbf{a}_a, \bar{\mathbf{a}}_a) & \text{for } |a| = 0 \text{ and } \omega_a = +1 \\ (\bar{\mathbf{b}}_a, -\mathbf{b}_a) & \text{for } |a| = 0 \text{ and } \omega_a = -1 \\ (\mathbf{c}_a, \bar{\mathbf{c}}_a) & \text{for } |a| = 1 \text{ and } \omega_a = +1 \\ (\bar{\mathbf{d}}_a, \mathbf{d}_a) & \text{for } |a| = 1 \text{ and } \omega_a = -1 \end{cases}. \quad (13.27)$$

These oscillators act on a Fock space with a vacuum state satisfying $\mathbf{a}_a |0\rangle = \bar{\mathbf{b}}_a |0\rangle = \mathbf{c}_a |0\rangle = \bar{\mathbf{d}}_a |0\rangle = 0$, such that an orthonormal basis is given by

$$|\mathbf{m}\rangle = |m_1, \dots, m_K\rangle = \frac{\left\{ \begin{smallmatrix} \bar{\mathbf{a}}_1 \\ \bar{\mathbf{b}}_1 \\ \bar{\mathbf{c}}_1 \\ \bar{\mathbf{d}}_1 \end{smallmatrix} \right\}^{m_1}}{\sqrt{m_1!}} \cdots \frac{\left\{ \begin{smallmatrix} \bar{\mathbf{a}}_K \\ \bar{\mathbf{b}}_K \\ \bar{\mathbf{c}}_K \\ \bar{\mathbf{d}}_K \end{smallmatrix} \right\}^{m_K}}{\sqrt{m_K!}} |0, \dots, 0\rangle, \quad (13.28)$$

¹⁵ Bars, Günaydin, "Unitary Representations of Noncompact Supergroups", *Commun. Math. Phys.* 91 (1983) 31

with $K = N + M = p + q + r + s$. Since the oscillators obey the standard conjugation $\mathbf{a}^\dagger = \bar{\mathbf{a}}$, $\mathbf{b}^\dagger = \bar{\mathbf{b}}$, $\mathbf{c}^\dagger = \bar{\mathbf{c}}$ and $\mathbf{d}^\dagger = \bar{\mathbf{d}}$, the generators are those of $u_{p,q|r+s}$, satisfying

$$E_{ab}^\dagger = \omega_a^{1+|a|} \omega_b^{1+|b|} E_{ba}. \quad (13.29)$$

Finally, the Fock space contains a series of representations labeled by the central charge $\mathbf{c} = \sum_a \mathbf{N}_a$ where the number operators have to be expressed in terms of oscillators \mathbf{a} , \mathbf{b} , \mathbf{c} and \mathbf{d} via (13.27). These representations are of highest- or lowest-weight type depending on the order of the different types of oscillators. The representation introduced in section 12.1 for the composite operators of $\mathcal{N} = 4$ SYM is precisely of this type, and we will specialize our construction in chapter 15.

13.4 Case study: spin $-s$ Heisenberg models

In the next chapter, we will show how the Q-operators we just defined can be evaluated, i.e. how their matrix elements can be calculated. For compact representations this is in principle straightforward, but quickly becomes complicated due to a combinatorial explosion of the number of terms in the \mathcal{R} -operators's matrix elements. For non-compact representations it is not at all obvious how to do this, since the matrix elements in general involve many infinite sums. To give the reader a preliminary idea of how such calculations can be done, we discuss the spin $-s$ Heisenberg models, include for example the spin -1 model appearing in QCD in the Regge limit.¹⁶ These models constitute the simplest non-trivial case which can be treated by the more general method presented in the next chapter.

¹⁶ References regarding this model can be found in section 11.3, where it appeared in relation to Grassmannian integrals.

While the formula for the Lax operators (13.12) is extremely compact, it is rather inconvenient for practical purposes where the matrix elements of the Lax operators and Q-operators are of interest. In particular, for non-compact representations we encounter infinite sums. To understand this problem we consider the \mathcal{R} -operators (13.12) which for the case of \mathfrak{gl}_2 are given by

$$\mathcal{R}_{\{a\}}(z) = e^{\bar{\xi}_{a\bar{a}} E_{a\bar{a}}} \frac{\Gamma(z + \frac{1}{2} - E_{\bar{a}\bar{a}})}{\Gamma(z + \frac{1}{2} - \mathbf{c})} e^{-\xi_{\bar{a}a} E_{\bar{a}a}}, \quad (13.30)$$

where $I \subseteq \{1, 2\}$. For infinite-dimensional representations the Lax operator contains two infinite sums emerging from the exponential functions. Using the algebraic relations in (13.2) we note that the Lax operators can be rewritten as

$$\mathcal{R}_{\{a\}}(z) = \sum_{n=-\infty}^{+\infty} (\bar{\xi}_{a\bar{a}} E_{a\bar{a}})^{\Theta(+n)|n|} \mathbb{M}_{\{a\}}(z) (-\xi_{\bar{a}a} E_{\bar{a}a})^{\Theta(-n)|n|}, \quad (13.31)$$

with $\Theta(-m) = \Theta(0) = 0$ and $\Theta(m) = 1$ for $m \in \mathbb{N}_+$. The middle part is given by an infinite sum and only depends on the Cartan elements

$$\mathbb{M}_{\{a\}}(z) = \frac{1}{|n|!} \frac{\Gamma(z + \frac{1}{2} - E_{\bar{a}\bar{a}})}{\Gamma(z + \frac{1}{2} - \mathbf{c})} {}_3F_2(E_{\bar{a}\bar{a}} - \lambda_1, E_{\bar{a}\bar{a}} - \lambda_2 + 1, -\mathbf{N}_{a\bar{a}}; 1 + |n|, E_{\bar{a}\bar{a}} + \frac{1}{2} - z; 1), \quad (13.32)$$

17 Note that in the rank 1 case the reformulation (13.31) with (13.32) is also valid for representations that are not of Jordan-Schwinger type.

with the \mathfrak{gl}_2 weights λ_1 and λ_2 .¹⁷

We are interested in highest-weight representations of the type discussed in section 13.3. To describe non-compact spin chains with spin $-s$, where s is a positive half integer, we take the Jordan-Schwinger realization (13.3) and perform a particle-hole transformation on the oscillators of type 1:

$$(\bar{\chi}_1, \chi_1) \rightarrow (-\bar{\mathbf{b}}, \bar{\mathbf{b}}), \quad (\bar{\chi}_2, \chi_2) \rightarrow (\bar{\mathbf{a}}, \mathbf{a}). \tag{13.33}$$

For convenience we use a notation different from the rest of this and the next chapters and label the states in the spin $-s$ representation as

$$|m\rangle_s = |2s - 1 + m, m\rangle, \tag{13.34}$$

cf. (13.28). The highest-weight state $|0\rangle_s$ then satisfies

$$E_{12}|0\rangle_s = 0, \quad E_{11}|0\rangle_s = -2s|0\rangle_s, \quad E_{22}|0\rangle_s = 0, \tag{13.35}$$

and the other states of the representation can be generated from this state by acting with the operator E_{21} . The representation has the \mathfrak{gl}_2 weights $\lambda_1 = -2s$ and $\lambda_2 = 0$, and the central charge takes the value $\mathbf{c}|m\rangle_s = -2s|m\rangle_s$.

Our goal is to obtain the matrix elements of the \mathcal{R} -operators in (13.30). From (13.20) we find that $\mathcal{R}_\emptyset(z) = 1$ and $\mathcal{R}_{\emptyset}(z) = \frac{1}{(z+1)_{2s}}$, where the Pochhammer symbol is defined by $(a)_n := \Gamma(a+n)/\Gamma(a)$ in terms of Gamma functions.¹⁸ It is rather straightforward to obtain the matrix elements of $\mathcal{R}_{\{2\}}$. They are polynomials in the spectral parameter z and can be obtained noting that the series representation of the hypergeometric function in (13.32) truncates, due to Gamma functions in the denominator with negative integer arguments. One finds

18 In the following we will sometimes consider Pochhammer symbols where a can be a negative integer. In this case we define the symbol using the identity $\frac{\Gamma(a+n)}{\Gamma(a)} = (-1)^n \frac{\Gamma(1-a)}{\Gamma(1-a-n)}$, which follows from Euler's reflection formula.

$$\begin{aligned} {}_s\langle \tilde{m} | \mathcal{R}_{\{2\}}(z) | m \rangle_s &= \sqrt{\frac{\max(m, \tilde{m})! \max(2s - 1 + m, 2s - 1 + \tilde{m})!}{\min(m, \tilde{m})! \min(2s - 1 + m, 2s - 1 + \tilde{m})!}} \\ &\times \bar{\xi}_{21}^{\Theta(\tilde{m}-m)|\tilde{m}-m|} \mathbb{M}_{\{2\}}(z, \mathbf{N}_{21}, |m - \tilde{m}|, \min(m, \tilde{m})) \xi_{12}^{\Theta(m-\tilde{m})|m-\tilde{m}|}, \end{aligned} \tag{13.36}$$

with the middle part which is diagonal in the auxiliary space

$$\mathbb{M}_{\{2\}}(z, \mathbf{N}_{21}, k, l) = (2s - 1 + l)! \sum_{p=0}^l \binom{l}{p} \frac{(\mathbf{N}_{21} + 1 + p - l)_{l-p} (z + \frac{1}{2} + 2s)_p}{(2s - 1 + p)! (k + l - p)!}. \tag{13.37}$$

Here $\Theta(-m) = \Theta(0) = 0$ and $\Theta(m) = 1$ for $m \in \mathbb{N}_+$.

However, as already noted in Frassek et al. (2013)¹⁹ the operator $\mathcal{R}_{\{1\}}$ yields infinite sums when evaluated naively, since there are only raising operators acting on the states, cf. (13.30). This makes it difficult to evaluate its matrix elements concretely in terms of rational functions. Nevertheless, as we will show in section 14.2, using the integral representation of the hypergeometric function and the Euler transformation the matrix elements can be obtained from (13.31)

19 Frassek, Łukowski, Meneghelli, Staudacher, "Baxter Operators and Hamiltonians for 'nearly all' Integrable Closed $\mathfrak{gl}(n)$ Spin Chains", 1112.3600

and written as

$$\begin{aligned}
 {}_s\langle \tilde{m} | \mathcal{R}_{\{1\}}(z) | m \rangle_s &= \sqrt{\frac{\max(m, \tilde{m})! \max(2s-1+m, 2s-1+\tilde{m})!}{\min(m, \tilde{m})! \min(2s-1+m, 2s-1+\tilde{m})!}} \\
 &\times (-\bar{\xi}_{12})^{\Theta(m-\tilde{m})|m-\tilde{m}|} \mathbb{M}_{\{1\}}(z, \mathbf{N}_{12}, |m-\tilde{m}|, \max(m, \tilde{m})) (-\bar{\xi}_{21})^{\Theta(\tilde{m}-m)|\tilde{m}-m|},
 \end{aligned} \tag{13.38}$$

with the middle part taking the simple form

$$\mathbb{M}_{\{1\}}(z, \mathbf{N}_{12}, k, l) = \frac{\mathbb{M}_{\{2\}}(z, \mathbf{N}_{12}, k, l-k)}{(z - \mathbf{N}_{12} - l + \frac{1}{2})_{2l-k+2s}}. \tag{13.39}$$

We see that also this non-polynomial \mathcal{R} -operator can be written in a very compact form and observe that the resulting expression is very similar to the polynomial \mathcal{R} -operator. In particular, both are simple rational functions of the spectral parameter and the auxiliary oscillators. The only difference is the dependence on the auxiliary space number operators in the denominator. This has important consequences for the analytic structure of the resulting Q-operators.

The matrix elements of the corresponding Q-operators (13.13) can now be derived as

$${}_s\langle \tilde{\mathbf{m}} | \mathbf{Q}_{\{a\}}(z) | \mathbf{m} \rangle_s = e^{iz\phi_a} \widehat{\text{tr}}_s \langle \tilde{m}_1 | \mathcal{R}_{\{a\}}(z) | m_1 \rangle_s \cdots {}_s\langle \tilde{m}_L | \mathcal{R}_{\{a\}}(z) | m_L \rangle_s. \tag{13.40}$$

The advantage of first evaluating the \mathcal{R} -operators in the quantum space and subsequently taking the trace in the auxiliary space is that we can restrict to individual magnon sectors with $M = \sum_{i=1}^L m_i = \sum_{i=1}^L \tilde{m}_i$. For each such sector, the Q-operators can then be realized as matrices of finite size. As we will show in Section 14.3, the matrix elements of the Q-operators corresponding to the \mathcal{R} -operators with non-truncating sums are non-rational functions and can be written in terms of the Lerch transcendent (Lerch zeta-function) defined as

$$\Phi_\ell^\tau(z) = \sum_{k=0}^{\infty} \frac{\tau^k}{(k+z)^\ell}. \tag{13.41}$$

To give the reader an impression of the resulting Q-functions we consider the concrete case of a spin chain with spin $-\frac{1}{2}$. For small length L and magnon number M we can diagonalize the Q-operators resulting from the monodromy construction directly. For the case $L = 2$ and $M = 0, 1, 2$ one easily obtains explicit though rather lengthy expressions for the eigenvalues and eigenvectors. Due to the constraint (13.21), there is only one independent twist parameter with $\phi_1 = -\phi_2$. For small values of ϕ_1 the eigenvalues corresponding to the highest-weight states of the untwisted spin chain are given by:

M	$Q_{\{1\}}(z)$	$Q_{\{2\}}(z)$
0	$2i\phi_1 [\psi'(-z - \frac{1}{2})] + \mathcal{O}(\phi_1^2)$	1
1	$2i\phi_1 \times (-4) \times [1 + (z+1)\psi'(-z - \frac{1}{2})] + \mathcal{O}(\phi_1^2)$	$(z+1) + \mathcal{O}(\phi_1)$
2	$2i\phi_1 \times 9 \times [(z+1) + (z^2 + 2z + \frac{13}{12})\psi'(-z - \frac{1}{2})] + \mathcal{O}(\phi_1^2)$	$(z^2 + 2z + \frac{13}{12}) + \mathcal{O}(\phi_1)$

Here the non-polynomial Q-functions are expressed in terms of the Polygamma function $\psi'(z) = \Phi_2^1(z)$. We observe that for fixed M , the prefactors of these functions in $Q_{\{1\}}$ are given by the functions $Q_{\{2\}}$, which are known in closed form and given by Hahn polynomials.²⁰ Expanding the factor $\Delta_{12} = 2i\phi_1 + \mathcal{O}(\phi_1^3)$ in the functional relation (13.17), we see that the functions $\frac{1}{2i\phi_1}Q_{\{1\}}(z)$ and $Q_{\{2\}}(z)$ satisfy the functional relations of the untwisted spin chain, where the factor Δ_{12} is not present.

13.5 Overview of non-compact Q-systems

Just as for the spin $-s$ models with $u_{1,1}$ symmetry we have just discussed, the Q-operators of spin chains with non-compact representations come in two types: they are either rational functions of the spectral parameter, or can be written in terms of functions with infinite ladders of poles, such as the Lerch transcendent (13.41), or generalizations of this function.

This analytic structure directly follows from the Lax operators given in (13.12). These operators naturally decompose into three factors, with exponentials acting on the left and on the right, and a diagonal part in terms of Gamma functions. As discussed for the spin $-s$ models, this elegant expression behaves very differently for \mathcal{R} -operators corresponding to the non-rational Q-operators of non-compact models. In this case, some of the oscillators are particle-hole transformed as in equation (13.27), and some of the exponentials appearing on the right (left) in the \mathcal{R} -operators (13.12) have only creation (annihilation) operators in the quantum space. Therefore the exponentials do not truncate to finite sums, and one has to sum over an infinite tower of states.²¹ These infinite sums result in rational expression for the matrix elements of the respective \mathcal{R} -operators, which contain both the spectral parameter as well as auxiliary space operators in the denominator, and lead to the special functions discussed above after taking the supertrace over the auxiliary space.

Before discussing how to perform such computations, we can use the structure of the Lax operators (13.12) for the non-compact oscillator representations (13.27), to give a survey of the Q-system of non-compact $u_{p,q|r+s}$ models. These Q-systems contain a total number of $2^{p+q+r+s}$ Q-operators built from the operators \mathcal{R}_I with $I \subseteq \{1, \dots, p+q+r+s\}$. Each level labeled by $k = |I|$ contains $\binom{p+q+r+s}{k}$ Q-operators. Interestingly, for only $2^{r+s}(2^p + 2^q)$ of all Q-operators all exponentials in the \mathcal{R} -operators as given in (13.12) truncate. This can be seen from the action of the exponentials on the states defined in (13.28).

²⁰ Korchemsky, "Quasiclassical QCD pomeron", [hep-th/9508025](#); and Eden, Staudacher, "Integrability and transcendentality", [hep-th/0603157](#)

²¹ Note that at this stage we do not consider the auxiliary space. Later on when evaluating Q-operators we will take the trace over the infinite-dimensional Fock space, see (13.13), but these infinite sums are actually relatively easy to compute.

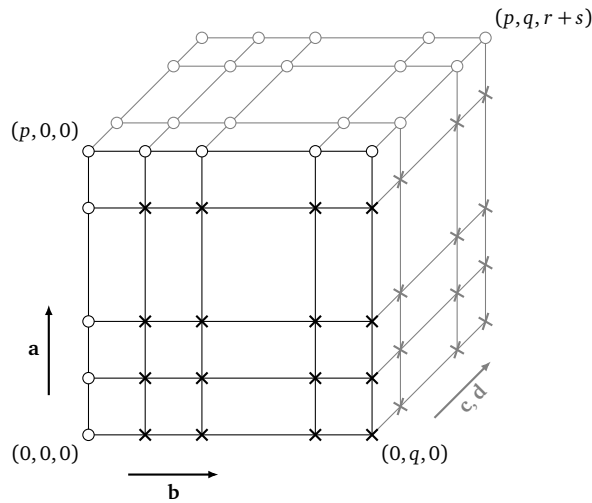


Figure 13.1: Distribution of rational and non-rational Q-operators for $u_{p,q|r+s}$. We show a projection of the Hasse diagram with Q-operators on the lattice point (i, j, k) . Rational Q-operators are marked with circle and non-rational ones with a cross.

This structure is visualized on a projection of the Hasse diagram in figure 13.1. In this diagram, each lattice point (i, j, k) represents the $\binom{p}{i}\binom{q}{j}\binom{r+s}{k}$ Q-operators with an index set including i bosonic indices which are not particle-holed transformed according to (13.27), j bosonic indices which are transformed, and k fermionic indices. Because of the nilpotency of the corresponding generators, the fermionic degrees of freedom do not change the truncating or non-truncating nature of the \mathcal{R} -operators. Therefore one finds that an \mathcal{R} -operator \mathcal{R}_I has matrix elements with truncating sums if:

- I does not contain any indices corresponding to bosonic oscillators that are particle-hole transformed.
- I contains all indices corresponding to bosonic oscillators that are not particle-hole transformed.

Consequently, the rational Q-operators are those on the lattice sites $(i, 0, k)$ and (p, j, k) . The \mathcal{R} -operators for the remaining non-rational Q-operators as given in equation (13.12) have $j(p-i)$ pairs of exponentials which do not truncate.

For the lowest level, these \mathcal{R} -operators have only p pairs of infinite sums, and in the next chapter we will derive different representations of these operators, that are simpler to evaluate, without calculating infinite sums. These operators are then sufficient to determine the whole Q-system.

Evaluating Q-operators

In section 13.5 we have seen that the majority of Q-operators for non-compact spin chains with $u_{p,r|r+s}$ symmetry are non-rational, and given in terms of functions with infinite ladders of poles. On the level of their constituent Lax operators, this analytic structure manifests itself in the appearance of infinite sums over intermediate states. These sums make it difficult to evaluate the Q-operators, i.e. to calculate explicit matrix elements, or even to see the analytic structure from first principles. For higher rank algebras, such as $u_{2,2|4}$ in the case of the $\mathcal{N}=4$ SYM spin chain at one-loop, even the rational Q-operators result in rather complicated expression for the matrix elements, and the evaluation of their Lax operators poses combinatorial difficulties, due to the large number of terms, most of which do not contribute to a given matrix element.

In this chapter, we want to show how to concretely evaluate such operatorial Q-systems for non-compact super spin chains, in terms of finite matrices for each magnon sector. This strategy exploits the block diagonal form of the Q-operators, and circumvents the problems posed by the infinite dimensional state space of these spin chains, based on the derivation of novel representations for the \mathcal{R} -operators which are easier to evaluate, and on the functional relations of the Q-system, that allow to focus on a subset of Q-operators.

We first describe a representation of the \mathcal{R} -operators which does not feature exponential functions of raising and lowering operators in section 14.1. This representation already solves much of the combinatorial difficulties, and allows to deduce the matrix elements for the polynomial cases. For the other operators, there are still infinite sums. In section 14.2 we derive a compact integral representation for the \mathcal{R} -operators of the lowest level involving hypergeometric functions, which facilitates practical calculations, and directly allows to write down formulas involving only finite sums. Using these results to efficiently calculate matrix elements of the lowest level \mathcal{R} -operators, we then show how to determine the entire operatorial Q-system in section 14.3. We first determine the matrix elements of the lowest level Q-operators in each magnon block, i.e. for each set of states with the same number of oscillator excitations, by calculating the necessary supertraces. Since these matrices are of finite size, we can use the functional relations to determine the other Q-operators in a computationally efficient way. Finally, section 14.4 collects some results on finite sum representa-

This chapter is based on the author's publication Frassek, Marboe, Meidinger, "Evaluation of the operatorial Q-system for non-compact super spin chains", 1706.02320.

tions for the \mathcal{R} -operators of higher levels. While we found that calculating the lowest level and then bootstrapping the Q-system is very efficient for practical calculations, the Lax operators for higher levels are still of theoretical interest. In particular we show that the problem quickly becomes very difficult, since operators involving more infinite sums require rather obscure identities to be written as finite sums.

Throughout this chapter, we aim to be explicit as possible, and provide all formulas necessary to calculate all Q-operators for $u_{p,q|r+s}$ invariant spin chains in arbitrary representations of Jordan-Schwinger form, in particular for $\mathcal{N} = 4$ SYM at one loop. This allows to fully automatize these calculations in computer algebra systems.¹

¹ We implemented our method in a Mathematica program which is available on request.

14.1 Ladder decomposition of \mathcal{R} -operators

As a first step towards a representation of the \mathcal{R} -operators which allows to understand the structure of their matrix elements, we can write \mathcal{R} -operators (13.12) without exponentials. Since the factors in these exponentials appear often in the following derivations, we define abbreviations for them:

$$Y_{a\bar{a}} = (-1)^{|a|+|\bar{a}||a|} \bar{\xi}_{a\bar{a}} \bar{\chi}_a \chi_{\bar{a}}, \quad X_{a\bar{a}} = (-1)^{|\bar{a}|+|a|+|\bar{a}||a|} \xi_{\bar{a}a} \bar{\chi}_{\bar{a}} \chi_a. \quad (14.1)$$

The main idea is to expand the exponentials and to combine terms with the same *difference* in the powers of the matching factors $X_{a\bar{a}}$ and $Y_{a\bar{a}}$ in the exponents. This can be done using the formula

$$e^{Y_{a\bar{a}}} f(\mathbf{N}_a, \mathbf{N}_{\bar{a}}) e^{-X_{a\bar{a}}} = \sum_{n=-\infty}^{+\infty} (Y_{a\bar{a}})^{\Theta(n)|n|} \sum_{k=0}^{\infty} \frac{(-1)^k Y_{a\bar{a}}^k X_{a\bar{a}}^k}{k!(|n|+k)!} f(\mathbf{N}_a - k, \mathbf{N}_{\bar{a}} + k) (-X_{a\bar{a}})^{\Theta(-n)|n|} \quad (14.2)$$

where $\Theta(-m) = \Theta(0) = 0$ and $\Theta(m) = 1$ for $m \in \mathbb{N}_+$. Using the identities

$$\bar{\chi}_a^k \chi_a^k = \frac{\Gamma(1 + \mathbf{N}_a)}{\Gamma(1 + \mathbf{N}_a - k)}, \quad \chi_a^k \bar{\chi}_a^k = (-1)^{k|a|} \frac{\Gamma(\mathbf{N}_a + k + (-1)^{|a|})}{\Gamma(\mathbf{N}_a + (-1)^{|a|})}, \quad (14.3)$$

we can express the factor $Y_{a\bar{a}}^k X_{a\bar{a}}^k$ as

$$Y_{a\bar{a}}^k X_{a\bar{a}}^k = (-1)^{|a|+|\bar{a}|} \frac{\Gamma(1 + \mathbf{N}_{a\bar{a}})}{\Gamma(1 + \mathbf{N}_{a\bar{a}} - k)} \frac{\Gamma(1 + \mathbf{N}_a)}{\Gamma(1 + \mathbf{N}_a - k)} \frac{\Gamma(\mathbf{N}_{\bar{a}} + k + (-1)^{|\bar{a}|})}{\Gamma(\mathbf{N}_{\bar{a}} + (-1)^{|\bar{a}|})}. \quad (14.4)$$

Applying equation (14.2) together with (14.4) to the \mathcal{R} -operator defined in (13.12), we find

$$\mathcal{R}_I(\mathbf{z}) = \sum_{\{n_{a\bar{a}}\}=-\infty}^{\infty} \left[\prod_{a, \bar{a}} (Y_{a\bar{a}})^{\Theta(n_{a\bar{a}})|n_{a\bar{a}}|} \right] \mathbb{M}_I(\mathbf{z}) \left[\prod_{a, \bar{a}} (-X_{a\bar{a}})^{\Theta(-n_{a\bar{a}})|n_{a\bar{a}}|} \right], \quad (14.5)$$

where the diagonal part is given by

$$\begin{aligned} \mathbb{M}_I(z) = & \sum_{\{k_{a\bar{a}}\}=0}^{\infty} \left[\prod_{a,\bar{a}} \frac{(-1)^{(|a|+|\bar{a}|+1)k_{a\bar{a}}}}{\Gamma(k_{a\bar{a}}+1)\Gamma(|n_{a\bar{a}}|+k_{a\bar{a}}+1)} \frac{\Gamma(1+\mathbf{N}_{a\bar{a}})}{\Gamma(1+\mathbf{N}_{a\bar{a}}-k_{a\bar{a}})} \right] \\ & \left[\prod_a \frac{\Gamma(1+\mathbf{N}_a)}{\Gamma(1+\mathbf{N}_a-\sum_{\bar{a}} k_{a\bar{a}})} \right] \left[\prod_{\bar{a}} \frac{\Gamma(\mathbf{N}_{\bar{a}}+(-1)^{|\bar{a}|}+\sum_a k_{a\bar{a}})}{\Gamma(\mathbf{N}_{\bar{a}}+(-1)^{|\bar{a}|})} \right] \\ & \frac{\Gamma(z+1-s_I-\sum_{\bar{a}} \mathbf{N}_{\bar{a}}-\sum_{a,\bar{a}} k_{a\bar{a}})}{\Gamma(z+1-s_I-c)}. \end{aligned} \quad (14.6)$$

The advantage of this representation is the fact that only a minimal number of raising and lowering operators remains. Note that for any matrix element of (14.2), only finitely many terms of the outer sums over the variables $n_{a\bar{a}}$ contribute, since the difference in occupation numbers between the bra and the ket state determine the possible powers of the $X_{a\bar{a}}$ and $Y_{a\bar{a}}$. In this sense, we call (14.5) a ladder decomposition, with (14.6) giving the diagonal contribution to the \mathcal{R} -operator. Note that this representation – compared to naively expressing the exponentials by their power series – already removes half of the sums. In particular, it removes a lot of combinatorial complexity, as there are no cross terms which vanish for a given matrix element.

So far we have not discussed the spectrum of the number operators. We implicitly assume that these operators act on a Hilbert space as given in (13.28). The spectrum of the \mathbf{N}_a then depends on whether the corresponding oscillator is particle-hole transformed, cf. (13.27). Depending on this spectrum, the remaining inner sums over the variables $k_{a\bar{a}}$ are infinite or not. Comparing with the classification of Q-operators as rational or non-rational as discussed in section 13.5, we see that the Gamma functions in the denominator of (14.6) effectively truncate all sums for the Lax operators of rational Q-operators. For the other Lax operators, a sufficient number of operators \mathbf{N}_a have a negative spectrum, such that at least some sums remain infinite. In the following, we will transform (14.6) into a representation where the infinite sums are evaluated.

14.2 Lowest level \mathcal{R} -operators for oscillator representations of $u_{p,q|r+s}$

For the \mathcal{R} -operators corresponding to non-rational Q-operators, some of the sums in equation (14.6) are still infinite. The operators of the lowest level, with an index set $I = \{a\}$ containing just a single element, in general have the smallest number of such sums, and the outer sums over the variables $n_{a\bar{a}}$ in (14.5) are completely fixed by the occupation numbers such that only a single term contributes to each matrix element. This means that the diagonal part $\mathbb{M}_{\{a\}}$ directly gives this matrix element, up to combinatorial factors from oscillator algebra. Moreover these operators are sufficient to generate the entire Q-system, due to the functional relations (13.17) and (13.18), and the fact that $\mathbf{Q}_{\emptyset}(z) = 1$.

Therefore we focus on these operators, and will now derive a different formula for them, which allows to calculate matrix elements without performing infinite sums.

We first specialize the expression given in (14.5) and (14.6) to these \mathcal{R} -operators which we can write as

$$\mathcal{R}_{\{a\}}(z) = \sum_{\{n_{\bar{a}}\}=-\infty}^{\infty} \left[\prod_{\bar{a}} (Y_{a\bar{a}})^{\Theta(n_{\bar{a}})|n_{\bar{a}}|} \right] \mathbb{M}_{\{a\}}(z, \{\mathbf{N}\}, \{n\}) \left[\prod_{\bar{a}} (-X_{a\bar{a}})^{\Theta(-n_{\bar{a}})|n_{\bar{a}}|} \right], \quad (14.7)$$

with X and Y given in (14.1), and where the diagonal part is

$$\begin{aligned} \mathbb{M}_{\{a\}}(z, \{\mathbf{N}\}, \{n\}) = & \sum_{\{k_{\bar{a}}\}=0}^{\infty} \prod_{\bar{a}} \left[\frac{(-1)^{(|a|+|\bar{a}|+1)k_{\bar{a}}} \Gamma(1 + \mathbf{N}_{a\bar{a}})}{k_{\bar{a}}! (|n_{\bar{a}}| + k_{\bar{a}})! \Gamma(1 + \mathbf{N}_{a\bar{a}} - k_{\bar{a}})} \frac{\Gamma(\mathbf{N}_{\bar{a}} + (-1)^{|\bar{a}}| + k_{\bar{a}})}{\Gamma(\mathbf{N}_{\bar{a}} + (-1)^{|\bar{a}}|)} \right] \\ & \frac{\Gamma(\mathbf{N}_a + 1)}{\Gamma(\mathbf{N}_a + 1 - \sum_{\bar{a}} k_{\bar{a}})} \frac{\Gamma(z + 1 - \sum_{\bar{a}} (\mathbf{N}_{\bar{a}} + k_{\bar{a}} - \frac{1}{2}(-1)^{|\bar{a}}|))}{\Gamma(z + 1 - \mathbf{c} - \frac{1}{2} \sum_{\bar{a}} (-1)^{|\bar{a}}|)}. \end{aligned} \quad (14.8)$$

Our aim is to transform this expression for the diagonal part into a form which can directly be evaluated, even for non-compact spin chains. To achieve this, we have to remove the infinite sums. As it turns out, the most compact expression we can obtain is an integral formula, from which expressions in terms of finite sums can also be generated. Since the intermediate formulas are quite lengthy, we only sketch the derivation of this representation.

We want to perform all sums over the $k_{\bar{a}}$ in (14.8). Consider the first sum, which we take to be over some index \bar{b} . This sum can be written as an expression involving Gamma functions and the following hypergeometric function:

$${}_3F_2 \left(\begin{matrix} \sum_{\bar{a} \neq \bar{b}} k_{\bar{a}} - \mathbf{N}_a & -\mathbf{N}_{a\bar{b}} & \mathbf{N}_{\bar{b}} + (-1)^{|\bar{b}} \\ -z + \frac{1}{2} \sum_{\bar{a}} (-1)^{|\bar{a}} + \sum_{\bar{a} \neq \bar{b}} (\mathbf{N}_{\bar{a}} + k_{\bar{a}}) + \mathbf{N}_{\bar{b}} & 1 + |n_{\bar{b}}| \end{matrix}; (-1)^{|a|+|\bar{b}|} \right). \quad (14.9)$$

Since the other summation variables appear in the arguments of this function, the other sums cannot be taken easily. To remedy this, and to disentangle the sums, one can use integral representations of the hypergeometric function. The type of integral however depends on the spectrum of the operator \mathbf{N}_a , which in turn depends on the choice of real form $u_{p,q|r+s}$, see section 13.3. If the oscillator with index a is bosonic and particle-hole transformed, $\omega_a = -1$, the first argument ($\sum_{\bar{a} \neq \bar{b}} k_{\bar{a}} - \mathbf{N}_a$) of the hypergeometric function takes positive integer values, and we can use the standard Euler type integral, expressing the function ${}_3F_2$ as an integral involving the function ${}_2F_1$, integrating over the interval $(0, 1)$ on the real line:

$$\begin{aligned} & {}_{q+1}F_q \left(\begin{matrix} a_0 & a_1 & \cdots & a_q \\ b_0 & b_1 & \cdots & b_{q-1} \end{matrix}; z \right) \\ &= \frac{\Gamma(b_0)}{\Gamma(a_0)\Gamma(b_0 - a_0)} \int_0^1 dt t^{a_0-1} (1-t)^{b_0-a_0-1} {}_qF_{q-1} \left(\begin{matrix} a_1 & \cdots & a_q \\ b_1 & \cdots & b_{q-1} \end{matrix}; tz \right). \end{aligned} \quad (14.10)$$

It converges for $\text{Re}(b_0) > \text{Re}(a_0) > 0$ and $|z| \leq 1$.

For all other cases, the Gamma function $\Gamma(N_a + 1 - \sum_{\bar{a}} k_{\bar{a}})$ in the denominator of (14.8) truncates the range of the summation variables such that the argument $(\sum_{\bar{a} \neq \bar{b}} k_{\bar{a}} - N_a)$ of the hypergeometric function takes non-positive integer values. For such arguments, one can use an analytic continuation of the Euler integral employing the Pochhammer contour \mathcal{P} , shown in figure 14.1,

$${}_{q+1}F_q \left(\begin{matrix} a_0 & a_1 & \cdots & a_q \\ b_0 & b_1 & \cdots & b_{q-1} \end{matrix} ; z \right) = \frac{\Gamma(b_0)}{\Gamma(a_0)\Gamma(b_0 - a_0)} \frac{1}{(1 - e^{2\pi i a_0})(1 - e^{2\pi i (b_0 - a_0)})} \int_{\mathcal{P}} dt t^{a_0-1} (1-t)^{b_0-a_0-1} {}_qF_{q-1} \left(\begin{matrix} a_1 & \cdots & a_q \\ b_1 & \cdots & b_{q-1} \end{matrix} ; tz \right). \quad (14.11)$$

This can be understood as follows: the arcs around 0 and 1 do not contribute, and thus the integral contour consists of four times the path from 0 to 1, each time with a different phase from crossing the branch cuts; these phases are canceled by the prefactor. The integral converges if a_0 and $(b_0 - a_0)$ are not positive integers. For negative integers however, the integral dramatically simplifies. Assume a_0 is a negative integer or zero. Then the integrand has a pole at zero instead of a branch point. Therefore, the contribution of the parts of the integration contour that go from 0 to 1 or from 1 to 0 cancel pairwise, since no phase is picked up going around the origin. Nevertheless the integral is non-zero, since now the arcs around zero contribute; on each of two sheets they give the residue at the origin, with a relative phase. The prefactor in (14.11) is regular at these points in parameter space, since

$$\lim_{a_0 \rightarrow -n} (\Gamma(a_0)(1 - e^{2\pi i a_0}))^{-1} = -\frac{(-1)^n \Gamma(n+1)}{2\pi i}. \quad (14.12)$$

Also, the remaining factor of $(1 - e^{2\pi i b_0})$ in (14.11) cancels against the phases from the two sheets. We therefore have the contour integral representation

$${}_{q+1}F_q \left(\begin{matrix} a_0 & a_1 & \cdots & a_q \\ b_0 & b_1 & \cdots & b_{q-1} \end{matrix} ; z \right) = (-1)^{a_0} \frac{\Gamma(b_0)\Gamma(1-a_0)}{\Gamma(b_0 - a_0) 2\pi i} \oint_{t=0} dt t^{a_0-1} (1-t)^{b_0-a_0-1} {}_qF_{q-1} \left(\begin{matrix} a_1 & \cdots & a_q \\ b_1 & \cdots & b_{q-1} \end{matrix} ; tz \right) \quad (14.13)$$

which is valid for $a_0 \in -\mathbb{N}$, including $a_0 = 0$.

Using the appropriate integral formulas to rewrite the hypergeometric function (14.9), one finds that all subsequent summations decouple, and can be performed easily using the series representation of the hypergeometric function ${}_2F_1$. We then arrive at the result

$$\mathbb{M}_{\{a\}}(z, \{\mathbf{N}\}, \{n\}) = \int dt \frac{t^{-N_a-1}}{(1-t)^{z+1-c-\frac{1}{2}\sum_{\bar{a}}(-1)^{|\bar{a}|}}} \prod_{\bar{a}} \frac{1}{|n_{\bar{a}}|!} {}_2F_1 \left(\begin{matrix} N_{\bar{a}} + (-1)^{|\bar{a}|} - N_{a\bar{a}} \\ 1 + |n_{\bar{a}}| \end{matrix} ; (-1)^{|\bar{a}|+|a|} t \right), \quad (14.14)$$

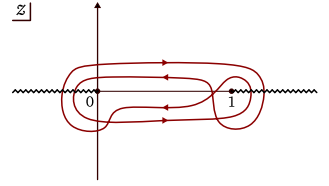


Figure 14.1: The Pochhammer contour.

where \mathbf{c} is the central charge defined in (13.11) and the integration is

$$\int dt = \begin{cases} \frac{(-1)^{N_a}}{\Gamma(-N_a)} \int_0^1 dt & \text{if } |a| = 0 \text{ and } \omega_a = -1 \\ \frac{\Gamma(1 + N_a)}{2\pi i} \oint_{t=0} dt & \omega_a = 1 \text{ or } |a| = 1 \end{cases}. \quad (14.15)$$

This means that for truncating \mathcal{R} -operators, the integral just computes a residue, while for the non-truncating ones, it is an integral over the interval $(0, 1)$. Note that strictly speaking, the integral is only convergent for appropriately chosen values of the spectral parameter z ; this however poses no problem, since the result for any matrix element is a rational function which can be analytically continued to any value of the spectral parameter.

While it might seem that we did not gain much by writing the potentially infinite sums of the \mathcal{R} -operator in terms of an integral, this integral is in fact trivial to evaluate, by expanding the integrand and either taking a simple residue, or evaluating the line integral in terms of a Beta function. We will present some examples for these calculations in the following: momentarily, we give derivations of the formulas for the spin $-s$ models discussed in section 13.4, and then provide a finite sum formula for the general case. In section 15.2 we calculate the Q-functions of the BMN vacuum in twisted $\mathcal{N} = 4$ SYM. These calculation involve concrete matrix elements of the operators, which we now obtain from the formulas given above.

Matrix elements

Given the \mathcal{R} -operators of the lowest level (14.7) with the integral representation of the diagonal part (14.14), explicit matrix elements $\langle \tilde{\mathbf{m}} | \mathcal{R}_{\{a\}}(z) | \mathbf{m} \rangle$ with the states defined in (13.28) can be obtained using oscillator algebra. First note that the values of the summation variables $n_{\bar{a}}$, $\bar{a} \in \bar{I}$ in (14.7) are fixed by the difference in occupation numbers as

$$n_{\bar{a}} = -\omega_{\bar{a}}(\tilde{m}_{\bar{a}} - m_{\bar{a}}), \quad (14.16)$$

because each of the corresponding oscillators only appears in a single factor $X_{a\bar{a}}$ and a single factor $Y_{\bar{a}a}$ in (14.7). The powers of the oscillators with index a in the left and right factors are

$$N_\ell = \sum_{\bar{a}} \Theta(n_{\bar{a}}) |n_{\bar{a}}| \quad \text{and} \quad N_r = \sum_{\bar{a}} \Theta(-n_{\bar{a}}) |n_{\bar{a}}|. \quad (14.17)$$

After acting with these operators, the occupation numbers of the state on which the diagonal part $\mathbb{M}_{\{a\}}$ acts are given by

$$\hat{m}_a = \tilde{m}_a - \omega_a N_\ell = m_a - \omega_a N_r, \quad \hat{m}_{\bar{a}} = \begin{cases} \max(m_{\bar{a}}, \tilde{m}_{\bar{a}}) & \text{if } \omega_{\bar{a}} = 1 \\ \min(m_{\bar{a}}, \tilde{m}_{\bar{a}}) & \text{if } \omega_{\bar{a}} = -1 \end{cases}. \quad (14.18)$$

For the different types of oscillators, given in (13.27), this sets the number operators in (14.14) to

$$\mathbf{N}_c = \begin{cases} \bar{\mathbf{a}}_c \mathbf{a}_c & \rightarrow & \hat{m}_c & |c| = 0 \text{ and } \omega_c = +1 \\ -1 - \bar{\mathbf{b}}_c \mathbf{b}_c & \rightarrow & -1 - \hat{m}_c & |c| = 0 \text{ and } \omega_c = -1 \\ \bar{\mathbf{c}}_c \mathbf{c}_c & \rightarrow & \hat{m}_c & |c| = 1 \text{ and } \omega_c = +1 \\ 1 - \bar{\mathbf{d}}_c \mathbf{d}_c & \rightarrow & 1 - \hat{m}_c & |c| = 1 \text{ and } \omega_c = -1 \end{cases}. \quad (14.19)$$

Finally, collecting all combinatorial factors arising from the oscillator algebra, we can write the matrix elements as

$$\begin{aligned} \langle \tilde{\mathbf{m}} | \mathcal{R}_{\{a\}}(z) | \mathbf{m} \rangle = & \zeta_{a1}^{\Theta(\omega_1(m_1 - \tilde{m}_1))|\omega_1(m_1 - \tilde{m}_1)|} \dots \zeta_{aK}^{\Theta(\omega_K(m_K - \tilde{m}_K))|\omega_K(m_K - \tilde{m}_K)|} \\ & (-1)^{\sum_{\bar{a}} |n_{\bar{a}}| c_{a\bar{a}}} \left(\frac{\sqrt{\tilde{m}_a! m_a!}}{\hat{m}_a!} \right)^{\omega_a} \prod_{\bar{a}} \sqrt{\frac{\max(m_{\bar{a}}, \tilde{m}_{\bar{a}})!}{\min(m_{\bar{a}}, \tilde{m}_{\bar{a}})!}} \mathbb{M}_{\{a\}}(z, \{\hat{m}_i\}, \{\omega_{\bar{a}}(m_{\bar{a}} - \tilde{m}_{\bar{a}})\}) \\ & \zeta_{K\bar{a}}^{\Theta(-\omega_K(m_K - \tilde{m}_K))|\omega_K(m_K - \tilde{m}_K)|} \dots \zeta_{1\bar{a}}^{\Theta(-\omega_1(\tilde{m}_1 - m_1))|\omega_1(\tilde{m}_1 - m_1)|}, \end{aligned} \quad (14.20)$$

where $K = p + q + r + s$ for the algebra $u_{p,q|r+s}$, \mathbb{M} is given in (14.14), and the sign is determined by

$$\begin{aligned} c_{a\bar{a}} = & \left[(|a| + |\bar{a}|) \Theta(n_{\bar{a}}) + (1 + |a||\bar{a}|) \Theta(-n_{\bar{a}}) \right] + \frac{1}{2} \left[(|a| + 1)(1 - \omega_a) \Theta(n_{\bar{a}}) + (|\bar{a}| + 1)(1 - \omega_{\bar{a}}) \Theta(-n_{\bar{a}}) \right] \\ & + \left[(|a| + |\bar{a}|) \sum_c |c| (\tilde{m}_c \Theta(n_{\bar{a}}) + m_c \Theta(-n_{\bar{a}})) \right] + \left[\sum_{c < \bar{a}} |a||c| (\tilde{m}_c \Theta(n_{\bar{a}}) + m_c \Theta(-n_{\bar{a}}) + \delta_{c\bar{a}}) \right] \\ & + \left[\sum_{c < \bar{a}} |\bar{a}||c| ((\Theta(n_c) + \tilde{m}_c) \Theta(n_{\bar{a}}) + (\Theta(-n_c) + m_c) \Theta(-n_{\bar{a}})) \right]. \end{aligned} \quad (14.21)$$

Here we define $n_a = 0$.

Derivation of the \mathcal{R} -operators for the spin $-s$ models

The integral representation for \mathcal{R} -operators of the lowest level, given in (14.7) together with (14.14), can easily be evaluated in practise. To show that it also serves as a good starting point to obtain representations in terms of finite sums, we now derive the formulas (13.36), (13.37), (13.38) and (13.39) for the \mathcal{R} -operators of the spin $-s$ spin chains considered in section 13.4. For these models, both oscillators are bosonic, $|\cdot| = (0, 0)$, and the first oscillator is particle-hole transformed, $\omega = (-1, +1)$. The central charge is constrained to $\mathbf{c} = -2s$, such that the states are given by $|m\rangle_s = |2s - 1 + m, m\rangle$, cf. (13.34).

We begin with the operator $\mathcal{R}_{\{2\}}$, which involves only truncating sums. The matrix elements ${}_s \langle \tilde{m} | \mathcal{R}_{\{2\}}(z) | m \rangle_s$ can be determined from (14.7) by noting that the summation variable n_1 is fixed to be $n_1 = \tilde{m} - m$, and that the diagonal part then acts on a state $|\hat{m}\rangle_s$ with $\hat{m} = \min(m, \tilde{m})$, cf. (14.16) and (14.18). Using this it is straightforward to show that the general structure of the Lax operator exactly matches (13.36). The diagonal part $\mathbb{M}_{\{2\}}$ could in principle be

derived directly from expression (14.8); we nevertheless start from the generally applicable formula (14.14) expressing it as a contour integral. This integral can be evaluated by plugging in the series representations of the hypergeometric function and of the power of $(1 - t)$,

$$\begin{aligned}
 & {}_s \langle \hat{m} | \mathbb{M}_{\{2\}}(z) | \hat{m} \rangle_s \\
 &= \frac{\hat{m}!}{|m - \tilde{m}|!} \frac{1}{2\pi i} \oint_{t=0} dt t^{-\hat{m}-1} (1-t)^{-z-\frac{1}{2}-2s} {}_2F_1 \left(\begin{matrix} 1-2s-\hat{m} - \mathbf{N}_{21} \\ 1+|\tilde{m}-m| \end{matrix}; t \right) \\
 &= \frac{\hat{m}!}{2\pi i} \oint_{t=0} \frac{dt}{t^{\hat{m}+1}} \left[\sum_{\ell=0}^{\infty} \frac{(z + \frac{1}{2} + 2s)_{\ell}}{\ell!} t^{\ell} \right] \left[\sum_{k=0}^{\hat{m}+2s-1} \frac{(2s + \hat{m} - k)_k (1 + \mathbf{N}_{21} - k)_k}{(|\tilde{m} - m| + k)! k!} t^k \right] \\
 &= \sum_{k=0}^{\hat{m}} \binom{\hat{m}}{k} \frac{(z + \frac{1}{2} + 2s)_{\hat{m}-k} (1 + \mathbf{N}_{21} - k)_k (2s + \hat{m} - k)_k}{(|\tilde{m} - m| + k)!}, \tag{14.22}
 \end{aligned}$$

which is the same as (13.37).

Next we turn to the non-truncating \mathcal{R} -operator $\mathcal{R}_{\{1\}}$. For each matrix element, the summation variable is fixed to $n_2 = m - \tilde{m}$, and the diagonal part acts on $|\hat{m}\rangle_s$, where now $\hat{m} = \max(m, \tilde{m})$. One finds that the form of the matrix elements in (13.38) is reproduced by (14.7). The diagonal part (14.14) is then given by

$$\begin{aligned}
 & {}_s \langle \hat{m} | \mathbb{M}_{\{1\}}(z) | \hat{m} \rangle_s = \frac{(-1)^{2s+\hat{m}}}{(2s-1+\hat{m})! |\tilde{m}-m|!} \\
 & \quad \times \int_0^1 dt t^{2s-1+\hat{m}} (1-t)^{-z-\frac{1}{2}-2s} {}_2F_1 \left(\begin{matrix} \hat{m}+1 - \mathbf{N}_{12} \\ 1+|\tilde{m}-m| \end{matrix}; t \right). \tag{14.23}
 \end{aligned}$$

To write the matrix elements as finite sums, we have to apply the Euler transformation ${}_2F_1(n, b; m; z) = (1-z)^{m-n-b} {}_2F_1(m-n, m-b; m; z)$ to the hypergeometric function. Then this function can be written as a finite sum and the integral can be evaluated using the integral representation of the Beta function:

$$\begin{aligned}
 & {}_s \langle \hat{m} | \mathbb{M}_{\{1\}}(z) | \hat{m} \rangle_s \tag{14.24} \\
 &= \frac{(-1)^{2s+\hat{m}}}{(2s-1+\hat{m})! |\tilde{m}-m|!} \int_0^1 dt t^{2s-1+\hat{m}} (1-t)^{-z-\frac{1}{2}-2s-\min(m, \tilde{m})+\mathbf{N}_{12}} \\
 & \quad \times {}_2F_1 \left(\begin{matrix} -\min(m, \tilde{m}) \\ 1+|\tilde{m}-m| \end{matrix}; t \right) \\
 &= \sum_{k=0}^{\min(m, \tilde{m})} \frac{(-1)^{2s+\hat{m}}}{(2s-1+\hat{m})!} \frac{(1 + \min(m, \tilde{m}) - k)_k (1 + |\tilde{m} - m| + \mathbf{N}_{12})_k}{k! (|\tilde{m} - m| + k)!} \\
 & \quad \times \int_0^1 dt t^{2s-1+\hat{m}+k} (1-t)^{-z-\frac{1}{2}-2s-\min(m, \tilde{m})+\mathbf{N}_{12}} \\
 &= \sum_{k=0}^{\min(m, \tilde{m})} \frac{(-1)^{2s+\hat{m}}}{(2s-1+\hat{m})!} \frac{(1 + \min(m, \tilde{m}) - k)_k (1 + |\tilde{m} - m| + \mathbf{N}_{12})_k}{k! (|\tilde{m} - m| + k)!} \\
 & \quad \times B(2s + \hat{m} + k, -z + \frac{1}{2} - 2s - \min(m, \tilde{m}) + \mathbf{N}_{12}). \tag{14.25}
 \end{aligned}$$

This expression is identical to (13.39), upon using $B(x, y) = \frac{\Gamma(x)\Gamma(y)}{\Gamma(x+y)}$.

These calculations can be generalized to other algebras and representations, and thus all matrix elements are rational functions and can be written as finite sums, using nothing more than the Euler transformations on all hypergeometric functions with non-truncating series representations and then performing the resulting Beta integral. We will now derive these formulas for the general case.

Finite sum representation for lowest level \mathcal{R} -operators

Evaluating the integral formula in (14.14) is a very efficient way to determine matrix elements of both polynomial as well as non-polynomial \mathcal{R} -operators. It is however also possible to directly derive finite sum expressions from the integral representation using the same ideas as in the previous section.

Here one has to treat the truncating and the non-truncating case, corresponding to the two integration contours in (14.15), separately. In the truncating case, evaluating the residue returns the expression given in (14.8), which can be expressed in terms of number operators for the particle-hole transformed oscillators (13.27); then all sums are manifestly finite.

For the non-truncating operators $\mathcal{R}_{\{a\}}$ with $|a| = 0$ and $\omega_a = -1$, one can evaluate the integral as follows: For notational convenience, we first decompose the set $\bar{I} = \bar{I}_a \cup \bar{I}_b \cup \bar{I}_c \cup \bar{I}_d$ into indices corresponding to the different types of oscillators in (13.27). Note that the integral (14.14) contains one hypergeometric function for each index $\bar{a} \in \bar{I}$. Applying the Euler transformation to the hypergeometric functions corresponding to the subset \bar{I}_a , using the series expansion of all such functions and subsequently performing the Beta integral, we find

$$\begin{aligned} \mathbb{M}_{\{a\}} = & \sum_{\{k_{\bar{a}}\}=0}^{\infty} \frac{(-1)^{1+\mathbf{N}_{b_a}}}{\mathbf{N}_{b_a}!} \frac{1}{\prod_{\bar{a} \in \bar{I}} k_{\bar{a}}! (|n_{\bar{a}}| + k_{\bar{a}})!} \\ & \prod_{\bar{a} \in \bar{I}_a} (|n_{\bar{a}}| - \mathbf{N}_{a_{\bar{a}}})_{k_{\bar{a}}} (|n_{\bar{a}}| + \mathbf{N}_{a_{\bar{a}}} + 1)_{k_{\bar{a}}} \prod_{\bar{a} \in \bar{I}_b} (-\mathbf{N}_{b_{\bar{a}}})_{k_{\bar{a}}} (-\mathbf{N}_{a_{\bar{a}}})_{k_{\bar{a}}} \\ & \prod_{\bar{a} \in \bar{I}_c} (-1)^{k_{\bar{a}}} (\mathbf{N}_{c_{\bar{a}}} - 1)_{k_{\bar{a}}} (-\mathbf{N}_{a_{\bar{a}}})_{k_{\bar{a}}} \prod_{\bar{a} \in \bar{I}_d} (-1)^{k_{\bar{a}}} (-\mathbf{N}_{d_{\bar{a}}})_{k_{\bar{a}}} (-\mathbf{N}_{a_{\bar{a}}})_{k_{\bar{a}}} \\ & B\left(-z + \mathbf{c} + \frac{1}{2} \sum_{\bar{a} \in \bar{I}} (-1)^{|\bar{a}|} + \sum_{\bar{a} \in \bar{I}_a} (\mathbf{N}_{a_{\bar{a}}} + |n_{\bar{a}}| - \mathbf{N}_{a_{\bar{a}}}), \mathbf{N}_{b_a} + 1 + \sum_{\bar{a} \in \bar{I}} k_{\bar{a}}\right), \end{aligned} \quad (14.26)$$

where we used the number operators of the oscillator representation of $u_{p,q|r+s}$, $\mathbf{N}_{a_a} = \bar{a}_a \mathbf{a}_a$ etc. All the Pochhammer symbols involving these operators are of the form $(-m)_k$ with $m \geq 0$ which gives $(-m)_k = (-1)^k \frac{\Gamma(m+1)}{\Gamma(m+1-k)}$, such that all sums truncate. Note that the fact that $|n_{\bar{a}} - \mathbf{N}_{a_{\bar{a}}}| \leq 0$ can be seen from the structure of the outer sums in (14.7), see also the discussion of explicit matrix elements, especially equation (14.18).

Despite being explicit, the finite sum expression (14.26) is rather lengthy. For concrete calculations it is therefore often more convenient to work with the integral formula, which in particular treats all \mathcal{R} -operators on nearly the same footing, the only difference being the contour of integration.

14.3 Generating the operatorial Q-system

The matrix elements for \mathcal{R} -operators of the lowest level which we calculated above are sufficient to generate the entire operatorial Q-system. Our strategy is to first combine these matrix elements into matrix elements of the respective Q-operators by taking products and tracing out the auxiliary Fock spaces. For each magnon block, these operators can be represented as explicit matrices of finite size. Systematically solving the functional relations, we determine all other Q-operators in a given magnon block.

Evaluating the supertrace for the lowest level

Using the matrix elements of the \mathcal{R} -operators of the lowest level given in (14.20), one can construct matrix elements of the full Q-operators. For states of length L these matrix elements are given by

$$\begin{aligned} & \left(\langle \tilde{\mathbf{m}}^{(L)} | \dots \langle \tilde{\mathbf{m}}^{(1)} | \right) \mathbf{Q}_{\{a\}}(z) \left(| \mathbf{m}^{(1)} \rangle \dots | \mathbf{m}^{(L)} \rangle \right) \\ &= (-1)^{\sum_{i < j} |\tilde{\mathbf{m}}^{(i)}| (|\mathbf{m}^{(i)}| + |\tilde{\mathbf{m}}^{(i)}|)} e^{iz\phi_a} \widehat{\text{str}} \left(\langle \tilde{\mathbf{m}}^{(1)} | \mathcal{R}_{\{a\}}(z) | \mathbf{m}^{(1)} \rangle \dots \langle \tilde{\mathbf{m}}^{(L)} | \mathcal{R}_{\{a\}}(z) | \mathbf{m}^{(L)} \rangle \right). \end{aligned} \quad (14.27)$$

Here we denote the Graßmann degree of the state $| \mathbf{m}^{(i)} \rangle$ by $| \mathbf{m}^{(i)} |$. The matrix elements of the \mathcal{R} -operators are given in formula (14.20), together with the integral representation (14.14), and can easily be evaluated by hand, or using a computer algebra system such as Mathematica.

Of course these matrix elements still depend on the auxiliary space operators $\bar{\xi}_{a\bar{a}}$ and $\xi_{a\bar{a}}$. To evaluate (14.27), one first commutes all the auxiliary space operators either to the left or to the right, and combines them into number operators $\mathbf{N}_{a\bar{a}}$ as far as possible. All terms with any remaining raising or lowering operators can then be dropped since they are non-diagonal. Note that the normalized supertrace defined in (13.15) factors into traces over the individual Fock spaces of the different auxiliary space oscillators, $\widehat{\text{str}} = \prod_{a,b} \widehat{\text{str}}_{ab}$, where $\widehat{\text{str}}_{ab}$ traces out the oscillator (ξ_{ab}, ξ_{ba}) . Each of these traces is then given in terms of ordinary sums over the diagonal terms. As discussed in section 13.2, some of the bosonic traces however need to be regularized, by giving the twist angles small imaginary parts.

Only a closed set of few different types of sums can occur when calculating the traces $\widehat{\text{str}}_{ab}$, including sums over rational functions and the Lerch transcendent (13.41). For the Q-operators of the lowest level, the following formulas are therefore sufficient to perform the occurring sums. First, for polynomials in the number operators, we can use

$$\widehat{\text{str}}_{ab} \mathbf{N}_{ab}^k = \begin{cases} \frac{\sum_{n=0}^k \binom{k}{n} \left(\frac{\tau_a}{\tau_b} \right)^{n+1-\delta_{k,0}}}{\left(1 - \frac{\tau_a}{\tau_b} \right)^k} & \text{bosonic} \\ \left(\frac{\tau_a}{\tau_a - \tau_b} \right)^{1-\delta_{k,0}} & \text{fermionic} \end{cases}, \quad (14.28)$$

where $\langle k \rangle_n$ are the Eulerian numbers defined by

$$\langle k \rangle_n = \sum_{j=0}^{n+1} (-1)^j \binom{k+1}{j} (n-j+1)^k. \quad (14.29)$$

Here and in the following we abbreviate the twist angles via $\tau_a = \exp(-i\phi_a)$.

For the non-rational Q-operators, we also need the Lerch transcendent Φ defined in (13.41), since the matrix elements of the \mathcal{R} -operators are rational functions of the number operators. Concretely one encounters traces of the form

$$\widehat{\text{str}}_{ab} \frac{\mathbf{N}_{ab}^k}{(\mathbf{N}_{ab} + r)^\ell} = \begin{cases} \frac{\tau_b - \tau_a}{\tau_b} \sum_{m=0}^k \binom{k}{m} (-r)^{k-m} \Phi_{\ell-m}^{\tau_a/\tau_b}(r) & \text{bosonic} \\ \frac{1}{\tau_b - \tau_a} \left(\delta_{k,0} \tau_b \frac{1}{r^\ell} - \tau_a \frac{1}{(r+1)^\ell} \right) & \text{fermionic} \end{cases}. \quad (14.30)$$

If further traces have to be evaluated, summation formulas for the Lerch transcendent can be used

$$\widehat{\text{str}}_{ab} \Phi_\ell^\tau(\mathbf{N}_{ab} + r) = \begin{cases} \frac{\tau_b - \tau_a}{\tau_b - \tau_a} \left(\tau \Phi_\ell^\tau(r) - \frac{\tau_a}{\tau_b} \Phi_\ell^{\tau_a/\tau_b}(r) \right) & \text{bosonic} \\ \frac{\tau_b}{\tau_b - \tau_a} \left(\tau_b \Phi_\ell^\tau(r) - \tau_a \Phi_\ell^\tau(r+1) \right) & \text{fermionic} \end{cases}, \quad (14.31)$$

and the general case

$$\widehat{\text{str}}_{ab} \mathbf{N}_{ab}^k \Phi_\ell^\tau(\mathbf{N}_{ab} + r) \quad (14.32)$$

$$= \begin{cases} \frac{\tau_b - \tau_a}{\tau_b} \left\{ \frac{\delta_{k,0} + \sum_{t=1}^k \langle t-1 \rangle \left(\frac{\tau_a/\tau_b}{1 - \tau_a/\tau_b} \right)^t}{\left(1 - \frac{\tau_a/\tau_b}{\tau} \right)^{k+1}} \Phi_\ell^\tau(r) - \frac{1}{\tau} \sum_{s=0}^k \binom{k}{s} \frac{\delta_{s,k} + \sum_{t=1}^{k-s} \langle t-1 \rangle \left(\frac{\tau_a/\tau_b}{1 - \tau_a/\tau_b} \right)^t}{\left(1 - \frac{\tau_a/\tau_b}{\tau} \right)^{k-s+1}} \right. \\ \left. \times \left[\left(\sum_{j=0}^s \binom{s}{j} (1-r)^{s-j} \Phi_{\ell-j}^{\tau_a/\tau_b}(r-1) \right) - \delta_{s,0} \frac{1}{(r-1)^\ell} \right] \right\} & \text{bosonic} \\ \frac{1}{\tau_b - \tau_a} \left(\tau_b \delta_{k,0} \Phi_\ell^\tau(r) - \tau_a \Phi_\ell^\tau(r+1) \right) & \text{fermionic} \end{cases}.$$

Given that the matrix elements of the \mathcal{R} -operators are rational functions of the auxiliary space number operators, and that one can use partial fraction decompositions to expand terms with complicated denominators, it is evident that these types of supertraces are the only ones which can appear. This implies that all matrix elements of the lowest level Q-operators are either rational functions or – for non-compact Q-operators – can be written in terms of the Lerch transcendent. We note that one can usually reduce the number of terms containing this function using the identity

$$\Phi_k^\tau(z+1) = \frac{1}{\tau} \left(\Phi_k^\tau(z) - \frac{1}{z^k} \right). \quad (14.33)$$

Due to the remaining u_1^{N+M} invariance which persists in the presence of twists, the Q-operators are block diagonal. These blocks correspond to sectors with a fixed number of magnons; they are labeled by the total excitation numbers $\sum_{i=1}^L m_a^{(i)}$ of the oscillators of the representation of $u_{p,q|r+s}$, see (13.28). By construction, one also needs to specify the number of sites L . For each such magnon block, the matrix elements can therefore be combined into a matrix of finite size. This gives the operatorial form of Q-operators in a subspace of the infinite-dimensional Hilbert space of non-compact models.

Constructing the Q-system from functional relations

Knowing Q-operators with a single index as explicit matrices for a given magnon block, one can produce all operators with multiple indices by solving the QQ-relations (13.17) and (13.18).² A naive way of solving the bosonic relation (13.17) however involves a matrix inversion, which is problematic given that the Q-operators are expressed in terms of special functions.

A more efficient strategy is to first calculate the Q-operators with one bosonic and one fermionic index $Q_{\{a,b\}}$ with $|a| \neq |b|$. To obtain these, we need to solve the first order difference equation given by (13.18):

$$Q_{\{a,b\}}(z) - Q_{\{a,b\}}(z + 1) = -\Delta_{ab} Q_{\{a\}}(z + \frac{1}{2}) Q_{\{b\}}(z + \frac{1}{2}), \quad |a| \neq |b|. \quad (14.34)$$

The formal solution to this equation can be written in terms of the discrete analogue of integration, which we denote by Σ and which is defined by

$$\Sigma[f(z) - f(z + 1)] = f(z) + \mathcal{P}, \quad (14.35)$$

where \mathcal{P} is periodic, $\mathcal{P}(z) = \mathcal{P}(z + 1)$. The discrete integral can be written as a sum, $\Sigma[f(z)] = \sum_{n=0}^{\infty} f(z+n)$, whenever this sum converges. For the Q-operators with one bosonic and one fermionic index we can thus write

$$Q_{\{a,b\}}(z) = -\Delta_{ab} \Sigma[Q_{\{a\}}(z + \frac{1}{2}) Q_{\{b\}}(z + \frac{1}{2})] \quad |a| \neq |b|. \quad (14.36)$$

It is important to note that in contrast to the untwisted case, the arbitrary periodic function \mathcal{P} is fixed to be zero if we require the Q-operators obtained from (14.36) to be identical to the monodromy construction, since \mathcal{P} is incompatible with the exponential scaling in terms of the twist phases.

When solving the difference equation (14.36) for non-compact Q-operators, the sums lead to generalizations of the Lerch transcendent (13.41), which we define by³

$$\Phi_{a_1, a_2, \dots, a_n}^{\tau_1, \tau_2, \dots, \tau_n}(z) = \sum_{0 \leq k_1 < k_2 < \dots < k_n} \frac{\tau_1^{k_1} \tau_2^{k_2} \dots \tau_n^{k_n}}{(z + k_1)^{a_1} (z + k_2)^{a_2} \dots (z + k_n)^{a_n}}. \quad (14.37)$$

Here the number of parameters n is arbitrary. Note that the variables τ_i will be given in terms of the twist variables, but here the indices are not those of the oscillators, but just label the arguments. It is clear from the definition that the generalized Lerch transcendent satisfies the following shift identity, generalizing equation (14.33):

$$\Phi_{a, a_1, \dots, a_n}^{\tau, \tau_1, \dots, \tau_n}(z) = \frac{\tau_1 \dots \tau_n}{z^a} \Phi_{a_1, \dots, a_n}^{\tau_1, \dots, \tau_n}(z + 1) + \tau \tau_1 \dots \tau_n \Phi_{a, a_1, \dots, a_n}^{\tau, \tau_1, \dots, \tau_n}(z + 1). \quad (14.38)$$

Importantly, Φ -functions satisfy so called stuffle-relations, e.g.

$$\Phi_{a_1}^{\tau_1} \Phi_{a_2}^{\tau_2} = \Phi_{a_1, a_2}^{\tau_1, \tau_2} + \Phi_{a_1 + a_2}^{\tau_1 \tau_2} + \Phi_{a_2, a_1}^{\tau_2, \tau_1}. \quad (14.39)$$

These can be used to linearize all products of these functions.

In the generation of the full Q-system, we need to apply the discrete integration Σ to the following four classes of functions, which form a closed set.

² We assume that these functional relations hold. Using the approach we present here, recovering the known expression for $Q_{\bar{z}}$ given in (13.20) constitutes a non-trivial check.

³ The treatment here is equivalent to that of η -functions given in Marboe, Volin, "Quantum spectral curve as a tool for a perturbative quantum field theory", 1411.4758 and Gromov, Levkovich-Maslyuk, "Quantum Spectral Curve for a cusped Wilson line in $\mathcal{N} = 4$ SYM", 1510.02098. The Lerch transcendents are related to η -functions used in the Quantum Spectral Curve literature by $\Phi_{a_1, a_2, \dots, a_n}^{\tau_1, \tau_2, \dots, \tau_n}(z) = i^n \eta_{a_1, a_2, \dots, a_n}^{\tau_1, \tau_2, \dots, \tau_n}(iz)$. To our knowledge, this class of functions has not been studied in the mathematics literature.

Polynomials The discrete integral of monomial, $\Sigma(\tau^z z^a)$ is another polynomial with an overall exponential factor of the form $p(z) = \tau^z(c_a z^a + \dots + c_0)$ satisfying the constraint $p(z) - p(z + 1) = \tau^z z^a$. This constraint fixes $p(z)$ completely.⁴

Shifted inverse powers From the definition of the generalized Lerch transcendent one finds

$$\Sigma \left[\frac{\tau^z}{(z+m)^a} \right] = \tau^z \Phi_a^\tau(z+m). \quad (14.40)$$

Terms of the form $\frac{\tau^z \Phi}{(z+m)^a}$ Note that

$$\Sigma \left[\frac{\tau^z \Phi_{a_1, a_2, \dots, a_n}^{\tau_1, \tau_2, \dots, \tau_n}(z+1)}{z^a} \right] = \tau^z \Phi_{a, a_1, a_2, \dots, a_n}^{\tau, \tau_1, \tau_2, \dots, \tau_n}(z). \quad (14.41)$$

To evaluate $\Sigma \left[\frac{\tau^z \Phi_{a_1, a_2, \dots, a_n}^{\tau_1, \tau_2, \dots, \tau_n}}{(z+m)^a} \right]$, use (14.38) to align the shifts of the spectral parameter in the denominator and the numerator, and then use (14.41).

Terms of the form $\tau^z z^a \Phi$ To evaluate products of monomials and generalized Lerch transcendent, one can use the finite difference analogue of partial integration,

$$\Sigma [f(g - g^{[2]})] = fg - \Sigma [g^{[2]}(f - f^{[2]})]. \quad (14.42)$$

For $\Sigma[\tau^z z^a \Phi_{a_1, a_2, \dots, a_n}^{\tau_1, \tau_2, \dots, \tau_n}]$, set $f = (\tau_1 \cdots \tau_n)^z \Phi_{a_1, a_2, \dots, a_n}^{\tau_1, \tau_2, \dots, \tau_n}$ and $g - g^{[2]} = \left(\frac{\tau}{\tau_1 \cdots \tau_n}\right)^z z^a$. This can be used recursively until no terms of this type are present.

Due to the property $\mathbf{Q}_\emptyset = 1$, it is possible to write all other Q-operators as determinants of $\mathbf{Q}_{\{a\}}$ and $\mathbf{Q}_{\{a,b\}}$ with $|a| \neq |b|$ without any inversions, see e.g. Tsuboi (2010, 2013); Gromov et al. (2015):⁵

$$\mathbf{Q}_{\{a_1, \dots, a_m, b_1, \dots, b_n\}} = \frac{\prod_{i=1}^m \prod_{j=1}^n \Delta_{a_i b_j}}{\prod_{1 \leq i < j \leq m} \Delta_{a_i a_j} \prod_{1 \leq i < j \leq n} \Delta_{b_i b_j}} \quad (14.43)$$

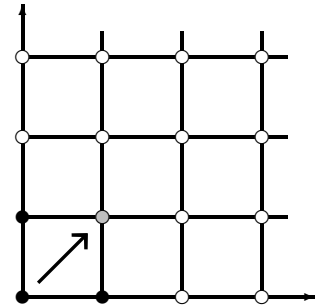
$$\times \begin{cases} (-1)^{(n-m)m} \epsilon^{k_1, \dots, k_n} \prod_{r=1}^m \frac{1}{\Delta_{a_r b_{k_r}}} \mathbf{Q}_{\{a_r, b_{k_r}\}}^{[*]} \prod_{s=1}^{n-m} \mathbf{Q}_{\{b_{k_m+s}\}}^{[n-m+1-2s]} & m < n \\ \epsilon^{k_1, \dots, k_m} \prod_{r=1}^m \mathbf{Q}_{\{a_{k_r}, b_r\}} & m = n \\ (-1)^{(n-m)n} \epsilon^{k_1, \dots, k_m} \prod_{r=1}^n \frac{1}{\Delta_{a_{k_r} b_r}} \mathbf{Q}_{\{a_{k_r}, b_r\}}^{[*]} \prod_{s=1}^{m-n} \mathbf{Q}_{\{a_{k_{m+s}}\}}^{[m-n+1-2s]} & m > n \end{cases}$$

where $|a_j| = 0$ and $|b_j| = 1$, \star can take any value in $-|m-n|, -|m-n|+2, \dots, |m-n|-2, |m-n|$, and $\mathbf{Q}^{[n]} = \mathbf{Q}(z + \frac{n}{2})$. The prefactor is a consequence of the normalization we use for the Q-operators (13.13), and follows from the more well known determinant formulas if one compares the different normalizations discussed at the end of section 13.2. The procedure to construct all Q-operators in this way is shown in Figure 14.2. As a consequence of this construction, one finds that the Q-operators only develop poles at $z \in \mathbb{N}$ or $z \in \mathbb{N} + \frac{1}{2}$, depending on the number of indices.⁶

4 Note that in the untwisted case where $\tau = 1$, the polynomial is of degree $a + 1$ instead.

5 Tsuboi, "Solutions of the T-system and Baxter equations for supersymmetric spin chains", 0906.2039; Tsuboi, "Wronskian solutions of the T, Q and Y-systems related to infinite dimensional unitarizable modules of the general linear superalgebra $gl(M|N)$ ", 1109.5524; and Gromov, Kazakov, Leurent, Volin, "Quantum spectral curve for arbitrary state/operator in AdS_5/CFT_4 ", 1405.4857

number of fermionic indices in set I (\bar{c}, \bar{d})



number of bosonic indices in set I (\bar{a}, \bar{b})

Figure 14.2: Generation of the full Q-system from the set of $\mathbf{Q}_{\{a\}}$. The black arrow signals the need to solve a difference equation. All Q-operators on the white vertices can then be obtained from the determinant formulas.

6 We would like to thank Dmytro Volin for pointing out that in general there are (equivalent) conjugated solutions of the Q-system, which in our conventions have poles on the negative real half-axis. For a discussion see e.g. section 4 of Gromov, Kazakov, Leurent, Volin, "Quantum spectral curve for arbitrary state/operator in AdS_5/CFT_4 ", 1405.4857. We suspect that these solutions can be found by particle-hole transforming the oscillators in the auxiliary space.

14.4 Expressions for higher-level Lax operators

We have seen that the Q-operators of the lowest level are enough data to generate the whole Q-system, and therefore the integral representation given in (14.7) and (14.14), or equivalently the finite sum representation (14.26) are in a sense sufficient. Still it would be desirable from a theoretical perspective to have similar formulas for all \mathcal{R} -operators. The \mathcal{R} -operators are almost symmetric under exchanging the index set $I \leftrightarrow \bar{I}$ with its complement, as can be seen already from the formula (13.12); this allows to derive a similar integral representation for the operators of the highest level. We then discuss the remaining levels: while many operators can immediately be written as finite sums, using the same strategy as for the lowest level, more complicated cases quickly appear, which we discuss using a $u_{2,2}$ example.

Highest level \mathcal{R} -operators and their matrix elements

In section 14.2 we derived a representation of \mathcal{R} -operators for the lowest level of the Q-system which allows to evaluate their matrix elements. Here we summarize similar results for the \mathcal{R} -operators of the highest non-trivial level, i.e. those where the index set I contains all but a single index which we denote by \bar{a} .

According to equation (14.5) we can write these \mathcal{R} -operators as

$$\mathcal{R}_{\{\bar{a}\}}(z) = \sum_{\{n_a\}=-\infty}^{\infty} \left[\prod_a (Y_{a\bar{a}})^{\Theta(n_a)|n_a|} \right] \mathbb{M}_{\{\bar{a}\}}(z, \{\mathbf{N}\}, \{n\}) \left[\prod_a (-X_{a\bar{a}})^{\Theta(-n_a)|n_a|} \right], \quad (14.44)$$

where X and Y are given in (14.1). After performing an almost identical calculation as for the \mathcal{R} -operators with a single index, we can write the diagonal part as follows:

$$\begin{aligned} \mathbb{M}_{\{\bar{a}\}}(z, \{\mathbf{N}\}, \{n\}) &= -\frac{\Gamma(z+1+\frac{1}{2}(-1)^{|\bar{a}|})}{\Gamma(z+1-c-\frac{1}{2}(-1)^{|\bar{a}|})} \\ &\times \int dt \frac{(-t)^{N_{\bar{a}}+(-1)^{|\bar{a}|-1}}}{(1-t)^{z+1+\frac{1}{2}(-1)^{|\bar{a}|}}} \prod_a \frac{1}{|n_a|!} {}_2F_1 \left(\begin{matrix} -N_a - N_{a\bar{a}} \\ 1 + |n_a| \end{matrix}; (-1)^{|\bar{a}|+|a|} t \right). \end{aligned} \quad (14.45)$$

Here the integration again depends on whether the oscillator with index \bar{a} is particle-hole transformed or not,

$$\int dt = \begin{cases} \frac{1}{\Gamma(N_{\bar{a}}+(-1)^{|\bar{a}|})} \int_0^1 dt & \text{if } |a| = 0 \text{ and } \omega_a = +1 \\ (-1)^{N_{\bar{a}}+1} \frac{\Gamma(1-N_{\bar{a}}-(-1)^{|\bar{a}|})}{2\pi i} \oint_{t=0} dt & \text{else} \end{cases}. \quad (14.46)$$

We can easily obtain matrix elements $\langle \tilde{\mathbf{m}} | \mathcal{R}_{\{\bar{a}\}}(z) | \mathbf{m} \rangle$ from this representation. First we note that occupation numbers $\tilde{\mathbf{m}}$ and \mathbf{m} fix the values of the

summation variables n_a , $a \in I$ in (14.44) to $n_a = \omega_a(\tilde{m}_a - m_a)$. The powers of the \bar{a} oscillators in the left and right factors are $N_\ell = \sum_a \Theta(n_a)|n_a|$ and $N_r = \sum_a \Theta(-n_a)|n_a|$, such that the occupation numbers of the states on which the diagonal part acts are

$$\hat{m}_{\bar{a}} = \tilde{m}_{\bar{a}} + \omega_{\bar{a}} N_\ell = m_{\bar{a}} + \omega_{\bar{a}} N_r \quad \hat{m}_a = \begin{cases} \min(m_a, \tilde{m}_a) & \text{if } \omega_a = 1 \\ \max(m_a, \tilde{m}_a) & \text{if } \omega_a = -1 \end{cases}. \quad (14.47)$$

We can thus write the matrix elements as

$$\begin{aligned} \langle \tilde{\mathbf{m}} | \mathcal{R}_{\{\bar{a}\}}(z) | \mathbf{m} \rangle = & \xi_{1\bar{a}}^{\Theta(\omega_1(\tilde{m}_1 - m_1))|\omega_1(\tilde{m}_1 - m_1)|} \dots \xi_{K\bar{a}}^{\Theta(\omega_K(\tilde{m}_K - m_K))|\omega_K(\tilde{m}_K - m_K)|} \\ & (-1)^{\sum_a |n_a| c'_{\bar{a}\bar{a}}} \left(\frac{\hat{m}_{\bar{a}}!}{\sqrt{\tilde{m}_{\bar{a}}! m_{\bar{a}}!}} \right)^{\omega_{\bar{a}}} \prod_a \sqrt{\frac{\max(m_a, \tilde{m}_a)!}{\min(m_a, \tilde{m}_a)!}} \mathbb{M}(z, \{\hat{m}_b\}, \{\omega_a(\tilde{m}_a - m_a)\}) \\ & \xi_{\bar{a}K}^{\Theta(-\omega_K(\tilde{m}_K - m_K))|\omega_K(\tilde{m}_K - m_K)|} \dots \xi_{\bar{a}1}^{\Theta(-\omega_1(\tilde{m}_1 - m_1))|\omega_1(\tilde{m}_1 - m_1)|}, \end{aligned} \quad (14.48)$$

where the sign follows from

$$\begin{aligned} c'_{\bar{a}\bar{a}} = & \left[(|a| + |a||\bar{a}|)\Theta(n_a) + (1 + |a||\bar{a}|)\Theta(-n_a) \right] + \frac{1}{2} \left[(|a| + 1)(1 - \omega_a)\Theta(n_a) + (|\bar{a}| + 1)(1 - \omega_{\bar{a}})\Theta(-n_a) \right] \\ & + \left[(|a| + |\bar{a}|) \sum_c |c| (\tilde{m}_c \Theta(n_a) + m_c \Theta(-n_a)) \right] + \left[\sum_{c < \bar{a}} |\bar{a}| |c| (\tilde{m}_c \Theta(n_a) + m_c \Theta(-n_a) + \delta_{ca}) \right] \\ & + \left[\sum_{c < \bar{a}} |a| |c| ((\Theta(n_c) + \tilde{m}_c)\Theta(n_a) + (\Theta(-n_c) + m_c)\Theta(-n_a)) \right], \end{aligned} \quad (14.49)$$

cf. equations (14.20) and (14.21).

Intermediate levels

We have seen that the \mathcal{R} -operators of the lowest level can conveniently be written either using the integral representation (14.14) or as finite sums as in (14.8) for the truncating operators or (14.26) for the non-truncating ones. Here we want to discuss the generalization of such representations to the remaining levels of the Q-system. For the intermediate levels, note that the difficulty of deriving representations without infinite sums does not increase according to the level $|I|$ of the operators \mathcal{R}_I , but rather by the number of infinite sums, or more precisely by the number of indices $a \in I$ which correspond to bosonic and particle-hole transformed oscillators, $|a| = 0$ and $\omega_a = -1$. If no such indices appear in the index set of \mathcal{R}_I , the formula (14.6) contains no infinite sum to begin with. Furthermore, for the case that there is exactly one such index, one can apply the same strategy as was used for the lowest level. Let this index be b ; then one can perform all sums over the variables $k_{b\bar{a}}$ in (14.6), and obtain a formula with an integral as in section 14.2, as well as the remaining finite sums. This expression can then be written in terms of only finite sums, using the Euler transformation and performing a Beta integral, as for the lowest level.

The first case where much more severe difficulties arise can best be discussed using a concrete example. Consider a $u_{2,2}$ invariant model, with oscillators $\mathbf{a}_1, \mathbf{a}_2, \mathbf{b}_3$ and \mathbf{b}_4 . Then the operator $\mathcal{R}_{\{3,4\}}$ contains two particle-hole transformed indices. After performing similar calculations as for the lowest level, one finds the following representation in terms of finite sums and an integral:

$$\begin{aligned} \mathcal{R}_{\{3,4\}}(z) &= e^{-\sum_{a,\bar{a}} \bar{\xi}_{a\bar{a}} \mathbf{a}_a \mathbf{b}_{\bar{a}}} \Gamma(z - \mathbf{N}_{\mathbf{a}_1} - \mathbf{N}_{\mathbf{a}_2}) e^{-\sum_{a,\bar{a}} \xi_{a\bar{a}} \bar{\mathbf{a}}_a \bar{\mathbf{b}}_{\bar{a}}} \\ &= \sum_{\{n_{a\bar{a}}\}=-\infty}^{+\infty} \left[\prod_{a,\bar{a}} (-\bar{\xi}_{a\bar{a}} \mathbf{a}_a \mathbf{b}_{\bar{a}})^{\Theta(+n_{a\bar{a}})|n_{a\bar{a}}|} \right] \mathbb{M}_{\{3,4\}}(z) \left[\prod_{a,\bar{a}} (-\xi_{a\bar{a}} \bar{\mathbf{a}}_a \bar{\mathbf{b}}_{\bar{a}})^{\Theta(-n_{a\bar{a}})|n_{a\bar{a}}|} \right], \end{aligned} \tag{14.50}$$

where the indices run over $a \in I = \{1, 2\}$ and $\bar{a} \in \bar{I} = \{3, 4\}$. Here the diagonal part $\mathbb{M}_{\{3,4\}}(z)$ can be written as

$$\begin{aligned} \mathbb{M}_{\{3,4\}}(z) &= \frac{(-1)^{N_{\mathbf{b}_3} + N_{\mathbf{b}_4}}}{n_{14}! n_{24}! N_{\mathbf{b}_3}! N_{\mathbf{b}_4}!} \sum_{k_{13}, k_{23}=0}^{\infty} \frac{(k_{13} + k_{23} + N_{\mathbf{b}_3})!}{k_{13}! k_{23}! (k_{13} + n_{13})! (k_{23} + n_{23})!} \\ &\times \frac{(n_{13} - N_{\mathbf{a}_1})_{k_{13}} (n_{23} - N_{\mathbf{a}_2})_{k_{23}} (1 + n_{13} + N_{13})_{k_{13}} (1 + n_{23} + N_{23})_{k_{23}}}{(n_{13} + n_{23} + N_{13} + N_{23} - N_{\mathbf{b}_3} + 1 - z)_{k_{13} + k_{23} + N_{\mathbf{b}_3}}} \\ &\times \int_0^1 t^{N_{\mathbf{b}_4}} (1-t)^{c-z} {}_3F_2(N_{\mathbf{a}_1} + 1, 1 - n_{13} + N_{\mathbf{a}_1}, -N_{14}; 1 - k_{13} - n_{13} + N_{\mathbf{a}_1}, 1 + n_{14}; t) \\ &\times {}_3F_2(N_{\mathbf{a}_2} + 1, 1 - n_{23} + N_{\mathbf{a}_2}, -N_{24}; 1 - k_{23} - n_{23} + N_{\mathbf{a}_2}, 1 + n_{24}; t), \end{aligned} \tag{14.51}$$

where the central charge is $\mathbf{c} = N_{\mathbf{a}_1} + N_{\mathbf{a}_2} - N_{\mathbf{b}_3} - N_{\mathbf{b}_4} - 2$. The formula is reminiscent of the integral formula (14.14), but involves generalized hypergeometric functions. Indeed it is even possible to write the integral in terms of finite sums, using an analogue of the Euler transformation which can be found in Miller and Paris (2013).⁷ This identity is however rather involved and not very explicit, and requires finding the zeros of an auxiliary polynomial. This renders it difficult to treat more difficult cases with more infinite sums recursively. While we found that for practical calculations the lowest level operators and the functional relation are very efficient, it would certainly be desirable to further investigate useful representations of the higher levels. We leave this for future work.

⁷ Miller, Paris, "Transformation formulas for the generalized hypergeometric function with integral parameter differences", *Rocky Mountain J. Math.* 43 02 (2013) 291–327

Q-operators for $\mathcal{N} = 4$ SYM

The reason for developing the technology necessary to evaluate the Q-operators of non-compact integrable super spin chains, which we presented in the last chapter, is of course to apply them to the spin chain describing $\mathcal{N} = 4$ SYM at one loop, and beyond.

In this chapter, we first show in section 15.1 how to specialize the construction of Q-operators presented in the last chapters to the representation relevant for the description of single trace operators in $\mathcal{N} = 4$ SYM, discussed in section 12.1. Furthermore, we provide a dictionary between the notation and conventions used in the literature on Q-operators and in the previous chapters, and those commonly used to describe the Quantum Spectral Curve, see section 12.2. In principle, the Q-operators for arbitrary magnon blocks can then be computed using the methods and formulas from the last chapter. Here we focus on some example calculations, which allow to highlight a number of observations. In particular, we will see the impact of the twists, which are a necessary ingredient of the monodromy construction of Q-operators, but result in a spin chain describing a non-commutative version of $\mathcal{N} = 4$ SYM.

In section 15.2, we show that the formulas for the matrix elements of Q-operators derived in section 14.2 also allow straightforward calculations for entire classes of states. We exemplify this by calculating the remarkably non-trivial one-index Q-functions of the BMN vacuum in fully twisted $\mathcal{N} = 4$ SYM, for arbitrary length.

Finally, we discuss an example magnon block from a rank one subsector of the theory in section 15.3, focusing on the local conserved charges, the mixing of states, and on the untwisted limit of the model. This discussion allows to draw first conclusions on the interpretation of states as single trace operators in the non-commutative field theory, and subtleties regarding the use of the Quantum Spectral Curve to compute higher-loop corrections to the operatorial Q-system.

15.1 Representation and conventions

In this section we want to show how the Q-operator construction and the methods for their evaluation can be applied to the $\mathcal{N} = 4$ SYM spin chain at the one-

Some of the results presented in this chapter have appeared in the author's publication Frassek, Marboe, Meidinger, "Evaluation of the operatorial Q-system for non-compact super spin chains", 1706.02320.

loop level. To make comparisons to other approaches easier, we also show how to convert our expressions to the conventions commonly used in the literature on the Quantum Spectral Curve.

From our construction we obtain the Q-operators for the theory with a full diagonal twist. This generalizes the well-know γ_i and β deformations¹ and includes twists of the space-time part of the symmetries, such that the field theory is not only non-conformal, but even non-commutative.² The results can be specialized to the γ_i and β deformed cases, or to the untwisted theory by choosing the twist angles appropriately. While this leads to divergent matrix elements in the Q-operators, their eigenstates and higher charges remain finite.

To specialize our construction to $\mathcal{N}=4$ SYM at one-loop, we first restrict to the singleton representation of $u_{2,2|4}$ by choosing a grading and applying particle-hole transformations as

$$\begin{aligned} (|a\rangle)_{a=1}^8 &= (0, 0, 1, 1, 1, 1, 0, 0), \\ (\omega_a)_{a=1}^8 &= (+1, +1, -1, -1, -1, -1, -1, -1), \end{aligned} \tag{15.1}$$

and requiring the vanishing of the central charge $\mathbf{c} = 0$. Comparing with (13.27), this given the representation of the fields of $\mathcal{N}=4$ SYM in terms of the oscillators $(\bar{\mathbf{a}}_1, \bar{\mathbf{a}}_2, \bar{\mathbf{d}}_1, \bar{\mathbf{d}}_2, \bar{\mathbf{d}}_3, \bar{\mathbf{d}}_4, \bar{\mathbf{b}}_1, \bar{\mathbf{b}}_2)$ introduced in section 12.1. With this choices, the representation has the scalar field \mathcal{Z} as the lowest-weight state:

$$|\mathcal{Z}\rangle = \bar{\mathbf{d}}_1 \bar{\mathbf{d}}_2 |0\rangle = |0, 0, 1, 1, 0, 0, 0, 0\rangle. \tag{15.2}$$

Comparing the conventions we used so far to describe Q-operators with the notation used in the Quantum Spectral Curve literature, cf. section 12.2, we see that they are related as follows. First, bosonic and fermionic indices are treated separately in QSC notation. To obtain Q-functions with the expected asymptotics, we call the Q-operators of the lowest level

$$\begin{aligned} (\mathbf{Q}_a)_{a=1}^8 &= (\mathbf{Q}_{\emptyset|1}, \mathbf{Q}_{\emptyset|2}, \mathbf{Q}_{1|\emptyset}, \mathbf{Q}_{2|\emptyset}, \mathbf{Q}_{3|\emptyset}, \mathbf{Q}_{4|\emptyset}, \mathbf{Q}_{\emptyset|3}, \mathbf{Q}_{\emptyset|4}) \\ &= (\mathbf{Q}_1, \mathbf{Q}_2, \mathbf{P}_1, \mathbf{P}_2, \mathbf{P}_3, \mathbf{P}_4, \mathbf{Q}_3, \mathbf{Q}_4), \end{aligned} \tag{15.3}$$

where the second equality defines the operators which appear in the $\mathbf{P}\mu$ and $\mathbf{Q}\omega$ systems of the Quantum Spectral Curve, cf. equation (12.11). To furthermore obtain the twist variables which were used in the discussion of the fully twisted QSC in Kazakov et al. (2016)³, we set

$$(e^{-i\phi_a})_{a=1}^8 = (\tau_a)_{i=a}^8 = (y_1, y_2, x_1, x_2, x_3, x_4, y_3, y_4). \tag{15.4}$$

Finally, the spectral parameter used in the QSC is related to ours by $z + \frac{1}{2} = iu$, and instead of the Lerch transcendents, the non-rational Q-operators are written in terms of so-called η -functions, which absorb factors of i in their definition and in the twisted case are given by

$$\eta_a^x(u) := \sum_{k=0}^{\infty} \frac{x^k}{(u + ik)^a}, \tag{15.5}$$

see for example appendix F of Gromov and Levkovich-Maslyuk (2016b),⁴ and

¹ Leigh, Strassler, “Exactly marginal operators and duality in four-dimensional $\mathcal{N}=1$ supersymmetric gauge theory”, [hep-th/9503121](#); Lunin, Maldacena, “Deforming field theories with $U(1) \times U(1)$ global symmetry and their gravity duals”, [hep-th/0502086](#); and Frolov, “Lax pair for strings in Lunin–Maldacena background”, [hep-th/0503201](#)

² See Beisert, Roiban, “Beauty and the twist: The Bethe ansatz for twisted $\mathcal{N} = 4$ SYM”, [hep-th/0505187](#) for a discussion of the subtleties which arise when trying to deduce the precise non-commutative field theory from the integrable spin chain description.

³ Kazakov, Leurent, Volin, “T-system on T-hook: Grassmannian Solution and Twisted Quantum Spectral Curve”, [1510.02100](#)

⁴ Gromov, Levkovich–Maslyuk, “Quantum Spectral Curve for a cusped Wilson line in $\mathcal{N} = 4$ SYM”, [1510.02098](#)

footnote 3 on page 172 for the relation between generalized eta functions and Lerch transcendents. These conventions ensure that the poles of non-polynomial Q-operators are located at the points required by the Quantum Spectral Curve.

15.2 Q-functions for the BMN vacuum in fully twisted $\mathcal{N}=4$ SYM

As a first application of the formulas derived for the matrix elements of the lowest level Q-operators in the last chapter to $\mathcal{N}=4$ SYM, and in order to give some further examples how they can be used in practice, we calculate the matrix elements of the single-index Q-operators with the BMN vacuum $\text{tr } \mathcal{Z}^L$ of arbitrary length L in fully twisted $\mathcal{N}=4$ SYM. Since these states constitute their own “magnon blocks”, we directly obtain the corresponding Q-functions in this case. Despite the fact that the BMN vacua are the most trivial states of the theory, we will see that in the presence of twists, their Q-functions are rather complicated.

\mathcal{R} -operators

We consider the matrix element of the single index \mathcal{R} -operators given in (14.14) with (14.20) between two scalars of type \mathcal{Z} , given in terms of occupation numbers in (15.2). For these matrix elements, there are no combinatorial factors and no signs. Since we look at matrix elements on the diagonal, all outer summation variables $n_{\bar{a}}$ in (14.7) are zero, and therefore there are no auxiliary space operators. This means that the values of the number operators in the diagonal part are fixed by $m_A = \tilde{m}_A = \hat{m}_A = (0, 0, 1, 1, 0, 0, 0, 0)$, cf. (14.18). Thus we only have to evaluate this diagonal part, given in (14.14).

If we denote the hypergeometric functions appearing in this equation as $F_{a\bar{a}}$, with indices matching those of the auxiliary space number operator that appears as a parameter, we can plug in the occupation numbers to obtain

$$F_{a\bar{a}} = \begin{cases} (1-t)^{N_{a\bar{a}}} & |a| = 0, \bar{a} = 1, 2, 3, 4 \\ 1 + tN_{a\bar{a}} & |a| = 1, \bar{a} = 1, 2, 3, 4 \\ 1 & \bar{a} = 5, 6, 7, 8 \end{cases} . \quad (15.6)$$

These functions determine the integrals appearing in the diagonal part (14.14). We start with evaluating the integral for \mathcal{R}_1 and find

$$\langle \mathcal{Z} | \mathcal{R}_1 | \mathcal{Z} \rangle = \frac{1}{2\pi i} \oint_{t=0} dt t^{-1} (1-t)^{-z-\frac{3}{2}+N_{12}+N_{13}+N_{14}} = 1 . \quad (15.7)$$

The calculation is identical for \mathcal{R}_2 such that

$$\langle \mathcal{Z} | \mathcal{R}_2 | \mathcal{Z} \rangle = 1 . \quad (15.8)$$

The next two types of matrix elements are likewise trivial, for \mathcal{R}_3 one finds

$$\langle \mathcal{Z} | \mathcal{R}_3 | \mathcal{Z} \rangle = \frac{1}{2\pi i} \oint_{t=0} dt t^{-1} (1-t)^{-z-\frac{1}{2}} (1+t\mathbf{N}_{31})(1+t\mathbf{N}_{32})(1+t\mathbf{N}_{34}) = 1, \quad (15.9)$$

and similarly for \mathcal{R}_4

$$\langle \mathcal{Z} | \mathcal{R}_4 | \mathcal{Z} \rangle = 1. \quad (15.10)$$

The other \mathcal{R} -operators have non-trivial matrix elements; for the polynomial operator \mathcal{R}_5 we have to evaluate a residue,

$$\begin{aligned} \langle \mathcal{Z} | \mathcal{R}_5 | \mathcal{Z} \rangle &= \frac{1}{2\pi i} \oint_{t=0} dt t^{-2} (1-t)^{-z-\frac{1}{2}} (1+t\mathbf{N}_{5,1})(1+t\mathbf{N}_{5,2})(1+t\mathbf{N}_{5,3})(1+t\mathbf{N}_{5,4}) \\ &= z + \frac{1}{2} + \mathbf{N}_{51} + \mathbf{N}_{52} + \mathbf{N}_{53} + \mathbf{N}_{54}, \end{aligned} \quad (15.11)$$

and a similar calculation gives for \mathcal{R}_6

$$\langle \mathcal{Z} | \mathcal{R}_6 | \mathcal{Z} \rangle = z + \frac{1}{2} + \mathbf{N}_{61} + \mathbf{N}_{62} + \mathbf{N}_{63} + \mathbf{N}_{64}. \quad (15.12)$$

The remaining operators are non-truncating, and the integrals are of Euler type, yielding a Beta function. For \mathcal{R}_7 ,

$$\begin{aligned} \langle \mathcal{Z} | \mathcal{R}_7 | \mathcal{Z} \rangle &= - \int_0^1 dt (1-t)^{-z-\frac{3}{2}+\mathbf{N}_{71}+\mathbf{N}_{72}+\mathbf{N}_{73}+\mathbf{N}_{74}} \\ &= \frac{1}{z + \frac{1}{2} - \mathbf{N}_{71} - \mathbf{N}_{72} - \mathbf{N}_{73} - \mathbf{N}_{74}}. \end{aligned} \quad (15.13)$$

Note that here we assume that the spectral parameter takes values such that the integral converges. Since the matrix elements of the Lax operators are rational functions, we can always perform this analytic continuation. \mathcal{R}_8 works in the same way,

$$\langle \mathcal{Z} | \mathcal{R}_8 | \mathcal{Z} \rangle = \frac{1}{z + \frac{1}{2} - \mathbf{N}_{81} - \mathbf{N}_{82} - \mathbf{N}_{83} - \mathbf{N}_{84}}. \quad (15.14)$$

Q-functions

We now calculate the actual Q-functions as

$$\langle \mathcal{Z}^L | \mathbf{Q}_a(z) | \mathcal{Z}^L \rangle = \widehat{\text{str}} \left(\langle \mathcal{Z} | \mathcal{R}_a(z) | \mathcal{Z} \rangle \right)^L, \quad (15.15)$$

where the BMN vacuum of length L is $|\mathcal{Z}^L\rangle = |\mathcal{Z}\rangle^{\otimes L}$ with $|\mathcal{Z}\rangle$ given in (15.2). Note that we ignore the exponential prefactor in the definition of the Q-operators, since it carries no information from the monodromy construction and depends on the conventions used for the Q-system, cf. section 13.2. From the expression for the matrix elements of the corresponding \mathcal{R} -operators given in (15.7), (15.8), (15.9) and (15.10) we see that

$$\langle \mathcal{Z}^L | \mathbf{Q}_a(z) | \mathcal{Z}^L \rangle = 1, \quad a = 1, 2, 3, 4. \quad (15.16)$$

For the other Q-functions, the traces lead to non-trivial expression. Using the multinomial theorem and the formula for the supertrace of polynomials in the number operators given in (14.28) we find for $\mathbf{Q}_{\{5\}}$,

$$\begin{aligned}
 \langle \mathcal{Z}^L | \mathbf{Q}_5(z) | \mathcal{Z}^L \rangle &= \widehat{\text{str}} \left[z + \frac{1}{2} + \mathbf{N}_{51} + \mathbf{N}_{52} + \mathbf{N}_{53} + \mathbf{N}_{54} \right]^L \\
 &= \widehat{\text{str}} \sum_{k+k_0+k_1+k_2+k_3+k_4=L} \binom{L}{k \ k_0 \ k_1 \ k_2 \ k_3 \ k_4} \frac{z^k}{2^{k_0}} \mathbf{N}_{51}^{k_1} \mathbf{N}_{52}^{k_2} \mathbf{N}_{53}^{k_3} \mathbf{N}_{54}^{k_4} \\
 &= \sum_{k=0}^L z^k \left[\sum_{k_0+k_1+k_2+k_3+k_4=L-k} \binom{L}{k \ k_0 \ k_1 \ k_2 \ k_3 \ k_4} \right. \\
 &\quad \left. \frac{\sum_{\ell_3=0}^{k_3} \binom{k_3}{\ell_3} \left(\frac{\tau_5}{\tau_3}\right)^{\ell_3+1-\delta_{k_3,0}} \sum_{\ell_4=0}^{k_4} \binom{k_4}{\ell_4} \left(\frac{\tau_5}{\tau_4}\right)^{\ell_4+1-\delta_{k_4,0}}}{2^{k_0} \left(\frac{\tau_5}{\tau_5-\tau_1}\right)^{\delta_{k_1,0}-1} \left(\frac{\tau_2}{\tau_5-\tau_2}\right)^{\delta_{k_2,0}-1} \left(1-\frac{\tau_5}{\tau_3}\right)^{k_3} \left(1-\frac{\tau_5}{\tau_4}\right)^{k_4}} \right].
 \end{aligned} \tag{15.17}$$

The Q-function $\langle \mathcal{Z}^L | \mathbf{Q}_{\{6\}}(z) | \mathcal{Z}^L \rangle = \langle \mathcal{Z}^L | \mathbf{Q}_{\{5\}}(z) | \mathcal{Z}^L \rangle |_{\tau_5 \rightarrow \tau_6}$ is obtained by a simple relabeling of the result for $\mathbf{Q}_{\{5\}}$, as was the case for the corresponding \mathcal{R} -operators.

We discuss the non-rational Q-functions in more detail, to showcase how the Lerch transcendent emerge from the supertraces. Considering $\mathbf{Q}_{\{7\}}$,

$$\langle \mathcal{Z}^L | \mathbf{Q}_7(z) | \mathcal{Z}^L \rangle = \widehat{\text{str}} (-1)^L \frac{1}{(-z - \frac{1}{2} + \mathbf{N}_{71} + \mathbf{N}_{72} + \mathbf{N}_{73} + \mathbf{N}_{74})^L}, \tag{15.18}$$

we can use (14.30) to first evaluate the fermionic traces, which still yield a rational expression,

$$\begin{aligned}
 \langle \mathcal{Z}^L | \mathbf{Q}_7(z) | \mathcal{Z}^L \rangle &= \widehat{\text{str}}_{71} \widehat{\text{str}}_{72} \frac{(-1)^L}{(\tau_4 - \tau_7)(\tau_3 - \tau_7)} \left[\frac{\tau_4 \tau_3}{(-z - \frac{1}{2} + \mathbf{N}_{71} + \mathbf{N}_{72})^L} \right. \\
 &\quad \left. - \frac{(\tau_3 + \tau_4) \tau_7}{(-z + \frac{1}{2} + \mathbf{N}_{71} + \mathbf{N}_{72})^L} + \frac{\tau_7^2}{(-z + \frac{3}{2} + \mathbf{N}_{71} + \mathbf{N}_{72})^L} \right].
 \end{aligned} \tag{15.19}$$

Now we take the first bosonic trace which according to (14.30) generates Lerch transcendent, summing up the poles in number operators,

$$\begin{aligned}
 \langle \mathcal{Z}^L | \mathbf{Q}_7(z) | \mathcal{Z}^L \rangle &= \widehat{\text{str}}_{71} \frac{(-1)^L (\tau_2 - \tau_7)}{\tau_2 (\tau_4 - \tau_7) (\tau_3 - \tau_7)} \left[\tau_4 \tau_3 \Phi\left(\frac{\tau_7}{\tau_2}, L, -z - \frac{1}{2} + \mathbf{N}_{71}\right) \right. \\
 &\quad \left. - (\tau_3 + \tau_4) \tau_7 \Phi\left(\frac{\tau_7}{\tau_2}, L, -z + \frac{1}{2} + \mathbf{N}_{71}\right) + \tau_7^2 \Phi\left(\frac{\tau_7}{\tau_2}, L, -z + \frac{3}{2} + \mathbf{N}_{71}\right) \right].
 \end{aligned} \tag{15.20}$$

Since the remaining auxiliary space number operator appears in the argument of the Lerch transcendent, we have to evaluate the last trace using (14.31):

$$\begin{aligned}
 \langle \mathcal{Z}^L | \mathbf{Q}_7(z) | \mathcal{Z}^L \rangle &= \frac{(-1)^L (\tau_2 - \tau_7) (\tau_1 - \tau_7)}{(\tau_4 - \tau_7) (\tau_3 - \tau_7) (\tau_1 - \tau_2)} \sum_{i=1,2} \frac{(-1)^i}{\tau_i} \left[\tau_4 \tau_3 \Phi\left(\frac{\tau_7}{\tau_i}, L, -z - \frac{1}{2}\right) \right. \\
 &\quad \left. - (\tau_3 + \tau_4) \tau_7 \Phi\left(\frac{\tau_7}{\tau_i}, L, -z + \frac{1}{2}\right) + \tau_7^2 \Phi\left(\frac{\tau_7}{\tau_i}, L, -z + \frac{3}{2}\right) \right].
 \end{aligned} \tag{15.21}$$

Finally the identity (14.33) allows to simplify this expression to

$$\begin{aligned} \langle \mathcal{Z}^L | \mathbf{Q}_7(z) | \mathcal{Z}^L \rangle &= \frac{(\tau_2 - \tau_7)(\tau_1 - \tau_7)}{(\tau_4 - \tau_7)(\tau_3 - \tau_7)} \left[\right. \\ &\quad \frac{1}{(z + \frac{1}{2})^L} + (-1)^L \frac{(\tau_2 - \tau_3)(\tau_2 - \tau_4)}{(\tau_1 - \tau_2)\tau_2} \Phi\left(\frac{\tau_7}{\tau_2}, L, -z - \frac{1}{2}\right) \\ &\quad \left. + (-1)^L \frac{(\tau_1 - \tau_3)(\tau_1 - \tau_4)}{(\tau_2 - \tau_1)\tau_1} \Phi\left(\frac{\tau_7}{\tau_1}, L, -z - \frac{1}{2}\right) \right]. \end{aligned} \quad (15.22)$$

The calculation proceeds similarly for $Q_{\{8\}}$, and gives

$$\langle \mathcal{Z}^L | \mathbf{Q}_{\{8\}}(z) | \mathcal{Z}^L \rangle = \langle \mathcal{Z}^L | \mathbf{Q}_{\{7\}}(z) | \mathcal{Z}^L \rangle |_{\tau_7 \rightarrow \tau_8}. \quad (15.23)$$

Note that these results can easily be converted into the conventions used for the (twisted) Quantum Spectral Curve, as outlined in section 15.1 above.

The calculations we presented here do not only provide a good example of the efficiency of the method developed in the last chapter, allowing the calculation of an entire class of Q-functions from first principles. They also showcase the fact that these functions tend to become extremely involved, already for comparatively simple states, due to the presence of twists.

15.3 A matrix example: local charges, untwisting, and single trace operators

The BMN vacuum is of course rather special, since it is an eigenstate of the model and – in a Bethe Ansatz language – features no excitations, or magnons. To give the reader an impression of the Q-operators in non-trivial magnon blocks, we now discuss an example from a rank one subsector, and present explicit matrices. We calculated these representations of the Q-operators using a Mathematica implementation of the method developed in chapter 14.

We consider a magnon block in one of the closed subsectors of the theory which enjoys $\mathfrak{su}_{1,1}$ invariance in the untwisted case. States in this sector are tensor products of the states

$$\mathcal{D}_{21}^k \mathcal{Z} = |0, k, 1, 1, 0, 0, k, 0\rangle, \quad (15.24)$$

and its magnon blocks have total occupation numbers $(0, S, L, L, 0, 0, S, 0)$, where L is the length and the spin S counts the number of excitations. The block with $L = S = 2$ is three-dimensional, and the Q-operators can be written as 3×3 matrices in the number basis

$$\begin{aligned} (1, 0, 0) &\sim \mathcal{Z} \otimes (\mathcal{D}_{21}^2 \mathcal{Z}), \\ (0, 1, 0) &\sim (\mathcal{D}_{21} \mathcal{Z}) \otimes (\mathcal{D}_{21} \mathcal{Z}), \\ (0, 0, 1) &\sim (\mathcal{D}_{21}^2 \mathcal{Z}) \otimes \mathcal{Z}. \end{aligned} \quad (15.25)$$

It is well-known that the local conserved charges of the model can be extracted from the Q-operators which correspond to the momentum-carrying levels of the Bethe Ansatz, see for example Frassek and Meneghelli (2013)⁵ for an in-depth discussion of the bosonic case. For $\mathcal{N}=4$ SYM, this means that we have to consider the central Q-operators, with two bosonic and two fermionic indices.

⁵ Frassek, Meneghelli, "From Baxter Q-Operators to Local Charges", 1207.4513

In the following, we pick the operator $\mathbf{Q}_{12|12}(u)$ as an example, using the QSC-like conventions from section 15.1, and the normalization with standard QQ-relations given in (13.24) and described in more detail there. In the basis (15.25), this operator takes the form

$$\mathbf{Q}_{12|12}(u) = \left(\frac{x_1 x_2}{y_1 y_2} \right)^{iu - \frac{1}{2}} \frac{(x_1 - x_2)(y_1 - y_2)}{(x_1 - y_1)(x_1 - y_2)(x_2 - y_1)(x_2 - y_2)} \times \begin{pmatrix} -u^2 - 2iu \frac{y_2 + y_3}{y_2 - y_3} + \frac{3y_2^2 + 2y_2 y_3 + 3y_3^2}{4(y_2 - y_3)^2} & -2iu \frac{y_3}{y_2 - y_3} + \frac{y_3(y_2 + y_3)}{(y_2 - y_3)^2} & \frac{2y_3^2}{(y_2 - y_3)^2} \\ -2iu \frac{y_2}{y_2 - y_3} + \frac{y_2(y_2 + y_3)}{(y_2 - y_3)^2} & -u^2 - iu \frac{y_2 + y_3}{y_2 - y_3} + \frac{y_2^2 + 6y_2 y_3 + y_3^2}{4(y_2 - y_3)^2} & -2iu \frac{y_3}{y_2 - y_3} + \frac{y_3(y_2 + y_3)}{(y_2 - y_3)^2} \\ \frac{2y_2^2}{(y_2 - y_3)^2} & -2iu \frac{y_2}{y_2 - y_3} + \frac{y_2(y_2 + y_3)}{(y_2 - y_3)^2} & -u^2 - 2iu \frac{y_2 + y_3}{y_2 - y_3} + \frac{3y_2^2 + 2y_2 y_3 + 3y_3^2}{4(y_2 - y_3)^2} \end{pmatrix}. \quad (15.26)$$

As already observed in the case of the BMN vacuum, the twists lead to rather involved expressions for the matrix elements.

The most important conserved charges are the momentum p of the states, which we can extract in the form of the shift operator $\mathcal{S} = e^{ip}$,

$$\mathcal{S} = \frac{\mathbf{Q}_{12|12}(u + \frac{i}{2})}{\mathbf{Q}_{12|12}(u - \frac{i}{2})} = \frac{y_1 y_2}{x_1 x_2} \begin{pmatrix} 0 & 0 & 1 \\ 0 & \frac{y_2}{y_3} & 0 \\ \frac{y_2^2}{y_3^2} & 0 & 0 \end{pmatrix}, \quad (15.27)$$

and the Hamiltonian

$$\mathcal{H} = \frac{d}{du} \log \frac{\mathbf{Q}_{12|12}(u + \frac{i}{2})}{\mathbf{Q}_{12|12}(u - \frac{i}{2})} \Big|_{u=0} = i \begin{pmatrix} -3 & \frac{y_2 + y_3}{y_2} & \frac{y_2^2 + y_3^2}{2y_2^2} \\ \frac{y_2 + y_3}{y_3} & -4 & \frac{y_2 + y_3}{y_2} \\ \frac{y_2^2 + y_3^2}{2y_3^2} & \frac{y_2 + y_3}{y_3} & -3 \end{pmatrix}. \quad (15.28)$$

These matrices are diagonalized by the following states,

$$\begin{aligned} X &= \left(-\frac{y_3}{y_2}, 0, 1 \right) \xrightarrow{\text{untwist}} (-1, 0, 1), \\ K &= \left(\frac{y_3}{y_2}, -\frac{y_2 + y_3 + \sqrt{y_2^2 + 34y_2 y_3 + y_3^2}}{4y_2}, 1 \right) \xrightarrow{\text{untwist}} (1, 2, 1), \\ D &= \left(\frac{y_3}{y_2}, -\frac{y_2 + y_3 - \sqrt{y_2^2 + 34y_2 y_3 + y_3^2}}{4y_2}, 1 \right) \xrightarrow{\text{untwist}} (1, 1, 1), \end{aligned} \quad (15.29)$$

where we also indicate the states to which they flow when taking the untwisting

limit $x_a = y_i = 1$. The shift eigenvalues of the states are given by

$$\begin{aligned}\mathcal{S} X &= -\frac{y_1 y_2^2}{x_1 x_2 y_3} X \xrightarrow{\text{untwist}} -X, \\ \mathcal{S} K &= \frac{y_1 y_2^2}{x_1 x_2 y_3} K \xrightarrow{\text{untwist}} K, \\ \mathcal{S} D &= \frac{y_1 y_2^2}{x_1 x_2 y_3} D \xrightarrow{\text{untwist}} D.\end{aligned}\tag{15.30}$$

We see that the state X is (twisted) antisymmetric and has momentum π in the untwisted model. It therefore does not belong to the spectrum of $\mathcal{N}=4$ SYM. The primary K and D , the descendant of the length two BMN vacuum however obey the zero-momentum condition after removing the twists. To interpret them as single trace operators defined using the ordinary product⁶ in the twisted theory, one has to parametrize the twist such that $\frac{y_1 y_2^2}{x_1 x_2 y_3} = 1$. While the shift operator \mathcal{S} is still twisted under this constraint, all states have the same momentum as in the untwisted case. We will discuss this in more generality below.

Finally, the energies of the states are

$$\begin{aligned}\mathcal{H} X &= -i \frac{y_2^2 + 6y_2 y_3 + y_3^2}{2y_2 y_3} X \xrightarrow{\text{untwist}} -4i X, \\ \mathcal{H} K &= i \frac{y_2^2 - 14y_2 y_3 + y_3^2 - (y_2 + y_3) \sqrt{y_2^2 + 34y_2 y_3 + y_3^2}}{4y_2 y_3} K \xrightarrow{\text{untwist}} -6i K, \\ \mathcal{H} D &= i \frac{y_2^2 - 14y_2 y_3 + y_3^2 + (y_2 + y_3) \sqrt{y_2^2 + 34y_2 y_3 + y_3^2}}{4y_2 y_3} D \xrightarrow{\text{untwist}} 0,\end{aligned}\tag{15.31}$$

and the corresponding anomalous dimensions are given by $\gamma = 2ig^2 \mathcal{H}$, where the coupling is defined by $g = \frac{\sqrt{\lambda}}{4\pi}$.

It is also possible to directly get the untwisted charges in operator form. The procedure was used in Bazhanov et al. (2010)⁷ for the Heisenberg spin chain, and is discussed for supersymmetric models on the eigenvalue level in Kazakov et al. (2016).⁸ For each level of the Q-system, one so-called distinguished Q-operator can be recovered by multiplying any of the operators of this level by its inverse, evaluated at some arbitrary value of the spectral parameter, and then removing the twists. For our example, this yields

$$\begin{aligned}\mathbf{Q}_{12|12}^{\text{untwist}}(u; u_0) &= \lim_{x_a, y_i \rightarrow 1} \frac{\mathbf{Q}_{12|12}(u)}{\mathbf{Q}_{12|12}(u_0)} = \frac{1}{24u_0^3 - 2u_0} \\ &\times \begin{pmatrix} (u+u_0)(4u_0u + 8u_0^2 - 1) & -8u_0(u-u_0)(u+u_0) & (u-u_0)(4u_0u - 8u_0^2 + 1) \\ -8u_0(u-u_0)(u+u_0) & 2u_0(8u^2 + 4u_0^2 - 1) & -8u_0(u-u_0)(u+u_0) \\ (u-u_0)(4u_0u - 8u_0^2 + 1) & -8u_0(u-u_0)(u+u_0) & (u+u_0)(4u_0u + 8u_0^2 - 1) \end{pmatrix},\end{aligned}\tag{15.32}$$

and the untwisted shift operator and Hamiltonian follow from the same formulas (15.27) and (15.28) as in the twisted case, simply substituting the untwisted Q-operator $\mathbf{Q}_{12|12}^{\text{untwist}}$ for the twisted one. These operators are independent of the

⁶ I.e. not using the non-commutative star product, see Beisert, Roiban, "Beauty and the twist: The Bethe ansatz for twisted $\mathcal{N}=4$ SYM", [hep-th/0505187](https://arxiv.org/abs/hep-th/0505187) for a discussion of this point.

⁷ Bazhanov, Lukowski, Meneghelli, Staudacher, "A Shortcut to the Q-Operator", [1005.3261](https://arxiv.org/abs/1005.3261)

⁸ Kazakov, Leurent, Volin, "T-system on T-hook: Grassmannian Solution and Twisted Quantum Spectral Curve", [1510.02100](https://arxiv.org/abs/1510.02100)

normalization point u_0 . Note that only one untwisted Q-operator per level can be generated as in (15.32). While a general recipe for untwisting the other Q-functions by rotating the Q-functions appropriately can be found in Kazakov et al. (2016),⁹ a systematic approach to the untwisting of operatorial Q-systems remains an important open problem.

9 Kazakov, Leurent, Volin, “T-system on T-hook: Grassmannian Solution and Twisted Quantum Spectral Curve”, 1510.02100

To conclude this chapter, we briefly give an overview of general states. While we picked a particular example for the preceding discussion, essentially any Q-operator for any magnon block can be calculated using the method developed in chapter 14, which can quite easily be implemented using a computer algebra system. The twisted shift operator, defined in equation (15.27), has a rather simple structure, since its eigenvalues follow from the number of excitations, as each magnon picks up a characteristic twist when the state is rotated. This allows to discuss the interpretation of the spin chain states in some generality. The eigenvalues of the shift operator for a state are given in terms of its oscillator excitations by

$$\frac{Q_{12|12}(+\frac{i}{2})}{Q_{12|12}(-\frac{i}{2})} = e^{2\pi i \frac{k}{L}} \left(\frac{y_1^{n_{a_1}} y_2^{n_{a_2}}}{x_1^{n_{d_1}} x_2^{n_{d_2}} x_3^{n_{d_3}} x_4^{n_{d_4}} y_3^{L+n_{b_1}} y_4^{L+n_{b_2}}} \right)^{\frac{1}{L}}. \quad (15.33)$$

Here, the first factor with $k \in \mathbb{N}$ is a root of unity and corresponds to the eigenvalue of the state for vanishing twists. For twisted $\mathcal{N}=4$ SYM, one first has to restrict the Hilbert space to the twisted cyclic states, where the first factor is 1, i.e. $k=0$. In order to have a correspondence with single trace operators, i.e. ordinary products of fields with a cyclic trace over the color structure, it is however necessary to ensure that also the second factor is 1. Then, despite the fact that both the states as well as the shift operator depend on the twists, its eigenvalues are the same as for the untwisted spin chain.

We can see how this works in the case of the γ_i -deformed theory. Here, in addition to the general constraint $x_1 x_2 x_3 x_4 = y_1 y_2 y_3 y_4 = 1$, the twists of the AdS/conformal part of the symmetry vanish, $y_1 = y_2 = y_3 = y_4 = 1$. In addition, the remaining twists are parametrized by the three parameters γ_i , with a dependence on the excitation numbers:

$$\begin{aligned} x_1 &= e^{\frac{i}{2}\gamma_1(n_{d_4}-n_{d_3})} e^{\frac{i}{2}\gamma_2(n_{d_2}-n_{d_4})} e^{\frac{i}{2}\gamma_3(n_{d_2}-n_{d_3})}, \\ x_2 &= e^{\frac{i}{2}\gamma_1(n_{d_3}-n_{d_4})} e^{\frac{i}{2}\gamma_2(n_{d_3}-n_{d_1})} e^{\frac{i}{2}\gamma_3(n_{d_4}-n_{d_1})}, \\ x_3 &= e^{\frac{i}{2}\gamma_1(n_{d_1}-n_{d_2})} e^{\frac{i}{2}\gamma_2(n_{d_4}-n_{d_2})} e^{\frac{i}{2}\gamma_3(n_{d_1}-n_{d_4})}, \\ x_4 &= e^{\frac{i}{2}\gamma_1(n_{d_2}-n_{d_1})} e^{\frac{i}{2}\gamma_2(n_{d_1}-n_{d_3})} e^{\frac{i}{2}\gamma_3(n_{d_3}-n_{d_2})}. \end{aligned} \quad (15.34)$$

This parametrization removes the redundancy in the twists by ensuring that the constraint $x_1 x_2 x_3 x_4 = 1$ is satisfied; moreover, it renders $x_1^{n_{d_1}} x_2^{n_{d_2}} x_3^{n_{d_3}} x_4^{n_{d_4}} = 1$. Therefore the shift eigenvalues (15.33) are indeed given by roots of unity.

For the fully twisted theory, a similar parametrization is likely required, using six independent parameters, and a relation involving the six $\mathfrak{psu}_{2,2|4}$ charges of the states, generalizing (15.34).

In principle, the matrix representatives of the Q-operators in each magnon block can be used as input data for perturbative calculations using the Quantum Spectral Curve, along the lines of Marboe and Volin (2015).¹⁰ Indeed, this is the main motivation for the work presented in this and the last chapters. Some subtle issues have however to be overcome: the reparametrization of the twists just discussed introduces a novel source of dependence on the anomalous dimension into higher-loop calculations, which will be interesting to investigate;¹¹ while the QSC is believed to have the same structure for the fully twisted theory, its perturbative behavior remains to be investigated. More importantly, the operatorial form of the QSC might pose further challenges. For example, we expect that the consistency of these calculations will require some magnon blocks to be fused into larger matrices, capturing the length-changing effects at higher loop order, which prevents a QISM construction of the Q-operators in the first place. It will be exciting to see this effect emerging from the viewpoint of the QSC. In general, being able to obtain eigenstates at high loop order promises to deepen our understanding of the $\text{AdS}_5/\text{CFT}_4$ system as an integrable model. In particular it might shed new light on the question of how integrability emerges from the field theory.

¹⁰ Marboe, Volin, “Quantum spectral curve as a tool for a perturbative quantum field theory”, [1411.4758](#)

¹¹ In preliminary experiments with the Quantum Spectral Curve, we indeed found that such a constraint is necessary for the consistency of the calculations.

Conclusion

In this thesis we investigated the interpretation of form factors as states of the integrable spin chain model underlying $\mathcal{N} = 4$ SYM at weak coupling. To this end, we developed on-shell methods for this class of quantities. We also showed that nonplanar on-shell functions, which are related to those of form factors, exhibit partial Yangian invariance beyond the planar limit; some of them even play a role as intertwiners on the spin chain. To make progress towards a way of calculating the states of the integrable model at higher loop order, we developed efficient methods to calculate Baxter Q-operators for non-compact super spin chains, which can be used as input data for the yet to be investigated operatorial form of the Quantum Spectral Curve. Here we summarize our main results.

In the first of the three parts of this thesis we developed and investigated some on-shell methods for form factors. In particular this shows that the corresponding formulations and techniques are applicable to partially off-shell quantities.

We first showed in chapter 3 how BCFW recursion relations lead to diagrammatic representations of tree-level form factors of the chiral stress-tensor multiplet which are almost identical to amplitude on-shell diagrams, but contain the minimal form factor as an additional vertex. These diagrams inherit many of the properties of their amplitude counterparts; in particular we described how many of them can be understood by inverse soft factors, and how permutations can be associated to them.

Building on the observation that form factor “top-cell” diagrams (corresponding to top dimensional forms on the Grassmannian) are related to the amplitude top-cell diagrams by the simple mapping, shown graphically in (3.15), replacing a box diagram by the minimal form factor, we developed a Grassmannian picture for the off-shell kinematics of the form factor, and a method to glue the minimal form factor into arbitrary on-shell diagrams in chapter 4. These tools then allowed to obtain a Grassmannian integral representation for form factors, given in equations (4.24) and (4.25). This is the main result of the first part of this work, and a first indication that Grassmannian, or generally geometric formulations exist for objects which are more general than scattering amplitudes, in particular for quantities involving off-shell kinematics. We furthermore translated the Grassmannian integral to twistor (equation (4.39)) and momentum twistor space (equation (4.60)), and calculated a variety of example form factors from

this representation. In chapter 5, we derived the BCFW contour prescription for the NMHV integral, given in equation (5.21), which allows to calculate all form factors with this MHV degree. To make progress towards an understanding of the contour for all form factors, we investigated the Graßmannian representation of the connected prescription for form factors in chapter 6. Remarkably we found that in contrast to the amplitude case, this formulation cannot easily be mapped to the Graßmannian integral derived from on-shell diagrams, and thus seem to provide a rather different representations of the same quantity.

In the second part of this thesis, building on the on-shell diagrams we developed for form factor, we investigated the integrability properties of on-shell functions with arbitrary operator insertions, as well as nonplanar amplitude on-shell functions. We proved hidden symmetries of these quantities and discussed their interpretation as spin chain states.

In chapter 8, we turned the on-shell diagram construction for form factors of the chiral stress-tensor multiplet into an integrability-based R-operator formalism, which generalized the amplitude version by considering the minimal form factor as an additional vacuum state. This leads to deformations of the form factors, and allows to easily investigate the integrability-related symmetries of the functions. We explicitly showed that, while not Yangian invariant, form factor on-shell functions are annihilated by integrable transfer matrices, see equation (8.27). They can thus be considered as eigenstates of the spin chain model. The construction also allowed us to consider on-shell functions with an insertion of an arbitrary operator, which likewise are eigenstates of the transfer matrix, with eigenvalues related to those of the single trace operator in the spectral problem (equation (8.38)). We furthermore showed in chapter 10 that in addition to the symmetries generated by the transfer matrix, a part of the Yangian invariance of “pure” on-shell functions persists in the presence of the operator insertion; these symmetries are given in equation (10.15).

As a further generalization, we considered nonplanar on-shell diagrams and the corresponding on-shell functions, which play a role as leading singularities in nonplanar loop calculations, and bear some resemblance with form factor on-shell functions. In chapter 9, we defined an action of Yangian generators on these diagrams, using the RTT formalism and restricting to individual boundaries of the diagrams, on which a well-defined ordering of states is possible. We found that in this sense, nonplanar on-shell functions are, remarkably, still partially Yangian invariant; the higher levels of the Yangian still annihilate them, as presented in equation (9.16). The first few levels of symmetries are broken, with the number of broken symmetries governed by the amount of nonplanarity in a precise way. We derived additional symmetries which are given in equation (9.24), and are written in terms of the transfer matrix. A main result of this chapter is the identity (9.21) for diagrams on cylinders. It is essentially a conservation law of higher charges and can be interpreted as an intertwining relation, and allows to think of these diagrams as members of the commuting family of operators of the integrable model.

All the quantities we discussed have representations in terms of Graßmann-

ian integrals. In chapter 11 we proved a curious relation (equation (11.13)) that maps the $\mathfrak{gl}_{4|4}$ transfer matrix, acting on such an integral, to a \mathfrak{gl}_k transfer matrix acting on the integrand. This relation, as well as a related formula for the generators of the Yangian, can conveniently be used to check and investigate the symmetries we derived for Grassmannian integrals corresponding to different types of on-shell diagrams. The map between spin chains is also quite interesting in its own right, and we started a preliminary study of the spin chains that have the Grassmannian integrands as eigenstates. In particular we showed that the MHV case corresponds to an integrable model which previously appeared in the context of high energy scattering in QCD.

In the final, third part of this thesis, we turned to the states of the integrable model behind planar $\mathcal{N}=4$ SYM describing single trace operators, and investigated Baxter Q-operators for the spin chain at the one-loop level. Given the recent successes of the Quantum Spectral Curve, which describes the eigenvalues of these operators at finite coupling in a beautiful and concise way, the development of methods to calculate the Q-operators at one loop is an important step to lift the QSC to the full operatorial form of the Q-system, and thus to calculate the states of the model at higher loop order.

After reviewing single trace operators, the QSC, and Q-operators in chapter 12, we gave a derivation of the Lax operators necessary for the monodromy construction of Q-operators of rational super spin chains with Jordan-Schwinger type representations, in chapter 13. We defined these Q-operators and their functional relations, and discussed the relevant representations of the non-compact algebras $\mathfrak{u}_{p,q|r+s}$. For these representations, the Lax and consequently also the Q-operators are given in terms of infinite sums over intermediate states, rendering concrete calculations extremely difficult. We exemplified this problem, as well as our solution for spin $-s$ Heisenberg models. Based on the form of the Lax operators, we then discussed the structure of the Q-system for the general case, where the knowledge about the infinite sums allows to separate the Q-operators into two classes, with distinct analytic structures.

In chapter 14, we then developed a general method to explicitly evaluate such non-compact Q-systems, providing all necessary formulas for practical calculations. We first derived an integral representation of the Lax operators of the lowest level which does not feature infinite sums. This allows to calculate the matrix elements of the operators between states in the physical space. We provided formulas to evaluate the supertraces giving the matrix elements of the corresponding Q-operators in terms of a restricted class of special functions. Since the Q-operators are block diagonal, these matrix elements can be assembled into finite representative matrices for each magnon sector, and all other Q-operators can be then recovered by solving the functional QQ-relations.

Finally, we applied this much more general technology to $\mathcal{N}=4$ SYM at one loop in chapter 15. We showed how it can be used to calculate the Q-functions of the BMN vacuum state in fully twisted $\mathcal{N}=4$ SYM for arbitrary length. Using a magnon block from a rank one sector of theory as an example, we discussed further important aspects, such as the calculation of the local charges, and the

untwisting of the model. Since the presence of twists for the space-time part of the symmetry algebra renders the field theory described by this spin chain non-commutative, we furthermore discussed parametrizations of the twists which are necessary to interpret the cyclic states as single trace operators. This aspect is all the more important for using the Q-operators we calculated as input data for perturbative calculations using the Quantum Spectral Curve, as we are doing in ongoing work. Via this approach, the methods we developed here are a crucial first step for obtaining the eigenstates of the model – twisted and untwisted – at higher loop order. We hope that this information will shed new light on the mysterious way in which integrability emerges from a four-dimensional field theory.

Open problems & directions for future research

One of the features which sets on-shell diagrams and the associated Graßmannian integrals for form factors apart from their amplitude counterparts is the necessity of multiple top-cell diagrams. The fact that these diagrams are related by cyclic relabellings is clearly an indication that the formalism does not take the color structure of form factors, with the operators a color singlet, properly into account. Is it possible to have a single top-cell diagram for form factors? We expect that if this is the case, one will likely have to consider nonplanar diagrams.

To make the Graßmannian integral a useful tool for the calculation of any form factor, a general expression for the contour is needed, extending our result for NMHV form factors presented in chapter 5. While it is possible to attack this problem via the BCFW recursion relations, an approach using the connected prescription would likely be more fruitful, as it was for amplitudes. However, as chapter 6 showed, the relation of this formulation to the Graßmannian integral seems to be rather subtle for form factors. We hope that further investigations of this issue will provide a better understanding of both representations of form factors. It might also be interesting to consider the idea that reality conditions on the kinematics uniquely determine the contour in this context.¹

The program of investigating on-shell diagrams and related ideas for form factors closely mirrors previous developments for amplitudes, but currently, results at loop level are completely missing. In particular it remains to be shown whether all loop recursion relations similar to those in equation (2.40) exist. One could also ask if some “formfactorhedron” space exists, which describes form factors in a purely geometric way, generalizing the amplituhedron.² Hints for such a generalization might come from the on-shell diagram representation of the amplituhedron,³ and its relation to the Yangian,⁴ as well as similar constructions for correlation functions.⁵

Finally, it is natural to wonder whether on-shell diagrams and Graßmannian integrals can be adopted to a wider range of quantities, such as generalized form factors with multiple operator insertion, or even correlation functions without

1 Kanning, Ko, Staudacher, “Graßmannian integrals as matrix models for non-compact Yangian invariants”, [1412.8476](#)

2 Arkani-Hamed, Trnka, “The Amplituhedron”, [1312.2007](#); and Arkani-Hamed, Trnka, “Into the Amplituhedron”, [1312.7878](#)

3 Bai, He, “The Amplituhedron from Momentum Twistor Diagrams”, [1408.2459](#)

4 Ferro, Łukowski, Orta, Parisi, “Yangian Symmetry for the Tree Amplituhedron”, [1612.04378](#)

5 Chicherin, Doobary, Eden, Heslop, Korchemsky, Mason, Sokatchev, “Correlation functions of the chiral stress-tensor multiplet in $\mathcal{N} = 4$ SYM”, [1412.8718](#); and Eden, Heslop, Mason, “The Correlahedron”, [1701.00453](#)

any external on-shell states. It would also be desirable to investigate insertions of arbitrary single trace operators (in particular from an integrability viewpoint, see chapter 8). The fact that ideas presented in this work have already been successfully used for off-shell gluons parametrized via Wilson lines in Bork and Onishchenko (2017a)⁶ raises hope that they are indeed more widely applicable.

The most pressing question concerning the symmetries derived in Part II of this work, for form factor and nonplanar on-shell functions, is how constraining they ultimately turn out to be.

For nonplanar on-shell diagrams, a starting point for such an investigation could be the recent work Bourjaily et al. (2016),⁷ which presented a classification of on-shell forms on the Grassmannian $G(3, 6)$. It would be very interesting to see whether the top-forms given there are completely determined from the symmetries derived in chapter 9; for this task, applying the symmetry generators directly on the level of the form using the mapping discussed in chapter 11 could prove very useful.

Nonplanar on-shell diagrams do not represent full contributions to the amplitude or its integrand. Given the remarkable properties amplitudes in $\mathcal{N}=4$ SYM seem to enjoy even in subleading contributions of the $\frac{1}{N}$ expansion,⁸ we think that the hidden symmetries of the nonplanar leading singularities might serve as well-motivated candidate symmetries which might be lifted to (parts of) the amplitude integrand. In particular we would like to stress that the RTT formulation circumvents the necessity to use dual momenta which are unavailable in the nonplanar case.

In a broader context we hope that having discovered at least traces of integrability for quantities appearing in nonplanar $\mathcal{N}=4$ SYM is a motivation to reconsider the problem of integrability beyond the planar limit in more generality, in particular in the light of recent advances for correlation functions.⁹

From a spin chain perspective, it would furthermore be interesting to see if some kind of Bethe Ansatz allows to determine nonplanar and form factor on-shell functions. For Yangian invariants, such an Ansatz was developed in Frassek et al. (2014),¹⁰ but not fully worked out for the case of the $\mathcal{N}=4$ SYM spin chain. In both cases such a generalization of the Bethe Ansatz would be rather novel, as the monodromy and transfer matrices act only on a subset of the spin chain sites; again there might be interesting intersections with the work on correlation functions, in particular the lowest order “tailoring” picture. Of course, the question of how to incorporate general operators poses itself also here.

Concerning the interpretation of the Grassmannian integral as a map between two different spin chains which we presented in chapter 11, many questions remain open. We clearly lack an understanding of why it works, and how it can be used. It would be desirable to find further \mathfrak{gl}_k invariant states on the spin chain describing the form on the Grassmannian, and to see what they correspond to in $\mathcal{N}=4$ SYM. Since the Yangian generates positive diffeomorphisms on the Grassmannian,¹¹ it would also be interesting to give a geometric interpretation to the higher charges of the integrable model, generated by transfer matrices.

6 Bork, Onishchenko, “Wilson lines, Grassmannians and gauge invariant off-shell amplitudes in $\mathcal{N}=4$ SYM”, [1607.02320](#)

7 Bourjaily, Franco, Galloni, Wen, “Stratifying On-Shell Cluster Varieties: the Geometry of Non-Planar On-Shell Diagrams”, [1607.01781](#)

8 Bern, Herrmann, Litsey, Stankowicz, Trnka, “Logarithmic Singularities and Maximally Supersymmetric Amplitudes”, [1412.8584](#); Arkani-Hamed, Bourjaily, Cachazo, Trnka, “Singularity Structure of Maximally Supersymmetric Scattering Amplitudes”, [1410.0354](#); and Bern, Herrmann, Litsey, Stankowicz, Trnka, “Evidence for a Nonplanar Amplituhedron”, [1512.08591](#)

9 Basso, Komatsu, Vieira, “Structure Constants and Integrable Bootstrap in Planar $\mathcal{N}=4$ SYM Theory”, [1505.06745](#); Fleury, Komatsu, “Hexagonalization of Correlation Functions”, [1611.05577](#); Basso, Coronado, Komatsu, Lam, Vieira, Zhong, “Asymptotic Four Point Functions”, [1701.04462](#); and Eden, Sfondrini, “Tessellating cushions: four-point functions in $\mathcal{N}=4$ SYM”, [1611.05436](#)

10 Frassek, Kanning, Ko, Staudacher, “Bethe Ansatz for Yangian Invariants: Towards Super Yang–Mills Scattering Amplitudes”, [1312.1693](#)

11 Arkani-Hamed, Bourjaily, Cachazo, Goncharov, Postnikov, Trnka, “Scattering Amplitudes and the Positive Grassmannian”, Cambridge University Press, 2016, [1212.5605](#)

The derivations we gave for the mapping between transfer matrices in equation (11.13) did not exploit any special properties of the $\mathcal{N}=4$ SYM spin chain. Given that formulas resembling the Grassmannian integral appear to be generically good representations of Yangian invariants for \mathfrak{gl}_n and $\mathfrak{gl}_{n|m}$, the mapping could possibly be generalized to any pair of algebras, also for spin chains with compact representations. We suspect that this could be used to find novel relations between integrable models.

The method we presented in section 14.3 generates the higher levels of the Q-operator system by solving the functional relations with the lowest level as input data. While this is an efficient approach for practical calculations, it would be satisfying from a theoretical perspective to derive formulas representing general \mathcal{R} -operators in a more explicit way. In particular, it is likely that some form of integral formula would be useful to factor the contributions of different sums. The preliminary results presented in section 14.4 suggest that for non-compact Q-operators, identities of more complicated hypergeometric functions will be needed to exploit the recursive structure.

The oscillator construction of Q-operators used here is not the only approach investigated in the literature, there are other methods based on integral kernels¹² or group characters.¹³ To our knowledge, these different formulations have never been directly compared or brought into a unified language, but we strongly suspect that this will lead to valuable insights.

Conceptually, it is very unsatisfying to work with the fully twisted spin chain; the model is not the “physical” model we are actually interested in, and the symmetry is massively broken. On a technical level, this leads to horrendous expressions, cf. the examples presented in chapter 15, which are amongst the simplest ones in the theory. There exists a method developed by Pronko and Stroganov¹⁴ and brought into operatorial form in Bazhanov et al. (2010),¹⁵ which leads to untwisted Q-operators for the Heisenberg spin chain. However, no generalization to higher rank is known, and the definitions involve matrix inversion and do not follow the standard monodromy construction. It is an important open question to develop some formalism for untwisted Q-operators, for $\mathcal{N}=4$ SYM and more general spin chains; a good starting point for such an investigation is untwisting procedure developed in Kazakov et al. (2016)¹⁶ for the individual Q-functions of general rational spin chains.

Our main motivation for developing methods for the efficient calculation of Q-operators for non-compact spin chains was of course their application to $\mathcal{N}=4$ SYM and the Quantum Spectral Curve. Since the QSC is an algebraic Q-system, we strongly suspect that non-perturbative Q-operators exist for the integrable model behind $\mathcal{N}=4$ SYM. Since the spin chain picture – or at least the QISM construction – breaks down at higher loop order, because of length-changing effects, a construction of these Q-operators from first principles remains out of reach. Our idea, which we plan to spell out in future work, is to use the information available as of now, namely the one-loop Q-operators in their explicit matrix form developed here, and methods to solve the QSC perturbatively. Combining

¹² Belitsky, Derkachov, Korchemsky, Manashov, “Baxter Q-operator for graded $SL(2|1)$ spin chain”, [hep-th/0610332](#); Derkachov, Manashov, “R-matrix and baxter Q-operators for the noncompact $SL(N,C)$ invariant spin chain”, [nlin/0612003](#); Derkachov, Manashov, “Noncompact $sl(N)$ spin chains: BGG-resolution, Q-operators and alternating sum representation for finite dimensional transfer matrices”, [1008.4734](#); and Derkachov, Manashov, “Factorization of R-matrix and Baxter Q-operators for generic $sl(N)$ spin chains”, [0809.2050](#)

¹³ Kazakov, Leurent, Tsuboi, “Baxter’s Q-operators and operatorial Backlund flow for quantum (super)-spin chains”, [1010.4022](#)

¹⁴ Pronko, Stroganov, “Bethe equations ‘on the wrong side of equator’”, [hep-th/9808153](#)

¹⁵ Bazhanov, Łukowski, Meneghelli, Staudacher, “A Shortcut to the Q-Operator”, [1005.3261](#)

¹⁶ Kazakov, Leurent, Volin, “T-system on T-hook: Grassmannian Solution and Twisted Quantum Spectral Curve”, [1510.02100](#)

these methods, it should be possible to calculate the matrix elements of the Q-operators in a perturbative expansion to high loop order. Apart from providing hints towards a non-perturbative construction, these matrices would allow more direct comparisons with field theoretic calculations. Moreover, they would contain information on the eigenstates of the integrable model beyond one-loop, and even at wrapping order. From a field theory perspective these states are renormalization scheme dependent; it would be interesting to see which scheme is chosen by the integrable model. There are numerous, mostly technical, challenges towards this goal: One needs a procedure for untwisting the Q-operators, or a detailed understanding of the perturbative behavior of the twisted QSC; a better understanding of the potential subtleties of reading the QSC equations as operator statements; and finally, an efficient computer implementation to make these calculations feasible. We hope to address these challenges soon.

As of now, Q-operators paired with the Quantum Spectral Curve appear to be the only available source for data on the finite size states at higher loop order. Apart from other complications, the Q-operators provide a method of representing the higher-loop integrable model, but are explicitly not a way of diagonalizing it. Sklyanin's quantum Separation of Variables approach¹⁷ has been regarded as a promising avenue for a while and has recently been developed further for higher rank algebras.¹⁸ It will be interesting to see how these methods converge in the context of the Quantum Spectral Curve.

Another possible testing ground for the investigation of higher-loop states and Q-operators is the chiral field theory recently constructed as a strongly twisted limit of γ_i -deformed super Yang-Mills.¹⁹ Compared to full $\mathcal{N}=4$ SYM, the integrable model behind this theory is closer to an ordinary non-compact spin chain and may thus provide a fruitful setting for applying and extending the Q-operator techniques developed here.

17 Sklyanin, "Quantum inverse scattering method. Selected topics", [hep-th/9211111](#); and Sklyanin, "Separation of Variables. New Trends.", [solv-int/9504001](#)

18 Gromov, Levkovich-Maslyuk, Sizov, "New Construction of Eigenstates and Separation of Variables for $SU(N)$ Quantum Spin Chains", [1610.08032](#)

19 Gürdoğan, Kazakov, "New Integrable 4D Quantum Field Theories from Strongly Deformed Planar $\mathcal{N}=4$ Supersymmetric Yang-Mills Theory", [1512.06704](#), [Addendum: Phys. Rev. Lett. 117, no. 25, 259903 (2016)]; and Caetano, Gurdogan, Kazakov, "Chiral limit of $N=4$ SYM and ABJM and integrable Feynman graphs", [1612.05895](#)

ACKNOWLEDGMENTS

I first and foremost thank Matthias Staudacher for supervising this thesis, many interesting discussions, hints, ideas, and advice. I thank Jan Fokken, Christian Marboe, Dhritiman Nandan, Brenda Penante, Gregor Richter, Congkao Wen, Matthias Wilhelm, Leonard Zippelius and in particular Rouven Frassek for being great collaborators on many projects, sharing their insights and the countless exciting discussions. I would furthermore like to express my gratitude to all other people who work or worked in Matthias Staudacher's and Jan Plefka's groups at Humboldt university, in particular Christoph Sieg, Nils Kanning, Johannes Brödel, Laura Koster, Stijn van Tongeren, and Burkhard Eden. This work greatly benefited from Gregor Richter and Rouven Frassek carefully proofreading the manuscript. Many thanks for taking your time! I would furthermore like to thank Matthias Staudacher, Jan Plefka and Dmytro Volin for preparing the reports on this thesis. I am grateful to the Caltech particle theory group, and in particular Jaroslav Trnka, Enrico Herrmann, Chia-Hsien Shen, for providing hospitality during a visit. I would also like to express my appreciation to the organizers and speakers of the Les Houches School "Integrability: from statistical systems to gauge theory"; I learned incredibly much during these exceptional weeks. I thank GRK 1504 "Masse Spektrum Symmetrie" for providing funding for this work and for organizing the block courses with their inspiring lectures on particle physics and related topics. Finally I want to thank Gregor Richter for being a great office mate always up to discussion and coffee consumption, Michael Borinsky for many interesting discussions on topics beyond physics, and all people who supported me during the last years: ♡

BIBLIOGRAPHY

- ATLAS Collaboration, G. Aad *et al.*, “Observation of a new particle in the search for the Standard Model Higgs boson with the ATLAS detector at the LHC”, *Phys. Lett.* **B716** (2012) 1–29, [arXiv:1207.7214](#).
- T. Adamo, “Twistor actions for gauge theory and gravity”, PhD thesis, Cambridge U., DAMTP, 2013, [arXiv:1308.2820](#),
- O. Aharony, O. Bergman, D. L. Jafferis, and J. Maldacena, “ $\mathcal{N} = 6$ superconformal Chern-Simons-matter theories, M2-branes and their gravity duals”, *JHEP* **10** (2008) 091, [arXiv:0806.1218](#).
- O. Aharony, S. S. Gubser, J. M. Maldacena, H. Ooguri, and Y. Oz, “Large N field theories, string theory and gravity”, *Phys. Rept.* **323** (2000) 183–386, [arXiv:hep-th/9905111](#).
- L. F. Alday, D. Gaiotto, J. Maldacena, A. Sever, and P. Vieira, “An Operator Product Expansion for Polygonal null Wilson Loops”, *JHEP* **04** (2011) 088, [arXiv:1006.2788](#).
- L. F. Alday and J. Maldacena, “Comments on gluon scattering amplitudes via AdS/CFT”, *JHEP* **11** (2007) 068, [arXiv:0710.1060](#).
- L. F. Alday and R. Roiban, “Scattering Amplitudes, Wilson Loops and the String/Gauge Theory Correspondence”, *Phys. Rept.* **468** (2008) 153–211, [arXiv:0807.1889](#).
- M. Alfimov, N. Gromov, and V. Kazakov, “QCD Pomeron from AdS/CFT Quantum Spectral Curve”, *JHEP* **07** (2015) 164, [arXiv:1408.2530](#).
- N. Arkani-Hamed, J. Bourjaily, F. Cachazo, and J. Trnka, “Unification of Residues and Grassmannian Dualities”, *JHEP* **01** (2011) 049, [arXiv:0912.4912](#).
- N. Arkani-Hamed, J. L. Bourjaily, F. Cachazo, S. Caron-Huot, and J. Trnka, “The All-Loop Integrand For Scattering Amplitudes in Planar $\mathcal{N} = 4$ SYM”, *JHEP* **01** (2011) 041, [arXiv:1008.2958](#).
- N. Arkani-Hamed, J. L. Bourjaily, F. Cachazo, A. B. Goncharov, A. Postnikov, and J. Trnka, “Scattering Amplitudes and the Positive Grassmannian”, Cambridge University Press, 2016, [arXiv:1212.5605](#).
- N. Arkani-Hamed, J. L. Bourjaily, F. Cachazo, A. Postnikov, and J. Trnka, “On-Shell Structures of MHV Amplitudes Beyond the Planar Limit”, *JHEP* **06** (2015) 179, [arXiv:1412.8475](#).
- N. Arkani-Hamed, J. L. Bourjaily, F. Cachazo, and J. Trnka, “Singularity Structure of Maximally Supersymmetric Scattering Amplitudes”, *Phys. Rev. Lett.* **113** (2014), no. 26, 261603, [arXiv:1410.0354](#).

- N. Arkani-Hamed, F. Cachazo, and C. Cheung, “The Grassmannian Origin Of Dual Superconformal Invariance”, *JHEP* **03** (2010)c 036, [arXiv:0909.0483](#).
- N. Arkani-Hamed, F. Cachazo, C. Cheung, and J. Kaplan, “A Duality For The S Matrix”, *JHEP* **03** (2010)a 020, [arXiv:0907.5418](#).
- N. Arkani-Hamed, F. Cachazo, C. Cheung, and J. Kaplan, “The S-Matrix in Twistor Space”, *JHEP* **03** (2010)b 110, [arXiv:0903.2110](#).
- N. Arkani-Hamed, F. Cachazo, and J. Kaplan, “What is the Simplest Quantum Field Theory?”, *JHEP* **09** (2010) 016, [arXiv:0808.1446](#).
- N. Arkani-Hamed and J. Trnka, “Into the Amplituhedron”, *JHEP* **12** (2014)b 182, [arXiv:1312.7878](#).
- N. Arkani-Hamed and J. Trnka, “The Amplituhedron”, *JHEP* **10** (2014)a 030, [arXiv:1312.2007](#).
- Y. Bai and S. He, “The Amplituhedron from Momentum Twistor Diagrams”, *JHEP* **02** (2015) 065, [arXiv:1408.2459](#).
- Z. Bajnok, “Review of AdS/CFT Integrability, Chapter III.6: Thermodynamic Bethe Ansatz”, *Lett. Math. Phys.* **99** (2012) 299–320, [arXiv:1012.3995](#).
- T. Bargheer, N. Beisert, and F. Loebbert, “Boosting Nearest-Neighbour to Long-Range Integrable Spin Chains”, *J. Stat. Mech.* **0811** (2008) L11001, [arXiv:0807.5081](#).
- T. Bargheer, N. Beisert, and F. Loebbert, “Exact Superconformal and Yangian Symmetry of Scattering Amplitudes”, *J. Phys.* **A44** (2011) 454012, [arXiv:1104.0700](#).
- T. Bargheer, Y.-t. Huang, F. Loebbert, and M. Yamazaki, “Integrable Amplitude Deformations for $\mathcal{N} = 4$ Super Yang-Mills and ABJM Theory”, *Phys. Rev.* **D91** (2015), no. 2, 026004, [arXiv:1407.4449](#).
- I. Bars and M. Günaydin, “Unitary Representations of Noncompact Supergroups”, *Commun. Math. Phys.* **91** (1983) 31.
- B. Basso, “Exciting the GKP string at any coupling”, *Nucl. Phys.* **B857** (2012) 254–334, [arXiv:1010.5237](#).
- B. Basso, J. Caetano, L. Cordova, A. Sever, and P. Vieira, “OPE for all Helicity Amplitudes”, *JHEP* **08** (2015)a 018, [arXiv:1412.1132](#).
- B. Basso, J. Caetano, L. Cordova, A. Sever, and P. Vieira, “OPE for all Helicity Amplitudes II. Form Factors and Data Analysis”, *JHEP* **12** (2015)b 088, [arXiv:1508.02987](#).
- B. Basso, F. Coronado, S. Komatsu, H. T. Lam, P. Vieira, and D.-l. Zhong, “Asymptotic Four Point Functions”, 2017, [arXiv:1701.04462](#).
- B. Basso, S. Komatsu, and P. Vieira, “Structure Constants and Integrable Bootstrap in Planar $\mathcal{N} = 4$ SYM Theory”, 2015c, [arXiv:1505.06745](#).

- B. Basso, A. Sever, and P. Vieira, “Spacetime and Flux Tube S-Matrices at Finite Coupling for $\mathcal{N} = 4$ Supersymmetric Yang-Mills Theory”, *Phys. Rev. Lett.* **111** (2013), no. 9, 091602, [arXiv:1303.1396](#).
- M. T. Batchelor and A. Foerster, “Yang-Baxter integrable models in experiments: from condensed matter to ultracold atoms”, *J. Phys.* **A49** (2016), no. 17, 173001, [arXiv:1510.05810](#).
- R. J. Baxter, “Exactly solved models in statistical mechanics”, 1982,
- R. J. Baxter, “Perimeter Bethe ansatz”, *Journal of Physics A: Mathematical and General* **20** (1987), no. 9, 2557.
- R. J. Baxter, “Partition function of the eight vertex lattice model”, *Annals Phys.* **70** (1972) 193–228, [Annals Phys.281,187(2000)].
- V. V. Bazhanov, R. Frassek, T. Łukowski, C. Meneghelli, and M. Staudacher, “Baxter Q-Operators and Representations of Yangians”, *Nucl. Phys.* **B850** (2011) 148–174, [arXiv:1010.3699](#).
- V. V. Bazhanov, A. N. Hibberd, and S. M. Khoroshkin, “Integrable structure of $W(3)$ conformal field theory, quantum Boussinesq theory and boundary affine Toda theory”, *Nucl. Phys.* **B622** (2002) 475–547, [arXiv:hep-th/0105177](#).
- V. V. Bazhanov, T. Łukowski, C. Meneghelli, and M. Staudacher, “A Shortcut to the Q-Operator”, *J. Stat. Mech.* **1011** (2010) P11002, [arXiv:1005.3261](#).
- V. V. Bazhanov, S. L. Lukyanov, and A. B. Zamolodchikov, “Integrable structure of conformal field theory. 2. Q operator and DDV equation”, *Commun. Math. Phys.* **190** (1997) 247–278, [arXiv:hep-th/9604044](#).
- V. V. Bazhanov, S. L. Lukyanov, and A. B. Zamolodchikov, “Integrable structure of conformal field theory. 3. The Yang-Baxter relation”, *Commun. Math. Phys.* **200** (1999) 297–324, [arXiv:hep-th/9805008](#).
- V. V. Bazhanov and Z. Tsuboi, “Baxter’s Q-operators for supersymmetric spin chains”, *Nucl. Phys.* **B805** (2008) 451–516, [arXiv:0805.4274](#).
- N. Beisert, V. Dippel, and M. Staudacher, “A Novel long range spin chain and planar $\mathcal{N} = 4$ super Yang-Mills”, *JHEP* **07** (2004) 075, [arXiv:hep-th/0405001](#).
- N. Beisert, C. Kristjansen, and M. Staudacher, “The Dilatation operator of conformal $\mathcal{N} = 4$ Super Yang-Mills theory”, *Nucl. Phys.* **B664** (2003) 131–184, [arXiv:hep-th/0303060](#).
- N. Beisert and R. Roiban, “Beauty and the twist: The Bethe ansatz for twisted $\mathcal{N} = 4$ SYM”, *JHEP* **08** (2005) 039, [arXiv:hep-th/0505187](#).
- N. Beisert, “The complete one loop dilatation operator of $\mathcal{N} = 4$ Super Yang-Mills theory”, *Nucl. Phys.* **B676** (2004) 3–42, [arXiv:hep-th/0307015](#).

- N. Beisert, “The $su(2|3)$ dynamic spin chain”, *Nucl. Phys.* **B682** (2004) 487–520, [arXiv:hep-th/0310252](#).
- N. Beisert, “The $SU(2|2)$ dynamic S-matrix”, *Adv. Theor. Math. Phys.* **12** (2008) 945–979, [arXiv:hep-th/0511082](#).
- N. Beisert, “On Yangian Symmetry in Planar $\mathcal{N} = 4$ SYM”, in “Quantum chromodynamics and beyond: Gribov-80 memorial volume. Proceedings, Memorial Workshop devoted to the 80th birthday of V.N. Gribov, Trieste, Italy, May 26-28, 2010”, pp. 175–203, 2011, [arXiv:1004.5423](#).
- N. Beisert, J. Broedel, and M. Rosso, “On Yangian-invariant regularization of deformed on-shell diagrams in $\mathcal{N} = 4$ super-Yang-Mills theory”, *J. Phys.* **A47** (2014) 365402, [arXiv:1401.7274](#).
- N. Beisert, B. Eden, and M. Staudacher, “Transcendentality and Crossing”, *J. Stat. Mech.* **0701** (2007) P01021, [arXiv:hep-th/0610251](#).
- N. Beisert and D. Erkal, “Yangian symmetry of long-range $gl(N)$ integrable spin chains”, *J. Stat. Mech.* **0803** (2008) P03001, [arXiv:0711.4813](#).
- N. Beisert *et al.*, “Review of AdS/CFT Integrability: An Overview”, *Lett. Math. Phys.* **99** (2012) 3–32, [arXiv:1012.3982](#).
- N. Beisert, A. Garus, and M. Rosso, “Yangian Symmetry and Integrability of Planar $\mathcal{N} = 4$ Supersymmetric Yang-Mills Theory”, *Phys. Rev. Lett.* **118** (2017), no. 14, 141603, [arXiv:1701.09162](#).
- N. Beisert, D. Müller, J. Plefka, and C. Vergu, “Integrability of smooth Wilson loops in $\mathcal{N} = 4$ superspace”, *JHEP* **12** (2015) 141, [arXiv:1509.05403](#).
- N. Beisert and M. Staudacher, “The $\mathcal{N} = 4$ SYM integrable super spin chain”, *Nucl. Phys.* **B670** (2003) 439–463, [arXiv:hep-th/0307042](#).
- N. Beisert and M. Staudacher, “Long-range $psu(2,2|4)$ Bethe Ansätze for gauge theory and strings”, *Nucl. Phys.* **B727** (2005) 1–62, [arXiv:hep-th/0504190](#).
- A. V. Belitsky, S. E. Derkachov, G. P. Korchemsky, and A. N. Manashov, “Baxter Q-operator for graded $SL(2|1)$ spin chain”, *J. Stat. Mech.* **0701** (2007) P01005, [arXiv:hep-th/0610332](#).
- A. V. Belitsky, S. Hohenegger, G. P. Korchemsky, E. Sokatchev, and A. Zhiboedov, “From correlation functions to event shapes”, *Nucl. Phys.* **B884** (2014) 305–343, [arXiv:1309.0769](#).
- S. Belliard and E. Ragoucy, “Nested Bethe ansatz for ‘all’ closed spin chains”, *J. Phys.* **A41** (2008) 295202, [arXiv:0804.2822](#).
- S. Bellucci, P. Y. Casteill, J. F. Morales, and C. Sochichiu, “Spin bit models from nonplanar $N = 4$ SYM”, *Nucl. Phys.* **B699** (2004) 151–173, [arXiv:hep-th/0404066](#).

- I. Bena, J. Polchinski, and R. Roiban, “Hidden symmetries of the $\text{AdS}_5 \times S^5$ superstring”, *Phys. Rev.* **D69** (2004) 046002, [arXiv:hep-th/0305116](#).
- P. Benincasa, “On-shell diagrammatics and the perturbative structure of planar gauge theories”, 2015, [arXiv:1510.03642](#).
- P. Benincasa and D. Gordo, “On-shell diagrams and the geometry of planar $N < 4$ SYM theories”, 2016, [arXiv:1609.01923](#).
- N. Berkovits and J. Maldacena, “Fermionic T-Duality, Dual Superconformal Symmetry, and the Amplitude/Wilson Loop Connection”, *JHEP* **09** (2008) 062, [arXiv:0807.3196](#).
- Z. Bern, J. J. Carrasco, L. J. Dixon, H. Johansson, and R. Roiban, “The Ultraviolet Behavior of $N=8$ Supergravity at Four Loops”, *Phys. Rev. Lett.* **103** (2009) 081301, [arXiv:0905.2326](#).
- Z. Bern, J. J. M. Carrasco, H. Johansson, and D. A. Kosower, “Maximally supersymmetric planar Yang-Mills amplitudes at five loops”, *Phys. Rev.* **D76** (2007) 125020, [arXiv:0705.1864](#).
- Z. Bern, L. J. Dixon, D. C. Dunbar, and D. A. Kosower, “One loop n point gauge theory amplitudes, unitarity and collinear limits”, *Nucl. Phys.* **B425** (1994) 217–260, [arXiv:hep-ph/9403226](#).
- Z. Bern, L. J. Dixon, D. C. Dunbar, and D. A. Kosower, “Fusing gauge theory tree amplitudes into loop amplitudes”, *Nucl. Phys.* **B435** (1995) 59–101, [arXiv:hep-ph/9409265](#).
- Z. Bern, L. J. Dixon, and D. A. Kosower, “Dimensionally regulated pentagon integrals”, *Nucl. Phys.* **B412** (1994) 751–816, [arXiv:hep-ph/9306240](#).
- Z. Bern, E. Herrmann, S. Litsey, J. Stankowicz, and J. Trnka, “Logarithmic Singularities and Maximally Supersymmetric Amplitudes”, *JHEP* **06** (2015) 202, [arXiv:1412.8584](#).
- Z. Bern, E. Herrmann, S. Litsey, J. Stankowicz, and J. Trnka, “Evidence for a Nonplanar Amplituhedron”, *JHEP* **06** (2016) 098, [arXiv:1512.08591](#).
- H. Bethe, “Zur Theorie der Metalle”, *Zeitschrift für Physik* **71** (1931), no. 3, 205–226.
- L. Bianchi, V. Forini, and A. V. Kotikov, “On DIS Wilson coefficients in $\mathcal{N} = 4$ super Yang-Mills theory”, *Phys. Lett.* **B725** (2013) 394–401, [arXiv:1304.7252](#).
- L. V. Bork, “On form factors in $\mathcal{N} = 4$ SYM theory and polytopes”, *JHEP* **12** (2014) 111, [arXiv:1407.5568](#).
- L. V. Bork and A. I. Onishchenko, “Four dimensional ambitwistor strings and form factors of local and Wilson line operators”, 2017c, [arXiv:1704.04758](#).

- L. V. Bork and A. I. Onishchenko, “Grassmannian integral for general gauge invariant off-shell amplitudes in $\mathcal{N} = 4$ SYM”, *JHEP* **05** (2017)a 040, [arXiv:1610.09693](#).
- L. V. Bork and A. I. Onishchenko, “Wilson lines, Grassmannians and gauge invariant off-shell amplitudes in $\mathcal{N} = 4$ SYM”, *JHEP* **04** (2017)b 019, [arXiv:1607.02320](#).
- J. L. Bourjaily, “Positroids, Plabic Graphs, and Scattering Amplitudes in Mathematica”, 2012, [arXiv:1212.6974](#).
- J. L. Bourjaily, S. Franco, D. Galloni, and C. Wen, “Stratifying On-Shell Cluster Varieties: the Geometry of Non-Planar On-Shell Diagrams”, *JHEP* **10** (2016) 003, [arXiv:1607.01781](#).
- J. L. Bourjaily, E. Herrmann, and J. Trnka, “Prescriptive Unitarity”, 2017, [arXiv:1704.05460](#).
- J. L. Bourjaily, J. Trnka, A. Volovich, and C. Wen, “The Grassmannian and the Twistor String: Connecting All Trees in $\mathcal{N} = 4$ SYM”, *JHEP* **01** (2011) 038, [arXiv:1006.1899](#).
- A. Brandhuber, O. Gurdogan, R. Mooney, G. Travaglini, and G. Yang, “Harmony of Super Form Factors”, *JHEP* **10** (2011)b 046, [arXiv:1107.5067](#).
- A. Brandhuber, P. Heslop, and G. Travaglini, “A Note on dual superconformal symmetry of the $\mathcal{N} = 4$ super Yang-Mills S-matrix”, *Phys. Rev.* **D78** (2008)b 125005, [arXiv:0807.4097](#).
- A. Brandhuber, P. Heslop, and G. Travaglini, “MHV amplitudes in $\mathcal{N} = 4$ super Yang-Mills and Wilson loops”, *Nucl. Phys.* **B794** (2008)a 231–243, [arXiv:0707.1153](#).
- A. Brandhuber, E. Hughes, R. Panerai, B. Spence, and G. Travaglini, “The connected prescription for form factors in twistor space”, *JHEP* **11** (2016) 143, [arXiv:1608.03277](#).
- A. Brandhuber, B. Spence, G. Travaglini, and G. Yang, “Form Factors in $\mathcal{N} = 4$ Super Yang-Mills and Periodic Wilson Loops”, *JHEP* **01** (2011)a 134, [arXiv:1011.1899](#).
- V. M. Braun, S. E. Derkachov, and A. N. Manashov, “Integrability of three particle evolution equations in QCD”, *Phys. Rev. Lett.* **81** (1998), 2020–2023, [arXiv:hep-ph/9805225](#).
- L. Brink, O. Lindgren, and B. E. W. Nilsson, “The Ultraviolet Finiteness of the $\mathcal{N} = 4$ Yang-Mills Theory”, *Phys. Lett.* **B123** (1983) 323–328.
- L. Brink, J. H. Schwarz, and J. Scherk, “Supersymmetric Yang-Mills Theories”, *Nucl. Phys.* **B121** (1977) 77–92.

- R. Britto, F. Cachazo, and B. Feng, “Generalized unitarity and one-loop amplitudes in $\mathcal{N} = 4$ super-Yang-Mills”, *Nucl. Phys.* **B725** (2005)b 275–305, [arXiv:hep-th/0412103](#).
- R. Britto, F. Cachazo, and B. Feng, “New recursion relations for tree amplitudes of gluons”, *Nucl. Phys.* **B715** (2005)a 499–522, [arXiv:hep-th/0412308](#).
- R. Britto, F. Cachazo, B. Feng, and E. Witten, “Direct proof of tree-level recursion relation in Yang-Mills theory”, *Phys. Rev. Lett.* **94** (2005)c 181602, [arXiv:hep-th/0501052](#).
- J. Broedel, M. de Leeuw, and M. Rosso, “A dictionary between R-operators, on-shell graphs and Yangian algebras”, *JHEP* **06** (2014)b 170, [arXiv:1403.3670](#).
- J. Broedel, M. de Leeuw, and M. Rosso, “Deformed one-loop amplitudes in $\mathcal{N} = 4$ super-Yang-Mills theory”, *JHEP* **11** (2014)a 091, [arXiv:1406.4024](#).
- F. Cachazo, S. He, and E. Y. Yuan, “Scattering equations and Kawai-Lewellen-Tye orthogonality”, *Phys. Rev.* **D90** (2014), no. 6, 065001, [arXiv:1306.6575](#).
- J. Caetano, O. Gurdogan, and V. Kazakov, “Chiral limit of $N = 4$ SYM and ABJM and integrable Feynman graphs”, 2016, [arXiv:1612.05895](#).
- S. Caron-Huot, “Loops and trees”, *JHEP* **05** (2011) 080, [arXiv:1007.3224](#).
- S. Caron-Huot and S. He, “Jumpstarting the All-Loop S-Matrix of Planar $\mathcal{N} = 4$ Super Yang-Mills”, *JHEP* **07** (2012) 174, [arXiv:1112.1060](#).
- CMS** Collaboration, S. Chatrchyan *et al.*, “Observation of a new boson at a mass of 125 GeV with the CMS experiment at the LHC”, *Phys. Lett.* **B716** (2012) 30–61, [arXiv:1207.7235](#).
- D. Chicherin, S. Derkachov, and R. Kirschner, “Yang-Baxter operators and scattering amplitudes in $\mathcal{N} = 4$ super-Yang-Mills theory”, *Nucl. Phys.* **B881** (2014) 467–501, [arXiv:1309.5748](#).
- D. Chicherin and R. Kirschner, “Yangian symmetric correlators”, *Nucl. Phys.* **B877** (2013) 484–505, [arXiv:1306.0711](#).
- D. Chicherin, R. Doobary, B. Eden, P. Heslop, G. P. Korchemsky, L. Mason, and E. Sokatchev, “Correlation functions of the chiral stress-tensor multiplet in $\mathcal{N} = 4$ SYM”, *JHEP* **06** (2015) 198, [arXiv:1412.8718](#).
- S. E. Derkachov, G. P. Korchemsky, J. Kotanski, and A. N. Manashov, “Noncompact Heisenberg spin magnets from high-energy QCD. 2. Quantization conditions and energy spectrum”, *Nucl. Phys.* **B645** (2002) 237–297, [arXiv:hep-th/0204124](#).
- S. E. Derkachov, G. P. Korchemsky, and A. N. Manashov, “Noncompact Heisenberg spin magnets from high-energy QCD: 1. Baxter Q operator and separation of variables”, *Nucl. Phys.* **B617** (2001) 375–440, [arXiv:hep-th/0107193](#).

- S. E. Derkachov, G. P. Korchemsky, and A. N. Manashov, “Noncompact Heisenberg spin magnets from high-energy QCD. 3. Quasiclassical approach”, *Nucl. Phys.* **B661** (2003) 533–576, [arXiv:hep-th/0212169](#).
- S. E. Derkachov and A. N. Manashov, “R-matrix and baxter Q-operators for the noncompact $SL(N,C)$ invariant spin chain”, *SIGMA* **2** (2006) 084, [arXiv:nlin/0612003](#).
- S. E. Derkachov and A. N. Manashov, “Factorization of R-matrix and Baxter Q-operators for generic $sl(N)$ spin chains”, *J. Phys.* **A42** (2009) 075204, [arXiv:0809.2050](#).
- S. E. Derkachov and A. N. Manashov, “Noncompact $sl(N)$ spin chains: BGG-resolution, Q-operators and alternating sum representation for finite dimensional transfer matrices”, *Lett. Math. Phys.* **97** (2011) 185–202, [arXiv:1008.4734](#).
- L. J. Dixon, “Calculating scattering amplitudes efficiently”, in “QCD and beyond. Proceedings, Theoretical Advanced Study Institute in Elementary Particle Physics, TASI-95, Boulder, USA, June 4-30, 1995”, pp. 539–584, 1996, [arXiv:hep-ph/9601359](#).
- L. J. Dixon, “A brief introduction to modern amplitude methods”, in “Proceedings, 2012 European School of High-Energy Physics (ESHEP 2012): La Pommeraye, Anjou, France, June 06-19, 2012”, pp. 31–67, 2014, [arXiv:1310.5353](#).
- L. Dolan and P. Goddard, “Gluon Tree Amplitudes in Open Twistor String Theory”, *JHEP* **12** (2009) 032, [arXiv:0909.0499](#).
- L. Dolan, C. R. Nappi, and E. Witten, “Yangian symmetry in $D = 4$ superconformal Yang-Mills theory”, in “Proceedings, 3rd International Symposium on Quantum theory and symmetries (QTS3): Cincinnati, USA, September 10-14, 2003”, pp. 300–315, 2004, [arXiv:hep-th/0401243](#).
- P. Dorey, “Exact S matrices”, in “Conformal field theories and integrable models. Proceedings, Eotvos Graduate Course, Budapest, Hungary, August 13-18, 1996”, pp. 85–125, 1996, [arXiv:hep-th/9810026](#).
- V. G. Drinfeld, “Hopf algebras and the quantum Yang-Baxter equation”, *Sov. Math. Dokl.* **32** (1985) 254–258, [Dokl. Akad. Nauk Ser. Fiz.283,1060(1985)].
- V. G. Drinfeld, “Quantum groups”, *J. Sov. Math.* **41** (1988) 898–915.
- J. M. Drummond and L. Ferro, “The Yangian origin of the Grassmannian integral”, *JHEP* **12** (2010)b 010, [arXiv:1002.4622](#).
- J. M. Drummond and L. Ferro, “Yangians, Grassmannians and T-duality”, *JHEP* **07** (2010)a 027, [arXiv:1001.3348](#).
- J. M. Drummond, J. Henn, G. P. Korchemsky, and E. Sokatchev, “On planar gluon amplitudes/Wilson loops duality”, *Nucl. Phys.* **B795** (2008)b 52–68, [arXiv:0709.2368](#).

- J. M. Drummond, J. Henn, G. P. Korchemsky, and E. Sokatchev, “Dual superconformal symmetry of scattering amplitudes in $\mathcal{N} = 4$ super-Yang-Mills theory”, *Nucl. Phys.* **B828** (2010) 317–374, [arXiv:0807.1095](#).
- J. M. Drummond and J. M. Henn, “All tree-level amplitudes in $\mathcal{N} = 4$ SYM”, *JHEP* **04** (2009) 018, [arXiv:0808.2475](#).
- J. M. Drummond, G. P. Korchemsky, and E. Sokatchev, “Conformal properties of four-gluon planar amplitudes and Wilson loops”, *Nucl. Phys.* **B795** (2008)a 385–408, [arXiv:0707.0243](#).
- J. M. Drummond, J. M. Henn, and J. Plefka, “Yangian symmetry of scattering amplitudes in $\mathcal{N} = 4$ super Yang-Mills theory”, *JHEP* **05** (2009) 046, [arXiv:0902.2987](#).
- P. Du, G. Chen, and Y.-K. E. Cheung, “Permutation relations of generalized Yangian Invariants, unitarity cuts, and scattering amplitudes”, *JHEP* **09** (2014) 115, [arXiv:1401.6610](#).
- B. Eden, P. Heslop, G. P. Korchemsky, and E. Sokatchev, “The super-correlator/super-amplitude duality: Part I”, *Nucl. Phys.* **B869** (2013) 329–377, [arXiv:1103.3714](#).
- B. Eden, P. Heslop, and L. Mason, “The Correlahedron”, 2017, [arXiv:1701.00453](#).
- B. Eden and A. Sfondrini, “Tessellating cushions: four-point functions in $\mathcal{N} = 4$ SYM”, 2016, [arXiv:1611.05436](#).
- B. Eden and M. Staudacher, “Integrability and transcendentality”, *J. Stat. Mech.* **0611** (2006) P11014, [arXiv:hep-th/0603157](#).
- H. Elvang, D. Z. Freedman, and M. Kiermaier, “Recursion Relations, Generating Functions, and Unitarity Sums in $\mathcal{N} = 4$ SYM Theory”, *JHEP* **04** (2009) 009, [arXiv:0808.1720](#).
- H. Elvang and Y.-t. Huang, “Scattering Amplitudes”, 2013, [arXiv:1308.1697](#).
- H. Elvang and Y.-t. Huang, “Scattering Amplitudes in Gauge Theory and Gravity”, Cambridge University Press, 2015,
- H. Elvang, Y.-t. Huang, C. Keeler, T. Lam, T. M. Olson, S. B. Roland, and D. E. Speyer, “Grassmannians for scattering amplitudes in 4d $\mathcal{N} = 4$ SYM and 3d ABJM”, *JHEP* **12** (2014) 181, [arXiv:1410.0621](#).
- O. T. Engelund and R. Roiban, “Correlation functions of local composite operators from generalized unitarity”, *JHEP* **03** (2013) 172, [arXiv:1209.0227](#).
- J. Escobedo, N. Gromov, A. Sever, and P. Vieira, “Tailoring Three-Point Functions and Integrability”, *JHEP* **09** (2011) 028, [arXiv:1012.2475](#).

- L. Faddeev, “Instructive history of the quantum inverse scattering method”, *Acta Applicandae Mathematicae* **39** (1995) 69–84, [10.1007/BF00994626](https://doi.org/10.1007/BF00994626).
- L. D. Faddeev, “Algebraic aspects of Bethe Ansatz”, *Int. J. Mod. Phys.* **A10** (1995) 1845–1878, [arXiv:hep-th/9404013](https://arxiv.org/abs/hep-th/9404013).
- L. D. Faddeev, “How algebraic Bethe ansatz works for integrable model”, in “Relativistic gravitation and gravitational radiation. Proceedings, School of Physics, Les Houches, France, September 26–October 6, 1995”, pp. pp. 149–219, 1996, [arXiv:hep-th/9605187](https://arxiv.org/abs/hep-th/9605187).
- L. D. Faddeev and G. P. Korchemsky, “High-energy QCD as a completely integrable model”, *Phys. Lett.* **B342** (1995) 311–322, [arXiv:hep-th/9404173](https://arxiv.org/abs/hep-th/9404173).
- P. Fendley, K. Schoutens, and B. Nienhuis, “Lattice fermion models with supersymmetry”, *J. Phys.* **A36** (2003) 12399–12424, [arXiv:cond-mat/0307338](https://arxiv.org/abs/cond-mat/0307338).
- A. Ferber, “Supertwistors and Conformal Supersymmetry”, *Nucl. Phys.* **B132** (1978) 55–64.
- L. Ferro, T. Łukowski, C. Meneghelli, J. Plefka, and M. Staudacher, “Harmonic R-matrices for Scattering Amplitudes and Spectral Regularization”, *Phys. Rev. Lett.* **110** (2013), no. 12, 121602, [arXiv:1212.0850](https://arxiv.org/abs/1212.0850).
- L. Ferro, T. Łukowski, C. Meneghelli, J. Plefka, and M. Staudacher, “Spectral Parameters for Scattering Amplitudes in $\mathcal{N} = 4$ Super Yang-Mills Theory”, *JHEP* **01** (2014)a 094, [arXiv:1308.3494](https://arxiv.org/abs/1308.3494).
- L. Ferro, T. Łukowski, A. Orta, and M. Parisi, “Yangian Symmetry for the Tree Amplituhedron”, 2016, [arXiv:1612.04378](https://arxiv.org/abs/1612.04378).
- L. Ferro, T. Łukowski, and M. Staudacher, “ $\mathcal{N} = 4$ scattering amplitudes and the deformed Grassmannian”, *Nucl. Phys.* **B889** (2014)b 192–206, [arXiv:1407.6736](https://arxiv.org/abs/1407.6736).
- T. Fleury and S. Komatsu, “Hexagonalization of Correlation Functions”, *JHEP* **01** (2017) 130, [arXiv:1611.05577](https://arxiv.org/abs/1611.05577).
- S. Franco, D. Galloni, B. Penante, and C. Wen, “Non-Planar On-Shell Diagrams”, *JHEP* **06** (2015) 199, [arXiv:1502.02034](https://arxiv.org/abs/1502.02034).
- R. Frassek, “Q-operators, Yangian invariance and the quantum inverse scattering method”, PhD thesis, Humboldt University Berlin, 2014, [arXiv:1412.3339](https://arxiv.org/abs/1412.3339).
- R. Frassek, “Algebraic Bethe ansatz for Q-operators: The Heisenberg spin chain”, *J. Phys.* **A48** (2015), no. 29, 294002, [arXiv:1504.04501](https://arxiv.org/abs/1504.04501).
- R. Frassek, N. Kanning, Y. Ko, and M. Staudacher, “Bethe Ansatz for Yangian Invariants: Towards Super Yang-Mills Scattering Amplitudes”, *Nucl. Phys.* **B883** (2014) 373–424, [arXiv:1312.1693](https://arxiv.org/abs/1312.1693).

- R. Frassek, T. Łukowski, C. Meneghelli, and M. Staudacher, “unpublished”.
- R. Frassek, T. Łukowski, C. Meneghelli, and M. Staudacher, “Oscillator Construction of $su(n|m)$ Q-Operators”, *Nucl. Phys.* **B850** (2011) 175–198, [arXiv:1012.6021](#).
- R. Frassek, T. Łukowski, C. Meneghelli, and M. Staudacher, “Baxter Operators and Hamiltonians for ‘nearly all’ Integrable Closed $gl(n)$ Spin Chains”, *Nucl. Phys.* **B874** (2013) 620–646, [arXiv:1112.3600](#).
- R. Frassek, C. Marboe, and D. Meidinger, “Evaluation of the operatorial Q-system for non-compact super spin chains”, *JHEP* **09** (2017) 18, [arXiv:1706.02320](#).
- R. Frassek and D. Meidinger, “Yangian-type symmetries of non-planar leading singularities”, *JHEP* **05** (2016) 110, [arXiv:1603.00088](#).
- R. Frassek, D. Meidinger, D. Nandan, and M. Wilhelm, “On-shell diagrams, Grassmannians and integrability for form factors”, *JHEP* **01** (2016) 182, [arXiv:1506.08192](#).
- R. Frassek and C. Meneghelli, “From Baxter Q-Operators to Local Charges”, *J. Stat. Mech.* **1302** (2013) P02019, [arXiv:1207.4513](#).
- R. Frassek and I. M. Szecsenyi, “Q-operators for the open Heisenberg spin chain”, *Nucl. Phys.* **B901** (2015) 229–248, [arXiv:1509.04867](#).
- S. Frolov, “Lax pair for strings in Lunin-Maldacena background”, *JHEP* **05** (2005) 069, [arXiv:hep-th/0503201](#).
- J. Fuksa and R. Kirschner, “Correlators with sl_2 Yangian symmetry”, *Nucl. Phys.* **B914** (2017) 1–42, [arXiv:1608.04912](#).
- Z. Gao and G. Yang, “Y-system for form factors at strong coupling in AdS_5 and with multi-operator insertions in AdS_3 ”, *JHEP* **06** (2013) 105, [arXiv:1303.2668](#).
- E. Gardi, “Infrared singularities in multi-leg scattering amplitudes”, *PoS LL2014* (2014) 069, [arXiv:1407.5164](#).
- T. Gehrmann, J. M. Henn, and T. Huber, “The three-loop form factor in $\mathcal{N} = 4$ super Yang-Mills”, *JHEP* **03** (2012) 101, [arXiv:1112.4524](#).
- M. Gekhtman, M. Shapiro, and A. Vainshtein, “Poisson Geometry of Directed Networks in an Annulus”, *Journal of the European Mathematical Society* **14** (2012) 541–570, [arXiv:0901.0020](#).
- M. B. Green, J. H. Schwarz, and L. Brink, “ $\mathcal{N} = 4$ Yang-Mills and N=8 Supergravity as Limits of String Theories”, *Nucl. Phys.* **B198** (1982) 474–492.
- P. A. Griffiths and J. Harris, “Principles of algebraic geometry”, Wiley, New York, NY, 1994.

- M. T. Grisaru, M. Rocek, and W. Siegel, “Zero Three Loop beta Function in $\mathcal{N} = 4$ Superyang-Mills Theory”, *Phys. Rev. Lett.* **45** (1980) 1063–1066.
- N. Gromov, V. Kazakov, S. Leurent, and D. Volin, “Quantum Spectral Curve for Planar $\mathcal{N} = 4$ Super-Yang-Mills Theory”, *Phys. Rev. Lett.* **112** (2014), no. 1, 011602, [arXiv:1305.1939](#).
- N. Gromov, V. Kazakov, S. Leurent, and D. Volin, “Quantum spectral curve for arbitrary state/operator in $\text{AdS}_5/\text{CFT}_4$ ”, *JHEP* **09** (2015) 187, [arXiv:1405.4857](#).
- N. Gromov and F. Levkovich-Maslyuk, “Quantum Spectral Curve for a cusped Wilson line in $\mathcal{N} = 4$ SYM”, *JHEP* **04** (2016) 134, [arXiv:1510.02098](#).
- N. Gromov and F. Levkovich-Maslyuk, “Quark-anti-quark potential in $\mathcal{N} = 4$ SYM”, *JHEP* **12** (2016) 122, [arXiv:1601.05679](#).
- N. Gromov, F. Levkovich-Maslyuk, and G. Sizov, “New Construction of Eigenstates and Separation of Variables for $\text{SU}(N)$ Quantum Spin Chains”, 2016b, [arXiv:1610.08032](#).
- N. Gromov, F. Levkovich-Maslyuk, and G. Sizov, “Quantum Spectral Curve and the Numerical Solution of the Spectral Problem in $\text{AdS}_5/\text{CFT}_4$ ”, *JHEP* **06** (2016)a 036, [arXiv:1504.06640](#).
- S. S. Gubser, I. R. Klebanov, and A. W. Peet, “Entropy and temperature of black 3-branes”, *Phys. Rev.* **D54** (1996) 3915–3919, [arXiv:hep-th/9602135](#).
- S. S. Gubser, I. R. Klebanov, and A. M. Polyakov, “Gauge theory correlators from noncritical string theory”, *Phys. Lett.* **B428** (1998) 105–114, [arXiv:hep-th/9802109](#).
- S. S. Gubser and I. R. Klebanov, “Absorption by branes and Schwinger terms in the world volume theory”, *Phys. Lett.* **B413** (1997) 41–48, [arXiv:hep-th/9708005](#).
- S. S. Gubser, I. R. Klebanov, and A. A. Tseytlin, “String theory and classical absorption by three-branes”, *Nucl. Phys.* **B499** (1997) 217–240, [arXiv:hep-th/9703040](#).
- M. Günaydin and N. Marcus, “The Spectrum of the S^5 Compactification of the Chiral $N=2$, $D=10$ Supergravity and the Unitary Supermultiplets of $U(2, 2/4)$ ”, *Class. Quant. Grav.* **2** (1985) L11.
- M. Günaydin, D. Minic, and M. Zagermann, “4D doubleton conformal theories, CPT and IIB string on $\text{AdS}_5 \times S^5$ ”, *Nucl. Phys.* **B534** (1998) 96–120, [arXiv:hep-th/9806042](#), [Erratum: *Nucl. Phys.* **B538**, 531(1999)].
- Ö. Gürdoğan and V. Kazakov, “New Integrable 4D Quantum Field Theories from Strongly Deformed Planar $\mathcal{N} = 4$ Supersymmetric Yang-Mills Theory”, *Phys. Rev. Lett.* **117** (2016), no. 20, 201602, [arXiv:1512.06704](#), [Addendum: *Phys. Rev. Lett.* **117**, no. 25, 259903(2016)].

- R. Haag, J. T. Lopuszanski, and M. Sohnius, “All Possible Generators of Supersymmetries of the S Matrix”, *Nucl. Phys.* **B88** (1975) 257.
- C. Hagendorf, “Spin chains with dynamical lattice supersymmetry”, *J. Stat. Phys.* **150** (2013) 609–657, [arXiv:1207.0357](#).
- C. Hagendorf and J. Liénardy, “Open spin chains with dynamic lattice supersymmetry”, *J. Phys.* **A50** (2017), no. 18, 185202, [arXiv:1612.02951](#).
- G. G. Hartwell and P. S. Howe, “(N, p, q) harmonic superspace”, *Int. J. Mod. Phys.* **A10** (1995) 3901–3920, [arXiv:hep-th/9412147](#).
- S. He and Z. Liu, “A note on connected formula for form factors”, *JHEP* **12** (2016) 006, [arXiv:1608.04306](#).
- S. He and Y. Zhang, “Connected formulas for amplitudes in standard model”, *JHEP* **03** (2017) 093, [arXiv:1607.02843](#).
- J. M. Henn and J. C. Plefka, “Scattering Amplitudes in Gauge Theories”, *Lect. Notes Phys.* **883** (2014) pp.1–195.
- E. Herrmann and J. Trnka, “Gravity On-shell Diagrams”, *JHEP* **11** (2016) 136, [arXiv:1604.03479](#).
- P. Heslop and A. E. Lipstein, “On-shell diagrams for $\mathcal{N} = 8$ supergravity amplitudes”, *JHEP* **06** (2016) 069, [arXiv:1604.03046](#).
- A. Hodges, “Eliminating spurious poles from gauge-theoretic amplitudes”, *JHEP* **05** (2013) 135, [arXiv:0905.1473](#).
- S. A. Huggett and K. P. Tod, “An Introduction to Twistor Theory”, 1994.
- R. A. Janik, “The $AdS_5 \times S^5$ superstring worldsheet S-matrix and crossing symmetry”, *Phys. Rev.* **D73** (2006) 026009, [arXiv:hep-th/0603038](#).
- R. A. Janik, “Review of AdS/CFT Integrability, Chapter III.5: Lüscher Corrections”, *Lett. Math. Phys.* **99** (2012) 277–297, [arXiv:1012.3994](#).
- P. Jordan, “Der Zusammenhang der symmetrischen und linearen Gruppen und das Mehrkörperproblem”, *Zeitschrift für Physik* **94** (1935), no. 7, 531–535.
- N. Kanning, Y. Ko, and M. Staudacher, “Grassmannian integrals as matrix models for non-compact Yangian invariants”, *Nucl. Phys.* **B894** (2015) 407–421, [arXiv:1412.8476](#).
- N. Kanning, T. Lukowski, and M. Staudacher, “A shortcut to general tree-level scattering amplitudes in $\mathcal{N} = 4$ SYM via integrability”, *Fortsch. Phys.* **62** (2014) 556–572, [arXiv:1403.3382](#).
- V. Kazakov, S. Leurent, and Z. Tsuboi, “Baxter’s Q-operators and operatorial Backlund flow for quantum (super)-spin chains”, *Commun. Math. Phys.* **311** (2012) 787–814, [arXiv:1010.4022](#).

- V. Kazakov, S. Leurent, and D. Volin, “T-system on T-hook: Grassmannian Solution and Twisted Quantum Spectral Curve”, *JHEP* **12** (2016) 044, [arXiv:1510.02100](#).
- I. R. Klebanov, “World volume approach to absorption by nondilatonic branes”, *Nucl. Phys.* **B496** (1997) 231–242, [arXiv:hep-th/9702076](#).
- R. Kleiss and W. Stirling, “Spinor techniques for calculating $p\bar{p} \rightarrow W_{\pm}/Z_0 + \text{jets}$ ”, *Nuclear Physics B* **262** (1985), no. 2, 235 – 262.
- A. Knutson, T. Lam, and D. Speyer, “Positroid Varieties: Juggling and Geometry”, *ArXiv e-prints*, 2011 [arXiv:1111.3660](#).
- T. Kojima, “Baxter’s Q-operator for the W-algebra WN ”, *J. Phys.* **A41** (2008), no. 35, 355206, [arXiv:0803.3505](#).
- G. P. Korchemsky, “Bethe ansatz for QCD pomeron”, *Nucl. Phys.* **B443** (1995) 255–304, [arXiv:hep-ph/9501232](#).
- G. P. Korchemsky, “Quasiclassical QCD pomeron”, *Nucl. Phys.* **B462** (1996) 333–388, [arXiv:hep-th/9508025](#).
- G. P. Korchemsky, “Review of AdS/CFT Integrability, Chapter IV.4: Integrability in QCD and $N < 4$ SYM”, *Lett. Math. Phys.* **99** (2012) 425–453, [arXiv:1012.4000](#).
- L. Koster, V. Mitev, M. Staudacher, and M. Wilhelm, “All tree-level MHV form factors in $\mathcal{N} = 4$ SYM from twistor space”, *JHEP* **06** (2016) 162, [arXiv:1604.00012](#).
- L. Koster, V. Mitev, M. Staudacher, and M. Wilhelm, “Composite Operators in the Twistor Formulation of $\mathcal{N} = 4$ Supersymmetric Yang-Mills Theory”, *Phys. Rev. Lett.* **117** (2016), no. 1, 011601, [arXiv:1603.04471](#).
- L. Koster, V. Mitev, M. Staudacher, and M. Wilhelm, “On Form Factors and Correlation Functions in Twistor Space”, *JHEP* **03** (2017) 131, [arXiv:1611.08599](#).
- C. Kristjansen, “Review of AdS/CFT Integrability, Chapter IV.1: Aspects of Non-Planarity”, *Lett. Math. Phys.* **99** (2012) 349–374, [arXiv:1012.3997](#).
- P. P. Kulish, “Integrable graded magnets”, *J. Sov. Math.* **35** (1986) 2648–2662, [Zap. Nauchn. Semin.145,140(1985)].
- P. P. Kulish, N. Yu. Reshetikhin, and E. K. Sklyanin, “Yang-Baxter Equation and Representation Theory. 1.”, *Lett. Math. Phys.* **5** (1981) 393–403.
- H. Lehmann, K. Symanzik, and W. Zimmermann, “Zur Formulierung quantisierter Feldtheorien”, *Il Nuovo Cimento (1955-1965)* **1** (1955), no. 1, 205–225.
- R. G. Leigh and M. J. Strassler, “Exactly marginal operators and duality in four-dimensional $N=1$ supersymmetric gauge theory”, *Nucl. Phys.* **B447** (1995) 95–136, [arXiv:hep-th/9503121](#).

- L. N. Lipatov, “Asymptotic behavior of multicolor QCD at high energies in connection with exactly solvable spin models”, *JETP Lett.* **59** (1994) 596–599, [arXiv:hep-th/9311037](#), [Pisma Zh. Eksp. Teor. Fiz.59,571(1994)].
- L. N. Lipatov, “Evolution equations in QCD”, in “Perspectives in hadronic physics. Proceedings, Conference, Trieste, Italy, May 12-16, 1997”, pp. 413–427, 1997.
- F. Loebbert, D. Nandan, C. Sieg, M. Wilhelm, and G. Yang, “On-Shell Methods for the Two-Loop Dilatation Operator and Finite Remainders”, *JHEP* **10** (2015) 012, [arXiv:1504.06323](#).
- F. Loebbert, C. Sieg, M. Wilhelm, and G. Yang, “Two-Loop $SL(2)$ Form Factors and Maximal Transcendentality”, *JHEP* **12** (2016) 090, [arXiv:1610.06567](#).
- J. Lovoie, T. J. Osler, and R. Tremblay, “Fractional derivatives and special functions”, *SIAM review* **18** (1976), no. 2, 240–268.
- O. Lunin and J. M. Maldacena, “Deforming field theories with $U(1) \times U(1)$ global symmetry and their gravity duals”, *JHEP* **05** (2005) 033, [arXiv:hep-th/0502086](#).
- M. Lüscher, “Volume Dependence of the Energy Spectrum in Massive Quantum Field Theories. 1. Stable Particle States”, *Commun. Math. Phys.* **104** (1986) 177.
- Z. Maassarani and S. Wallon, “Baxter equation for the QCD odderon”, *J. Phys.* **A28** (1995) 6423–6434, [arXiv:hep-th/9507056](#).
- N. J. MacKay, “Introduction to Yangian symmetry in integrable field theory”, *Int. J. Mod. Phys.* **A20** (2005) 7189–7218, [arXiv:hep-th/0409183](#).
- M. Magro, “Review of AdS/CFT Integrability, Chapter II.3: Sigma Model, Gauge Fixing”, *Lett. Math. Phys.* **99** (2012) 149–167, [arXiv:1012.3988](#).
- J. Maldacena and A. Zhiboedov, “Form factors at strong coupling via a Y-system”, *JHEP* **11** (2010) 104, [arXiv:1009.1139](#).
- J. M. Maldacena, “The Large N limit of superconformal field theories and supergravity”, *Int. J. Theor. Phys.* **38** (1999) 1113–1133, [arXiv:hep-th/9711200](#), [Adv. Theor. Math. Phys.2,231(1998)].
- S. Mandelstam, “Light Cone Superspace and the Ultraviolet Finiteness of the $\mathcal{N} = 4$ Model”, *Nucl. Phys.* **B213** (1983) 149–168.
- C. Marboe and V. Velizhanin, “Twist-2 at seven loops in planar $\mathcal{N} = 4$ SYM theory: full result and analytic properties”, *JHEP* **11** (2016) 013, [arXiv:1607.06047](#).
- C. Marboe, V. Velizhanin, and D. Volin, “Six-loop anomalous dimension of twist-two operators in planar $\mathcal{N} = 4$ SYM theory”, *JHEP* **07** (2015) 084, [arXiv:1412.4762](#).

- C. Marboe and D. Volin, “Quantum spectral curve as a tool for a perturbative quantum field theory”, *Nucl. Phys.* **B899** (2015) 810–847, [arXiv:1411.4758](#).
- C. Marboe and D. Volin, “Fast analytic solver of rational Bethe equations”, *J. Phys.* **A50** (2017)a, no. 20, 204002, [arXiv:1608.06504](#).
- C. Marboe and D. Volin, “The full spectrum of AdS5/CFT4 I: Representation theory and one-loop Q-system”, 2017b, [arXiv:1701.03704](#).
- C. Matsui, “Spinon excitations in the spin-1 XXZ chain and hidden supersymmetry”, *Nucl. Phys.* **B913** (2016) 15–33, [arXiv:1607.04317](#).
- D. Meidinger and V. Mitev, “Dynamic Lattice Supersymmetry in $gl(n|m)$ Spin Chains”, *J. Statist. Phys.* **156** (2014) 1199, [arXiv:1312.7021](#).
- D. Meidinger, D. Nandan, B. Penante, and C. Wen, “A note on NMHV form factors from the Grassmannian and the twistor string”, *JHEP* **09** (2017) 24, [arXiv:1707.00443](#).
- C. Meneghelli, “Superconformal Gauge Theory, Yangian Symmetry and Baxter’s Q-Operator”, PhD thesis, Humboldt University Berlin, 2011.
- R. R. Metsaev and A. A. Tseytlin, “Type IIB superstring action in $AdS_5 \times S^5$ background”, *Nucl. Phys.* **B533** (1998) 109–126, [arXiv:hep-th/9805028](#).
- A. Miller and R. Paris, “Transformation formulas for the generalized hypergeometric function with integral parameter differences”, *Rocky Mountain J. Math.* **43** 02 (2013) 291–327.
- J. A. Minahan and K. Zarembo, “The Bethe ansatz for $\mathcal{N} = 4$ Super Yang-Mills”, *JHEP* **03** (2003) 013, [arXiv:hep-th/0212208](#).
- A. I. Molev, “Yangians and their applications”, *Handbook of Algebra* **3** (2003) 907–959, [arXiv:math/0211288](#).
- A. Molev, M. Nazarov, and G. Olshansky, “Yangians and classical Lie algebras”, *Russ. Math. Surveys* **51** (1996) 205, [arXiv:hep-th/9409025](#).
- D. Müller, H. Münkler, J. Plefka, J. Pollok, and K. Zarembo, “Yangian Symmetry of smooth Wilson Loops in $\mathcal{N} = 4$ super Yang-Mills Theory”, *JHEP* **11** (2013) 081, [arXiv:1309.1676](#).
- V. P. Nair, “A Current Algebra for Some Gauge Theory Amplitudes”, *Phys. Lett.* **B214** (1988) 215–218.
- D. Nandan, C. Sieg, M. Wilhelm, and G. Yang, “Cutting through form factors and cross sections of non-protected operators in $\mathcal{N} = 4$ SYM”, *JHEP* **06** (2015) 156, [arXiv:1410.8485](#).
- D. Nandan, A. Volovich, and C. Wen, “A Grassmannian Étude in NMHV Minors”, *JHEP* **07** (2010) 061, [arXiv:0912.3705](#).
- D. Nandan and C. Wen, “Generating All Tree Amplitudes in $\mathcal{N} = 4$ SYM by Inverse Soft Limit”, *JHEP* **08** (2012) 040, [arXiv:1204.4841](#).

- M. L. Nazarov, “Quantum Berezinian and the classical Capelli identity”, *Letters in Mathematical Physics* **21** (1991), no. 2, 123–131.
- S. J. Parke and T. R. Taylor, “An Amplitude for n Gluon Scattering”, *Phys. Rev. Lett.* **56** (1986) 2459.
- K. Peeters, J. Plefka, and M. Zamaklar, “Splitting spinning strings in AdS/CFT”, *JHEP* **11** (2004) 054, [arXiv:hep-th/0410275](#).
- B. Penante, “On-shell methods for off-shell quantities in $\mathcal{N} = 4$ Super Yang-Mills: from scattering amplitudes to form factors and the dilatation operator”, PhD thesis, Queen Mary, U. of London, 2016, [arXiv:1608.01634](#),
- R. Penrose, “Twistor algebra”, *J. Math. Phys.* **8** (1967) 345.
- R. Penrose, “The Central programme of twistor theory”, *Chaos Solitons Fractals* **10** (1999) 581–611.
- A. Postnikov, “Total positivity, Grassmannians, and networks”, 2006, [arXiv:math/0609764](#).
- G. P. Pronko and Yu. G. Stroganov, “Bethe equations ‘on the wrong side of equator’”, *J. Phys.* **A32** (1999) 2333–2340, [arXiv:hep-th/9808153](#).
- R. Roiban, M. Spradlin, and A. Volovich, “A Googly amplitude from the B model in twistor space”, *JHEP* **04** (2004)a 012, [arXiv:hep-th/0402016](#).
- R. Roiban, M. Spradlin, and A. Volovich, “On the tree level S matrix of Yang-Mills theory”, *Phys. Rev.* **D70** (2004)b 026009, [arXiv:hep-th/0403190](#).
- R. Roiban and A. Volovich, “All conjugate-maximal-helicity-violating amplitudes from topological open string theory in twistor space”, *Phys. Rev. Lett.* **93** (2004) 131602, [arXiv:hep-th/0402121](#).
- M. A. Shifman, A. I. Vainshtein, and V. I. Zakharov, “Remarks on Higgs Boson Interactions with Nucleons”, *Phys. Lett.* **B78** (1978) 443–446.
- E. K. Sklyanin, “Quantum inverse scattering method. Selected topics”, 1991, [arXiv:hep-th/9211111](#).
- E. K. Sklyanin, “Separation of Variables. New Trends.”, 1995, [arXiv:solv-int/9504001](#).
- M. F. Sohnius and P. C. West, “Conformal Invariance in $\mathcal{N} = 4$ Supersymmetric Yang-Mills Theory”, *Phys. Lett.* **B100** (1981) 245.
- M. Spradlin and A. Volovich, “From Twistor String Theory To Recursion Relations”, *Phys. Rev.* **D80** (2009) 085022, [arXiv:0909.0229](#).
- M. Staudacher, “The Factorized S-matrix of CFT/AdS”, *JHEP* **05** (2005) 054, [arXiv:hep-th/0412188](#).
- L. Susskind, “The World as a hologram”, *J. Math. Phys.* **36** (1995) 6377–6396, [arXiv:hep-th/9409089](#).

- B. Sutherland, “Exact Solution of a Two-Dimensional Model for Hydrogen-Bonded Crystals”, *Phys. Rev. Lett.* **19** Jul (1967) 103–104.
- G. ’t Hooft, “A Planar Diagram Theory for Strong Interactions”, *Nucl. Phys.* **B72** (1974)a 461.
- G. ’t Hooft, “A Two-Dimensional Model for Mesons”, *Nucl. Phys.* **B75** (1974)b 461–470.
- G. ’t Hooft and M. J. G. Veltman, “Scalar One Loop Integrals”, *Nucl. Phys.* **B153** (1979) 365–401.
- Z. Tsuboi, “Solutions of the T-system and Baxter equations for supersymmetric spin chains”, *Nucl. Phys.* **B826** (2010) 399–455, [arXiv:0906.2039](#).
- Z. Tsuboi, “Wronskian solutions of the T, Q and Y-systems related to infinite dimensional unitarizable modules of the general linear superalgebra $gl(M|N)$ ”, *Nucl. Phys.* **B870** (2013) 92–137, [arXiv:1109.5524](#).
- W. L. van Neerven, “Infrared Behavior of On-shell Form-factors in a $\mathcal{N} = 4$ Supersymmetric Yang-Mills Field Theory”, *Z. Phys.* **C30** (1986) 595.
- P. Vieira and T. Wang, “Tailoring Non-Compact Spin Chains”, *JHEP* **10** (2014) 35, [arXiv:1311.6404](#).
- F. Wilczek, “Decays of Heavy Vector Mesons Into Higgs Particles”, *Phys. Rev. Lett.* **39** (1977) 1304.
- M. Wilhelm, “Amplitudes, Form Factors and the Dilatation Operator in $\mathcal{N} = 4$ SYM Theory”, *JHEP* **02** (2015) 149, [arXiv:1410.6309](#).
- E. Witten, “Anti-de Sitter space and holography”, *Adv. Theor. Math. Phys.* **2** (1998) 253–291, [arXiv:hep-th/9802150](#).
- E. Witten, “Perturbative gauge theory as a string theory in twistor space”, *Commun. Math. Phys.* **252** (2004) 189–258, [arXiv:hep-th/0312171](#).
- A. B. Zamolodchikov, “Thermodynamic Bethe Ansatz in Relativistic Models. Scaling Three State Potts and Lee-Yang Models”, *Nucl. Phys.* **B342** (1990) 695–720.
- B. I. Zwiebel, “From Scattering Amplitudes to the Dilatation Generator in $\mathcal{N} = 4$ SYM”, *J. Phys.* **A45** (2012) 115401, [arXiv:1111.0083](#).